Nitrogen signaling in the mature endodermis of *Arabidopsis* and its role in microbe-elicited soil nitrogen utilization

Inaugural-Dissertation

zur

Erlangung des Doktorgrades

der Mathematisch-Naturwissenschaftlichen Fakultät

der Universität zu Köln

vorgelegt von

Noah David Kürtös

aus Ludwigsburg, Deutschland

Köln

2023

Die vorliegende Arbeit wurde am Max-Planck-Institut für Pflanzenzüchtungsforschung in Köln in der Abteilung für Pflanzen-Mikroben Interaktionen (Direktor: Prof. Dr. Paul Schulze-Lefert), in der Arbeitsgruppe von Dr. Tonni Grube Andersen durchgeführt.

Unterstützt durch:

Max Planck Institute for Plant Breeding Research

IMPRS Cologne/Düsseldorf

Erstgutachtende*r: Prof. Dr. Paul Schulze-Lefert

Zweigutachtende*r: Prof. Dr. Stanislav Kopriva

Drittgutachtende*r: Dr. Anne Krapp

Prüfungsvorstizende*r: Prof. Dr. Bart Thomma

Protokollführende*r: Dr. Tonni Grube Andersen

Tag der Prüfung: 05.12.2023

1 Table of contents:

2 Abstract

Nitrogen is a key component to life. The bioavailability of nitrogen (N), in the form of ammonium (NH_4^+) and nitrate (NO_3^-), in soil ecosystem varies strongly and it often is a growth limiting factor for plants. Therefore, plants have evolved an arsenal of nitrogen signalling and uptake mechanisms to forage nitrogen from their environment. Once taken up by the root, nitrogen amongst other nutrients, is transported to other organs of the plant through the central vascular cylinder. To prevent the leakage of nutrients out of the vasculature, it is surrounded by a barrier tissue: the endodermis. We have only recently started to understand how the reinforcement of endodermal cell walls by lignin and suberin is coordinated with the plant nutrient status and especially the role of nitrogen remained unresolved. Here we found that, in *Arabidopsis thaliana*, nitrogen starvation leads to an increase of endodermal suberization and that endodermal nitrogen signalling and suberization are required to facilitate microbe-dependent growth promotion after nitrogen fertilizer application to agricultural soil. Tissue-specific post-transcriptional analysis of nitrogen starved plants revealed, that in the mature primary root, the high affinity nitrate transporter *NRT2.1* and the high affinity ammonium transporter *AMT1.5* are upregulated in the outer cortex layer above the suberized endodermis. Similarly, coumarin biosynthesis appears to be distinctively regulated in the mature root under nitrogen starvation. The scopoletin synthesizing gene *F6'H1* and the fraxetin synthesizing gene *S8H* are upregulated in the mature cortex, while the sideretin synthesizing gene *CYP82C4* is downregulated. Moreover, the nitrate transceptor *NPF6.3* and the transcription factor *NIGT1.3* are upregulated specifically in the endodermis of nitrogen starved plants. Manipulation of nitrogen signalling by overexpressing the nitrate responsive transcription factor NLP7, in the endodermis specifically, leads to higher sensitivity to nitrate and resulted in a reduction of suberization under nitrate re-supply. When grown in nitrogen-fertilized natural soil NLP7 overexpression leads to a loss of microbe-dependent growth promotion. Similarly, the *f6'h1* mutant, which is unable to produce coumarins, is unable to benefit from nitrogen fertilization. Our results demonstrate that the endodermis, likely through *NPF6.3* and *NIGT1.3*, plays a central role in coordinating plant nitrogen homeostasis. The distinct modulation of the root microbiome, through secreted secondary metabolites, has gained recent attention. It appears to be an integral tool for the adaption of plants to nutrient limiting conditions. How plant-microbial relationships are established and communicated across a closed endodermal barrier will be a key question of upcoming research.

3 Introduction

3.1 Nitrogen is an essential plant macro nutrient.

Nitrogen (N), together with carbon, oxygen and hydrogen is one of the four key components for the formation of organic life (S. L. Miller, 1953). It is estimated to be the seventh most abundant element in the universe (0.11%) (Croswell, 1996). Elemental nitrogen (N_2) constitutes the vast majority (78%) of earth's atmosphere. Due to its triple bond, elemental dinitrogen (N_2) is an inert gas. Because of that, elemental nitrogen does not contribute to the pool of biologically available nitrogen, often rendering it a limiting factor in many ecosystems. In fact, the concentration of nitrogen in the earth crust is low (0.002 %) (Mark Winter, 2023; Ohyama & Sueyoshi, 2010) but elemental nitrogen can be made bioavailable by natural atmospheric deposition, anthropogenic chemical fixation or biological fixation. The nitrogen cycle describes the turnover of biologically fixed nitrogen between species and ecosystems (Vitousek et al., 2002). In eukaryotic organisms, nitrogen constitutes between 1% (*Laguncularia racemosa,* white mangrove) and 15% (*Epinephelus niveatus*, snowy grouper*)* of the total dry mass (Barbarino & Lourenço, 2009), primarily in protein form (Novoa & Loomis, 1981).

For land plants, nitrogen dry weight content is estimated at 1.5% (Marschner, 1995). In aboveground tissue of winter oilseed rape (*Brassica napus*), 45.3% of nitrogen can be associated with photosynthetic activity, 10-15% with nucleic acids and ribosomes, and 8% with structural properties such as cell walls (Harrison et al., 2009; T. Liu et al., 2018). Nitrogen containing defense compounds vary greatly across species, but can constitute up to 20% of leaf nitrogen in almondbark (*Prunus turneriana*) (R. E. Miller & Woodrow, 2008). The remaining 20-30% of plant nitrogen are not directly involved in any metabolic processes and are considered storage N. Until its remobilization for the growth of new tissue, nitrogen is either stored as inorganic nitrogen in the form of nitrate (NO_3^-), or as organic nitrogen in the form of amino acids (AAs) or storage proteins (T. Liu et al., 2018). Nitrate can constitute up to 36% of total nitrogen in the shoots of perennial ryegrass (*Lolium perenne*) (Millard, 1988) and is mainly stored in the central vacuole of the plant cell (Tegeder & Masclaux-Daubresse, 2018). Depending on plant species, between 50% (birch, *Betula pendula*) and 90% (tomato, *Lycopersicon esculentum*) of total nitrogen is allocated to the shoot, while the remaining 10% to 50% are allocated to the root system. However, the distribution of available nitrogen between root and shoot depends on the nutrient status and photosynthetic rate of the plant, and different species employ different redistribution strategies (Ågren & Franklin, 2003).

3.1.1 Nitrogen is a limiting factor for modern agriculture resulting in heavy nitrogen fertilizer usage.

In natural ecosystems nitrogen is one of the major growth limiting factors. Due to the inert nature of N_2 in the atmosphere there are little potential inputs of bioavailable nitrogen. Sporadic fixation of atmospheric nitrogen by lightning or volcanic eruptions is estimated to provide ca. 0.24kg N ha^{-1} annually, which represents 3% of preindustrial global nitrogen fixation. The remaining 97% are fixed by prokaryotic organisms (Barth et al., 2023; Hill et al., 1980). Biological nitrogen fixation occurs mostly by free living or plant associated bacteria. Free living heterotrophic bacteria have been shown to contribute up to 20kg N ha^{-1} per year. The symbiotic

relationship of water ferns (*Azolla spp.*) with a cyanobacterium (*Anabaena azollae*) has been demonstrated to be able to fix up to 600kg N ha^{-1} per year (Wagner, 2011).

Most nitrogen will be fixed as organic nitrogen within organisms and cycled between them. In this way, as so-called protein-precipitation, nitrogen is bound in the aboveground foliage of forests. Thus, available nitrogen would be stable over time. However, available nitrogen is still removed from ecosystems. While free organic, carbon-bound nitrogen and cationic, reduced mineral nitrogen (ammonium, NH_4^+) show low mobility in soil, nitrogen in its oxidized anionic forms (nitric oxide, NO; nitrite, NO_2^-; nitrogen dioxide, NO_2 and nitrate, NO_3^-) is highly mobile in the soil and can be washed out of topsoil layers by nutrient leaching. Moreover, during microbial, anaerobic metabolism, available nitrogen is removed from the soil resulting in denitrification. In contrast to other essential mineral elements, both oxidized and reduced nitrogen compounds have a gaseous phase resulting in nitrogen loss through volatilization (Berhe et al., 2014; Lehmann & Schroth, 2009; Vitousek et al., 2002). Besides these chemical processes, nitrogen bound in plant foliage can also be physically removed from ecosystems by forest fires, deforestation and agricultural harvest. The net nitrogen output of forest fires and deforestation is highly variable, because forest fires often result in remobilization of protein-precipitated nitrogen in the form of free-soil mineral nitrogen, while deforested areas are often replaced with agricultural systems. However, both have been associated to increased nitrogen leaching from affected ecosystems (Christensen, 1973; Guiry et al., 2020).

On present-day earth (status 2019), half (46%) of the total land mass is used for agriculture. In the last two hundred years, the area used for crop production quadrupled (Ritchie & Roser, 2019). However, in the same timeframe, global population increased tenfold (Mathieu et al., 2023). The British Association for the Advancement of Science already predicted in 1898 that a growing demand for food could eventually no longer be met with the amount of land available for agricultural farming, and indeed, while the cropland per capita initially increased to a peak of 0.5 ha per capita in 1910, it declined thereafter, and today only 0.22 ha are available per person (O'Neill, 2022; Ritchie & Roser, 2019; Topham, 1985). It was already known then, that the addition of certain materials increases soil fertility, and thus crop production. Yet, already at the brink of the 20th century the three known sources of nitrogen fertilizer - bird guano off the coast of South America, mineral nitrate reserves in the Atacama Desert, and charcoal distilled ammonium sulphate - were forecast to be exhausted mid-century (Topham, 1985).Thus, in 1908, the two chemists Fritz Haber and Carl Bosch started to investigate the industrial synthesis of ammonia (NH_3) from atmospheric nitrogen and water. Already four years later, this work resulted in the first industrial ammonia plant using their *Haber–Bosch* process in Ludwigshafen, Germany. Today, while scaled up, the principle of the process remains the same for which Nobel Prizes were awarded to Fritz Haber in 1919 and to Carl Bosch in 1931. In brief, pure elemental hydrogen (H_2) gas is obtained by steam reformation from methane. Pure elemental nitrogen (N_2) gas is obtained by air separation via cryogenic distillation. One unit of N_2 and three units of H_2 are then merged in a pressured vessel, which is cooled to 400-500°C. Here, the gasses are adsorbed onto a magnetite (Fe_3O_4) catalyst. The high pressure and low temperature shift the equilibrium towards ammonia (Equation 1). Hydrogen, Nitrogen and ammonium are desorbed from the catalyst and ammonia is removed from the gas by cryogenic distillation, before the remaining reactants, H_2 and N_2, are recycled onto the catalyst (Topham, 1985). The current global NH_3 production through this process is estimated at 150

10^9 kg (Smith et al., 2020). Ammonia can be converted to nitric acid HNO_3 and subsequently all mineral nitrogen salts (Benvenuto & Plaumann, 2021). Currently, 80% of industrially fixed nitrogen is used for fertilizer production (Erisman et al., 2008). This is equivalent to $100 \cdot 10^9$ kg of fixed nitrogen or 80 kg N ha^{-1} of arable land. Yet, nitrogen fertilizers are not distributed equally, and thus, up to 380 kg N ha^{-1} are locally introduced into agricultural ecosystems (Figure 1A) (Ritchie & Roser, 2019). In soil ecosystems, the availability of inorganic nitrogen can vary from 10^{-3} M to $10 \cdot 10^{-2}$ M, and 10^{-6} M to 10^{-3} M, for nitrate and ammonium, respectively. In addition to mineral nitrogen, plants can also take up organic nitrogen in the form of amino acids (AAs) from the soil. AAs can constitute between 10% to 40% of the total soluble N in soils with concentrations ranging between 10^{-7} M and 10^{-2} M (Gioseffi et al., 2012; Jones et al., 2005), greatly depending on the ecological context (Raab et al., 1999). Heavy supply of biologically available nitrogen, introduced through industrial fertilizers, leads to high level of nitrate and ammonium into the soil. This allows for ammonium to be converted into nitrate by autotrophic nitrifying bacteria (Prosser, 1990). As a result, fertilizer nitrogen, in the form of nitrate, is leached into the lower soil levels and eventually into the ground water system (J. Fan et al., 2017; Lehmann et al., 2003; Lehmann & Schroth, 2009). Annually $10 \cdot 10^9$ kg of nitrogen end up in surface water this way, equivalent to 10% of the nitrogen fixed via the Haber-Bosch process (data from 2010) (van Puijenbroek et al., 2019). Eventually, leached nitrogen becomes unavailable for agricultural ecosystems and resulting in elevated nitrogen levels in freshwater reservoirs and river deltas. Here, excessive nitrogen availability fosters rapid algal blooms. Covering the whole surface of entire water bodies, algal blooms obstruct the penetration of light to lower levels and cause local littoral flora and fauna to die off. Furthermore, high photosynthesis rates deplete dissolved carbon, thereby elevating water pH levels. In the aftermath, the decomposition of these blooms consumes oxygen and creates hypoxic environments, rendering them uninhabitable (Figure 1B) (Chislock et al., 2013). In summary, while the chemical fixation of nitrogen has revolutionized agriculture, a new challenge has also arisen; as it has become clear that efficient usage of nitrogen fertilizer is also crucial for high yielding and sustainable agriculture.

3.1.2 Plants employ different strategies to optimize their nitrogen use efficiency.

To reach the goal of increasing agricultural nitrogen use efficiency, it is crucial to understand which strategies different plants employ to obtain nitrogen in their natural, nitrogen-limited ecosystems. As mentioned above, nitrogen, in contrast to all other mineral nutrients, is not added to the soil nutrient pool by weathering, but by atmospheric fixation. This unique interaction with the atmosphere, as well as the low mobility of reduced (NH_4^+) and organic nitrogen versus the high mobility of oxidized nitrogen (NO_3-), result in drastic differences of soil nitrogen availability in space and time (Glass, 2010). In aerobic soils, the main form of inorganic N is nitrate, while in flooded soils or anaerobic wetlands, the main form of inorganic N is ammonium (G. Xu et al., 2012). Currently, most domesticated crop plants are flowering (clade *Angiosperm*), vascular plants (clade *Tracheophytes*). These are primarily cereals (family *Poaceae,* 70%), leguminous plants (family *Fabaceae*, 18%), or oilseed plants (family *Brassicaceae*, 4%) (Figure 1C) (Ritchie & Roser, 2019). To sustain their aboveground vegetative and reproductive tissue, these plants take up mineral nutrients and water from the soil via their below-ground root system. While agricultural values have traditionally focused on above-ground traits, such as grain size, yield, and straw length, the root system is gaining

attention as an important contributor to plant health. The root system architecture (RSA) can dynamically adapt to the plant's requirements by changing the directionality and branching of its primary and lateral roots, in order to forage nutrients from the soil (Giehl & von Wirén, 2014; Gruber et al., 2013).

The effect of nitrogen on RSA has been shown in the roots of rice (*Oryza sativa*), amongst all essential mineral nutrients tested, plants only display nutritropism towards ammonium (Yamazaki et al., 2020). Moreover, in the extensively studied model organism *Arabidopsis thaliana* (commonly: thale cress, family: *Brassicaceae*), both ammonium (NH_4^+) and nitrate (NO_3^-) have been shown to directly and locally influence RSA under standardized laboratory conditions. While local supply of NH_4^+ leads to an increase in lateral root number, as well as first and second order lateral root growth, local supply of NO_3^- doesn't influence the number of lateral roots, but increases the elongation of first order lateral roots (Meier et al., 2020). Together, these results highlight those plants indeed sense the presence and quality of mineral nitrogen, and show specific behaviorisms in order to optimize their nutrient uptake efficiency.

Another adaptation of plants to limited soil nitrogen, is the recruitment of beneficial microbes into their roots. Some flowering plants within the *Rosid I* clade of *eudicotyledon* plants can develop specialized root organs, so-called 'nodules', in which they host nitrogen-fixing bacteria, making them independent from mineral nitrogen sources. Within this N_2-fixing clade (NFC) the hypothesized predisposition for nodulation first appeared about $100 \cdot 10^6$ years ago. Considering that plants moved from sea to land already 10^9 years ago, *Fabaceae* nodulation is a relatively recent development in evolutionary history (de Vries & Archibald, 2018). Yet, they have been part of human agriculture from the very beginning in the form of, e.g., the name-giving faba beans (*Vicia faba)* and lentils (*Vicia lens*). Amongst other attributes they have been praised by the ancient greeks for their "soil invigorating" purposes (Fred, 1932), and to this day, leguminous plants such as clover (*Trifolium spp.*) are valued as "green manure", and actively incorporated into crop cycles (Arevalo et al., 2005) in order to provide additional nitrogen to the field. The ability to beneficially interact with nitrogen-fixing bacteria is suggested to be conserved across plant lineages (Garrido-Oter et al., 2018). There is also evidence for non-leguminous plants living intimately with nitrogen fixing bacteria. As an example, it has been recently shown by Van Deynze et al. (2018), that aerial roots of a maize landrace (*Zea Maize* from Sierra Mixe, Oaxaca, Mexico*,* family *Poaceae*), secrete mucilage, which recruits and hosts microbial communities of diazotrophic bacteria. According to the study, these plants retrieve between 29 and 82% of their nitrogen through this interaction. Moreover, this unique interaction is may be the decisive factor allowing this landrace to outperform her sister landraces. Understanding the molecular mechanisms underlying nitrogen sensing, signaling, and homeostasis, will contribute to our understanding of how plants interact with their environment, and how these interactions impact crop yield.

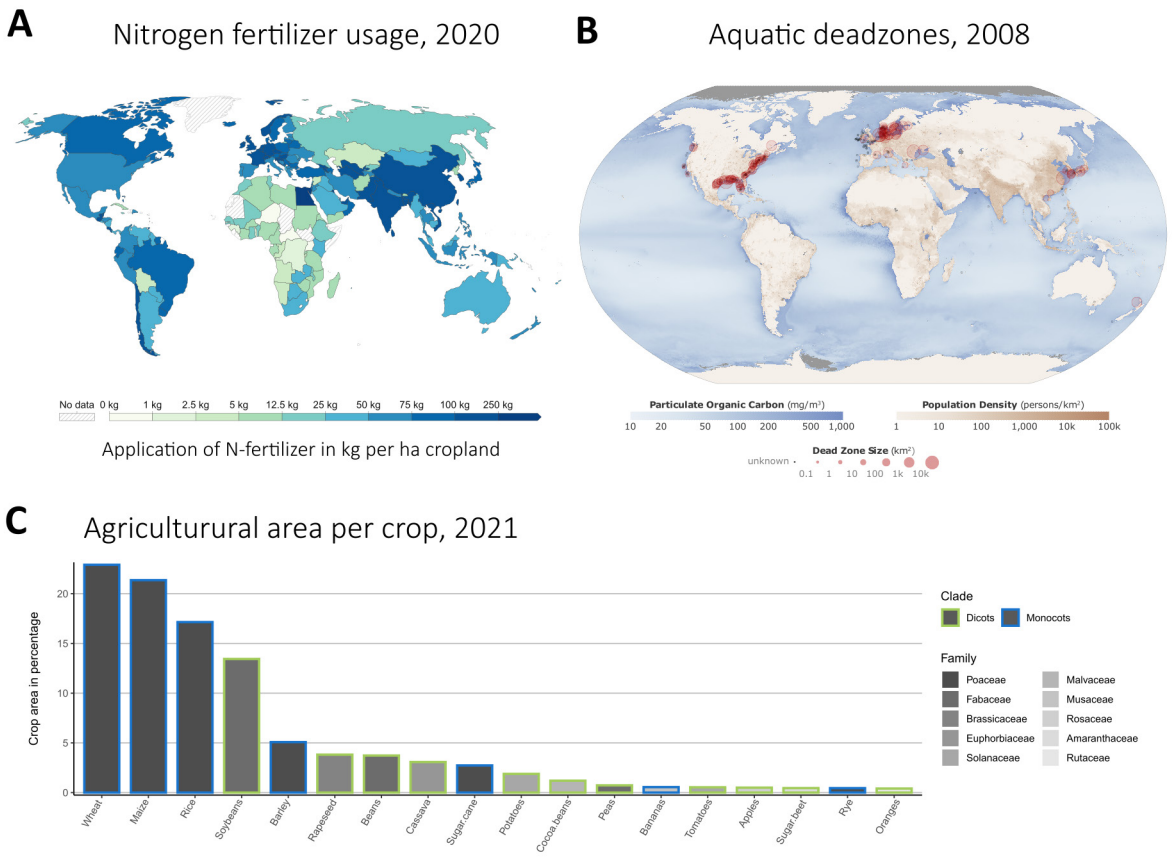

Figure 1: ***Agricultural relevance of nitrogen fertilizer usage: A*** *Distribution of nitrogen fertilizer usage, modified after Ritchie & Roser, 2019.* ***B*** *Spread of aquatic hypoxic 'dead zones' as read out for eutrophication and overfertilization, taken from Diaz & Rosenberg, 2008* ***C*** *Land usage per crop separated by clade and family. Only data for food crops was provided, data from Ritchie & Roser, 2019*

$$N_2 + 3\,H_2 \rightleftharpoons 2\,NH_3$$

Equation 1: ***Ammonia equilibrium exploited in the Haber-Bosch-Principle****: The reaction to ammonium is exothermic. All three molecules can be considered ideal gases with a volume of 22.4 L mol^{-1}*

3.2 Molecular mechanisms of plant nitrogen homeostasis

Although the ability to form root nodules is an advantageous trait, it is not essential for plant survival, since land plants presumably lived on terrestrial soil for the majority of the last 1 10^9 years without it. Moreover, even plants that can undergo nodule formation don't always do so (Streeter, 1985; Wong, 1988). Whilst nodule symbiosis provides the host plant with fixed nitrogen, the plant in turn provides the symbiotic bacteria with primary metabolites (Bezrutczyk et al., 2018; Strodtman & Emerich, 2015). To balance, and conditionally restrain this metabolically costly relationship, nodule formation is restricted in the presence of sufficient mineral nitrogen sources (Streeter, 1985). Similarly, depending on carbon and water availability, which affects photosynthetic rates, nodule formation and supply are also adjusted by the host according to nutrient and water availability (Parvin et al., 2020). Further, plants are adjusting their nitrogen uptake capacity in accordance to nitrogen availability (Breazeale, 1906). A prerequisite for the plant to make any of these adjustments is its ability sense both, the external availability of nitrogen in the soil, as well as its own internal nitrogen status and

demand. For this, plants have evolved sophisticated nitrogen sensing mechanisms (Gent & Forde, 2017).

3.2.1 Extracellular nitrogen sensing

Nitrogen sensing and uptake are tightly intertwined, and accordingly, all identified NO_3^-, NH_4^+ and AA sensing proteins serve an additional function as plasma membrane-localized nitrogen transporters (Ho & Tsay, 2010; O'brien et al., 2016). In *Arabidopsis thaliana*, apoplastic NO_3^- levels are sensed by the dual affinity nitrate transceptor AtNPF6.3[1] (NRT1.1, *AT1G12110*) (Tsay et al., 1993). However, the exact details how it exerts its functions are not yet understood. To date, at least four different modes of NPF6.3-dependent signaling have been proposed (Armijo & Gutiérrez, 2017). In brief; at low nitrate levels, NPF6.3 acts as a decoupled dimeric high affinity transporter (Figure 2, top) (Armijo & Gutiérrez, 2017; Fang et al., 2021; Krapp et al., 2014; Muratore et al., 2021; O'Brien et al., 2016; Parker & Newstead, 2014; Rashid et al., 2018, 2020; Ye et al., 2019). Upon binding nitrate to the binding site of protomer A, the CIPK23-CBL9 (CIPK, CBL-Interacting Protein Kinase; CBL, Calcineurin-B like Protein) protein complex is phosphorylating NPF6.3, increasing its the nitrate transport rate. Phosphorylation of NPF6.3 by CIPK23-CBL9 triggers secondary CIPK23-CBL9-dependent nitrate responses, including calcium influx, protein phosphorylation and transcriptional changes. In contrast, at high nitrate levels, NPF6.3 is dephosphorylated and NPF6.3 dimers have a low transport rate (Bouguyon et al., 2015; Parker & Newstead, 2014; Rashid et al., 2020). Similarly, Members of the high affinity AMMONIUM TRANSPORTER (AMT) family undergo a similar process of concentration dependent autoregulation. It has been shown that AMT1.1 and AMT1.3 form active homo- or heterotrimers. With increasing ammonium concentrations, these complexes are phosphorylated, reducing the ammonium influx (Lanquar et al., 2009; Straub et al., 2017; Wu et al., 2019). Apoplastic ammonium concentrations are thus stably maintained between 1mM and 2mM, independent of external ammonium supply (Yuan et al., 2007). Although similar transceptor models as for NO_3^- have been proposed for NH_4^+, a sensory complex at the plasma membrane has not yet been identified and it has been suggested that ammonium is instead sensed via its cytoplasmic concentration, or indirectly with nitrogen containing metabolites serving as proxy (Bai, Zhou, et al., 2014). Similarly, the perception of external amino acids and urea as nitrate sources is still debated. While transporters have been identified for both, soil amino acid concentrations are usually several orders of magnitude lower than cellular amino acid concentrations – depending on nitrogen status – can range between $0.1 \cdot 10^{-6}$M and $10 \cdot 10^{-3}$M (Gioseffi et al., 2012; Jones et al., 2005; Raab et al., 1999). Also, free urea is rapidly reduced to ammonia (NH_3) or ammonium (NH_4^+) (Muratore et al., 2021). Recently, GLUTAMATE RECEPTOR LIKE (GLR) amino-acid gated $Na^+/K^+/Ca^{2+}$ transporters have been suggested to serve as AA sensors (Kang & Turano, 2003; Weiland et al., 2015). However, due to their substrate promiscuity it has remained difficult to

[1] The NRT1/PTR FAMILY (NPF) is a 53-member transporter gene family in *Arabidopsis thaliana*. Named after the first described *NITRATE TRANSPORTER 1.1* (*NRT1.1/CHL1*) (Tsay et al., 1993), several genes within the family were associated to nitrate transport (aliases: *NRT1.2* to *NRT1.16*) and/or other compounds, including chloride (Cl^-), glucosinolates (GSL), auxin (IAA), abscisic acid (ABA), jasmonates (JA) and gibberellins (GA) (detailed review by Corratgé-Faillie & Lacombe, 2017). For the sake of consistency, they will be referred to as NPF genes in this work and, if applicable, their respective NRT1 alias as well as gene identifier will be added upon first mentioning as it is referenced on arabidopsis.org (Berardini et al., 2015).

connect them directly to nitrogen sensing (Gent & Forde, 2017). In conclusion, while NPF6.3 represents an intricate system to sense fluctuations in extracellular NO_3^- concentrations, nitrogen levels are also sensed within the cell. Moreover, for ammonium and amino acids, this appears to be the primary sensory mechanism.

3.2.2 Intracellular nitrogen sensing and signaling cascades

3.2.2.1 Intracellular nitrate sensing by NLP proteins

In addition to NPF6.3-dependent nitrate sensing at the plasma membrane, NIN-LIKE PROTEIN 7 (NLP7) was shown to directly bind nitrate and then relocate from the cytosol into the nucleus, where it acts as transcription factor to activate the expression of genes involved in nitrogen uptake (K. H. Liu et al., 2022). Retention of NLP7 in the nucleus is crucial for its activity (Marchive et al., 2013)and dependent on phosphorylation by the CALCIUM DEPENDENT PROTEIN KINASES 10, 30 and 32 (CPK10, CPK30, CPK32). Interestingly, these CPKs are in turn activated by NPF6.3-dependent calcium waves, which links the NLP7-dependent N-responses to the plasma membrane nitrate sensing (K. H. Liu et al., 2020; Mu & Luo, 2019). Evolutionary analysis suggests that both, the nitrate binding-ability of NLP7 and its functional dependence on phosphorylation, are conserved across plant species (Durand et al., 2023; Mu & Luo, 2019). Seven of the nine NLP homologues in *Arabidopsis thaliana* – NLP 2,4,5,6,7,8 and 9 – have been directly demonstrated or suggested to be involved in nitrate signaling (K. H. Liu et al., 2020, 2022). However, A similar sensing role by directly binding nitrate has so-far only been shown for NLP2 (Durand et al., 2023) (Figure 2, left).

3.2.2.2 Is the tonoplast localized RLK CAP1 sensing cytosolic ammonium?

Cytosolic ammonium could be sensed in three distinct manners. First, ammonium could be directly bound by a sensor, similar to nitrate being bound by NLP7. Second, changes in ammonium dependent nitrogen metabolism may serve as a proxy for cytosolic availability. And third, the influx of ammonium (NH_4^+) or ammonia (NH_3) may result in a changed cytosolic pH, which could serve as an indirect signal for changes in ammonium homeostasis. Regarding the latter, it has been shown that AMT-dependent apoplastic acidification leads to the import of protonated auxin into cortical cells, which ultimately facilitates lateral root emergence (Meier et al., 2020). Regarding the first suggestion, the tonoplast-localized $[Ca^{2+}]_{cyt}$-ASSOCIATED PROTEIN KINASE 1 (CAP1),a member of the 17-member CrRLK1s (*Catharanthus roseus* RECEPTOR LIKE KINASEs) family, has been indicated to convey the cytosolic NH_4^+ status via calcium signaling. However, evidence of CAP1 directly binding the NH_4^+ ion is still missing (Bai, Ma, et al., 2014; Y. Liu & Von Wirén, 2017) (Figure 2, bottom).

3.2.2.3 N-assimilation by primary nitrogen metabolism

Most evidence points towards a direct regulation of ammonium homeostasis by primary N-metabolism. At this stage, nitrate and ammonium sensing converge, as nitrate is reduced to ammonium and eventually incorporated into AAs. In this process, cytosolic nitrate (NO_3^-) is first reduced to nitrite (NO_2^-) by the NITRATE REDUCTASE (NR). This step has been identified as rate limiting within the nitrate assimilation pathway, and is dependent on the redox cofactors flavin adenine dinucleotide (FAD), heme-Fe and molybdenum-molybdopterin (Mo-MPT). Here, both NADH and NADPH can act as electron donors for FAD (Campbell, 2001; Chamizo-Ampudia et al., 2017). Next, the generated nitrite is imported into the chloroplast (Sanz-Luque et al., 2015). Within the stroma of the chloroplast, nitrite is further reduced to ammonium (NH_4^+)

by the NITRITE REDUCTASE (NiR), which carries a [4Fe-4S] cluster and a siroheme as prosthetic groups. Reduced ferredoxin (Fd_{red}), generated by photosynthesis, is used as an electron donor in this process. Alternatively, NADPH can be used as an electron donor. Still within the chloroplast, ammonium is incorporated into glutamate through GLUTAMATE SYNTHASE (GOGAT), using 2-oxoglutarate as a substrate and Fd_{red}, NAD or NADPH as electron donors. Ultimately, another ammonium moiety can be added by the GLUTAMINE SYNTHETASE (GS), hydrolyzing ATP and using glutamate and ammonium as substrate. All other amino acids and nitrogen compounds are then synthesized via transamination (Hawkesford et al., 2023; Okumoto & Pilot, 2011; Russell, 2009; Sanz-Luque et al., 2015; Vallon & Spalding, 2009). Although homologues of the algal nitrite transporter *Chlamydomonas reinhardtii CrNAR1.1*, namely *Cucumus sativus NITR1-L* and *CsNITR1-S*, have been suggested to facilitate the import of nitrite into the chloroplast in those organisms, it is still not known how nitrite is imported into the chloroplast of vascular plants (Chamizo-Ampudia et al., 2017; Sugiura et al., 2007). Similarly, little is known about the import of NH_4^+ into the chloroplast. However, the *Arabidopsis thaliana* AMT1.2 protein contains a predicted plastid transit peptide site, and could therefore facilitate this process (Howitt & Udvardi, 2000). Export of synthesized amino acids from the chloroplast is currently believed to be facilitated by members of the PREPROTEIN AND AMINO ACID TRANSPORTER (PRAT) superfamily (Pudelski et al., 2010). In roots, nitrogen assimilation into amino acids mainly occurs through synthesis from glutamine by cytosplasmic GS (Howitt & Udvardi, 2000) and a study in barley (*Hordeum vulgare*) has shown that in the early stages of nitrogen assimilation, glutamine levels in roots increased 20-fold, even at the expense of decreasing levels of glutamic and aspartic acid (Oji & Izawa, 1971) (Figure 2, right).

In conclusion, at the plasma membrane nitrogen is sensed in the form of nitrate by the transceptor NPF6.3. In the cytoplasm, nitrate is sensed by NLP transcription factors. Further nitrate is then reduced and integrated into glutamate in the plastid or directly into glutamine in the cytosol. Thus, in the cytosol glutamine and nitrate function as direct proxies of plant nitrogen status (Figure 2).

3.2.2.4 Post-translational responses to nitrogen supply

Nitrate transport, sensing and the primary nitrate response (PNR) are tightly intertwined. Post-translational modifications of the proteins involve may serve to quickly integrate responses into cellular function (W. Wang et al., 2020). For example, nitrate resupply has been shown to reduce phosphorylation of the high affinity nitrate transporter NRT2.1, resulting in its rapid deactivation (Jacquot et al., 2020). In addition, phosphorylation of AMT1.1 increases its transport activity (Qin et al., 2020). Next to these two examples, also post-translational regulation of ammonium transport and assimilation via the highly conserved TARGET OF RAPAMYCIN (TOR) kinases has also been suggested. Although a direct connection between glutamine and TOR or its downstream targets remains elusive, it was shown that glutamine, together with nitrate and ammonium, and in the presence of sucrose, leads to the activation of TOR. Concomitantly, inhibition of TOR leads to decreased ammonium uptake and upregulation of NITRATE REDUCTASE (NR) and NITRITE REDUCTASE (NiR) resulting in increased Glutamine levels. As a result, NR, NiR and GS, but also CAP1, were hypothesized as potential targets for TOR to regulate nitrogen assimilation (Courbier, 2023; Ingargiola et al., 2023).

3.2.2.5 Transcriptional regulation of nitrogen status is integrated with nutrient status responses

The transcriptional response to nitrate has been extensively studied in the context of nitrogen starvation and the PNR after nitrate re-supply. In the nucleus, NLP7 binds to DNA of nitrate responsive genes at conserved, 43 base pair (bp) long regulatory cis-element(s) (NRE). NREs are located in the 5'-promoter regions, between ca. 50 and 250 bp upstream of the translational start codon (Konishi & Yanagisawa, 2011, 2013). NLP7 has been found bind to the promoters of 851 genes at their NRE, including 25% of genes that were miss regulated in the *nlp7* mutant, and equivalent to ca 2% of all putative genes in *Arabidopsis thaliana.* These findings highlight the central and direct involvement of NLP7 in nitrate-dependent transcriptional regulation (The Arabidopsis Genome Initiative, 2000; Vidal et al., 2020; L. Zhao et al., 2018). Genes regulated as part of the transcriptional primary nitrate response can be categorized into transcription factors, transporters, hormone synthesis genes or transporters, nitrogen metabolism, signaling, or non-categorizable genes (e.g. the proteasome scaffolding genes *BTB DOMAINE CONTAINING PROTEIN1 (BT1)* and *BT2* (Sato et al., 2016)). Transcription factors and signaling related genes, such as MAP kinases or CIPKs, furthermore influence each other, thereby creating a dense web of feedback loops. In the context of nitrogen homeostasis, genes involved in transport, nitrate reduction and nitrogen-assimilation, as well as regulatory transcription factors, deserve special attention. Both high and low affinity NO_3^- and NH_4^+ transporters, of the *NPF (NPF6.3/NRT1.1, NRT1.2, NRT1.8), NRT2 (NRT2.1, 2.2, 2.4, 2.5, 2.6., 2.7), AMT1 (AMT1.1, AMT1.3, AMT1.4)* families, as well as *AMT2,* have been shown to be regulated within the PNR. Moreover, the nitrate reductases *NIA1, NIA2*, and the nitrite reductase *NiR1*, for which the NRE was first discovered, are directly bound by PNR transcription factors. Finally, nitrogen assimilation is also directly regulated, primarily via glutamate (11/25 genes), glutamine (5/28 genes), aspartate (4/28) and asparagine (3/28 genes) metabolism. NPR also affects the transcriptional regulation of transcriptional regulators themselves. These transcriptional regulators include, but are not limited to, *LATERAL BOUNDARY DOMAIN 37* (*LBD37), 38, 39* (involved *NRT2* and anthocyanin biosynthesis repression, (Rubin et al., 2009; Zhu et al., 2022)*, NITRATE-INDUCIBLE, GARP-TYPE TRANSCRIPTIONAL REPRESSOR 1..1 (NIGT1.1), 1.2, 1.3, 1.4* (involved in *NRT2* repression and integration of N and phosphorus (P) signaling (Maeda et al., 2018))*, ELONGATED HYPOCOTYL 5 (HY5)* (light induced and involved in long distance signaling and anthocyanin biosynthesis (Shin et al., 2013; X. Wang et al., 2023) *and NLP1, 3* (see above). Together, these results highlight the extend and variety of transcriptional changes by NPF6.3-depedent and -independent signaling mediated through NLP7 (Vidal et al., 2020).

While most transcriptional responses to nitrate appear to be NLP7-dependent, there is also some evidence for NLP7-independent transcriptional regulation. The transcription factor NRG2 has been shown to bind to NLP7, but also to induce NLP7-independent transcriptional changes upon nitrate supply. Moreover, transcriptional profiles of the *nrg2* mutant after nitrate treatment differed, depending on the presence of ammonium in the growth medium (N. Xu et al., 2016). In 2002, Rawat and colleagues identified that one *Arabidopsis thaliana AtAMT1* homologue, is negatively regulated by elevated glutamine levels. A similar negative feedback regulation has been described for *Oryza sativa AMT1.3* (but not *OsAMT1.1* and *OsAMT1.2)* (Sonoda et al., 2003). Taken together, these previous studies highlight that the transcriptional responses to

high ammonium, and thus glutamine levels, might differ across species, and that systemic transcriptional responses to either glutamine or ammonium have yet to be demonstrated.

While most research aimed to understand nitrogen signaling in plants, has focused on the resupply of nitrogen to nitrogen-starved plants, there is also evidence for transcriptional regulation of the response to nitrogen starvation. For example, the *NPF6.3*-dependent transcriptional repression of the high affinity nitrate transporter *NRT2.1* in high nitrate availability, is relieved under nitrogen starvation. Moreover, *NPF6.3* itself, as well as the transcription factors *LBD37, 38, 39* and *NLP7,* appear to be repressed under nitrogen starvation. In contrast, two high affinity nitrate transporters *NRT2.4* and *NRT2.5* have been identified as hallmarks of nitrogen starvation and highly transcribed in starved plants.

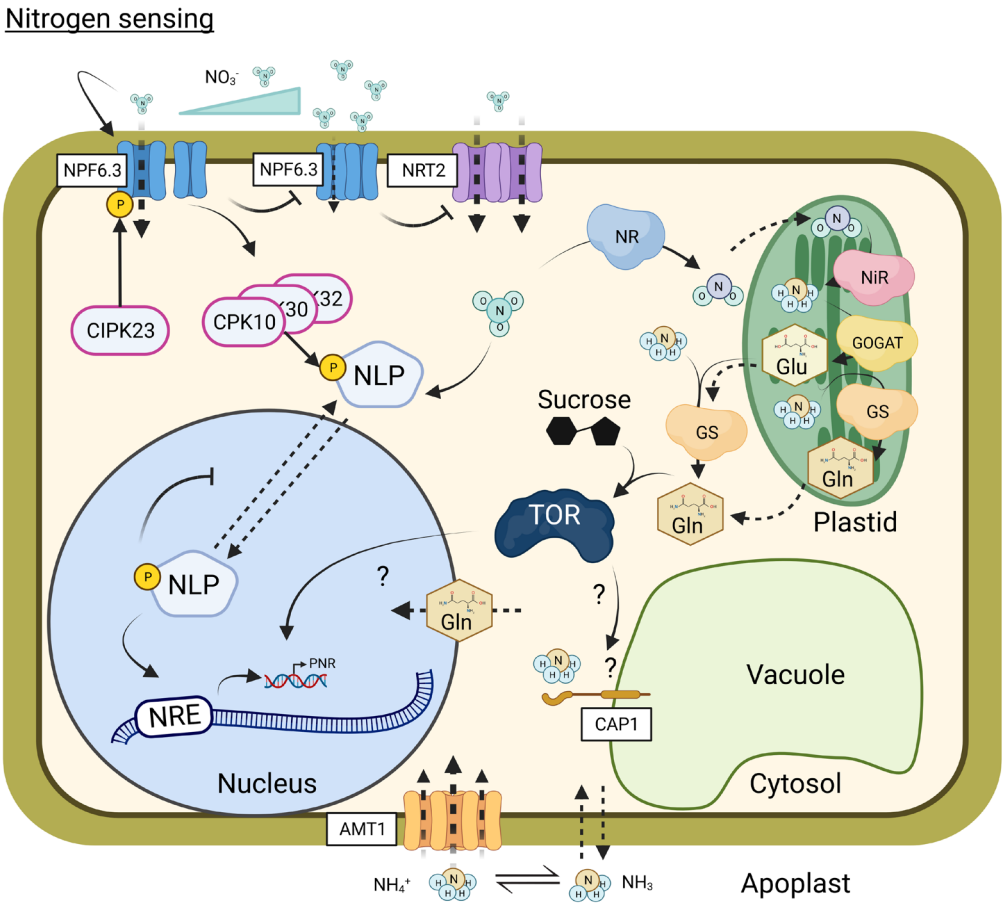

Figure 2: ***Overview of cellular nitrogen perception:*** *Nitrate is perceived at the plasma membrane by the dimer dual-affinity nitrate transceptor NRT1/PTR FAMILY, NITRATE TRANSPORTER 1 / PEPTIDE TRANSPORTER FAMILY 6.3 (NPF6.3), leading to its phosphorylation and activation by CBL-INTERACTING PROTEIN KINASE 23 (CIPK23). High levels of nitrate lead to NPF6.3 de-phosphorylation, resulting in low affinity nitrate import, as well as the dimer high affinity NITRATE TRANSPORTER2 (NRT2) family deactivation. Also, NPF6.3 signaling activates CALCIUM DEPENDENT KINASEs (CPKs) 10, 30 and 32, which phosphorylate NIN-LIKE PROTEIN 7 (NLP7). Phosphorylated NLP7 is retained in the nucleus where in binds DNA at nitrate responsive cis-elements (NRE) activating the primary nitrate response (PNR). In the cytosol nitrate can be reduced to nitrite (NO_2^-) by NITRATE REDUCTASE (NR). Nitrite gets imported into the chloroplast, where it is reduced to ammonium (NH_4^+) by the NITRITE REDUCTASE (NiR), before integrate into glutamate (Glu) by plastid localized GLUTAMINE OXOGLUTARATE AMINOTRANSFERASE, GLUTAMATE SYNTHASE (GOGAT). Another moiety of ammonium subsequently gets integrated by either plastid or cytosol localized GLUTAMINE SYNTHASE (GS). Alternatively, ammonium can be transported into the cytosol by trimer high affinity AMMONIUM TRANSPORTER 1 (AMT1) family or diffuse through the plasma membrane as uncharged ammonia NH_3. Cellular ammonium levels are potentially perceived by vacuolar [Ca2+]cyt-ASSOCIATED PROTEIN KINASE 1 or in coordination with sucrose and glutamine by TARGET OF RAPAMYCIN. Glutamine levels could directly or via TOR affect transcriptional regulation of PNR genes. Figure generated with biorender.com.*

3.2.3 Long distance nitrogen signaling

As nitrogen is assimilated from the soil, the local status needs to be communicated between the root and the shoot. Moreover, as roots can grow into different soil patches that may contain drastically different nitrogen concentrations, plants require mechanisms that allow for systemic communication of nitrogen status. This is also the case for nitrogen where amino acid availability, in particular glutamine, is a proxy for N-availability (Ijato et al., 2021; Oji & Izawa, 1971). However, the question whether amino acids are sensed as signaling molecules themselves, remains controversial (Gent & Forde, 2017; Ruffel, 2018). Plants have developed dedicated genetic networks to signal systemic nitrogen availability. For example, the shoot-to-root mobile transcription factor HY5 has been shown to integrate the shoot Carbon/Nitrogen status and to induce expression of *NRT2.1* in a photosynthate-dependent manner (X. Chen et al., 2016). Intriguingly, nitrogen starvation also leads to the expression of *C-TERMINALLY ENCODED PEPTIDEs* (*CEP*) and *CLAVATA/ESR-RELATED* (*CLE*), which have been associated to systemic signaling (Kiba et al., 2018; Kiba & Krapp, 2016; Maeda et al., 2018; Safi et al., 2021). CEP peptides are produced locally in nitrogen starved roots, they are transported to the shoot via the xylem, where they are perceived by the CEP-RECEPTORs 1 and 2 (CEPR1, CEPR2). Here they induce the production of CEP-DOWNSTREAM 1 and 2 (CEPD1, CEPD2), two glutaredoxin polypeptides. These are then, through the phloem, transported back to the root, where they induce *NRT2.1* but not *AMT1.1* expression (Ohkubo et al., 2017; Ruffel & Gojon, 2017; Tabata et al., 2014). A recent study highlighted the intersection between cytokinin (CK) and CEPD signaling and suggested CEPD glutaredoxin function to balance root growth and nitrogen acquisition with available photosynthates (Taleski et al., 2023). To a lesser extend the involvement of CLE2, 3, 5 and 7 and their recognition through the receptor kinase CLAVATA1 (CLV1) has been studied. The mobility of root derived CLE peptides, however, is suggested to be restricted to the root layers to locally repress lateral root emergence (Araya et al., 2014; Kiba & Krapp, 2016; Ruffel, 2018). Lastly, shoot-root-mobile microRNAs (miRs) could directly regulate protein translation. In *Arabidopsis miR169* has been suggested for this role. This microRNA is strongly downregulated upon nitrogen starvation and concomitantly its overexpression led to increased sensitivity to nitrogen limitation as well as altered expression of *NPF6.3* and *NRT2.1* (M. Zhao et al., 2011)

3.3 Nitrogen uptake into the plant root

3.3.1 Molecular nitrogen transport systems

With nitrogen present in soil in many different varieties and concentrations, the plant needs to be able to deploy different strategies to ensure sufficient N-uptake under fluctuating conditions. Plasticity of root development and, in particular, root anatomical features such as root hairs can help (Gruber et al., 2013). However, more sophisticated methods also exist. The plant has evolved low and high affinity uptake systems (LATS and HATS), including a whole arsenal of transporter proteins capable of facilitating nitrogen transport across the plasma membrane. Previous research revealed, that systemic nitrogen status signaling is responsible for local adaptations of root morphology. In part this occurs through local transcriptional regulation through signaling molecules such as hormones, peptides or transcription factors. Evidentially, this also requires tissue specific regulation of nitrogen transport. By now, the main players in plant nitrogen transport have been identified and partly associated to specific plant tissues

(reviewed by X. Fan et al., 2017; Hu et al., 2021; Kant, 2018; Muratore et al., 2021; Nacry et al., 2013; Noguero & Lacombe, 2016; O'brien et al., 2016; Tegeder & Masclaux-Daubresse, 2018) (Table 1).

For nitrate, this includes the NRT1/PTR FAMILY (NPF), which contains 53-members in *Arabidopsis thaliana*. This family is named after the first described NITRATE TRANSPORTER 1.1 (NRT1.1/NPF6.3) (Tsay et al., 1993), 16 genes within the family have been directly associated to nitrate transport (Vidal et al., 2020, Supplemental Table 1). However, due to the high variability in their pore region, NPF genes can transport a wide variety of substrates and e.g., NPF6.3 is also characterized as auxin transporter (Corratgé-Faillie & Lacombe, 2017). This wide diversity of substrate specificity and sequence variety within the NPF family has made it difficult to identify NPF-homologues in other plants that fulfill a similarly central role as *NPF6.3* in *Arabidopsis* (Figure 3). Besides NPF6.3 none of the NRT1 members has been shown to act as high affinity nitrate transporter and thus nitrate transporting members of the *NPF* family, i.e, *NRT1.1 – NRT1.16*, have been labelled as nitrate low affinity transport system (LATS). Plants also possess a high affinity transport system (HATS). Genes of the *NRT2* family have been identified to encode high affinity nitrate transporters (Orsel et al., 2002). In *Arabidopsis thaliana*, this family consist of seven members which are suggested to act as high affinity H^+/NO_3^-symporters (Lezhneva et al., 2014; Lupini et al., 2016). NRT2 transporters interact with NRT3.1 (*AtNAR2.1, AT5G50200*) and NRT3.2 proteins. Despite, not possessing any known transport activity loss of *NRT3* genes led to a reduction of nitrate import down by 96% (Kotur et al., 2012; Okamoto et al., 2006). Of the seven members of the NRT2 family, NRT2.1 – NRT2.6 are associated to the plasma membrane, whilst NRT2.7 is suggested to be tonoplast localized, loading nitrate into the vacuoles of developing seeds (Chopin et al., 2007). NRT2.1 and NRT2.2 contribute up to 80% to the inducible HATS (W. Li et al., 2007), but have been shown to be transcriptionally downregulated by constitutive nitrogen supply in an *NPF6.3*-dependent manner (Krouk et al., 2006). NRT2.4 and NRT2.5 have been associated to nitrogen starvation and the constitutive HATS in both roots and shoots (Kiba et al., 2012; Lezhneva et al., 2014). Also, for ammonium, high affinity ammonium transporters of the *AMT1* family have been identified. In *Arabidopsis thaliana* four of the five members, *AMT1.1, 1.2, 1.3* and *1.5* have been shown to be expressed in the roots. Moreover, AMT1.1 and AMT1.3 act in homo- or heterotrimers and have been shown to be inhibited by their phosphorylation in high ammonium availability. (Lanquar & Frommer, 2010; Qin et al., 2020; Wu et al., 2019; Yuan et al., 2007). Also, the only member of the *Arabidopsis AMT2* family*AMT2.1* has been associated to ammonium transport, albeit with lower affinity (Giehl et al., 2017). Due to the similarity of the ammonium and potassium ion in charge and size, potassium transporters are also likely to contribute to cellular NH_4^+ influx (Cuin et al., 2010). Lastly, as ammonia and ammonium are in a pH dependent equilibrium, at high concentrations and high pH, it cannot be ruled out that uncharged ammonia can diffuse unaided across the plasma membrane (Hoopen et al., 2010).

Urea and amino acids represent organic forms of nitrogen available in soil and are also used by plants as nitrogen source (Czaban et al., 2016). Although urea fertilizers contribute to more than 50% of the world's fertilizer, it is rapidly converted to mineral nitrogen forms by soil microorganisms (Finch et al., 2014). Amino acids are also demonstrated to be transported by members of the USUALLY MULTIPLE ACIDS MOVE IN AND OUT TRANSPORTER (UMAMIT) family. However, until now only six of the 44 members in *Arabidopsis* have been

described and contributed rather to systemic nitrogen transport between different plant organs, rather than uptake from the soil (C. Zhao et al., 2021). Yet, three gene families have been associated to root amino acid uptake: *AMINO ACID PERMEASES (AAP) LYSINE/HISTIDINE-LIKE TRANSPORTERs (LHT)* and *PROLINE AND GLYCINE BETAINE TRANSPORTERS (ProTs)* (Tegeder & Masclaux-Daubresse, 2018). One of them, *LHT6,* has been suggested to import acidic amino acids, as well as, glutamine and alanine from the rhizosphere (Perchlik et al., 2014).

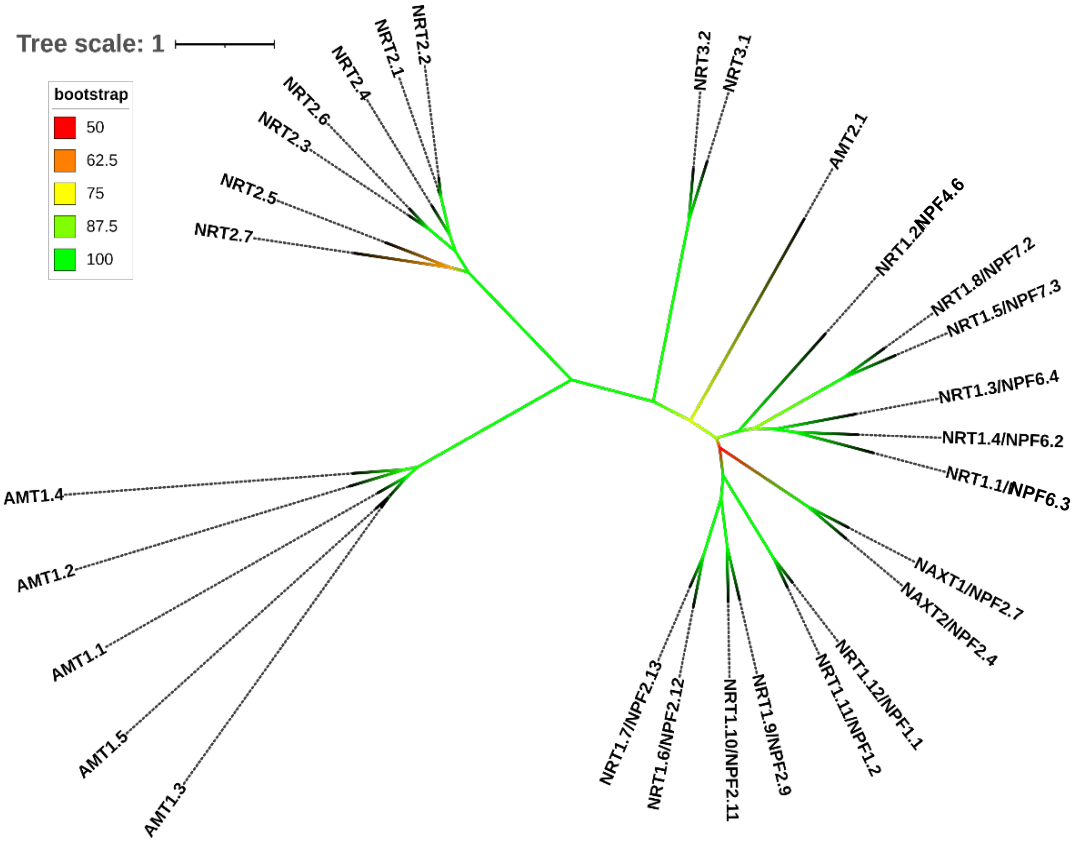

Figure 3: ***Genetic phylogeny of described and putative nitrogen related transporters****. The genetic tree layout was done with iTOL, multiple sequence alignment done by Oliver Johanndrees with RAxML on whole genomic sequences from TAIR*

3.3.2 Spatial organization of nitrogen uptake

Some of the above-mentioned transporters have been shown to be expressed in different tissues of the root. For example, the high ammonium transporter *AMT1.2* was shown to be expressed in the endodermis in younger roots and in the cortex in the mature root (Yuan et al., 2007). Also, *NRT2.1* was shown to be specific to the outer cell layers of the root, the epidermis, cortex and endodermis (Wirth et al., 2007). However, this information is inferred from microscopical imaging of transcriptional or translational fluorescent reporters, which are often imaged under sufficient nutrient conditions and also maybe are not directly comparable. Thus, it is difficult to comparatively assess the localization of different transporters in different root maturation zones and tissues (Table 1) and to connect this information to the extensive transcriptional information that has been gathered on nitrate – and nitrogen – signaling in the last 30 years. Nitrogen is taken up into the root and following the flow of water. The transport from root to shoot occurs mostly through the apoplastic xylem (Tyree, 2003; Van Bel, 1984, 1990). The root contains a complicated system that serves to provide filters that exclude

unwanted compounds from entering the root and prevent nutrients from flowing back into the soil. For this function, in particular the cell layer surrounding the vasculature, the endodermis, has gained attention. Moreover, the different expression of transporters along the longitudinal axis of the root suggests that different young and mature root tissues might play different roles in nitrogen uptake from the soil. In order to investigate what these roles might be, it is crucial to understand the morphological differences between young and mature root tissue.

*Table 1: **List of genes associated to plant nitrogen transport and their respective function in plants**. The list is accumulated and cross referenced by the reviews indicted in the last column as well as the review by* Vidal et al., 2020*. Although extensive literature is available on nitrogen transporters, it cannot be excluded that some already described functions of nitrogen transporters were overlooked or not mentioned here for other reasons. Only genes from* Arabidopsis thaliana *are mentioned. Protein, gene and compound descriptions can also be found in the List of abbreviations*

N-Form	Family	Gene	Alias	Organ	Tissue-specificity in roots	Tissue-specificity in shoots	Function	Reviewed by
Nitrate	NPF	*NPF1.1*	*NRT1.12*	Leaf		Source leaf	Phloem loading	(O'brien et al., 2016; Tegeder & Masclaux-Daubresse, 2018)
		NPF1.2	*NRT1.11*	Leaf		Source leaf	Phloem loading	(O'brien et al., 2016; Tegeder & Masclaux-Daubresse, 2018)
		NPF2.3		Root			Xylem loading	(Kant, 2018; O'brien et al., 2016)
		NPF2.7	*NAXT1*	Mature root	Cortex		Low affinity efflux	(Kant, 2018; Muratore et al., 2021; O'brien et al., 2016)
		NPF2.9	*NRT1.9*				Xylem to phloem transfer	(Kant, 2018; O'brien et al., 2016)
		NPF2.12	*NRT1.6*	Flower			Import Phloem unloading	(Kant, 2018)
		NPF2.13	*NRT1.7*	Leaf		Source leaf	Phloem loading	(O'brien et al., 2016; Tegeder & Masclaux-Daubresse, 2018)
		NPF4.6	*NRT1.2*	Root tip Young root Mature root	Epidermis, young Epidermis, mature Epidermis, root tip		Low affinity uptake	(Kant, 2018; Muratore et al., 2021; Nacry et al., 2013; O'brien et al., 2016)
		NPF5.5		Seed		Embryo	Phloem unloading	(O'brien et al., 2016)
		NPF6.2	*NRT1.4*	Leaf		Source leaf	Xylem unloading	(Kant, 2018; O'brien et al., 2016)
		NPF6.3	*NRT1.1*	Primary root tip Young root Emerging lateral root	Epidermis near root tips Cortex Endodermis, mature root		High affinity uptake Low affinity uptake Auxin transport Transceptor	(Hu et al., 2021; Kant, 2018; Muratore et al., 2021; Nacry et al., 2013; Noguero & Lacombe, 2016; O'brien et al., 2016)
		NPF7.2	*NRT1.8*	Root			Xylem unloading	(O'brien et al., 2016)
		NPF7.3	*NRT1.5*	Root			Xylem loading	(O'brien et al., 2016)
	NRT2	*NRT2.1*		Mature root	Epidermis Cortex Endodermis		High affinity uptake Suggested transceptor	(Hu et al., 2021; Kant, 2018; Muratore et al., 2021; Nacry et al., 2013; Noguero & Lacombe, 2016; O'brien et al., 2016)

N-Form	Family	Gene	Alias	Organ	Tissue-specificity in roots	Tissue-specificity in shoots	Function	Reviewed by
		NRT2.2		Mature root	Epidermis		High affinity uptake	(Kant, 2018; Muratore et al., 2021; Nacry et al., 2013; Noguero & Lacombe, 2016; O'brien et al., 2016)
		NRT2.3		Young roots, Mature root, Young shoot			Suggested high affinity uptake	Original publication: (Orsel et al., 2002)
		NRT2.4		Lateral Root Root tip Mature root Young root	Root tip epidermis Endodermis, young root Epidermis, mature root	Source leaf	High affinity uptake, Phloem loading	(Kant, 2018; Muratore et al., 2021; Noguero & Lacombe, 2016; Tegeder & Masclaux-Daubresse, 2018)
		NRT2.5		Root tip Mature root Young root	Root hairs Epidermis, young root Cortex Endodermis, root tip Epidermis, mature root	Source leaf	High affinity uptake, Phloem loading	(Kant, 2018; Muratore et al., 2021; Noguero & Lacombe, 2016; O'brien et al., 2016; Tegeder & Masclaux-Daubresse, 2018)
		NRT2.6		Mature and young root			Suggested high affinity uptake	Original publication: (Orsel et al., 2002)
		NRT2.7		Seed			Import into the seed cell vacuoles	(Kant, 2018; O'brien et al., 2016)
Ammonium	AMT1	*AMT1.1*		Root tip Root	Root hairs Epidermis Cortex		High affinity uptake	(Muratore et al., 2021; Nacry et al., 2013)
		AMT1.2		Root	Endodermis, young root Cortex, mature root		Retrieval from apoplast	(Muratore et al., 2021; Nacry et al., 2013)
		AMT1.3		Root tip Root	Root hairs Epidermis Cortex		High affinity uptake Suggested transceptor	(Muratore et al., 2021; Nacry et al., 2013)
		AMT1.5		Root tip Root	Root hairs Epidermis		Very high affinity uptake	(Muratore et al., 2021; Nacry et al., 2013)
	AMT2	*AMT2.1*		Root tip Root	Vasculature Cortex		High affinity transport, low affinity uptake	(Nacry et al., 2013, Giehl et al., 2017)
	AKT	*AKT1*					Unspecific ammonium and potassium import	(Muratore et al., 2021)
Amino acid	LHT	*LHT1*		Young root Mature root Root tip	Epidermis		High affinity uptake of neutral and acidic amino acids, His	(Muratore et al., 2021; Nacry et al., 2013)
		LHT6		Root	Root hairs Epidermis Cortex Endodermis		High affinity uptake of acidic amino acids, Gln, Ala	(Muratore et al., 2021)
	AAP	*AAP1*		Root Root tip Seed	Root hairs Epidermis Cortex		High affinity uptake of Glu, Ala, Gln, Pro, Ser Seed loading	(Muratore et al., 2021; Nacry et al., 2013; Tegeder & Masclaux-Daubteresse, 2018)
		AAP5		Root	Cortex		High affinity uptake of Arg, Lys	(Muratore et al., 2021)

N-Form	Family	Gene	Alias	Organ	Tissue-specificity in roots	Tissue-specificity in shoots	Function	Reviewed by
		AAP8		Seed Leaf			Seed loading Phloem unloading	(Nacry et al., 2013; Tegeder & Masclaux-Daubresse, 2018)
	UMAMIT	*UMAMIT11*					Phloem unloading	(Tegeder & Masclaux-Daubresse, 2018)
		UMAMIT14					Phloem unloading	(Tegeder & Masclaux-Daubresse, 2018)
		UMAMIT18		Leaf			Phloem unloading	(Tegeder & Masclaux-Daubresse, 2018)
		UMAMIT28		Seed			Seed loading	(Tegeder & Masclaux-Daubresse, 2018)
		UMAMIT29		Seed			Seed loading	(Tegeder & Masclaux-Daubresse, 2018)
	ProT	*ProT2*		Root	Cortex Epidermis		Uptake of Pro, Gly-betaine	(Muratore et al., 2021; Nacry et al., 2013)
Urea	SSS	*DUR3*		Root	Epidermis Cortex Vasculature, near xylem		High affinity uptake	(Muratore et al., 2021; Nacry et al., 2013)

3.4 The formation of root barriers is essential for nutrient homeostasis

3.4.1 In the young root the Casparian Strip is established as a primary apoplastic diffusion barrier

Nutrients taken up from the soil need to pass the outer root cell layers before reaching the stele for transport into above ground parts of the plant. They can either diffuse through the apoplast or be taken up into cells. Once in the cell, they can move along the symplastic pathway via cell-cell connecting funnels termed plasmodesmata or be exported to apoplast for further uptake by an adjacent cell which resembles the trans-cellular pathway (Barberon, 2017; Geldner, 2013; Ramakrishna & Barberon, 2019). In *Arabidopsis thaliana*, the outer cell layers consist of the epidermis, cortex and endodermis (Dolan et al., 1993; Webb et al., 2002). In light of these transport mechanisms the endodermis serves a protective role and restricts the apoplastic transport by Casparian strip (CS) thin lignified net between endodermal cells (Caspary, 1866; Geldner, 2013; Naseer et al., 2012) and the transcellular transport by suberin deposition around the cells (Andersen et al., 2018; Barberon et al., 2016; Krömer, 1903; Peterson & Enstone, 1996). After passing the endodermis the nutrients are taken up into the vasculature, for long distance transport towards the shoot.

3.4.2 Suberin as an adaptive secondary barrier

While the CS and its function are initiated in the young endodermal cells close to the apical root meristem after 10-15 cells (Kamiya et al., 2015), most endodermal cells develop suberin lamellae about 30-40 cells distal to the meristematic region (Andersen et al., 2015, 2018; Doblas, Geldner, et al., 2017). Suberin is deposited in the secondary cell wall and covering the entire surface of the cell. This insulates the endodermal cells by blocking access to the plasma-membrane (Peterson & Enstone, 1996). Suberin deposition does not occur

homogenously across all endodermal cells. Rather endodermal cells initiate suberization in a patchy manner (Patchy zone) before most endodermal cells are suberized (Suberized zone) (Barberon, 2017; Barberon et al., 2016; Doblas, Geldner, et al., 2017; Geldner, 2013). Intriguingly, some cells positioned adjacent to the underlying xylem poles remain unsuberized after the establishment of the suberized zone. These have been termed “passage cells” (PCs) as they are believed to provide a low-resistance radial flow path directly into the vasculature. (Kroemer, 1903; Peterson & Enstone, 1996). Although so far no function of PCs has been established, we recently gained hints that these cells might be involved in nutrient homeostasis (Andersen et al., 2018). These findings suggest a model where nutrients and/or biotic signals might be funnelled towards and through the endodermis via PCs (El-Showk & Mähönen, 2018; Robbins et al., 2014). Suberizing cells can be found in both above-ground (i.e., bark) and below-ground barrier tissues (e.g., periderm, exodermis, endodermis) (Woolfson et al., 2022). Although research in potato (*Solanum tuberosum*) (e.g., Soliday et al., 1979) and the name giving cork oak (*Quercus suber*) (e.g., Almeida et al., 2013; Silva et al., 2013) has highlighted the importance of suberin in pathogen and water stress resistance of the periderm and cork bark respectively, we only recently started to understand the importance of endodermal suberin deposition.

The suberin macromolecule consists of two distinct domains, an aliphatic domain consisting of long chain fatty acids and fatty alcohols (C18-C26), and an aromatic domain, consisting of phenylalanine-derived aromatic acids or alcohols such as ferulic and coumaric acid. These covalently polymerized through esterification of the three alcohol groups of glycerol to form mono- or di-acyl glycerols (MAG, DAG) with one aromatic component. Currently, there are two models about the organization of the suberin macromolecule. First, the ‘Two-Domain-Model’ where suberin monomers are linked to the primary cell walls at through their aromatic residues and then aliphatic and aromatic residues alternating creating the distinctive laminar pattern. Alternatively, the “Integrated Model” suggests a stronger subdivision of phenolic, hydrophilic, and aliphatic residues (Ursache et al., 2020; Woolfson et al., 2022)(Figure 4A, B). For synthesis of suberin monomers, metabolites from two separate pathways are required. First, the aromatic compounds are derived from the phenylpropanoid pathway (PPP) and second long aliphatic compounds derived from plastid primary metabolism (Dong & Lin, 2021; Jamet et al., 2021; Obata, 2019; Peng et al., 2008; Vishwanath et al., 2015; Woolfson et al., 2022). Several genes have been attributed, so suberin polymerization. This mainly includes members of the GDSL-TYPE ESTERASE/LIPASEs (GELP) 22, 38, 49, 51 and 96. A quintuple knockout of which was devoid of any endodermal suberization (Ursache et al., 2020). Suberin synthesis requires metabolites from both the phenylpropanoid pathway and from fatty acid metabolism. The availability of these resources likely influences suberin biosynthesis and vice versa regulation of suberin synthesis likely affects the production of other secondary metabolites. However, some transcriptional regulators have been directly associated to the regulation suberin biosynthesis. The transcription factor MYB41 has been shown to be a key positive regulator of suberin aliphatic compound biosynthesis (Kosma et al., 2014). On the other hand, MYB4 appears to be a negative regulator of the PPP and its tissue-specific overexpression in the endodermis was sufficient to abolish endodermal suberin deposition (Andersen et al., 2021). However, in the endodermis specifically also MYB53, 92 and 93 have been shown to modulate suberin (Shukla et al., 2021).

Endodermal suberization is dependent on the nutritional status of the plant. Iron, manganese, phosphate and zinc starvation result in a reduction of suberization. Sulphur and potassium starvation result in an increase of suberization and closure of passage cells (Andersen et al., 2018, 2021; Barberon et al., 2016). Recent observations in barley (*Hordeum vulgare*) also link endodermal suberization to nitrogen responses. Here an increase in suberization could be observed upon nitrogen depletion (Armand et al., 2019; Melino et al., 2021). However, the effect of nitrogen status on endodermal suberization of *Arabidopsis thaliana*, especially along the longitudinal axis has not been addressed. Endodermal suberization status appears to be positively regulated through ABA and negatively regulated through ethylene (Andersen et al., 2021; Barberon et al., 2016; Ursache et al., 2020).

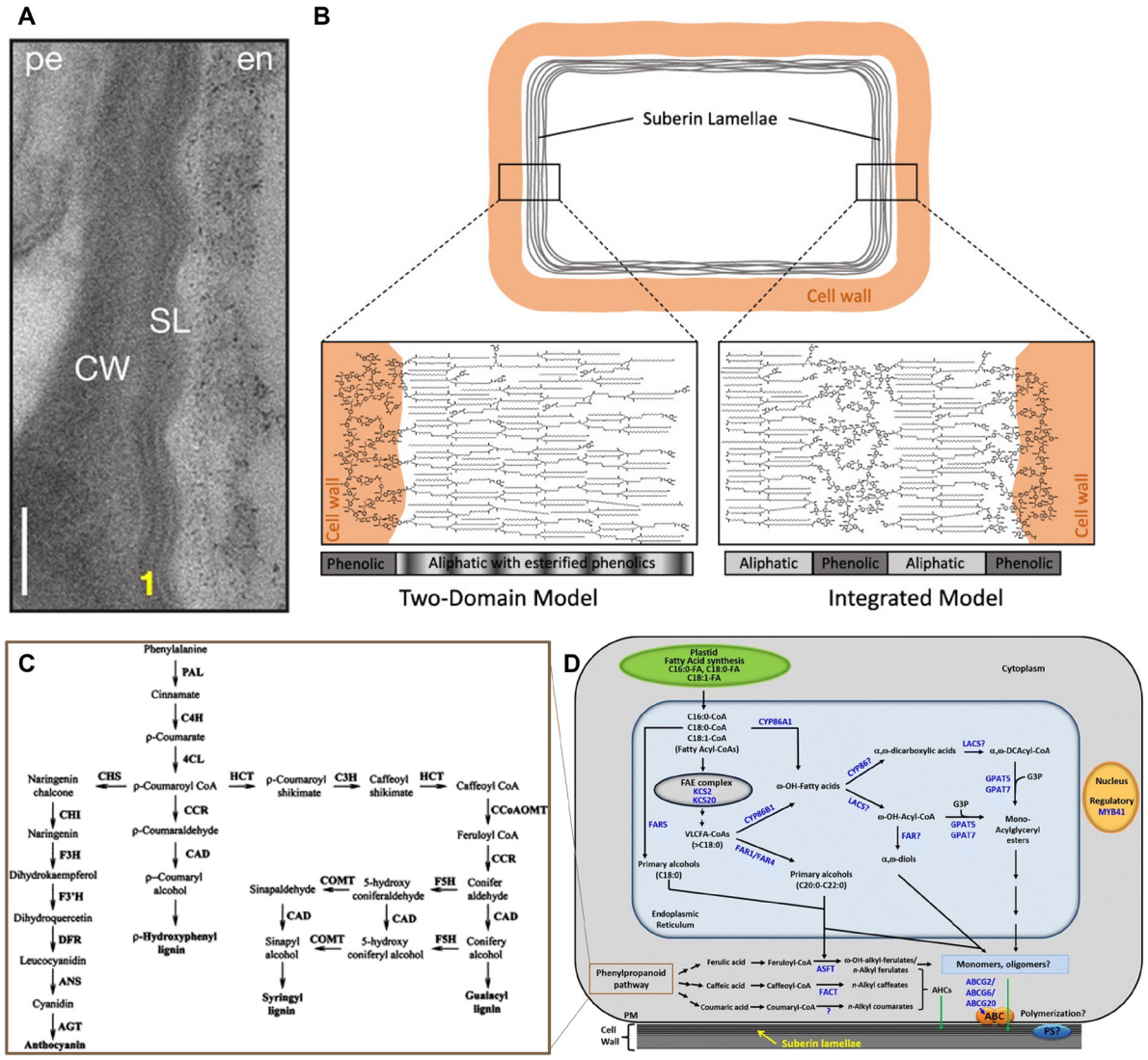

Figure 4: ***Physical and chemical structure of suberin and its synthesis.*** *A: TEM micrographs of root cross sections showing presence of suberin lamellae in wild-type. Scale bar = 20µm. pe = Pericycle, en = Endodermis, SL = Suberin Lamellae, CW = Cell Wall, 1 refers to the cross section depicted in the original figure (Ursache et al., 2020, Figure 4M). B: Proposed composition of the suberin macro molecule (Woolfson et al., 2022, Figure 1). C p-Coumaryl CoA is at the heart of the phenylpropanoid pathway required for a plethora of secondary metabolites such as anthocyanin, flavones, lignin, and suberin, Figure 1 from Peng et al 2008. (Dong & Lin, 2021; Obata, 2019; Peng et al., 2008). D Overview of main enzymes required for suberin synthesis, taken from Vishwanath et al., 2015, Figure 2. For detailed gene names see list of abbreviations*

3.4.3 Does endodermal suberization play a role in microbiome assembly determining soil nitrogen fate.

Plants assemble distinct microbial communities around their root (Wippel et al., 2021). A recent study connected the status of endodermal barriers to the assembly of plant microbiota. This appears to be actively modulated by the plant, as both plants cultivated in mono-association with bacterial strains showed differences in suberin deposition, but also mutants defective in endodermal barrier formation assemble different microbial communities when cultivated with a Synthetic Community (SynCom) of bacteria. Moreover, this modulation appeared to enhance the plant adaptation to nutritional stress. Nitrogen deficiency was not assessed in this study (Salas-González et al., 2020). A later study fortified the active role of the endodermis in plant-microbial interactions (Verbon et al., 2023). In regard to nitrogen-homeostasis, it is known that microbial communities, can improve plant growth under nitrogen limiting conditions and as mentioned above in extreme cases can provide the plant with up to 82% of their required nitrogen (Courty et al., 2015; Van Deynze et al., 2018; P. Yu et al., 2021). Plants have been shown to alter their shoot-to-root carbon allocation depending on environmental factors and further to exude a significant proportion (ca. 11%) of assimilated carbon into the rhizosphere (Bulgarelli et al., 2013, 2019; Parvin et al., 2020). Lastly, the presence of specific secondary metabolites, namely coumarins, flavonoids and glucosinolates have been shown independently to be crucial to convey beneficial effects of the microbial community (Harbort et al., 2020; Stringlis et al., 2018; Voges et al., 2019; Wolinska et al., 2021; P. Yu et al., 2021). Coumarins, flavonoids and suberin share coumaric acid, generated through the phenylpropanoid pathways, as a precursor molecule and it is likely that they are jointly regulated and integrate plant nutrient status and its microbial environment. In turn the microbial community has a strong effect in determining the fate of soil nitrogen where, depending on soil status, nitrate reduction to ammonium competes with denitrification (Putz et al., 2018). These two microbial processes have contrasting implications for the nitrogen status in the ecosystem. While denitrification leads to loss of aqueous (NO_3^-) or gaseous (NO, N_2O, N_2) nitrogen, nitrate reduction to ammonium (NH_4^+) leads to nitrogen retention in the soil. Metagenomic analysis of the capacity of soil microbiota to reduce nitrate can provide a diagnostic tool to assess the nitrogen retention capacity of microbial communities (Welsh et al., 2014). However, it remains unclear how -and if- these traits are actively modulated by host plants and integrated in their regulation of nitrogen homeostasis.

4 Aims of this work

The cumulative research introduced above has revealed key nitrogen transporters and their regulatory elements in the model plant *Arabidopsis thaliana*. In parallel, investigations into the localization of nitrogen transporters along the longitudinal axis of the root also highlighted differences in tissue specificity along the root. The establishment of diffusion barriers within the root ground tissue, namely the endodermal CS and suberin deposition, have been shown to be important for plant nutrient homeostasis (Andersen et al., 2018; Barberon et al., 2016; Kamiya et al., 2015). Moreover, two recent studies pointed towards a specific role of the endodermis in coordinating plant-microbe interactions (Salas-González et al., 2021; Verbon et al., 2023). Lastly, the importance of beneficial plant-microbe interactions in respect to plant nitrogen homeostasis – beyond the realm of nodulating plants – has gained traction (Van Deynze et al., 2018; P. Yu et al., 2021).

The work presented here aimed to connect the physiological response of endodermal suberin deposition to varying N-availability (1), as well as the tissue-specific transcriptional responses along the longitudinal axis of the primary root (2) and additionally the role of the endodermis in coordinating N-homeostasis in a natural environment (3).

To address points (1) and (2), plants were cultivated in an agar-based system, allowing for precise control of nitrogen availability. (1) Suberin deposition was directly assessed using fluorol yellow (FY) and fluorescent microscopy (described by Lux et al., 2005). (2) Compared to bulk tissue sequencing, tissue-specific sequencing approaches can reveal previously hidden plant responses. In addition, Translating Ribosome Affinity purification (TRAP) does not require the production of protoplasts. Instead, mRNA can be harvested from specific tissues of bulk samples, and also such tissue with strong cell-to-cell connections or cell wall modifications, including the endodermis (Mustroph et al., 2009; Thellmann et al., 2020). Here, TRAP was used to directly compare the transcriptional response of the young and mature ground tissue, i.e. cortex and endodermis, in nitrogen-starved and nitrogen-sufficient conditions. To address point (3), the key-transcription factor of nitrogen-signaling, NLP7, was overexpressed specifically in the mature endodermis. The impact of manipulating N-signaling in the endodermis specifically was then assessed in both axenic, plate-based experiments, as well as more natural, soil-based experiments.

In the following, we show that endodermal suberization occurs earlier in nitrogen starvation, which can be reverted by nitrate supply (1). Further, we present a tissue-specific atlas, focusing on the ground tissues, of the young and mature primary root of *Arabidopsis thaliana*. Here we observe an upregulation of high affinity nitrogen uptake and the phenylpropanoid pathway in the mature cortex (2). Lastly, we show that manipulation of nitrogen-signaling, in the mature endodermis specifically, hampers the plant's ability to benefit from microbe-elicited nitrogen fertilizer usage (3).

5 Results

5.1 Nitrogen availability influences the onset of the endodermal suberin barrier and passage-cell aperture.

5.1.1 Nitrogen starvation leads to premature onset of suberization and decrease in endodermal passage cell occurrence.

First, we investigated the endodermal suberization pattern of roots grown under nitrogen-starvation (0mM N), nitrogen-limiting (0.11mM N), and sufficient nitrogen (30mM N) conditions on pH 5.8 buffered axenic agar plates without added carbon source. Staining of the root with Fluorol Yellow revealed that nitrogen limitation led to an earlier onset of suberization (Figure 5A). Quantification of root length and endodermal suberization at five and eight days after germination (DAG) showed, that both nitrogen limiting and nitrogen starvation conditions led to a similarly earlier onset of both patchy and full suberization, resulting in a smaller zone of patchy suberization and a larger zone of full suberization (Figure 5B). However, five DAG the absolute root length was also depending on the nitrogen availability and roots grown under nitrogen limited or starved conditions grew longer. This has been previously described as nitrogen foraging (Giehl & von Wirén, 2014; Gruber et al., 2013). At eight DAG primary root length was comparable across treatments and the time point was thus chosen for later experiments. The earlier onset of suberization under nitrogen limiting and starved conditions also coincided with passage cell closure at eight DAG, but not at five DAGs (Figure 5C).

Enhanced suberization has been shown before to be a compensatory mechanism for plants with defective CSs (Baxter et al., 2009) and to be dependent on the SGN3 receptor (Doblas, Smakowska-Luzan, et al., 2017). We tested whether the earlier onset of suberization upon nitrogen starvation could be dependent on CS-integrity. The *sgn3-3* mutant plants are able to sense and respond to complete N-starvation (0mM N) as wild-type, leading to an earlier onset of the patchy and fully suberized zone of the endodermis five and eight days after germination. However, eight days after germination the *sgn3-3* mutant showed no significant increase in suberization under N-limiting conditions (Figure 5B). Moreover, the *sgn3-3* mutant displayed no decrease in passage cell occurrence at neither of the timepoints. On the contrary, *sgn3-3* displayed increased passage cells in N-limiting and N-starvation conditions at five DAG (Figure 5C). Taken together, this indicates that SGN3 might play a secondary role to the nitrogen-starvation dependent overurbanization. It remains unclear whether SGN3 plays a CS-independent role in N-responses related to nitrogen foraging under limiting conditions.

5.1.2 Provision of nitrate (NO_3^-) as only nitrogen source promotes root growth and delays the onset of suberization

Mineral nitrogen is available to the plant root in the form of nitrate (NO_3^-) and ammonium (NH_4^+). To clarify the dynamics of suberin barrier formation, we compared root growth and suberization in roots of *Arabidopsis thaliana* wild-type plants (*Col-0*) exposed to varying nitrogen availability. We used a total concentration of 30mM N, which is commonly used 2:1 NO_3^-:NH_4^+ in 1/2 Murashige & Skoog (MS) plant growth media (Murashige & Skoog, 1962). The plants were grown on 1/2 MS-N agar plates, as well as plates re-supplied with either 30mM

NO_3^-, 30mM NH_4^+ or a 20mM-NO_3^-:10mM-NH_4^+ combination of both (control). In line with published results plants only supplied with ammonium displayed ammonium toxicity, which has recently been linked to shoot acidic stress (Hachiya et al., 2021). Ammonia-only supplied plants already showed reduced root growth at five DAG and failed to recover over the course of 13 days (Figure 5D, red). All treatments were added to 1/2MS-N media. Thus, to account for the imbalance in K^+ and SO_4^{2-} availability, plants were also supplied with 2:1 NO_3^-:NH_4^+ in the form of 20 mM KNO_3 and 5mM $(NH_4)_2SO_4$ (Figure 5D, light green). Plants grown with additional potassium and sulfate showed no difference in their root length when compared to those under control conditions until 11 DAG (Figure 5D, dark green). Plants grown without nitrogen displayed reduced root growth from 11 DAG and growth cessation occurred between 11 and 13 DAG (Figure 5D, grey). Further, we found that supplying NO_3^- as the only nitrogen source plants showed increased root growth continuously (Figure 5D, blue). Therefore, we focused on the analysis of suberization in plants grown either in control conditions (2:1 NO_3^-:NH_4^+), in nitrogen starvation (0 mM N) or supplied only with nitrate (30 mM KNO_3). During the transition from primary to secondary growth, the outer cell-layers undergo programmed cell death (PCD), shed and are replaced by the periderm. In a previous study, in plants grown under continuous light on 1/2 MS supplied with 1% sucrose, PCD was initiated from 8 DAG (Wunderling et al., 2018). In our experiments, periderm formation occurred from 9 DAG onward and was delayed to 11 DAG under nitrogen starvation (Figure 5E). When supplied with nitrate as the only nitrogen source, plants showed an increased patchy zone of endodermal suberization. To account for the effect of primary root elongation we also compared the roots at different time points but of comparable root length. This highlighted that indeed plants treated with nitrate showed a delay in the onset of both patchy and full endodermal suberization. In accordance plants grown under nitrogen starvation showed an earlier onset of both patchy and full endodermal suberization (Figure 5E,F). Despite a trend of increased passage cell occurrence in nitrate treated plants, the effect of nitrate treatment on passage cell occurrence could not be decoupled from endodermal suberization (Figure 5G). Based on these results, in the context of endodermal suberization nitrate and ammonium may be perceived separately and lead to distinct responses. Supplying the plants with nitrate as the sole nitrogen source delayed suberization. Nitrogen starvation consistently leads to an earlier onset of suberization. In this context, we wondered how endodermal responses and N-homeostasis are integrated during primary root growth.

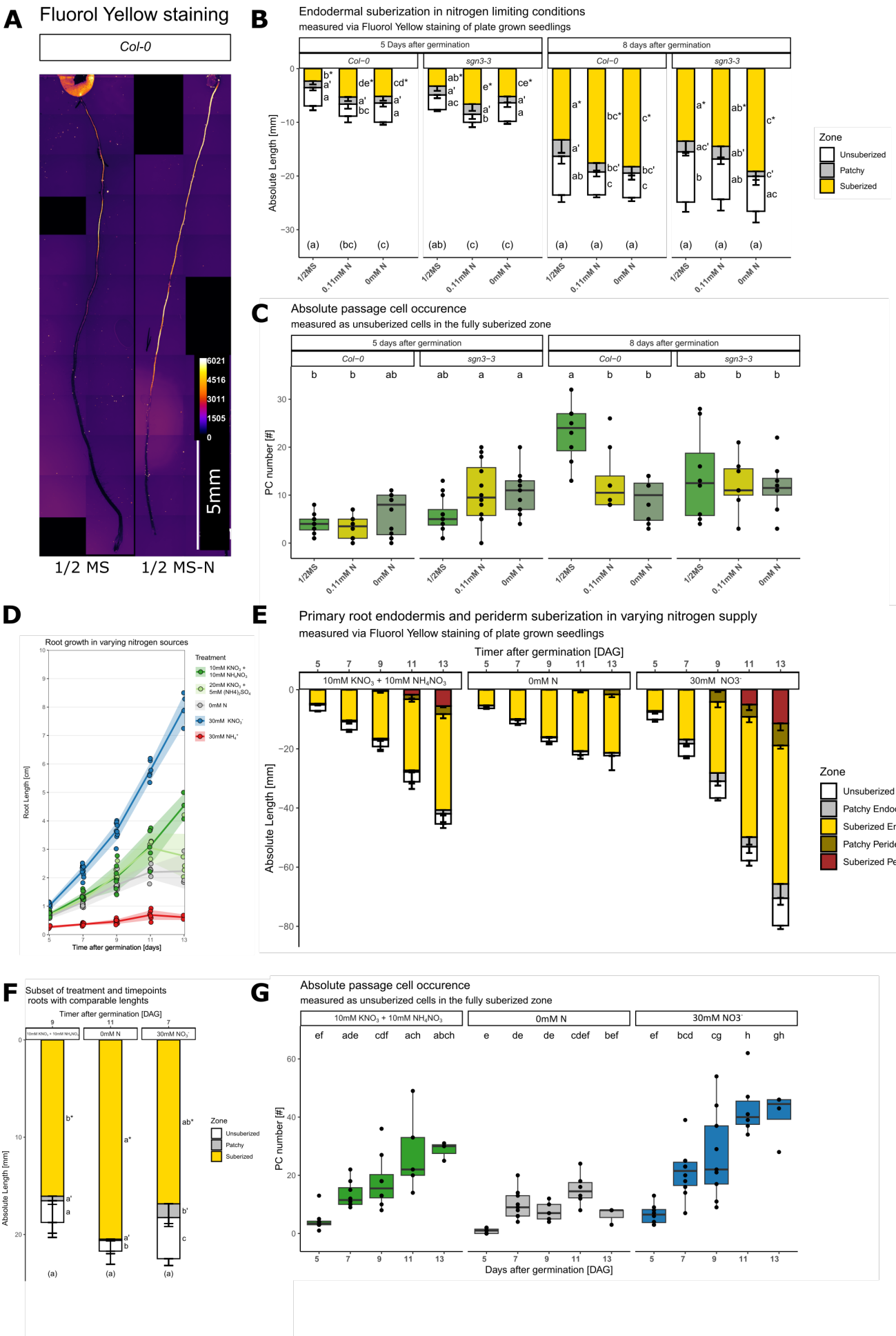
A
Fluorol Yellow staining
Col-0
6021
4516
3011
1505
0
5mm
1/2 MS
1/2 MS-N
B
Endodermal suberization in nitrogen limiting conditions
measured via Fluorol Yellow staining of plate grown seedlings
5 Days after germination
8 days after germination
Col−0
sgn3-3
Absolute Length [mm]
1/2MS
0.11mM N
0mM N
Zone
Unsuberized
Patchy
Suberized
C
Absolute passage cell occurence
measured as unsuberized cells in the fully suberized zone
PC number [#]
D
Root growth in varying nitrogen sources
Treatment
10mM KNO3 + 10mM NH4NO3
20mM KNO3 + 5mM (NH4)2SO4
0mM N
30mM KNO3-
30mM NH4+
Root Length [cm]
Time after germination [days]
E
Primary root endodermis and periderm suberization in varying nitrogen supply
measured via Fluorol Yellow staining of plate grown seedlings
Timer after germination [DAG]
10mM KNO3 + 10mM NH4NO3
0mM N
30mM NO3-
Absolute Length [mm]
Zone
Unsuberized Endodermis
Patchy Endodermis
Suberized Endodermis
Patchy Periderm
Suberized Periderm
F
Subset of treatment and timepoints
roots with comparable lenghts
Timer after germination [DAG]
Absolute Length [mm]
Zone
Unsuberized
Patchy
Suberized
G
Absolute passage cell occurence
measured as unsuberized cells in the fully suberized zone
PC number [#]
Days after germination [DAG]

Figure 5: ***Endodermal suberin deposition in varying nitrogen availability. A*** *Representative images of wild-type roots 8 DAG stained with Fluorol Yellow. Epifluorescence values obtained via using an epifluorescence stereomicroscope by exciting at 488nm (Lumencor LED) and GFP signal detection using a MF475-35 filter. False coloring for GFP signal intensity.* ***B*** *Quantification of endodermal suberization of seedlings grown for 5 DAG (n= 12) or 8 DAG (n = 8) in two separate experiments. Error bars indicate bi-directional standard deviation per zone as mean plus standard deviation. Statistics are performed as Tukey post-hoc HSD within each experiment and per zone as well as on the total root length. Statistics are indicated as: (a) = total root length, a = unsuberized zone, a' = patchy zone and a* = suberized zone.* ***C*** *Quantification of passage cells after 5 DAG (n = 12) or 8 DAG (n = 8). Passage cells are defined as unsuberized cells in the fully suberized zone. Statistics are performed as Tukey post-hoc HSD within each experiment.* ***D-G*** *Sample size:* $n_{5\ DAG}$ *= 4-8,* $n_{7\ DAG}$ *= 8-10,* $n_{9\ DAG}$ *= 7-9,* $n_{11\ DAG}$ *= 5-6 and* $n_{13\ DAG}$ *= 2-4.* ***D*** *Absolute root length of seedlings grown with different nitrogen sources. Line represents the mean value. Ribbon represents the standard deviation.* ***E*** *Subset for periderm and endodermis suberin quantification over time for "10mM* KNO_3 *+ 10mM* NH_4NO_3*", "0mM N" and "30mM* NO_3^-*" treatments.* ***F*** *Subset for endodermis suberin quantification over time for "10mM* KNO_3 *+ 10mM* NH_4NO_3*", "0mM N" and "30mM* NO_3^-*" treatments as well as for seven, nine and eleven DAG respectively. Tukey post-hoc HSD per zone as well as on the total root length indicated as described above.* ***G*** *Quantification of passage cells for "10mM* KNO_3 *+ 10mM* NH_4NO_3*", "0mM N" and "30mM* NO_3^-*" treatments. Statistics performed as Tukey post-hoc HSD.*

5.2 Translating Ribosome Affinity Profiling (TRAPseq) reveals tissue-specific nitrogen responses in the young and mature primary root.

5.2.1 Immuno-purification of ribosomal-bound mRNA from the meristematic and differentiated *Arabidopsis thaliana* root eight days after germination.

In order to resolve tissue specific transcriptional patterns of plants grown under nitrogen sufficient (1/2 MS, control) or nitrogen starved conditions (1/2 MS-N), we employed Translating Ribosome Affinity Purification based RNA sequencing (TRAPseq) (Thellmann et al., 2020). This yields profiles of ribosome bound mRNA and albeit no direct conclusion on the amounts of translated proteins can be drawn, TRAPseq data will be considered as post-transcriptome hereafter. The methodology and data processing of the TRAPseq is further elaborated in "15 Appendix I: Translating ribosome affinity purification as tool to resolve tissue-specific post-transcriptional profiles".

Next, we set out to probe the translational responses in different root zones. For this, we performed TRAP by expressing the TRAP-construct under promoters of genes, which were previously reported to be specific to the mature or young endodermis. For the mature endodermis we used the promoter of *ENDODERMIS LIPID TRANSFER PROTEIN* (pELTP, *AT2G48140*) (Barberon et al., 2016) and for the young endodermis we used the promoter of *SCARECROW* (pSCR, *AT3G54220*) (Mustroph et al., 2009; Vragović et al., 2015) respectively. For cortex-specific expression we used the promoter of *ENDOPEPTIDASE* (pPEP, *AT1G09750*) (Mustroph et al., 2009). Lastly, the tissue specific profiles were compared to profiles of mRNA extracted from a construct expressed ubiquitously under the promoter of *POLYUBIQUITIN 10* (pUBQ, *AT4G05320*) (Thellmann et al., 2020). To investigate the nitrogen starvation responses, we grew plants for eight days under nitrogen starvation (0mM N) or control conditions, which led to similar root lengths under all conditions (Figure 5B). We isolated GFP-tagged ribosomes from dissected young roots (ca. <0.5cm from the tip) and mature roots separately. The usage of a fluorescent protein as ribosomal tag allowed us to confirm the presence and localization of the polysomal complexes extracted for TRAP. Indeed, fluorescent signal was primarily observed in the nucleoli as well as the cytosol of the respective tissues (Supplemental figure 1).

5.2.2 Dimensionality reduction reveals gene clusters specific to the dissected root zone, tissue and treatment respectively

First, we assessed the quality of the generated TRAPseq data. After filtering the data for low counts across all conditions and trimmed mean of M values (TMM) normalization (Robinson & Oshlack, 2010), we performed a dimension reduction in the form of principle component analysis (PCA) on the whole dataset. PCA allowed us to reduce the dimensionality of our data and to find common vectors, while maintaining its variance (Gower, 1966; Jollife & Cadima, 2016). Here each vector represents one sample and each gene represents one dimension. To reduce the noisiness of the data and to allow for interpretation of the principal components, the data was subsetted for the dimensions containing the most variance (ntop = 500) (Love et al., 2014). These 500 genes represented 2.4% of the total genes that passed the low-count filtering but contributed to 14.7% of the total variation across all genes (15 Appendix I: Translating ribosome affinity purification as tool to resolve tissue-specific post-transcriptional profiles). Here the main difference between the samples could be explained by the root zone, i.e. the meristem enriched and mature root parts with the first component explaining 42% of the observed variance (Figure 6A,D). The second component, explaining 25% of the variance, can be attributed to the different promoters, hence the different tissues from which the mRNA was isolated (Figure 6A,B). Next, the third component explaining 13% of the variance can be attributed to the treatment, in this case nitrogen starvation (Figure 6B,C). Lastly, the fourth component (9% variance) appears to separate the tissues at a higher level. Here cortex, under the PEP promoter, the endodermis, under the ELTP, SCR and GPAT promoters and the total root, under the UBQ10 promoter, could be clearly distinguished (Figure 6C). Together, these first five principal components explain 88% of the variation of the most variable genes. In conclusion, PCA resulted in a clear separation of samples according to the experimental design and indicates that the obtained post-transcriptomes are tissue-specific. While the biggest difference between samples was indeed observable between the young and mature root, both young and mature root respond to nitrogen starvation. PCA only allows for limited insight into the relationship of the individual samples. Hence, we performed hierarchical clustering on the complete set of filtered, normalized and scaled counts (Ma et al., 2021) (15 Appendix I: Translating ribosome affinity purification as tool to resolve tissue-specific post-transcriptional profiles). Next, we reduced the dimensionality of our dataset by calculating the average library-size normalized count per gene and condition across all replicates, reducing the number of vectors from 53 to 14. The z-score of the mean counts was used for visualization (Figure 6E,F). We then repeated the hierarchical clustering on the averaged normalized counts as before and as expected the conditions now clustered into four levels only, but mimicking the previously described hierarchy of tissue dissection, an undescribed subdivision of the tissues, the promoter used and lastly the treatment (Figure 6F). Notably, the “pGPAT” samples grown under nitrogen starvation clustered as an outgroup closest to the joint cluster of the remaining mature endodermal samples (“ELTP” and “GPAT” promoter). In order to identify genes with similar behavior across conditions we performed k-means clustering (k = 36) (MacQueen, 1967). For easier visualization and to get an impression of the relationship between the individual clusters, the average z-score of all genes per cluster and condition was determined and used for hierarchical clustering according to the pairwise pearson correlation coefficients (Ma et al., 2021) (Figure 6G). This revealed gene clusters specific to the root zone,

tissues or treatment. In conclusion, PCA of the most variable genes could clearly divide the post-transcriptome according to the experimental design. Moreover, dimensionality reduction was sufficient to isolate individual gene clusters sized between 268 (k = 24) and 1445 (k = 4) individual genes, while preserving the variability of the dataset across conditions.

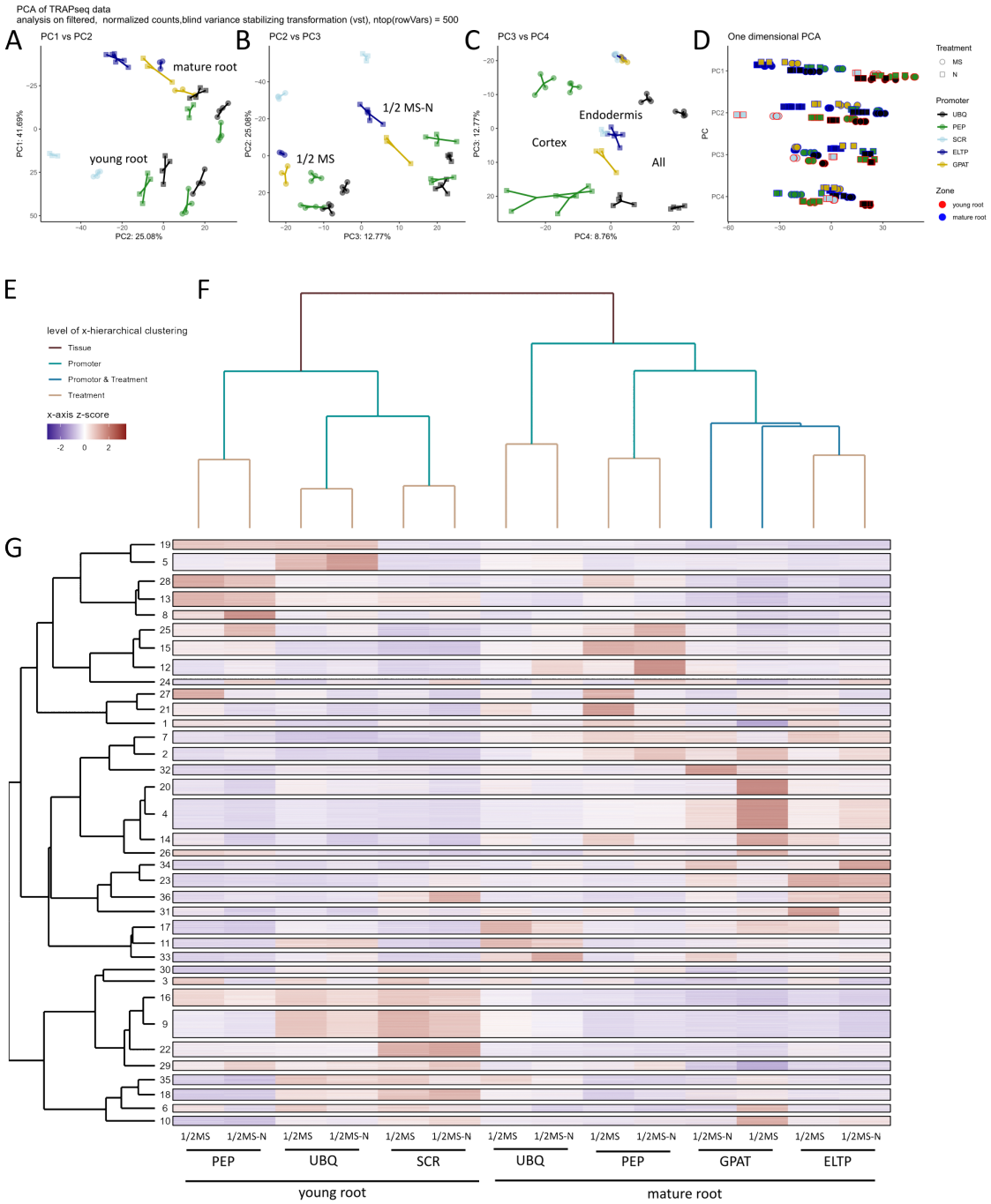

Figure 6: ***Dimensionality reduction of TRAPseq data. A-D*** *Principal component analysis was performed on the top 500 most variable genes after low count filtering and TMM normalization. Variance stabilizing transformation was performed before PCA. Segments indicate the calculated centroid of data points after PC calculation.* ***A*** *PCA plotting PC1 vs PC2. Dissection zones are manually annotated "young root" and "mature root".* ***B*** *PCA plotting PC2 vs PC3. Treatments are manually annotated manually as "1/2MS" for control samples and "1/2MS-N" for nitrogen starved profiles* ***C*** *PCA plotting for PC3 vs PC4. Tissues are annotated manually as "Cortex" for "pPEP" samples, "Endodermis" for "pSCR", "pELTP", "pGPAT5" samples and "All" for "pUBQ" samples.* ***D*** *One dimensional PC plotting for first four PCs. Dissection zone is added as point outline.* ***E-G*** *Heatmap for all genes after low count filtering and TMM normalization (n = 21179) plotted individually as tiles on the y-axis. Color indicates mean gene z-score per condition.* ***F*** *Hierarchical clustering performed across all conditions on mean gene z-score. Colors indicate node determining parameter.* ***G*** *Hierarchical clustering of clusters across all conditions determined by k-means clustering across all genes. Numbers indicate k-cluster name.*

5.2.3 TRAPseq cluster analysis reveals tissue specific nitrogen starvation responses, highlighting the mature section of the primary root

Next, we determined the specificity of the clusters according to different parameters of interest, i.e., condition, treatment, tissue and dissection zone. To resolve whether a cluster was significantly enriched for a specific parameter of interest, we performed a one-sided student's t-test on the z-scores of all genes within a cluster. For the purposes of the t-test the z-scores of all parameters, unequal to the parameter of interest were merged (15 Appendix I: Translating ribosome affinity purification as tool to resolve tissue-specific post-transcriptional profiles). When comparing our samples according to the first principal component, the dissection, into a meristem and mature root enriched section respectively, we saw that most clusters were either specific to the meristematic or mature primary root (Figure 7A).When performing a gene ontology (GO) enrichment on the conglomerated clusters for the meristem-enriched samples, we found that cell cycle processes (k6, k18, k35), DNA replication (k6, k9, k16) as well as root morphogenesis (k5, k8, k13, k19, 28) were significantly enriched (Supplemental figure 2A). In contrast, in the GO-enrichment analysis of the mature root-enriched samples, we primarily saw secondary metabolic process (k2, k12, k15, k17, k21, k23, k33), indole glucosinolate metabolic process (k15, k21, k32), but also responses to salicylic acid and immune system processes were enriched (k2, k12, k15, k21) (Supplemental figure 2A). Taken together, GO-enrichment and cluster-specificity revealed that distinct genetic networks work in concert in different zones (Figure 7A) and tissues (Figure 7B) along the root and allows us to investigate tissue specific transcriptional regulation upon nitrogen starvation (Figure 7C) that previously remained hidden in whole root transcriptomics.

5.2.4 The cortex and endodermis of the mature root are involved in the response to chronic nitrogen starvation

We next aligned DEGs from previously published TRAPseq datasets for the young endodermis and cortex, to the identified k-clusters of the present TRAPseq dataset generated in this study (Figure 7D). Across datasets, the clusters k28, k8, k25, k15 and k12 appeared to be robust for cortex-specific expression. Cluster k22 was specific for young endodermis post-transcriptome data and the clusters k23 and k36 were prominently featured in previous young endodermis data while they were assigned to the mature endodermis in the data set generated in this study (Figure 7D). Genes related to suberin synthesis and polymerization (Ursache et al. 2020), were primarily enriched in cluster k36. Next, we performed differentially expressed gene (DEG) analysis for nitrogen starvation induced genes. Fitting to the cluster association suberin synthesis genes were mostly represented in the endodermal TRAPseq profiles ("pSCR", "pELTP", "pGPAT") (Figure 6E, Supplemental figure 3). In conclusion, upon nitrogen starvation suberin synthesis genes are enriched in the young tissues of the root, specifically the endodermis. This corroborates our previous observation of a larger suberized zone and an earlier onset of suberin biosynthesis.

Next, we set out to map tissue-specific N-responses. For this we investigated genes induced upon nitrogen starvation irrespective of root zone or dissected tissue (Figure 6D). Both t-test and DEG analysis of the tissue-unspecific post-transcriptome ("pUBQ") analysis revealed clusters k12, k34, k24, k25, k33 to be responsive to nitrogen starvation (Figure 6D,

Supplemental figure 4A). These clusters were also associated to the mature root endodermis and cortex (Figure 6A, B). Cortex-associated cluster k12 showed the highest number of upregulated genes, while tissue-unspecific cluster k24, showed the highest average enrichment. Performing GO-enrichment on the most significantly upregulated genes, by adjusted p-value, per cluster (threshold = 25%, n = 127) (Supplemental figure 4A) revealed that upon nitrogen starvation genes involved in nitrate response, nitrogen metabolism, sucrose and starvation response as well as phenylpropanoid metabolism were upregulated (Supplemental figure 4). The response to nitrate was mainly present in cluster k12, starvation and carbohydrate response in cluster k24 and phenylpropanoid synthesis in cluster k8 (Supplemental figure 4). Interestingly, cluster k5, although only the 8th strongest induced cluster upon nitrogen starvation, revealed upregulation of transmembrane transport. The transmembrane transport gene ontology enrichment was also shared with the aforementioned cortex-specific clusters k12, k24 and k25 (Supplemental figure 4D). After identifying clusters k12, k24 and k25 to be relevant for the nitrogen starvation in the mature root we investigated them in further detail. Cluster k24, only containing 268 genes, showed comparably insignificant GO-enrichment, mainly attributed to abiotic stimuli, nutrient metabolism and nitrate response (Supplemental figure 4D). Cluster k12 (n = 747) and k25 (n = 627), besides enrichment in nitrogen cycle metabolic process and inorganic ion transmembrane transport, primarily showed responses associated to biotic factors such as salicylic acid response or immune system process (Supplemental figure 4C,E). These results indicate a common regulatory network, regulating abiotic responses together with biotic responses in the mature cortex of the root under nitrogen starvation. Cluster k12 especially drew our attention as it contains genes associated to high affinity ammonium uptake (i.e. *AMT1.5*), high affinity nitrate uptake (i.e.: *NRT2.1*) but also their regulation (i.e. *NLP7 and NRT3.1*). Furthermore, we also found the coumarin biosynthetic gene *S8H* in this cluster (Figure 7E). Coumarins, together with flavonoids, aromatic lignin-like compounds and suberin, are part of the phenylpropanoid pathway and share p-Coumarate, originating from phenylalanine, as an intermediate substrate (Shimizu, 2014) (Figure 4). We thus decided to investigate the families of genes found in this cluster in greater detail.

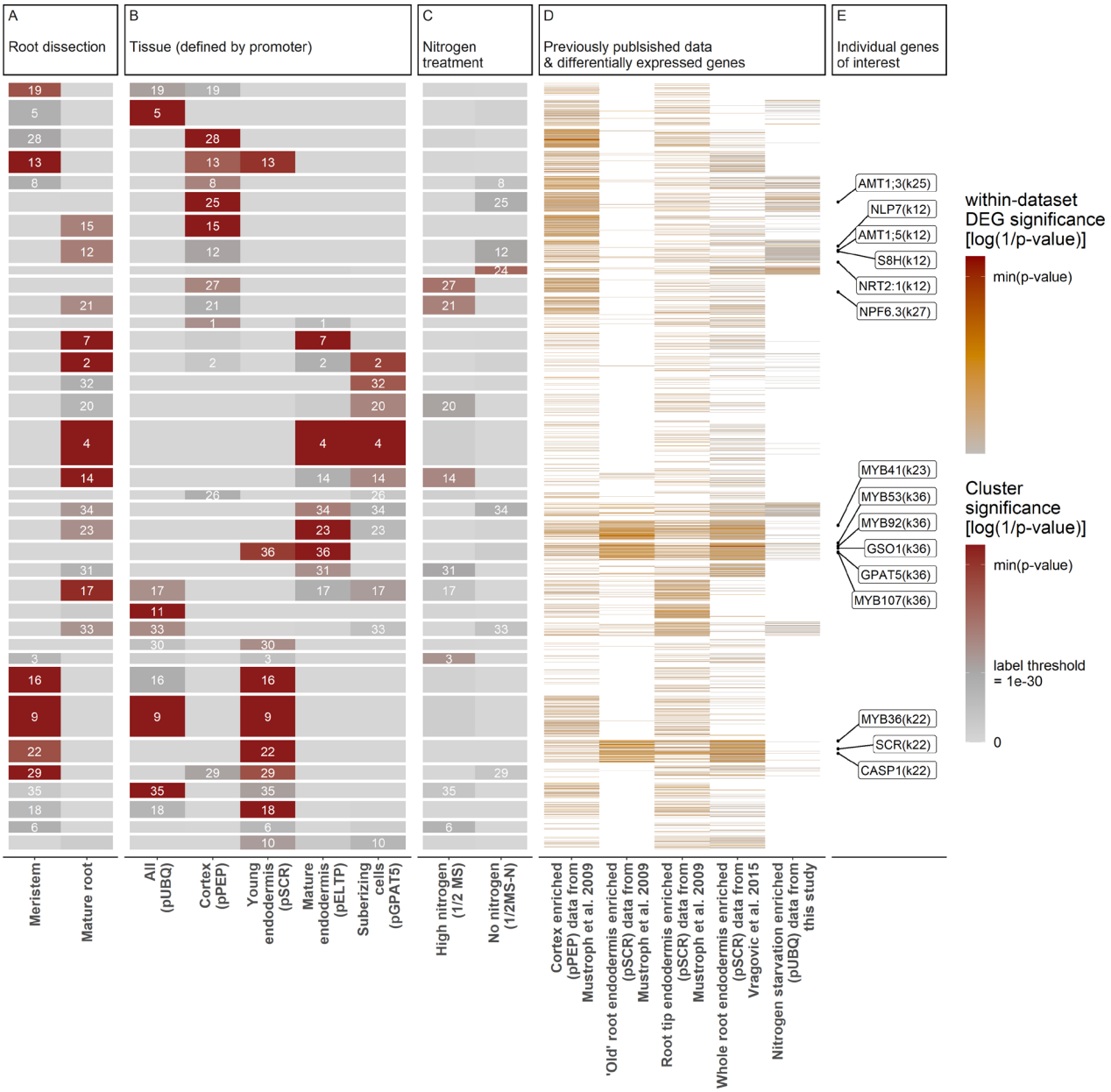

Figure 7: ***Cluster preference of TRAPseq data****. Cluster name, distribution and y-position corresponds to individual gene position as in Figure 6* ***A,B,C*** *Cluster significance was determined by one-sided t-test by subsetting the filtered, normalized, scaled counts of the indicated cluster and parameter of interest compared against all non-subsetted counts, i.e. counts which were not from the parameter of interest. Fill color (grey to red) indicates the level of significance. Clusters below the significance threshold ($p = 10^{-30}$) were labelled with the respective k-cluster number.* ***A*** *Comparison of all merged profiles from mature roots vs al merged profiles of young roots of 1/2 MS and 1/2 MS-N treatment.* ***B*** *Comparison of young and mature merged profiles for each tissue of 1/2 MS and 1/2 MS-N treatment* ***C*** *Comparison of treatments of young and mature profiles and all promoters.* ***D*** *Comparison of DEGs from previously published data sets or within this data set. Data from Mustroph et al. 2009 was provided as tissue and padj. Data from Vragović and Leal et al., was provided as raw counts and were analyzed with the same pipeline as TRAPseq data of this study. From this study DEG analysis was performed on merged young and mature roots of the pUBQ post-transcriptome only. Fill color (yellow to red) indicates significance as calculated individually within each dataset. DEGs were defined as padj<0.05 and log2(fold change)>1 if applicable.* ***E*** *Individual annotation of genes of interest. Numbers in brackets indicate the respective k-cluster. Dot and line indicate the respective position in the heatmap*

5.2.5 The synthesis of coumarins and suberin is both upregulated upon nitrogen starvation, albeit in different tissues

Through cluster specific GO-enrichment we found that phenylpropanoid biosynthesis was strongly enriched in cluster k8, which in turn was upregulated upon nitrogen starvation. When analyzing genes associated to the phenylpropanoid pathway (PPP), we found that those associated to clusters k8 and k12 showed the highest expression as well as induction by nitrogen starvation across tissues (Supplemental figure 4A, Supplemental figure 5). Phenylpropanoid synthesis genes associated to the other clusters were expressed to a lesser extent and didn't follow a clear pattern. When analyzing genes specific to the different branches of the PPP we found that genes involved in synthesis of hydroxycinnamates, which can serve as suberin monomers, to be strongly induced in the endodermis upon N-starvation. Genes involved in coumarin biosynthesis, were strongly upregulated in the cortex (Figure 8). Namely *FERULOYL-COA 6-HYDROXYLASE1* (*F6'H1*) and *SCOPOLETIN 8-HYDROXYLASE* (*S8H*) were strongly induced. F6'H1 catalyzes the production of scopoletin from ferulate, while S8H catalyzes the production of fraxetin from scopoletin (Figure 8D). Interestingly, CYP82C4, which catalyzes the production of sideretin was primarily expressed in the endodermis and strongly downregulated upon nitrogen starvation (Figure 8A,B,C). Preliminary results indicate that the upregulation of *F6'H1* and *S8H,* but not *CYP82C4* resulted in increased levels of scopoletin and fraxetin but not sideretin in the roots (Figure 8E). Moreover, the production and secretion of fraxetin by the root has been previously demonstrated to be crucial for iron mobilization and iron-starvation dependent beneficial plant-microbe interactions (Harbort et al., 2020). For the utilization of fraxetin both the iron transporter gene *IRON-REGULATED TRANSPORTER1* (*IRT1*) and the Fe^{3+}-Fe^{2+} iron reductase *FERRIC REDUCTION OXIDASE 2* (*FRO2*) are required. However, neither *IRT1* nor *FRO2* were upregulated upon nitrogen starvation. On the contrary both genes were downregulated upon nitrogen starvation (Supplemental figure 6B). Together this highlights the tissue specific and distinct regulation of phenylpropanoids, namely coumarins, in the mature root upon nitrogen starvation.

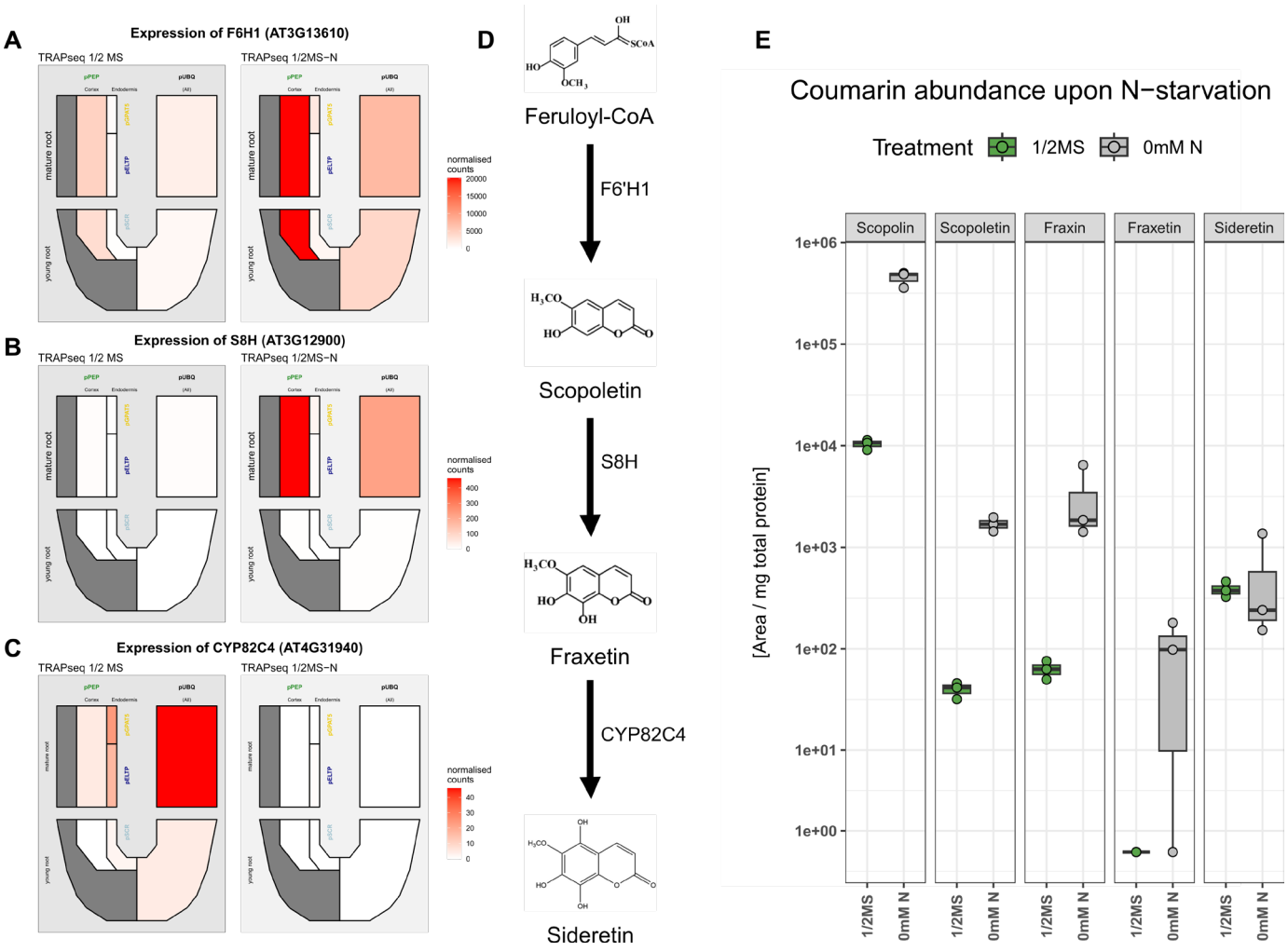

Figure 8: ***Tissue specific expression of Coumarin biosynthesis under nitrogen starvation. A,B,C*** *Minecraft-plots for the indicated gene after bioinformatic processing. One plot represents a young (bottom) and mature (top) primary root. Left part of the root depicts the tissue specific profiles for the cortex (pPEP) and endodermis (pGPAT, pELTP, pSCR, top to bottom). Right part of the root depicts the expression of UBQ whole root TRAPseq profiles. Left plot (gray background) indicates 1/2 MS condition and right plot indicates 1/2 MS-N condition. The colors indicate the respective mean normalized counts per conditions.* ***D*** *Biosynthetic pathway for coumarins branching off from the PPP.* ***E*** *GC-MS analysis of coumarins and their glycosylated forms, extracted from whole roots grown under TRAPseq conditions.*

5.2.6 *NLP* genes are upregulated upon nitrogen starvation accompanied by a strong increase in transcript levels of *NRT2* and *AMT* genes.

We found that all four of the root-expressed high affinity ammonium transporters (*AMT1*), as well as the low affinity ammonium transporter *AMT2* were upregulated upon nitrogen starvation. *AMT1.2* and *AMT1.5* could be found in the previously discussed clusters k24 and k12 respectively (Figure 9A,D). *AMT1.2* expression followed the previously described expression pattern and shows the strongest expression in the mature cortex, followed by the young endodermis (Yuan et al., 2007) (Supplemental figure 7A). All *AMT* transcripts were associated with the clusters k12, k24 and k25, whilst *AMT1.5* was the only one of cluster k12 (Supplemental figure 7A).

Similarly, we investigated the differential expression of the high affinity nitrate transporter family NRT2 (Figure 9B,E). We detected five out of the seven described homologues in our dataset, *NRT2.3* and *NRT2.6* were not detected. All NRT2s, besides the vacuolar nitrate

transporter *NRT2.7* were induced upon nitrogen starvation. Especially in the young endodermis, *NRT2.7* was significantly downregulated upon nitrogen starvation. Moreover, the nitrogen-starvation hallmark-genes *NRT2.4* and *NRT2.5* were strongly induced in our conditions. Notably, *NRT2.4* was mostly enriched in the young tissue-unspecific samples ("UBQ10") (Figure 9E). Strikingly and mostly pronounced in the mature root cortex, *NRT2.1* showed the highest expression in chronic nitrogen starvation (Figure 9B). The different *NRT2* genes were distributed across clusters k5, k12, k20, k33, with *NRT2.1* being the only one in k12, suggesting a distinct regulation (Figure 9D,E). Members of the NPF family associated with low affinity nitrogen uptake (NRT1 family) were mostly downregulated, upon chronic nitrogen starvation (Figure 9C,F). Upregulated members of NRT1 showed overall weak expression in our dataset with the exception of *NPF7.2 (NRT1.8)* and *NPF2.13 (NRT1.7).* The former was strongly induced in the mature root upon nitrogen starvation and has been previously associated with the removal of nitrate from the xylem sap (J. Y. Li et al., 2010), while the latter was less strongly expressed overall but showed increased mRNA levels in the endodermis and was previously associated with phloem loading (S. C. Fan et al., 2009) (Figure 9C). Previously, *NPF6.3* transcripts have been shown to be decreased upon nitrogen starvation (Loqué et al., 2003). In agreement with strong induction of *NRT2.1,* conversely *NRT1.1* expression was repressed in the cortex-specific, as well as UBQ10 TRAPseq profiles. Additionally, *NRT1.1* transcripts were increased in the endodermis (Figure 9C, Supplemental figure 7D)**.** This is in line with a lesser increase in *NRT2.1* transcripts in the endodermis (Figure 9B)**.**

One member of the nine genes in the NLP transcription factor family, *NLP7*, has been shown to be at the crossroads of nitrate and ammonium signaling and directly regulate the respective high affinity transport systems. NLP7 was demonstrated to directly bind the promoter of the high affinity nitrate transporter *NRT2.1* and to regulate *NRT2.1* expression mediating nitrate uptake (Maeda et al., 2018; Marchive et al., 2013). In agreement with the upregulation of *NRT2* genes (Figure 9B), *NLP* genes were also upregulated under nitrogen starvation (Supplemental figure 8). Least changes were observed in *NLP6* of cluster k19 (Figure 7). *NLP3* and *NLP9* showed the strongest relative induction upon nitrogen starvation. While the former was primarily induced in the young cortex, the latter was induced primarily in mautre-root associated samples across all tissues and was part of the late-endodermis associated cluster k34 (Figure 7). *NLP2*, *NLP5 and NLP7* were part of the previously discussed nitrogen-starvation clusters k24 and k12 respectively, and the induction of *NLP7* was strongest in the cortex of the mature root (Supplemental figure 7E). In conclusion, we observed that the high affinity uptake systems for ammonium and nitrate are upregulated in the mature cortex of primary roots grown under chronic nitrogen starvation. This is accompanied by upregulation of *NLP* genes.

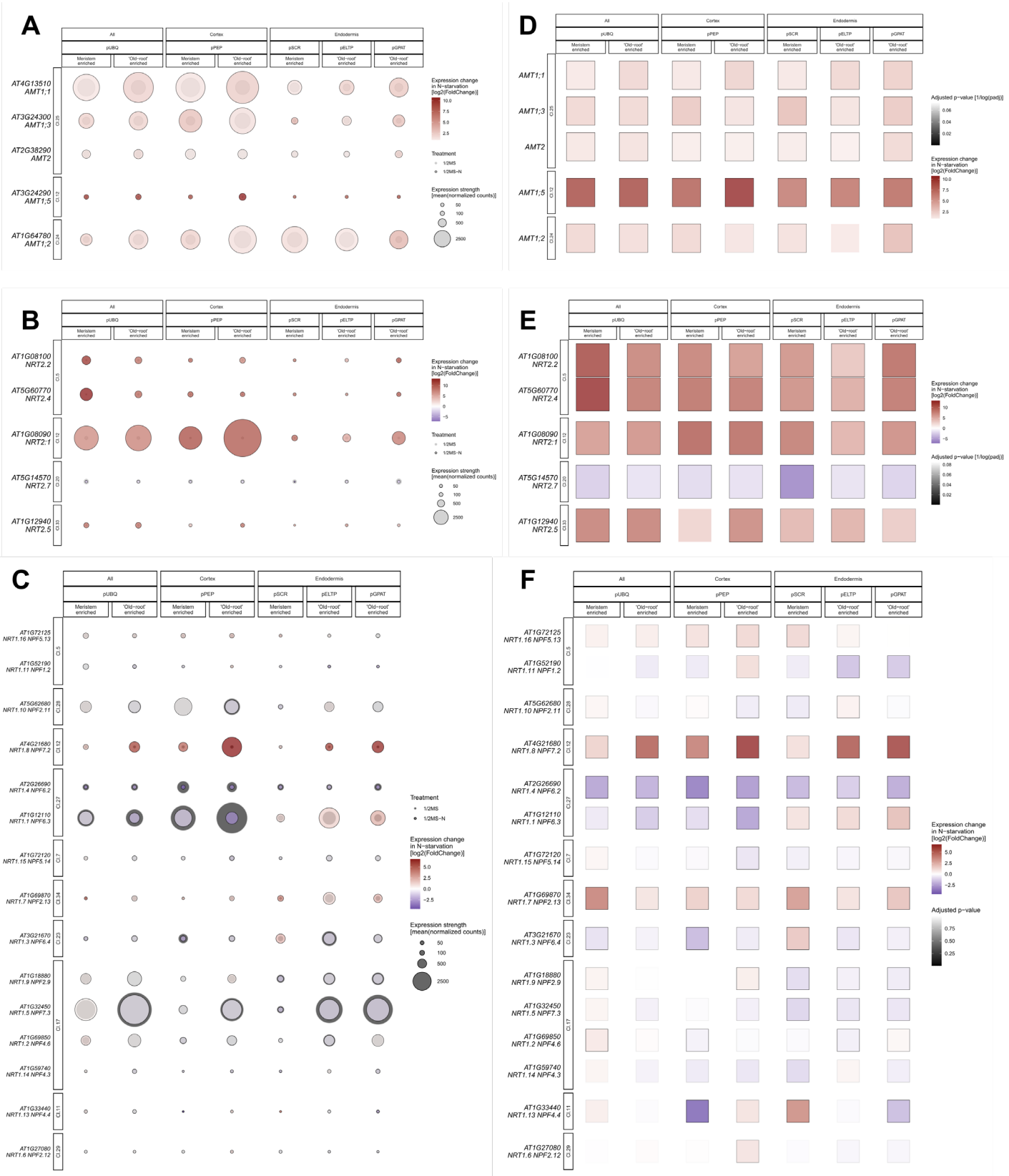

Figure 9: ***Expression of nitrogen uptake related genes: A,B,C*** *Halo-plots. Grey circles indicate the mean, normalized counts of TRAPseq profiles from 1/2 MS grown plants. Colored circles indicated the mean, normalized counts of TRAPseq profiles form 1/2 MS-N grown plants. Color indicates the log2(FoldChange). Accordingly, larger red circles indicate induction upon nitrogen starvation and smaller blue circles indicate repression upon nitrogen starvation. The x-axis is facetted for the tissue, then promoters, then young and mature root. The y-axis is facetted for the individual k-clusters. Genes are indicated by name and AGI.* ***D,E,F*** *Heatmap. Color indicates log2(FoldChange) as above and borders indicated adjusted p-values.* ***A,D*** *Genes of the AMT1 and AMT2 gene families.* ***B,E*** *Genes of the NRT2 family.* ***C,F*** *Subset of genes of the NPF family which have been classified as family of low affinity nitrate transporters NRT1. Sub plot structure e.g. as in Supplemental figure 3.*

5.2.7 Upon nitrogen starvation, *NIGT1.3* and *NPF6.3,* repressors of *NRT2* expression, are specifically induced in the endodermis while being repressed in all other tissues.

Upon nitrogen supply NLP7-dependent induction of *NRT2* is limited by the NLP7-dependent expression of the NRT2-repressing transcription factor family NIGT1 (Maeda et al., 2018; Safi et al., 2021). The NIGT1 family consists of four homologues in *Arabidopsis thaliana*. In line with elevated levels of *NRT2* transcripts, we observed that *NIGT1.1, NIGT1.2 and NIGT1.4* transcripts were strongly reduced across all tissues (Supplemental figure 9). This was not the case for *NIGT1.3*, which maintained its high expression in the cortex and furthermore was induced in the endodermis (Supplemental figure 9B, Supplemental figure 7F).

In conclusion, DEG-analysis showed that under nitrogen starvation, suberization is induced in the young endodermis. However, genes of the PPP were strongly induced in the mature part of the primary root (Figure 7D,E). Subsequently, genes related to coumarin biosynthesis were upregulated, leading to the increased production of scopoletin and fraxetin but not sideretin (Figure 8). Moreover, *NLP* genes and members of the HATS were induced in the mature cortex of the root, while most *NIGT1* genes and members of the LATS were downregulated (Figure 9, Supplemental figure 9). However, *NRT2.1* induction was weakest in the endodermis and concomitantly both *NPF6.3* and *NIGT1.3* were not downregulated but induced in the endodermis upon nitrogen starvation. Taken together, these results indicate that the endodermis plays a separate, previously overlooked role in coordinating nitrogen transporter regulation during chronic nitrogen starvation.

5.3 Overexpression of *NLP7* in the late endodermis leads to nitrate-dependent decrease in suberization

Nitrogen starvation leads to an earlier onset of the endodermal suberin barrier formation (Figure 5, Figure 7). At the transcriptional level, the endodermis and the cortex in the mature primary root are distinctly responding to the lack of nitrogen. To further probe this, we investigated how specific manipulation of nitrogen signaling in the endodermis, impacts the nitrogen signaling network locally and systematically. Here, we used the previously established late-endodermis promoter of *ELTP* to overexpress two representative nitrogen-regulatory transcription factors: NLP7 and NIGT1.1.

We first tested the suberization behavior of plants overexpressing NIGT1.1 (*pELTP::NIGT1.1*) and *NLP7* (*pELTP::NLS-NLP7*) under nitrogen limiting conditions. Two independent lines of *pELTP::NLS-NIGT1.1* plants showed a similar behavior of endodermal suberin deposition in nitrogen limiting conditions when compared to wild-type. In NLP7 overexpressing plants, low nitrogen conditions already led to a slightly delayed onset of suberin deposition compared to no nitrogen conditions. Furthermore, full supply of nitrogen even further delayed the onset of suberization. NLP7 overexpressing plants showed a strong decrease in fully suberized endodermis. Passage-cells are a key feature of the fully differentiated endodermis, as they represent remaining openings in the otherwise suberized endodermis. (Figure 5C, Andersen et al. 2018). In both plants overexpressing either NLP7 or NIGT1.1, passage cell occurrence was different from wild-type plants, but also between independent lines. In NLP7 overexpressing plants passage cell occurrence under 1/2 MS conditions was lower compared

to wild-type but increased in nitrogen limiting conditions. In *pELTP::NIGT1.1 #1-17* passage cell occurrence behaved like wild-type, while in *pELTP::NIGT1.1 #6-2* passage cell occurrence was unaffected by nitrogen availability and comparable to passage cell occurrence of wild-type plants grown under nitrogen limiting conditions (Figure 10B).

In contrast to lignin deposition, suberin deposition in the secondary cell wall is a dynamic process dependent on the plant nutrient status ((Andersen et al., 2018, 2021; Barberon et al., 2016; Ursache et al., 2020)). In *Col-0* suberin deposition was delayed when plants were supplied with nitrate only (Figure 5E,F). Similarly, in *pELTP::NLS-NLP7 #4-20* endodermal suberization is increased under nitrogen limiting conditions, while it was strongly decreased under nitrogen sufficient conditions (Figure 10A). Therefore, we investigated whether nitrogen supply after a period of starvation would result in a suberin pattern similar to plants continuously grown under sufficient nitrogen condition. To do so, plants were grown in on agar plates without nitrogen and after six days they were transferred to new plates containing 10 mM NH_4NO_3, 10 mM KNO_3, plates containing 30 mM KNO_3 or, as control, plates containing no nitrogen (Figure 10C). In wild-type plants, two days after transfer (2 DAT) from nitrogen starvation conditions to the respective treatments the primary root elongation after 8 days on nitrogen starvation was comparable to previous experiments (Figure 5B,E, Figure 10A). Wild-type plants grew to around 20 mm, whilst *NLP7* overexpressing plants were shorter only growing to ~16 mm (Figure 10D). Transferring wild-type plants to nitrogen-rich plates, independent of the nitrogen source, for 48h did not affect the onset of suberin in the patchy or fully suberized zone. In contrast, transferring plants overexpressing NLP7 to plates containing nitrogen resulted in a reduction of endodermal suberization. When transferred from 1/2 MS-N to 1/2 MS plates, containing 20mM nitrate and 10mM ammonium or to plates containing 30mM nitrate, the onset of suberin was delayed compared to plants transferred to continued nitrogen starvation. Thus, we conclude that suberization is decreased in NLP7 overexpressing plants in a nitrate dependent manner after nitrogen resupply.

Next, we compared the whole root transcriptome of wild-type plants versus *pELTP::NLS-NLP7 #4-20* after nitrate resupply. When performing PCA analysis as before, we saw that the respective wild-type lines *Col-0* and *pGPAT5::Citrine-SYP122* clustered closest together. The first principal component, explaining 57% of the variance, separated nitrogen starved samples (1/2 MS-N), regardless of genotype from samples grown under continuous nitrogen supply (1/2 MS, 8 DAG) or grown for two days on 30mM nitrate after six days of nitrogen starvation (30mM KNO_3 2 DAT). The second principal component, explaining 21% of the variance, separated the 1/2 MS 8 DAG samples from 30mM KNO_3 2 DAT samples but also *pELTP::NLS-NLP7* samples from wild-type samples. Under the assumption that NLP7 expression leads to an activation of nitrate responses, the second principal component explains the nitrate status of the plant (Figure 10E).

When performing DEG analysis we found that, TRAPseq analysis of nitrogen starved plants (Supplemental figure 3), suberin synthesis was upregulated in upon nitrogen starvation across all genotypes (Figure 10F). This included four of the five genes encoding for GDSL-like Lipase/Acylhydrolase (GELP) superfamily proteins *(GELP38, 49, 51 & 96)*, that have been previously described to be essential for endodermal suberization (Ursache et al., 2020). The same study also identified five members of the GELP family, that are involved in suberin

degradation (*GELP12, 55, 72, 73, 81*). These were either not detected (*GELP12, 55, 81*) or not differentially expressed (*GELP72, 73*) in our RNAseq dataset (Figure 10F). When comparing gene expression after nitrate treatment, we found that despite not showing indication of a reduction of endodermal suberin (Figure 10F), suberin synthesis was downregulated in all genotypes. In *pELTP::NLS-NLP7, GPAT5, GELP51* and *GELP96* showed a stronger decrease compared to wild-type plants (Figure 10F). Lastly, we observed that, as in TRAPseq analysis of nitrogen starved plants (Supplemental figure 9), members of the *NIGT1* family were downregulated upon nitrogen starvation, which was upregulated. However, in *pELTP::NLS-NLP7* plants *NIGT1.3* expression was stronger in 1/2 MS conditions and downregulated under nitrogen starvation. Conversely, and as demonstrated before (Maeda et al., 2018) all members of the *NIGT1* family were upregulated after nitrate resupply. In *pELTP::NLS-NLP7* plants *NIGT1.3* upregulation after nitrate resupply was stronger compared to wild-type plants (Supplemental figure 10). Taken together, we report that albeit nitrogen regulated suberin synthesis being similar between wild-type and *NLP7* overexpressing plants, endodermal overexpression of NLP7 is sufficient to delay endodermal suberization under nitrogen replete conditions in a dynamic manner. Furthermore, *NIGT1.3* is differentially regulated in *pELTP::NLS-NLP7* suggesting that NLP7 and NIGT1.3 act jointly in the endodermis to regulate nitrate dependent suberization responses.

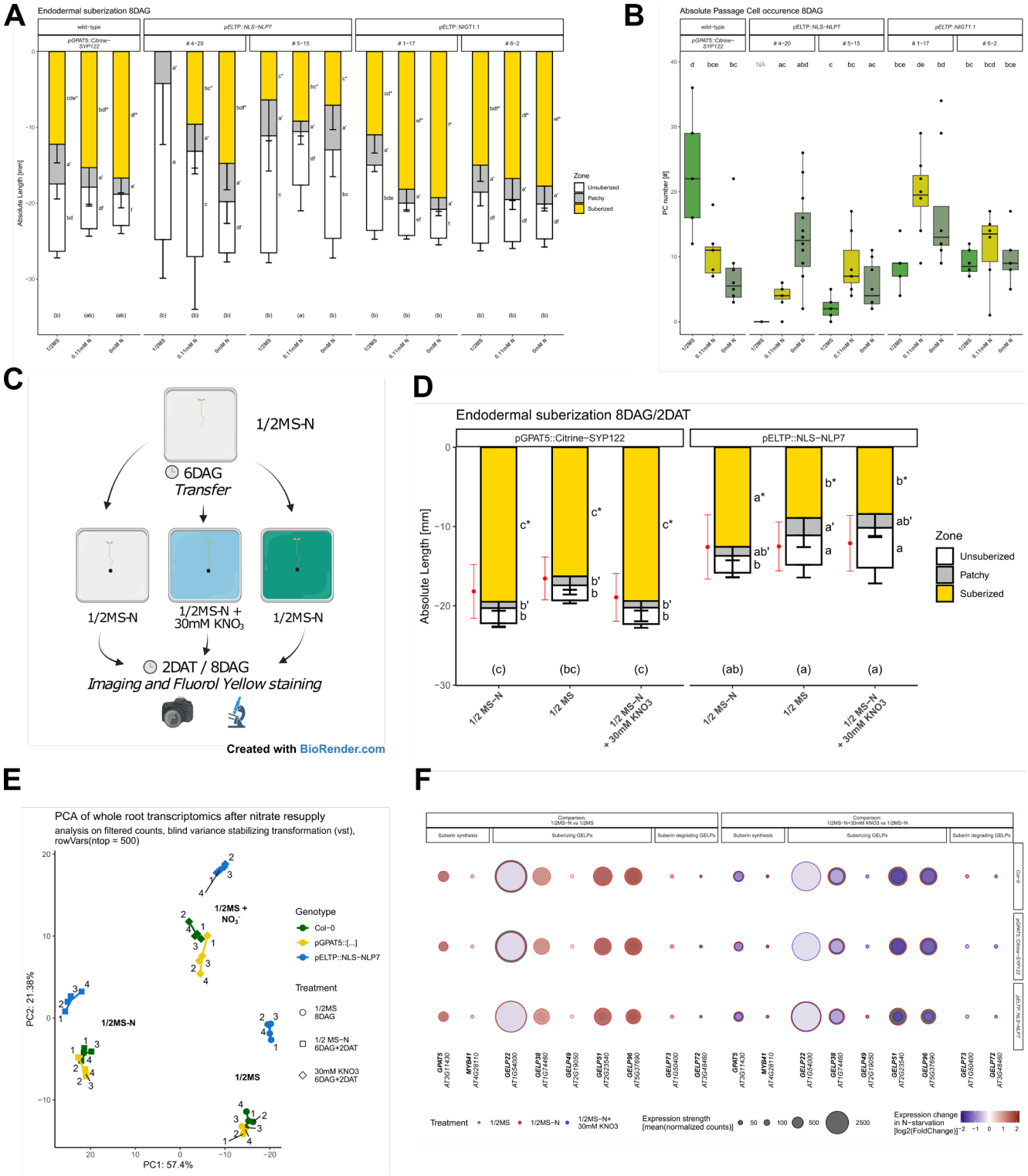

Figure 10: ***Endodermal overexpression of NLP7 leads to nitrate-dependent desuberization.*** *Error bars indicate bi-directional standard deviation per zone as mean plus standard deviation. Statistics are performed as Tukey post-hoc HSD within each experiment and per zone as well as on the total root length. Statistics are indicated as: (a) = total root length, a = unsuberized zone, a' = patchy zone and a* = suberized zone.* ***A*** *Endodermal suberin analysis of NLS-NLP7 and NIGT1.1 overexpressing plants.* ***B*** *Passage cell occurrence of NLP7 and NIGT1.1 overexpressing plants* ***C*** *Experimental setup for nitrogen transfer experiments* ***D*** *Suberin analysis two days after transfer. Red dots indicate the position of the root tip six DAG. Red error bars indicate the standard deviation. n = 8.* ***E*** *PCA analysis of RNAseq after transfer. Numbers indicate replicates.* ***F*** *Halo-plot for Suberin synthesis genes (GPAT5, MYB41) as well as suberin synthesis (GELP22,38,49,51,96) and degradation (GELP12,55,72,73,81) GELP genes* (Ursache et al., 2020)*. Genes not present in the halo plot didn't pass the filtering process due to low expression. Grey circles indicate the base mean, normalized counts of RNAseq profiles from 1/2 MS grown plants 8DAG. Colored circles indicated the mean, normalized counts of RNAseq profiles from 1/2 MS-N grown plants 6DAG + 2DAT. Fill color indicates the log2(FoldChange). Circle edge color indicates the treatment. The x-axis is facetted for the respective DEG analysis. The y-axis is facetted for genotypes. Genes are indicated by name and AGI on the x-axis.*

5.4 Nitrogen resupply into agricultural soils elicits growth promotion dependent on the microbial community and plant endodermal nitrogen signaling

5.4.1 Resupply of agricultural soil with nitrogen improves plant performance in wild-type plants but to a lesser extend in plants altered in endodermal nitrogen signaling

Despite the fact that nitrate-resupply led to a similar transcriptomic response across all genotypes (Figure 10F), it only led to decreased suberization in plants overexpressing NLP7 in the endodermis (Figure 10A). Hence, we ought to investigate the behavior of NLP7 overexpressing plants in a greenhouse environment grown on natural soil. As agricultural soils are often devoid of nitrogen (Vitousek et al., 2002), extensive fertilizer usage is common. Nevertheless, nitrogen remains a limiting resource for plants grown on these soils until immediate fertigation. Therefore, a quicker response to nitrogen supply, as observed in *pELTP::NLS-NLP7* plants, could have an effect on plant performance in agriculturally relevant conditions. Therefore, we established an experimental setup in nitrogen poor agricultural soil (Harbort et al., 2020). Here plants were supplied with either no fertilizer (rainwater), a fix amount of nitrogen-only fertilizer (Calcinite) or a fix amount of full fertilizer (Wuxal). One-week old plants were transferred to potting soil (80mg/L N, pH 5.8) versus Cologne Agricultural Soil (CAS) (10mg/kg N-NO_3, pH 7.5) which was supplied with 10L of rainwater, Calcinite ($\sum_N$=1000mg) or Wuxal ($\sum_N$ =1250mg) treatment over the course of 3 weeks (Figure 11A). Across all genotypes investigated, plants performed best when grown on potting soil, although the NLP7 overexpressing plants were noticeably smaller (Figure 11B). When grown on CAS, rosette fresh weight of wild-type plants was reduced by ~94%. Similarly, also NLP7 overexpressing plants showed even further reduced fresh weight. Furthermore, wild-type plants showed a dark-purple color, previously associated with anthocyanin accumulation in this soil (Figure 11C)(Rubin et al., 2009; Shen et al., 2023). NLP7 overexpressing plants didn't show purple coloration, but instead occasionally showed signs of early leaf senescence. Fertilization with Calcinite led to a significant increase in fresh weight only in wild-type compared to untreated soil (Figure 11B). Furthermore, the purple coloration of wild-type plants disappeared (Figure 11C). While irrigation with Wuxal led to a further increase in fresh-weight in wild-type plants, NLP7 overexpressing plants showed no increase in fresh weight compared to Calcinite treatment. Also, two out of the 16 plants investigated in this experiment showed severely stunted growth and chlorosis. This was the case for both independent *pELTP::NLS-NLP7* lines investigated (Figure 11B,C).

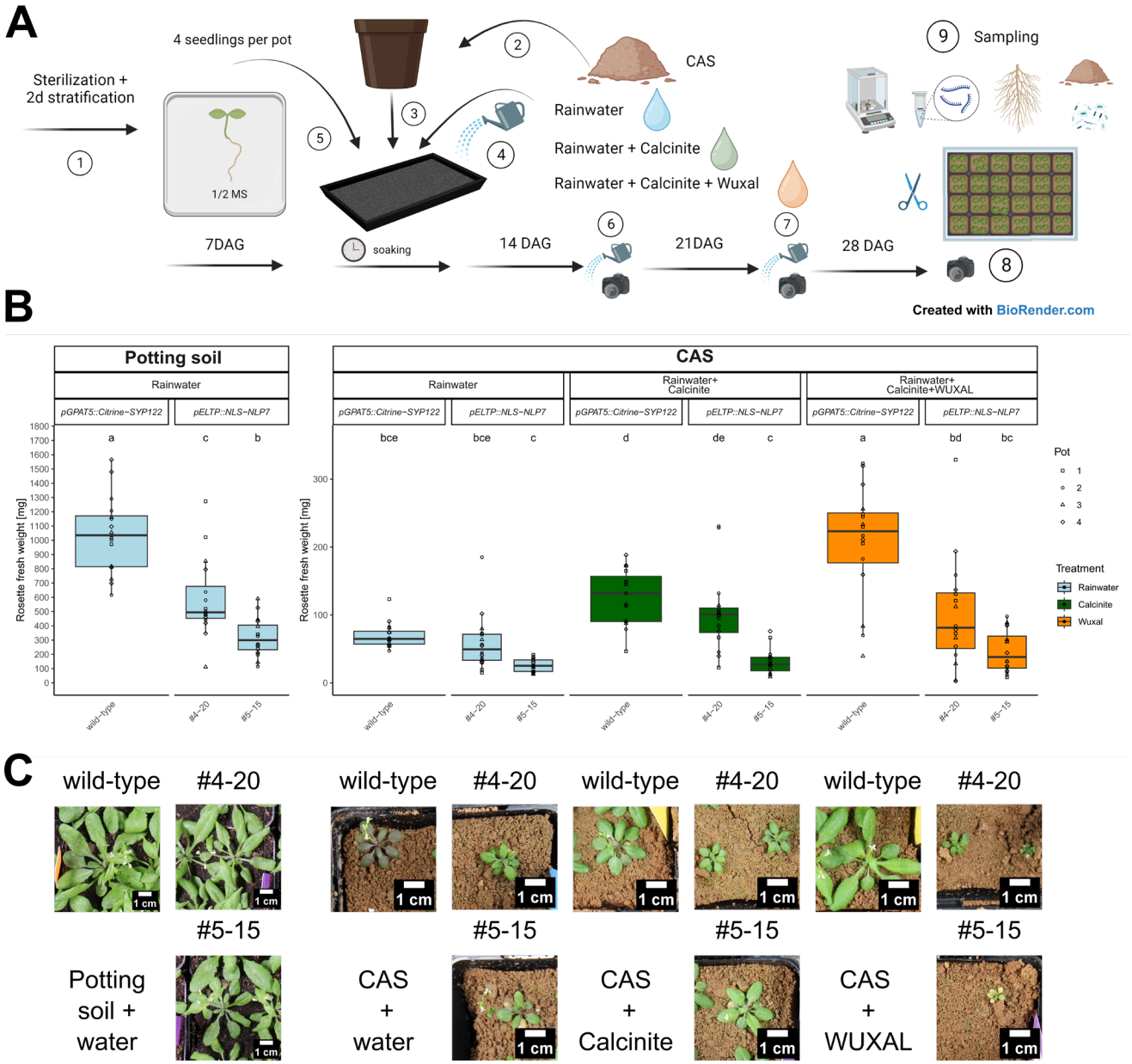

Figure 11: ***Nitrogen fertilizer resupply to agricultural soil increases growth. A*** *Exemplary experimental setup of all soil experiments. 1: Pre-germination and growth on 1/2 MS plates (with nitrogen). 2: Preparation of pots (9cm x 9cm, ca 500g soil). 3: Placing pots into trays. 4: Pre-incubate trays lined with capillary mats with respective irrigation treatment. 5: Transfer four plants from plate to pot. 6: Irrigate and image. 7: Irrigate and image. 8: Image and cut rosettes. 9: Sample required biological material.* ***B*** *Fresh weight of rosettes 4WAG Statistics are performed as tukey post-hoc HSD per soil-type.* ***C*** *Exemplary images of plants grown in the respective treatment. Same scale within each soil type.* ***B, C*** *Shared x-axis for genotype.*

5.4.2 Shoot growth promotion by nitrogen requires functional plant endodermal nitrogen signaling and is not directly connected to shoot nitrate content.

GELP51 and *GELP96* were strongly downregulated and endodermal suberization was decreased in NLP7 overexpressing plants upon nitrate resupply. The *gelp22 gelp38 gelp49 gelp51 gelp96* (*gelp*^{quintuple}) mutant is devoid of endodermal suberization (Ursache et al., 2020). Thus, we also included the *gelp*^{quintuple} mutant and its parental line *Col-0* into the following experiments. As observed before, *pELTP::NLS-NLP7* plants showed a reduction in shoot fresh weight, compared to wild-type plants, when grown on CAS and irrigated with deionized water (water). The *gelp*^{quintuple} mutant showed comparable fresh weight to *Col-0.* Supplying the soil

with Calcinite led to a significant increase in fresh weight in both wild-type genotypes. Neither *gelp*^{quintuple} *nor pELTP::NLS-NLP7* plants showed a significant increase in fresh weight upon Calcinite treatment. When cultivating the plants on sterilized soil, all genotypes grew smaller compared to natural soil. Both *gelp*^{quintuple} and *pELTP::NLS-NLP7* mutants showed reduced rosette fresh weight compared to their respective wild-types. None of the genotypes benefited from Calcinite treatment (Figure 12A).

Investigating the nitrate content of shoots via ion chromatography coupled mass spectrometry (IC-MS), revealed that wild-type plants indeed accumulated more nitrate in the shoot when treated with Calcinite compared to water treated plants. This was in agreement with their increased shoot fresh weight under these conditions. Despite the fact that the *gelp*^{quintuple} mutant showed similar shoot fresh weight, when treated with water, nitrate content was elevated in these plants. The nitrate content of *pELTP::NLS-NLP7* plants treated with water was comparable to those of their parental line. Neither *gelp*^{quintuple} nor *pELTP::NLS-NLP7* plants showed increased shoot nitrate content when treated with Calcinite. With the exception of *pELTP::NLS-NLP7,* shoot nitrate content of plants grown on sterile soil was reduced compared to plants cultivated on natural soil. Irrespective of genotype, shoot nitrogen content in plants grown on sterile soil was increased upon Calcinite treatment. In conclusion, relative shoot nitrate content didn't appear to be the determining factor for rosette fresh weight in sterile soil. In natural soil, an increased shoot nitrate content after Calcinite treatment, compared to water treatment, could be observed in plants with increased rosette fresh weight (Figure 12B).

5.4.3 A microbial community is required for growth promotion by nitrogen application

It was suggested that the microbial community aids plants in utilizing soil nitrogen effectively (Yu et al 2020). Furthermore, the partial leaf senescence and strong variation in rosette growth observed in plants overexpressing NLP7 (Figure 12B) could be an indicator for dysbiosis induced chlorosis (Chen et al. 2020). To investigate whether the former was the cause for the lack of growth promotion in sterilized soil, a soil wash was re-introduced into sterilized agricultural soil. Indeed, wild-type plants grown on soil, that was reinoculated with a putative natural community showed growth promotion when treated with Calcinite. As before, NLP7 overexpressing plants were unable to benefit from the Calcinite treatment, irrespective of whether a microbial community was present. No growth promotion was observed when the plants were inoculated with a 0.22µm sterile-filtered soil wash (mock). In conclusion, the soil microbial community appears to be required in facilitating nitrogen fertilizer growth promotion (Figure 12D).

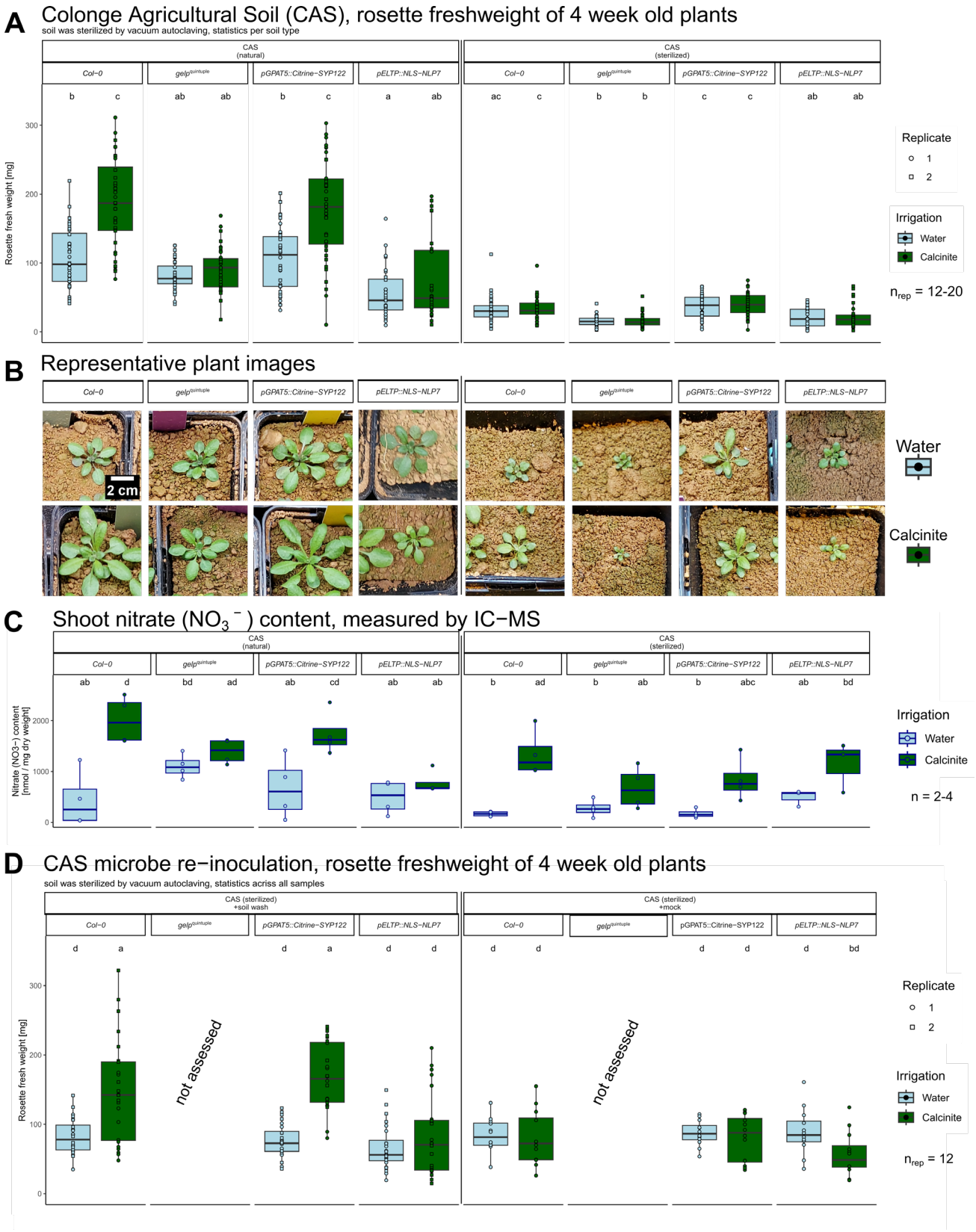

Figure 12: ***Nitrogen fertilizer use capacity is microbe dependent and disturbed in plants with modified endodermal suberin or nitrogen responses.*** *Sample size is indicated for each individual experiment. X-axis position is equal across all panels.* ***A*** *Rosette fresh weight 4WAG. Statistics per soil type as post-hoc tukey HSD.* ***B*** *Representative images of plants from the respective treatments. Images are of the same absolute size and scale is indicated in the leftmost upper picture.* ***C*** *Nitrate content measured via IC-MS. Statistics across all samples as post-hoc tukey HSD.* ***D*** *Rosette fresh weight 4WAG after re-inoculation of sterilized soil with a soil wash or sterile filtered soil wash (mock). Statistics across all samples as post-hoc tukey HSD, statistics were performed including the f6'h1 mutant used in this experiment (Table 9).*

5.4.4 Nitrogen treatment reshapes the natural bacterial community and results in shifts between the rhizosphere and the endosphere.

Nitrogen fertilizer induced growth promotion is microbe dependent, while the shoot nitrate content appears not to be. This raised the question, whether the quality of the microbial communities around the roots plays a role in communicating the soil nitrogen status to the shoots. Thus, we sequenced the 16S amplicon diversity of natural bacterial communities in and around roots of plants grown on natural and sterilized CAS after Calcinite treatment. Indeed, preliminary analysis shows that the soil sterilization procedure led to a decrease of the bacterial alpha diversity, observed as a decrease in the Shannon index (Shannon, 1948), in both unplanted soil, as well as the rhizosphere and endosphere of *Col-0* when compared to the respective natural soil (Figure 13A). This is in line with strongly reduced microbial growth and diversity *in vitro* (Supplemental figure 11D). Furthermore, the bacterial alpha diversity in sterile soil seems to be mostly unaffected by the nitrogen treatment of the soil (Figure 1A). In the rhizosphere of wild-type plants grown on natural soil diversity appeared to decrease after nitrogen treatment, which was not the case for neither *gelp*^{quintuple}, *pELTP::NLS-NLP7* nor *Col-0* samples extracted from sterilized soil (Figure 13A). An opposite trend was observable in the endosphere where bacterial alpha diversity was increased after Calcinitie treatment. This observation was independent of genotype and soil sterilization. Next, we investigated the bacterial beta diversity by performing principal coordinate analysis (PCoA) on the Bray Curtis dissimilarities (Bray & Curtis, 1957). The first two principal coordinates resolved 15% and 13% of the observed dissimilarity respectively and revealed three distinct clusters. First, independent of nitrogen treatment, all samples obtained from sterile soil clustered together. Second, samples obtained from the endosphere clustered together and third cluster contained both soil samples as well as rhizosphere samples (Figure 13B). The effect of the nitrogen treatment was less pronounced but clearly visible in rhizosphere samples from natural soil or samples obtained from sterile soil irrespective of compartment (Figure 13C). In this preliminary analysis, no clear effect of the genotype on the microbial structure was visible albeit endopshere samples of *gelp*^{quintuple} and *pELTP::NLS-NLP7* cluster further from the center when compared to wild-type plants (Figure 13D). Together these findings allow for the hypothesis that nitrogen-treatment results in a targeted modulation of the microbiome and warrant further investigation.

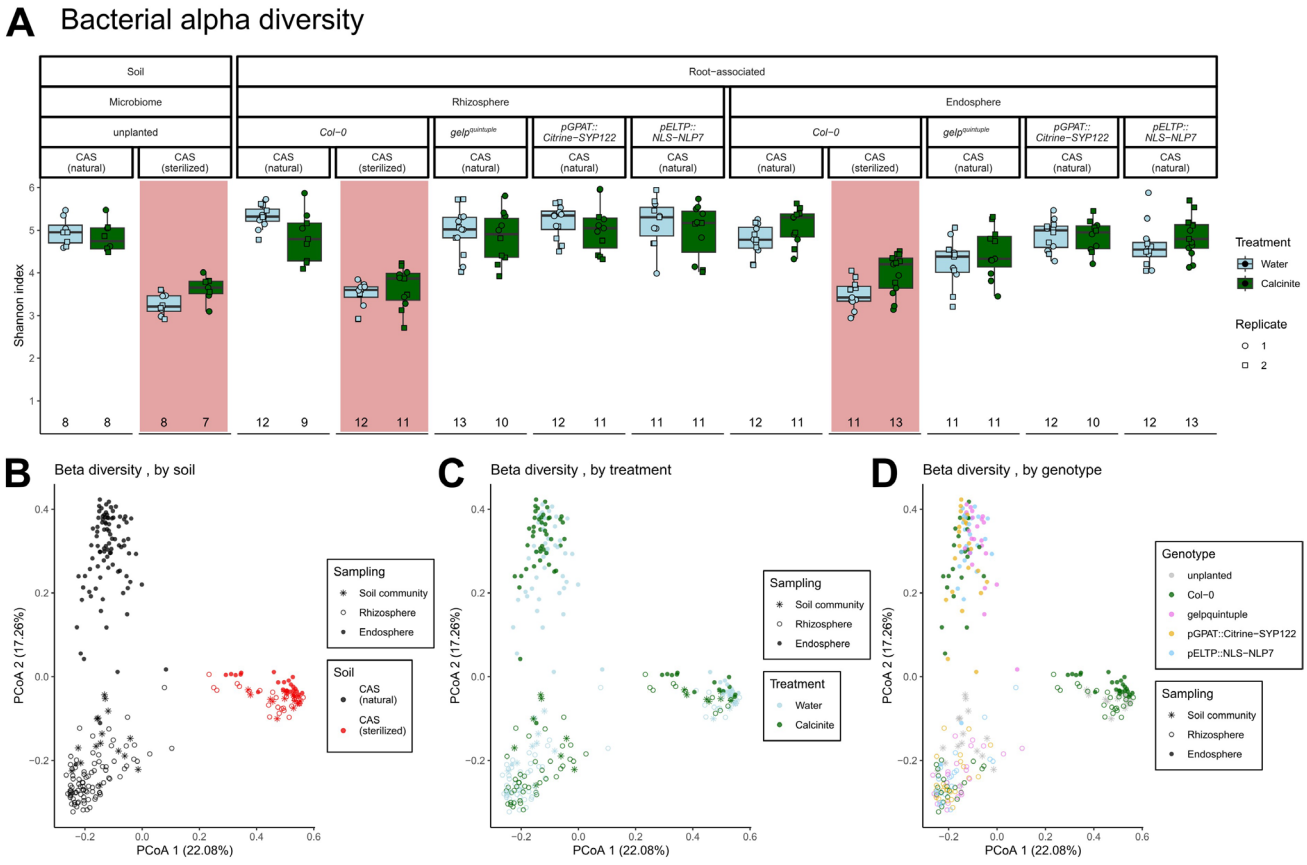

Figure 13: ***Diversity of the bacterial community.*** *Bacterial taxa were identified based on their 16S amplicon sequence as (Shen et al., 2023; Wippel et al., 2021)* ***A*** *Alpha diversity calculated as Shannon index* (Shannon, 1948)*, red rectangle indicate samples obtained from sterilized soil. Numbers below the boxplots indicate sample size* ***B,C,D*** *Beta diversity as Bray-Curtis dissimilarity.* ***B*** *Beta diversity soil.* ***C*** *Beta diversity treatment.* ***D*** *beta diversity genotype.*

5.4.5 Coumarin biosynthesis is required to facilitate microbe-nitrogen fertilizer utilization

Our previous experiments revealed that upon nitrogen starvation specific genes associated to secondary metabolism are upregulated in the cortex of the mature root (Figure 8). Namely, the scopoletin synthesis gene *F6'H1,* and the fraxetin synthesis gene *S8H.* The gene for sideretin synthesis *CYP82C4* and the ferrous iron importer *IRT1* are downregulated in nitrogen starvation (Figure 8, Supplemental figure 6, Supplemental figure 15). Moreover, manipulation of nitrogen signaling by overexpressing of NLP7 in the endodermis leads to a delayed onset of suberization and a hypersensitivity towards nitrate resupply. Further, glucosinolates have been shown before to be involved in the maintenance of microbial commensalism and dysbiosis (Wolinska et al., 2021). Based on this we selected an array of mutant lines deficient in coumarin biosynthesis (*f6'h1*), indole glucosinolates (*cyp79b2cyp79b3*), a combination of both *(f6'h1cyp79b2cyp79b3)*, high affinity ferrous iron uptake (*irt1*), high affinity ammonium uptake (*amt1.2*), high affinity nitrate uptake (*nrt2.1*) and lastly the mutant lacking the transcription factor *NLP7* (*nlp7*). We tested those mutants for their ability to utilize supplied nitrogen fertilizer. Mutant plants deficient in either ammonium, nitrate or iron uptake showed no impairment in nitrogen fertilizer utilization (Figure 14A). Mutant plants deficient in indolic glucosinolate synthesis still displayed growth promotion, albeit weaker. Both mutants impaired in coumarin production and NLP7-dependent nitrogen signaling were unable to benefit from

the supplied nitrogen. Moreover, coumarin biosynthesis mutant plants showed impaired growth in sterilized soil, regardless of nitrogen treatment. None of the investigated plants was able to benefit from nitrogen fertilizer supply in the sterilized soil. Furthermore, as previously shown the coumarin biosynthesis mutant *f6'h1* showed strong chlorosis under nitrogen-starved conditions, when only treated with water (Harbort et al., 2020). In conclusion this suggest that both nitrogen-signaling and coumarin biosynthesis are required to integrate the soil nitrogen

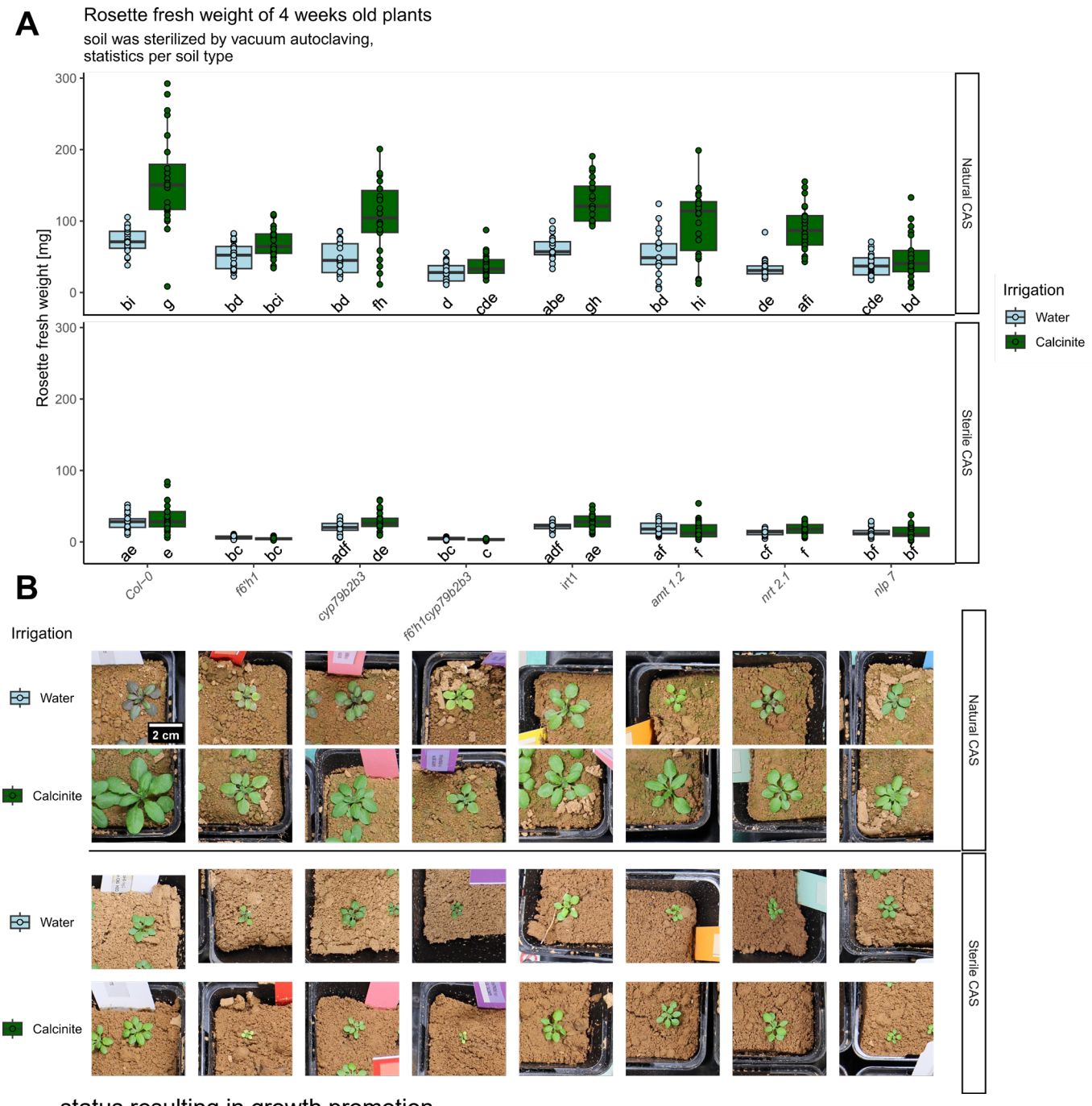

status resulting in growth promotion.

Figure 14: ***Nitrogen fertilizer use capacity is dependent on plant coumarin production and nitrogen signaling. A*** *Rosette fresh weight 4WAG. Statistics per soil type as post-hoc tukey HSD.* ***B*** *Representative images of plants from the respective treatments. Images are of the same absolute size and scale is indicated in the leftmost upper picture.*

6 Discussion

The root systems of vascular plants are essential for nutrient-acquisition from surrounding soil, and therefore form a nexus between soil and above-ground growth. In roots, the formation of lignified or suberized diffusion barriers is essential for selective nutrient-uptake. To date, three such diffusion barriers have been described. The first is the endodermis, which consists of an inner skin surrounding the central vascular cylinder (Geldner, 2013). The second is the exodermis, which consists of an additional outer cell layer (Hose et al., 2001). The third is the periderm, a structure which forms during secondary growth and surrounds the expanding root (Serra et al., 2022). The endodermis is the most prevalent of these diffusion barriers, as not all vascular plants form an exodermis, and the monocotyledons do not undergo secondary growth and therefore lack periderms. Indeed, formation of an endodermis appears ubiquitous amongst *Angiosperms*, and arguably all vascular plants (Yang et al., 2023). It is believed that the endodermis is crucial for the success of modern land plants (Raven, 1994) and today vascular plants dominate the planet contributing between 80-90% of the total biomass.(Bar-On et al., 2018; Erb et al., 2017). In the present study we expand our understanding on the endodermal barrier in the primary root and its implications for plant nitrogen homeostasis, and provide new insights into the importance of spatial N-signaling in the root for mounting of physiological N-responses in natural environments.

6.1 Regulation of endodermal suberin deposition may control the loss of soluble nitrogen out of the vasculature.

The endodermis undergoes two steps of differentiation. First, the lignified Casparian Strip (CS) is deposited between endodermal cells (Caspary, 1866; Naseer et al., 2012). Second, suberization occurs around endodermal cells (Krömer, 1903; Peterson & Enstone, 1996). A study based on the mutant *sgn3,* which has a defective CS but normal onset of suberization, revealed that the lack of a functional CS consistently led to a distinctive reduction in shoot potassium (K^+) (Pfister et al., 2014). In a separate study, the same group investigated the effect of the suberin barrier on nutrient homeostasis by overexpressing the suberin-degrading enzyme *CUTICLE DESTRUCTION FACTOR1* (CDEF1) in the endodermis. The resulting ablation of endodermal-suberin resulted in a similar reduction in K^+ (Barberon et al., 2016). In both studies, the abundance of nitrogen in the shoot could not be measured for technical reasons. Moreover, the experiments were conducted in nutrient replete hydroponic conditions. The work of Andersen et al., 2018; Barberon et al., 2016, as well as the present study show that nutrient availability impacts endodermal suberin deposition. Specifically, Potassium starvation has been shown to result in endodermal oversuberization, while the deprivation of other nutrients leads to desuberization (Barberon et al., 2016), suggesting a shared function of suberin deposition in these cases. Here, we have demonstrated that nitrogen starvation, like potassium starvation, leads to endodermal oversuberization. Similar to potassium, nitrate is a highly mobile nutrient (Tinker & Nye, 2000), and comprises at least part of a plant's internal nitrogen stores (Figure 12C). Accordingly, endodermal suberin deposition and the CS may play a vital role in maintaining plant nitrogen stores by prevent leakage of this nutrient from the vasculature. The upregulation of *SGN3* in nitrogen starved plants (Figure 7E) may indicate a crosstalk between endodermal barriers and nitrogen homeostasis. However, further studies are required to explore this potential connection. In this study, we investigated the performance

of the gelp^{quintuple}, a mutant devoid of endodermal suberin (Ursache et al., 2020) and *pELTP::NLS-NLP7*, a mutant overexpressing the transcription factor NLP7 in the endodermis, resulting in nitrate-dependent reduction in suberization (Figure 10). However, compared to their respective wild-types, both *gelp^{quintuple}* and *pELTP::NLS-NLP7* mutant plants showed no significant increase in shoot nitrate content when nitrogen fertilizer was applied to natural soil, which could account for the lack of growth promotion in these conditions (Figure 12C).

6.2 High affinity nitrogen transport is upregulated in nitrogen starvation: Controlling soil nitrogen uptake or nitrogen rectification?

Tissue-specific post-transcriptome analysis points towards high affinity nitrogen uptake being regulated in the cortex of the mature primary root under chronic nitrogen starvation. Interestingly, high affinity transport systems were upregulated in both the young and mature primary root (Figure 9A,B). Specifically, we also observed the high affinity ammonium transporter *AMT1.5*, high affinity nitrate transporter *NRT2.1,* and the PNR regulatory transcription factor *NLP7* in this cluster (Supplemental figure 7E).

During the early stages of seedling development, young roots depend on seed-stored nitrogen for their growth, and seed nitrogen content has been previously shown to correlate to soybean (*Glycine max*) performance under nitrogen limiting conditions (Naegle et al., 2005). In the conditions used for TRAPseq analysis, plants were grown for 8 days on media devoid of nitrogen. In these conditions, root growth cessation occurred between 11 and 13DAG (Figure 1E), which indicates that this is the limit of *Arabidopsis* survival solely based on seed N-supplies. Under the assumption that increased suberin is a mechanism to prevent the leakage of nutrients from the vasculature into the rhizosphere, this prompts the question of why high affinity transport is upregulated in the cortex of the mature root, while the endodermis underneath is increasing its suberization. Interestingly, *NPF7.2* (*NRT1.8*) and *NPF2.13* (*NRT1.7*), previously associated with xylem nitrogen unloading (J. Y. Li et al., 2010) and phloem loading (S. C. Fan et al., 2009) respectively, were amongst the members of the NPF family to be upregulated in nitrogen starvation conditions (Figure 9C,F). Thus, high affinity nitrogen transporters in the plasma membrane could serve to recover nitrogen, that leaked out of the root and this could be a mechanism to survive longer on seed nitrogen. Following differentiation, root cells don't move. Therefore, nitrogen delivered to the root meristem through the vasculature must pass through vascular cells, and pass by undifferentiated endodermal cells. To my knowledge, it is poorly understood whether nutrient supply of the meristem occurs through symplastic transport via plasmodesmata, active cell-to-cell-coupled transport, or passive apoplastic diffusion. In either case, leaking nitrate could be taken up by *NRT2.2* and *NRT2.4* in the meristematic zone itself and as cortical cells mature by cortex localized *NRT2.1.*

Another possible explanation for the upregulation of high affinity nitrogen transporters in the cortex could be the preparation of the root for increasing nitrogen levels in soil. Accordingly, the levels of locally available nitrogen fluctuate, even in n-deplete soils, and local nitrate levels can rapidly and locally increase (e.g. through the input of new organic matter through forest fires, animal droppings or decaying organisms themselves, or through changes in pH leading to an oxidation of NH_4^+ to NO_3^- increasing the solubility of nitrogen). Here the expression of high affinity nitrate transporters like *NRT2.1* would allow for the uptake of nitrogen into the

symplast, where it could be stored or symplastically transported into the vasculature. On one hand, it has been suggested that the transport of nutrients across the suberized endodermis could occur through plasmodesmata (Barberon, 2017; Ramakrishna & Barberon, 2019). On the other hand, endodermal suberization is reversable through the application of ethylene (Barberon et al., 2016) which could be facilitated by members of the GELP family (Ursache et al., 2020). In this study we were able to show that *pELTP::NLS-NLP7* plants are able to drastically reduce endodermal suberin deposition, if nitrate is resupplied after a previous period of nitrogen starvation (Figure 10D). Transcriptomic analysis indeed revealed that the downregulation of suberization was accompanied by upregulation of suberin degrading members of the *GELP* family (Figure 10F). Albeit, wild-type plants did not show a nitrate-dependent suberin reduction suggesting that another mechanism likely prevents N-dependent desuberization after nitrate-resupply. PCA of the whole root transcriptomics revealed that after NO_3^- resupply, profiles of both wild-type and *pELTP::NLS-NLP7* clustered closer to profiles of plants continuously grown on nitrogen sufficient media (1/2 MS) compared to profiles of plants grown continuously on nitrogen starvation (1/2 MS-N) (Figure 10E). Despite the difference in endodermal suberization phenotype, this indicates at least partial overlap between transcriptional reprogramming of wild-type plants and *pELTP::NLS-NLP7* plants. Although whether nitrate resupply is able to induce desuberization, and whether this occurs in natural conditions, remains to be investigated.

6.3 *NPF6.3* and *NIGT1.3* could act as a signaling module in the late endodermis integrating internal and/or external nitrogen status

When analyzing the expression pattern of known nitrogen transport gens (Figure 9C), we found that *NPF6.3* transcript levels decreased in the whole root, but increased in the endodermis (Figure 9C,F, Supplemental figure 7F). Also, we found *NIGT1.3* to be upregulated under nitrogen starvation, and especially in the endodermis, while the other 3 members of the *NIGT1* family were downregulated (Supplemental figure 9, Supplemental figure 10). Thus, our data suggests a specific role of the endodermis in nitrogen signaling where NIGT1.3 plays a distinct role in preventing N-responses. Investigations on *NPF6.3* have established its role as plasma membrane localized dual affinity transceptor (Bouguyon et al., 2015; Fang et al., 2021; Krouk et al., 2006; Parker & Newstead, 2014; Rashid et al., 2018; Sun & Zheng, 2015; Tsay et al., 1993) but also highlighting its function in alleviating ammonium toxicity (Xiao et al., 2022). Less is known in respect to the function of *NIGT1* genes. Arguing for a shared expression of *NPF6.3* and *NIGT1.3/1.4* at the root tip, the Medici et al., 2015suggested that both functions jointly, and potentially in coordination with NLP7, as NO_3^-/PO_4^{2-} signaling module. A later study then highlighted *NIGT1.1,1.2,1.3* and *1.4* for this role and showed that the four *NIGT1* genes are induced by nitrate resupply in an NLP7 dependent manner and subsequently repress high affinity nitrogen transporters such as *NRT2.1, NRT2.2* but also *NPF6.3* (Maeda et al., 2018). Moreover, they showed this repression is enforced by *PHR* during P_i-starvation. Lastly, a recent study has shown that *NIGT1* genes are crucial to repress the nitrogen starvation hallmark HATS transporters *NRT2.4* and *NRT2.5* after nitrogen is resupplied, and the authors suggested that *NIGTs* could regulate N-starvation responses through the modulation of reactive oxygen species (Safi et al., 2021). A distinctive role of NIGT1.3 has not been demonstrated so far. Based on previous findings and the observations of this study, we

propose that *NPF6.3* and *NIGT1.3* in the mature endodermis act jointly as a nitrogen signaling hub during nitrogen starvation, potentially integrating the systemic N-status through *NIGT1.3* dependent ROS modulation.

6.4 Passage cells in the otherwise suberized endodermis may form N-sensing hubs

Suberized endodermal cells are believed to be insulated from both the vascular and the cortical apoplast (2019; Krömer, 1903; Peterson & Enstone, 1996, visualized e.g.: Andersen et al., 2018; Kreszies et al., 2019). This would prevent nitrogen signaling in suberized endodermal cells, while an NLP7/NIGT1.3 module still could act as an intracellular module to sense the endodermal nitrogen status. NPF6.3 is located at the plasma membrane with the two nitrate binding sites located within a transmembrane domain and facing the apoplast respectively (Parker & Newstead, 2014). This begs the question why the transcription of *NPF6.3* would be maintained specifically in the mature endodermis under nitrogen starvation (Figure 9C,F). One feature of the suberized endodermis are passage cells, which remain open in the otherwise fully suberized endodermis. Since their discovery they have been hypothesized to be remaining openings for the “passage” of water and solutes (Krömer, 1903). However, their physiological function remained elusive and only recently a distinct regulatory mechanism to maintain passage cell aperture has been unveiled (Andersen et al., 2018). Moreover, it was shown that passage cells can still undergo suberization trough application of ABA and thus a model was proposed in which the suberization of the xylem pole associated endodermis is jointly regulated through modifying the threshold for joint ethylene and ABA signaling. In agreement with previous research which showed that overall endodermal suberization can be increased by ABA application and decreased by ethylene application (Barberon et al., 2016). In the study of Andersen et al., 2018, the physiological function of passage cells has been proposed to act in concert with the cortical and epidermal cell layers above to funnel nutrients into the vasculature or to exchange signaling molecules between the vasculature and the rhizosphere. We would like to expand on that model by proposing that NPF6.3 and NIGT1.3 could integrate nitrate-, and potentially phosphate-, signaling in passage cells. In support of this, a family of homologues of the described phosphate transporter *PHOSPHATE1* (PHO1)(Hamburger et al., 2002), *PHO1-H1* to *PHO1-H10*, has been associated with passage cells and transcriptional reporter analysis showed the expression of *PHO1, PHO1-H3, H5* and *H8* in passage cells (Andersen et al., 2018, Extended Data Figure 9). Indeed, we also observed an enrichment of these four genes in the mature endodermis (“ELTP”) TRAPseq profile (Supplemental figure 13A). Furthermore, besides *PHO1-H2* and *PHO1-H10* which were part of the cortex associated clusters k12 and k2 respectively, the remaining members of the *PHO1* family were part of the endodermis associated clusters k32, k23, k 31, k15, k22 and k10 (Supplemental figure 13B). Moreover, their expression was decreased upon nitrogen starvation (Supplemental figure 13B). In this study we also reported a reduction of passage cell occurrence and increased suberization under nitrogen starvation conditions (Figure 1C). In contrast, phosphate starvation was previously reported to lead to a reduction in suberization (Andersen et al., 2018). In nitrogen limiting conditions, the occurrence of passage cells appears to be dynamic, and preliminary data on the suberization and passage cell occurrence of four *Arabidopsis thaliana* accessions suggests that the onset of endodermal suberization and passage cell occurrence are not directly linked (Supplemental figure 14A,B)Taken together,

we are proposing a model in which a passage cell localized NPF6.3/NIGT1.3 module could integrate plant nitrogen availability.

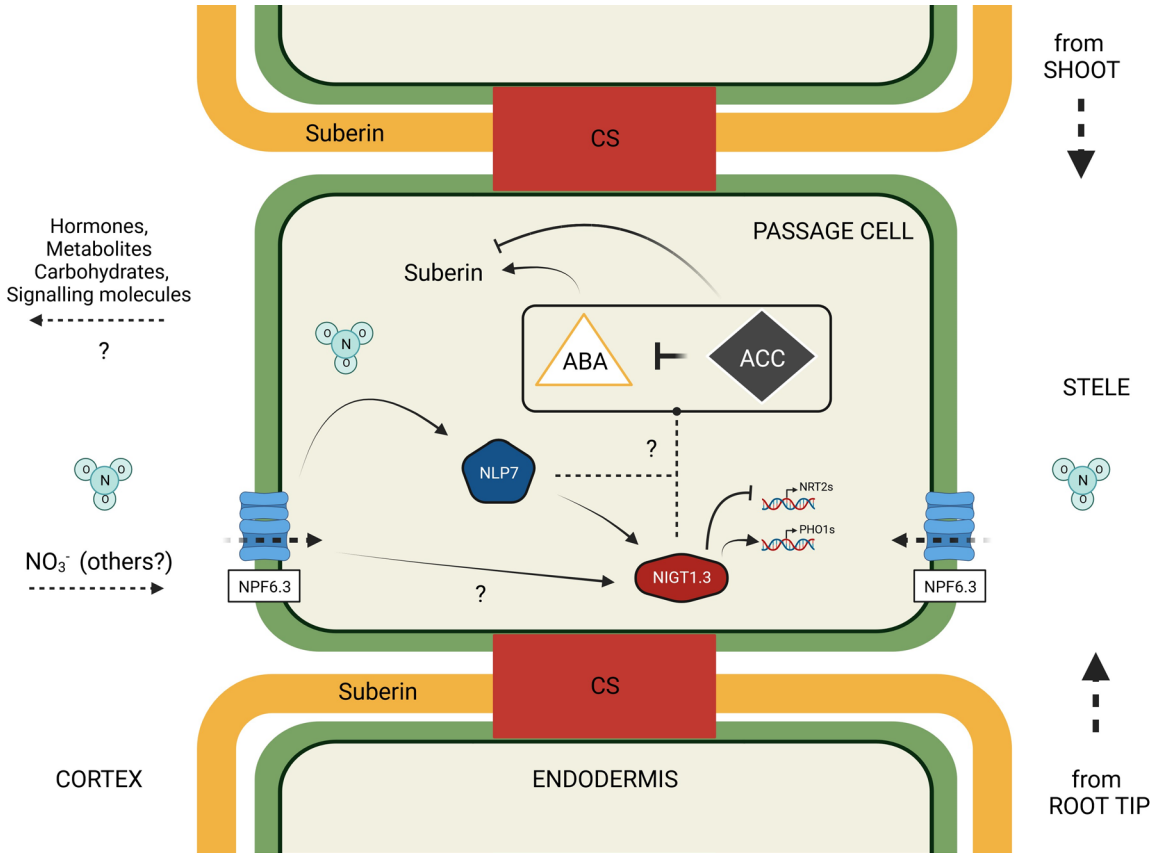

Figure 15: ***Model of endodermal NPF6.3/NIGT1.3 signaling module:*** *Under nitrogen starvation endodermal NPF6.3 and NIGT1.3 expression are maintained in mature endodermal cells, putatively in passage cells. NIGT1.3 represses the expression of high affinity nitrate transporters to prevent uptake of shoot or seed derived nitrate from the stele. NPF6.3 remains expressed and localized to the plasma membrane to sense changes in internal and/or external nitrogen status. NLP7 and NIGT1.3 monitor cellular N-status and potentially regulate endodermal suberization through modulating ABA and ethylene signaling. Created with biorender.com.*

6.5 Endodermal nitrogen signaling and root coumarin production could share an overlapping but not exclusive function in microbe elicited nitrogen and iron nutrition after nitrogen fertilization.

In this study we used the promoter of *ELTP* to overexpress a nuclear-localized version of the transcription factor NLP7 in the mature endodermis (*pELTP::NLS-NLP7 #4-20*) to specifically address the role of endodermal nitrogen-signaling in plant responses. This allowed us to circumvent direct influences on primary root development. This was in sharp contrast to a previously used NLP7 overexpression construct (*p35S::NLP7*), which ubiquitously overexpresses the *NLP7* gene (L. H. Yu et al., 2016). *pELTP::NLS-NLP7* showed no increase in primary root length across our experimental conditions (Figure 10A). However, when nitrate was supplied in the agar media, either from germination on or after a period of nitrogen starvation, *pELTP::NLS-NLP7* plants showed a drastic reduction in endodermal suberin deposition. This could be accounted for by both downregulation of suberin synthesis but also upregulation of suberin degradation (Figure 10 A, D, F). We hypothesize that the overexpression of NLP7 in the endodermis exaggerates the transcriptional response to nitrate. This suggested hypersensitivity led to decreased shoot fresh weight when plants were grown

on agricultural soil. Furthermore, *pELTP::NLS-NLP7* plants could not benefit from supplied nitrogen fertilizer to the same extent as wild-type plants (Figure 12B,D). Also, in wild-type plants, the increased growth after nitrogen fertilization was dependent on the microbial community in the soil (Figure 12B,D). A previous study has shown that maize (*Zea mays*) plants produce specific secondary metabolites, flavones, to enrich the rhizosphere with oxalobacteria, aiding in plant nitrogen provision (P. Yu et al., 2021). We hypothesized that a similar mechanism would be required to facilitate the observed microbe dependent growth promotion after nitrogen resupply.

TRAPseq analysis revealed that the majority of nitrogen DEG associate to the mature cortex (Supplemental figure 12, Figure 7C,E). In addition, nitrogen fertilizer growth promotion was lost in *pELTP::NLS-NLP7*, which modulates nitrogen signaling only in the late endodermis (Figure 11B, Figure 12A). Moreover, TRAPseq revealed an upregulation of coumarin biosynthetic genes (Figure 8). Interestingly the biosynthesis of scopoletin and fraxetin but not sideretin was upregulated in the mature root under nitrogen starvation (Figure 8). Root secreted scopoletin and fraxetin have been previously shown to be required to shape the microbiome in iron-limiting condition, facilitating microbe-assisted iron uptake. Sideretin appeared to be dispensable for this. In the present study we show evidence, that coumarins are needed to facilitate microbe assisted nitrogen uptake as well (Figure 14). Both scopoletin fraxetin were shown to be bateria- and fungicidal properties towards certain taxa (Buathong et al., 2019; Harbort et al., 2020; Mamatova et al., 2019; Napiroon et al., 2018; Stringlis et al., 2018). However, as not all organisms are equally susceptible to secreted coumarins and thus they have a selective function in the rhizosphere (Harbort et al., 2020). When analyzing the root transcriptome and post-transcriptome of plants grown without nitrogen source (Figure 8), we found *F6'H1* and *S8H* to be strongly induced while *CYP82C4* expression was repressed. Conversely, *F6'H1* and *S8H* were repressed when nitrate was resupplied after a period of nitrogen starvation and *CYP82C4* expression was increased. The endodermal overexpression of NLP7 did not influence this behavior (Supplemental figure 15A,B). Therefore, we suggest sideretin to have a special role during nitrogen resupply after starvation. Alternatively, a reduction in secreted scopoletin and fraxetin, could allow for the colonization of microbes which were inhibited before. Although, the antimicrobial role of sideretin has not been assessed, both scopoletin and fraxetin, have selective antimicrobial properties (Harbort et al., 2020). A reduction of alpha-diversity in the rhizosphere supports the idea of an antimicrobial action of secreted exudates under nitrogen resupply (Figure 13A). Perhaps, when nitrogen limitation is alleviated, reduction of rhizosphere diversity would be a means of reducing plant-bacteria competition for other - now limiting - nutrients, such as iron, in the soil niche. Although, bacterial quantity was not assessed in the present study, it would be interesting to investigate the nutrient usage of bacterial extracts from nitrogen fertilized rhizosphere samples versus samples of nitrogen starved plants.

Indeed, the iron reductase *FRO2* and the iron transporter *IRT1* are upregulated after nitrogen resupply (Supplementary Figure 15B). However, while the *f6'h1* mutant did not show growth promotion after nitrogen fertilization, the *irt1* mutant showed the same growth promotion as *Col-0* wild-type plants. In addition, on the one hand, the upregulation of *FRO2* and *IRT1*, as well as the reduction of rhizosphere alpha diversity after nitrate supply was not hampered in *pELTP::NLS-NLP7* plants (Figure 13A,B). On the other hand, the further upregulation of *S8H*

and *NRT2.1,* as observed in wild-type plants was not present in *pELTP::NLS-NLP7* (Supplemental figure 15B,D).These results indicate that, there might be an overlapping role of coumarins in facilitating microbe elicited nitrogen and iron nutrition. However, preliminary results show that joint provision of fraxetin and nitrogen, can't facilitate growth promotion of the *f6'h1* mutant but partly restores growth promotion in the *pELTP::NLS-NLP7* line (Supplemental figure 16B). Moreover, provision of chelated iron to nitrogen limited soil confers a growth benefit towards wild-type and *f6'h1* mutant plants but not *pELTP::NLS-NLP7* plants (Supplemental figure 16C). Albeit, joint provision of chelated iron and nitrogen to the soil did promote growth also of the *pELTP::NLS-NLP7* plants, while further enhancing growth promotion in wild-type and *f6'h1* mutant plants (Supplemental figure 16B,C). Taken together, with the fact that growth promotion was also lost in wildtype plants in sterile soil, when neither nitrogen nor iron where limiting (Figure 12, Figure 14), these results imply a shared but not completely overlapping function of coumarins in microbe elicited nitrogen and iron provision.

However, neither the iron uptake machinery after nitrate supply nor the ability of translocating nitrate to the shoot, were hampered in *pELTP::NLS-NLP7* observed in whole root transcriptomics and in sterilized soil grown plants, respectively (Supplemental figure 15B, Figure 12). Furthermore we observed that *pELTP::NLS-NLP7* grown in natural soil, didn't show purple coloration reminiscent of anthocyanin accumulation during nitrogen starvation (Liang & He, 2018; Peng et al., 2008), which has been demonstrated before to be mediated by *LBD* family transcription factors (Rubin et al., 2009). Further, unpublished work has shown a similar lack of anthocyanin production in plants with defective or enhanced Casparian Strip (CS) formation, highlighting the role of endodermal signaling in regulating shoot nitrogen status. (Shen et al., 2023). The usage of tissue specific expression of regulatory proteins allows us to address these questions in detail.

7 Outlook

Looking forward, we want to further investigate the cause of lost growth promotion in the plants with defective endodermal suberin deposition, *gelp*^{quintuple}, plants defective in coumarin biosynthesis *f6'h1* and plants with manipulated endodermal signaling, *pELTP::NLS-NLP7*.

First, as a functional microbial community appears to be required for conveying nitrogen fertilizer usage, we hypothesized that microbiome assembly would be affected in these mutants. A first analysis of 16S amplicon sequencing of wild-type plants on fertilized natural and sterilized soil conditions revealed structural changes in the rhizosphere of plants after fertilization. However, the specific changes of *gelp*^{quintuple} and *pELTP::NLS-NLP7* were not clear yet and will require further analysis. From the same samples also ITS amplicon libraries were produced to investigate the fungal community as well. Although coumarins have been demonstrated to possess antifungal properties (Mamatova et al., 2019; Stringlis et al., 2018) and have been implied in aiding plant phosphorus nutrition (Hiruma et al., 2016), the role of secondary metabolites in shaping the fungal the community and their respective role in nitrogen is not clear yet. However, despite *Arabidopsis* being unable to form symbiotic relationships with arbuscular mycorrhizal fungi (AMF), AMF taxa are enriched in its root microbiome (Fernández et al., 2019) and scopoletin has been suggested to play a role in their recruitment (Cosme et al., 2021). Further, AMF have been shown to impact plant nitrogen acquisition through fungal-bacterial interactions (Govindarajulu et al., 2005; Hestrin et al., 2019). Analysis of the bacterial and fungal microbiome may allow us to identify keystone taxa, aiding plants in nitrogen – and or iron - acquisition from the soil after nitrogen provision. Adding these to our repertoire of biofertilizers, soil inoculants or seed inoculants can improve the nitrogen use efficiency (NUE) after nitrogen fertilization.

Second, as discussed above, shoot growth promotion appeared to be not directly linked to shoot nitrogen status, as after nitrogen fertilization, nitrate was still translocated to the shoot in sterilized soil, where growth promotion was lost (Figure 12). To investigate this, we performed transcriptomic analysis on shoots of plants grown under these conditions Preliminary analysis of these profiles revealed that as expected photosynthesis and ammonia assimilation are strongly upregulated in wild-type plants after nitrogen provision (Supplemental figure 17B). Interestingly, *gelp*^{quintuple} and *pELTP::NLS-NL7* plants, which were unable to benefit from the supplied nitrogen fertilizer, showed little changes in neither up- nor downregulated genes (Supplemental figure 17A,C). Direct, comparison of wild-type plants to *pELTP::NLS-NLP7* plants showed few upregulated genes. However, we observed a strong downregulation of defense related genes (Supplemental figure 17D). Regulation defense and growth responses has been demonstrated to be critical for microbiome homeostasis (Ma et al., 2021). Our results indicate that a key component of nitrogen fertilizer usage efficiency is the switch from defense to growth. Whether the inability to do so is cause or result of a dysbiotic community in the rhizosphere remains to be investigated.

Lastly, although our results highlighted the importance of mature root nitrogen signaling and coumarin biosynthesis, it remains unclear how biotic and abiotic signals are conducted across the suberized endodermis. Across different ecotypes, we found passage cells in *Arabidopsis thaliana* to be a variable trait in nitrogen limiting conditions (Supplemental figure 14A,B). It is possible that passage cell occurrence contributes to the observed variability of plant responses

to limiting nitrogen (Supplemental figure 14C,D,E,F). New advancements in microscopy techniques (von Wangenheim et al., 2017), as well as an ever-expanding repertoire of genetic tools to genetically modify plants and microbes (Ordon, Kiel, et al., 2023; Ordon, Thouin, et al., 2023) will allow us to observe plant microbial interactions in living organisms with high spatial resolution. After establishing the core taxa relevant for microbe-elicited nitrogen fertilizer usage, key experiments would include; the validation of their sufficiency to elicit nitrogen fertilizer usage in gnotobiotic systems, the spatial resolution of the interactions required to do so and lastly to test if and which endodermal traits contribute to the recruitment or limitation of relevant strains.

7.1 Conclusion

The agricultural soil ecosystem is complex. Plants have to adapt to the biotic and abiotic soil properties as well as available nutrients. To do so plants have evolved extensive nutrient uptake systems (Marschner, 1995). Moreover, plants distinctively regulate their microbiome (Wippel et al., 2021). In this work we shed light on the importance of microbes in nitrogen fertilizer use efficiency. Moreover, we show that nitrogen signaling and secondary metabolism in the mature primary root of *Arabidopsis thaliana* play a role in the effective usage of available soil nitrogen. Together these findings allow us to establish tools to manipulate soil microbial communities through genetic modification of plants or bio fertilization, ultimately improving the soil fertilizer usage of agricultural systems and preventing leaching and subsequent eutrophication.

8 Materials and Methods

8.1 Materials

8.1.1 Plant material

All wild-type and mutant plants of the *Arabidopsis thaliana* ecotypes Col-0 and Van-0 (The European Arabidopsis Stock Centre - NASC) as well as Wid1-6 and Teb23-1 (Milena Malisic, unpublished) and *Camelina sativa* cultivars were cultivated and propagated at the Max Planck Institute for Plant Breeding Research, Carl-von-Linné Weg 10, Germany (Table 2). Transgenic plants for TRAP experiments expressing *BLRP-FLAG-RPL18-GFP* under the promoter of *UBQ10* (AT4G05320), *PEP* (AT1G09750), *SCR* (AT3G54220) *ELTP* (*EDA4*, AT2G48140) and *GPAT5* (AT3G11430) respectively (Barberon et al., 2016; Leal et al., 2022; Thellmann et al., 2020) were previously described or were generated in this study (Table 4). The TRAP line driven by the *SCR* promoter contained the FastRed fluorescent seed coat marker and fluorescence was confirmed via microscopy. Endodermal overexpression lines of NLS-NLP7 (AT4G24020) and NIGT1.1 (AT1G25550), expressed under the promoter of *ELTP* (AT2G48140) were transformed into *pGPAT5::Citrine-SYP122* (Andersen et al., 2018) and selected via the FastGreen seed coat marker (Shimada et al., 2010). T_2 lines were selected according to a 3:1 Mendelian segregation and fluorescent seeds were cultivated individually to obtain homozygous T_3 lines. If applicable, seed coat marker presence was confirmed via fluorescent stereo microscopy (Zeiss Axio Zoom.V16) before each experiment.

Table 2: List of plant species and ecotypes used for this study

Species	Ecotype	Latitude	Longitude	Collector	Source (for this work)
Arabidopsis thaliana	*Col-0*	38.3	-92.3	Albert Kranz	Charles Uhlmann
Arabidopsis thaliana	*Van-0*	49.2655	-123.206	Albert Kranz	Charles Copeland
Arabidopsis thaliana	*Wid1-6*	50.9821	6.8272	Klaus Schläppi & Nina Dombrowski	Milena Malisic
Arabidopsis thaliana	*Teb23-1*	44.292	11.784	Haruhiko Inoue et al.	Milena Malisic
Camelina sativa	*CAM63*	Sweden	Sweden	IÖF Malchow	IPK Gatersleben
Camelina sativa	*CAM134*	Sweden	Sweden	BAZ, Braunschweig Genetic Resources Centre	IPK Gatersleben
Camelina sativa	*CAM220*	Sweden	Sweden	BAZ, Braunschweig Genetic Resources Centre	IPK Gatersleben
Camelina sativa	*CAM277*	Germany	Germany	Asmus Sören Petersen	IPK Gatersleben

Table 3: List of Arabidopsis thaliana *mutant plants used for this study*

Species	Ecotype	Name	Mutated gene(s) AGI	Source (for this work)	Publication / ID
Arabidopsis thaliana	*Col-0*	*esb1-1*	AT2G28670	Tonni Grube Andersen	(Hosmani et al., 2013)
Arabidopsis thaliana	*Col-0*	*sgn3-3*	AT4G20140	Tonni Grube Andersen	(Pfister et al., 2014)

Species	Ecotype	Name	Mutated gene(s) AGI	Source (for this work)	Publication / ID
Arabidopsis thaliana	*Col-0*	*f6'h1*	AT3G13610	Milena Malisic	(Harbort et al., 2020)
Arabidopsis thaliana	*Col-0*	*irt1*	AT4G19690	Milena Malisic	(Harbort et al., 2020)
Arabidopsis thaliana	*Col-0*	*nlp7-1*	AT4G24020	Sandrine Ruffel	(L. H. Yu et al., 2016)
Arabidopsis thaliana	*Col-0*	*cyp79b2* *cyp79b3*	AT4G39950 AT2G22330	Thomas Ryohei Nakano	(Wolinska et al., 2021)
Arabidopsis thaliana	*Col-0*	*cyp79b2* *cyp79b3* *f6'h1*	AT4G39950 AT2G22330 AT3G13610	Makoto Tsuda	unpublished
Arabidopsis thaliana	*Col-0*	*amt1.2*	AT1G64780	NASC	SALK-202315C N690238 ID:60978
Arabidopsis thaliana	*Col-0*	*nrt2.1*	AT1G08090	NASC	SALK-035429C N662089 ID60978
Arabidopsis thaliana	*Col-0*	*gelp22-c1* *gelp38-c3* *gelp49-c1* *gelp51-c1* *gelp96-c1*	AT1G54000 AT1G74460 AT2G19050 AT2G23540 AT5G37690	Robertas Ursache	(Ursache et al., 2021)

Table 4: List of transgenic t-DNA insertion lines overexpressing proteins of interest used in this study

Donor Species	Parental line	Name	Lines	Associated gene(s) AGI	Source (For this work)	Publication
Arabidopsis thaliana, Aequorea victoria	*Col-0*	*pGPAT5:: Citrine-SYP122*	-	AT3G11430, AT3G52400	Tonni Grube Andersen	(Andersen et al., 2018)
Arabidopsis thaliana,	*Col-0*	*pCASP1:: CDEF1*	-	AT2G36100 AT4G30140	Tonni Grube Andersen	(Naseer et al., 2012)
Arabidopsis thaliana, Aequorea victoria	*pGPAT5:: Citrine-SYP122*	*pELTP:: NLS-NLP7-GFP*	#3-1, #7-5	AT2G48140 AT4G24020	Tonni Grube Andersen	unpublished
Arabidopsis thaliana	*pGPAT5:: Citrine-SYP122*	*pELTP:: NLS-NLP7*	#4-20, #5-15	AT2G48140 AT4G24020	Tonni Grube Andersen	unpublished
Arabidopsis thaliana, Aequorea victoria	*pGPAT5:: Citrine-SYP122*	*pELTP:: NIGT1.1-GFP*	#1-5, #3-7	AT2G48140 AT1G25550	Tonni Grube Andersen	unpublished
Arabidopsis thaliana	*pGPAT5:: Citrine-SYP122*	*pELTP:: NIGT1.1*	#1-17, #6-2	AT2G48140 AT1G25550	Tonni Grube Andersen	unpublished
Arabidopsis thaliana, Aequorea victoria	*Col-0*	*pUBQ:: BLRP-FLAG-GFP-RPL18*	#12, #17	AT1G09750 AT3G05590	Marie Barberon	(Thellmann et al., 2020)
Arabidopsis thaliana, Aequorea victoria	*Col-0*	*pPEP:: BLRP-FLAG-GFP-RPL18*	#4, #5	AT1G09750 AT3G05590	Marie Barberon	(Thellmann et al., 2020)

Donor Species	Parental line	Name	Lines	Associated gene(s) AGI	Source (For this work)	Publication
Arabidopsis thaliana, Aequorea victoria	*Col-0*	*pSCR:: BLRP-FLAG-GFP-RPL18*	#2-7-8	AT3G54220 AT3G05590	Tonni Grube Andersen	unpublished
Arabidopsis thaliana, Aequorea victoria	*Col-0*	*pELTP:: BLRP-FLAG-GFP-RPL18*	#9, #11	AT2G48140 AT3G05590	Marie Barberon	unpublished
Arabidopsis thaliana, Aequorea victoria	*Col-0*	*pGPAT:: BLRP-FLAG-GFP-RPL18*	#4, #7	AT3G11430 AT3G05590	Tonni Grube Andersen	Leal et al. 2022

8.1.2 Plant growth media

If not indicated otherwise, half-strength Caisson MSP01 (1/2 MS) or Caisson MSP21 (1/2 MS-N) were used. For the 0.11mM N limiting treatment, 0.037mM KNO_3 and 0.037mM NH_4NO_3 were added to Caisson MSP21 medium. For the K_2SO_4 control medium a surplus K^+ and SO_4^{2-} was supplemented onto Caisson MSP21 with final concentrations of 20mM KNO_3 and 5mM $(NH_4)_2SO_4$ mimicking MSP01 in its nitrogen content. Similarly, to control for a surplus K^+, 10mM KNO_3 and 10mM NH_4NO_3 was added to 1/2 MS-N, mimicking MSP01 in its nitrogen content. This medium was referred to as positive control. To all media, 10mM 2-(N-morpholino)ethanesulfonic acid (MES) was added as a buffering component and pH was adjusted to 5.8 using KOH. No sucrose was added to any media. Lastly 1% (w/v) Difco™ Granulated Agar was added before autoclaving the media using gravity steam sterilization at 120°C for 20min. Similarly, as for media containing individual concentrations of nitrogen, Caisson MSP21 was supplied with the indicated amount of either KNO_3 or $(NH_4)_2SO_4$ for nitrate and ammonium concentration gradients respectively.

Table 5: Composition of 'Caisson MSP01' medium: Murashige & Skoog Basal Salts, [+] Macronutrients, [+] Micronutrients. 2.165g/L of mineral salts were used for the preparation of 1/2 MS medium. Listed concentrations correspond to the final concentration in 1/2 MS medium

1/2 MS composition	Nutrient salt (name)	Nutrient salt (formula)	Molecular weight [g / mol]	Final concentration [µM]	Final concentration [mg / L]
Macronutrients	*Magnesiumsulphate anhydrous*	$MgSO_4$	120.37	750.6	90.4
	Potassium dihydrogen phosphate	KH_2PO_4	136.09	624.6	85.0
	Ammonium nitrate	NH_4NO_3	80.04	10307.3	825.0
	Potassium sulfate anhydrous	KH_2SO_4	136.09	0.0	0.0
	Potassium nitrate	KNO_3	101.1	9396.6	950.0
	Calcium dichloride anhydrous	$CaCl_2$	110.98	1496.7	166.1
Micronutrients	*Cobalt dichloride hexahydrate*	$CoCl_2 \cdot 6H_2O$	237.93	0.1	0.025
	Cupric sulfate pentahydrate	$CuSO_4 \cdot 5H_2O$	249.71	0.1	0.025
	Boric acid	H_3BO_3	61.83	50.1	3.1

1/2 MS composition	Nutrient salt (name)	Nutrient salt (formula)	Molecular weight [g / mol]	Final concentration [µM]	Final concentration [mg / L]
	Potassium iodide	KI	166	2.5	0.4
	Manganese Sulfate monohydrate	$MnSO4 \cdot H_2O$	169.02	50.0	8.5
	Disodium Molybdate dihydrate	$Na_2MoO_4 \cdot 2H_2O$	241.95	1.0	0.25
	Zinc sulfate heptahydrate	$ZnSO_4 \cdot 7H_2O$	136.3	31.5	4.3
	Ferrous sulfate heptahydrate	$FeSO_4 \cdot 7H_2O$	278.02	50.0	13.9
	Disodium-EDTA dihydrate	Na_2EDTA	372.24	50.0	18.6
	Potassium Chloride	KCl	74.55	0.0	0.0

Table 6: Composition of 'Caisson MSP21' medium: Murashige & Skoog Basal Salts, [+] Nitrogen Free, [+] Micronutrients [+] Macronutrients [+] Potassium Chloride [+] Potassium Sulfate. 1.565g/L of mineral salts were used for the preparation of 1/2 MS medium. Listed concentrations correspond to the final concentration in 1/2 MS medium. Fields highlighted in red display a reduction compared to 'Caisson MSP01'. Fields highlighted in green display an increase compared to 'Caisson MSP01'.

1/2 MS-N composition	Nutrient salt (name)	Nutrient salt (formula)	Molecular weight [g / mol]	Final concentration [µM]	Final concentration [mg / L]
Macro-nutrients	*Magnesiumsulphate anhydrous*	$MgSO_4$	120.37	750.6	90.4
	Potassium dihydrogen phosphate	KH_2PO_4	136.09	624.6	85.0
	Ammonium nitrate	NH_4NO_3	80.04	0.0	0.0
	Potassium sulfate anhydrous	KH_2SO_4	136.09	6017.7	818.9
	Potassium nitrate	KNO_3	101.1	0.0	0.0
	Calcium dichloride anhydrous	$CaCl_2$	110.98	1496.7	166.1
Micronutrients	*Cobalt dichloride hexahydrate*	$CoCl_2 \cdot 6H_2O$	237.93	0.1	0.025
	Cupric sulfate pentahydrate	$CuSO_4 \cdot 5H_2O$	249.71	0.1	0.025
	Boric acid	H_3BO_3	61.83	50.1	3.1
	Potassium iodide	KI	166	2.5	0.4
	Manganese Sulfate monohydrate	$MnSO4 \cdot H_2O$	169.02	50.0	8.5
	Disodium Molybdate dihydrate	$Na_2MoO_4 \cdot 2H_2O$	241.95	1.0	0.25
	Zinc sulfate heptahydrate	$ZnSO_4 \cdot 7H_2O$	136.3	31.5	4.3
	Ferrous sulfate heptahydrate	$FeSO_4 \cdot 7H_2O$	278.02	50.0	13.9
	Disodium-EDTA dihydrate	Na_2EDTA	372.24	50.0	18.6
	Potassium Chloride	KCl	74.55	4761.3	355.0

8.1.3 Fertilizer

For control 'Water' treatment de-ionized water (ddH_2O) from a tap within the greenhouse cabin was used. For 'Calcinite' treatment 7mL/L of a 9.3kg/100L stock solution (YaraTerra

CALCINIT, Yara GmbH) was used, resulting in an electric conductivity (EC) of 1.4 mS/m. For 'Wuxal' treatment 7mL/L Calcinite stock solution and 3mL/L of WUXAL (WUXAL Super 8-8-6, Hauert MANNA Düngerwerke GmbH) were used, resulting in an EC of 2.4 mS/s. The resulting nutrient concentrations are listed below (Table 7). The final concentration of 'Wuxal' treated soil is to be understood as additive value of all concentrations listed below.

Table 7: Fertilizer composition used for the greenhouse experiments. Molarity was calculated using selleckchem.com/molaritycalculator.jsp according to the "Formula" given. Final concentration is calculated using 7mL/L of 9.3kg/100L Calcinite stock solution and 3mL/L of WUXAL respectively. Ingredients were listed in German and the formula was constructed according to the translation.

Fertilizer	Ingredient (as listed)	Formula	Content	Final concentration [µM]	Final concentration [mg / L]
Calcinite	**N Gesamtstickstoff**	**N**	**15.5%**	**7 286**	**101.9**
	N Nitratstickstoff	$N\text{-}NO_3$	14.4%	6 692	93.70
	N Ammoniumstickstoff	$N\text{-}NH_4$	1.1%	551	7.16
	CaO wasserlösliches Calciumoxid	CaO	26.5%	3 076	172.52
Wuxal	**Gesamtstickstoff**	**N**	**8%**	**1 713**	**24.00**
	N als Nitratstickstoff	$N\text{-}NO3_3$	2.3%	492	6.90
	N als Ammoniumstickstoff	$N\text{-}NH_4$	3.7%	792	11.10
	N als Carbamidstickstoff	CH_4N_2O	2.0%	428	6.00
	Wasserlösliches Phosphat	P_2O_5	100 g/L	2 113	300
	Wasserlösliches Kaliumoxid	K_2O	75 g/L	2 386	225
	Wasserlösliches Bor	B	0.12 g/L	33	0.36
	Wasserlösliches Kupfer als Chelat von EDTA	Cu • C10H16N2O8	0.05 g/L	2	0.15
	Wasserlösliches Eisen als Chelat von EDTA	Fe • C10H16N2O8	0.25 g/L	13	0.75
	Wasserlösliches Mangan als Chelat von EDTA	Mn • C10H16N2O8	0.15 g/L	8	0.45
	Wasserlösliches Molybdän	Mo	0.01 g/L	0.3	0.03
	Wasserlösliches Zink als Chelat von EDTA	Zn • C10H16N2O8	0.05 g/L	2	0.15

8.1.4 Soil

As indicated, either potting soil (Blumavis, Profisubstrat E078 Deklarationstyp 3, pH 5.8) or Cologne agricultural soil (CAS) were used. For all experiments the same batch of soil 'CAS-16', extracted in April 2022 from a local site at the MPIPZ (GPS code : 50.958 N, 6.856 E) was used. In order to sterilize the soil, ~10kg soil were placed in an autoclaving bag and sterilized for 30min at 121°C in a vacuum autoclave (Systec VX-150). Maximum of five bags were autoclaved in one cycle and the vacuum was released once 90°C were reached. Afterwards, the soil was stored at 4°C until usage (<12 weeks after sterilization). Around 100kg of soil were sterilized in two batches (27. & 28.02.2023). To assess the effectiveness of the sterilization, ~5cm³ of either autoclaved and untreated soil were plated on 50% tryptic soy agar (Roth, CASO-Bouillon, X938, 30g/L) solidified with 1.5% (w/v) bactoagar (BD 214010) without antibiotics. Microbial growth was visually assessed 2 and 5 days after plating. The soil properties of CAS were previously assessed (Harbort et al., 2020). Additionally, after the

experiment to assess “nitrogen fertilizer usage of endodermis mutant lines” (8.2.4.3, CAS III) pH, nitrate (NO_3^-) and iron ($Fe^{2+/3+}$) were assessed before and after fertilizer treatment and autoclaving, respectively (Supplemental figure 11).

Table 8 Soil composition of “potting soil”used for the greenhouse experiments. Molarity was calculated using selleckchem.com/molaritycalculator.jsp according to the “Formula” given. Ingredients were listed in German and the formula was constructed according to the translation.

Soil	Ingredient (as listed)	Formula	Final concentration [µM]	Final concentration [mg / L]
Blumavis Profisubstrat E078 Deklarationstyp 3	**Stickstoff (N)**	N	5 710	80
	Kaliumoxid	K_2O	1 220	115
	Phosphat	P_2O_5	669	95
	Magnesium	Mg	3 290	80
	Salzgehalt	KCl	13 413	1000
	Spurenelemente	Fe, Cu, B, Zn	not indicated	not indicated

8.2 Methods

8.2.1 Seed preparation

Seeds were sterilized via Cl_2 gas sterilization. Briefly, seeds were filled into the curved bottom of 2mL Eppendorf tubes and placed into a desiccator under the fume hood. To generate Cl_2 gas, 100mL of 13% NaOCl solution (bleach) was placed in a beaker next to it. Then 10mL 37% HCl was carefully pipetted into the bleach. The desiccator was closed, and the seeds were incubated for 2-4 hours in the gas. Afterwards the desiccator was opened, and the tubes were closed underneath the fume hood. At a sterile bench the tubes were opened and incubated for 5-10min for the remaining Cl_2 to dissipate. Lastly, the seeds were suspended in 0.2% Difco™ Granulated Agar solution. The seeds were imbibed and stratified for 2 days at 4° in darkness before sowing (Lindsey et al., 2017) (16 Appendix II: TRAP protocol”).

8.2.2 Growth conditions

8.2.2.1 Pots

If not indicated otherwise, plants were propagated at 22h light at 21°C with 220 µmol/m²/s light intensity followed by 2h darkness at 21°C. If not indicated otherwise, all greenhouse experiments were carried out in a semi-closed greenhouse (50°57'24.1"N 6°51'34.1"E) under long-day conditions (16h light). The greenhouse chamber was separated from the rest of the building by a sluice where a UV-Lamp and fly-traps were installed to prevent infestation. The chamber itself was only entered wearing lab-coats, hairnets, shoe covers and gloves. Ventilation through the greenhouse roof was filtered by insect proof nets. To ensure long-day conditions the chamber was equipped with additional lamps (80µmol/m²/s) which were turned on from 06:00h-09:00h as well as, 18:00h-22:00h every day. The lamps were also activated when the intensity outside was measured below 180µmol/m²/s. The air temperature in the chamber was controlled between 16.5°C and 24°C (one-time measurement 08.02.2023).

8.2.2.2 Plates

For plate-based experiments, plates were transferred to the referred growth conditions directly after sowing. If not indicated differently, the plants were grown vertically at 16h light at 21°C with 140 µmol/m²/s light intensity followed by 8h darkness at 19°C (MPIPZ Hall 15, incubator 15.5.3, Hettich Elbanton PRC1700). Deviating from those conditions; for assessment of endodermal suberin (Figure 5B), at 5 DAG, the plants were grown at 50-75 µmol m^{-2} s^{-1} (n = 6) (H-O 9/10, Sanyo MIR-553) at 100-120 µmol m^{-2} s^{-1} or (PSL#3 H-K-17, SANYO MLR351). Also, for the assessment of endodermal suberin, 5 to 13 DAG the plants were grown (PSL#3 H-K-17, SANYO MLR351) at 100-120 µmol m^{-2} s^{-1} (Figure 5D,E,F,G). All light measurements were performed with a spectrometer (UPRtek, PG100N).

8.2.3 Plate based experiments

8.2.3.1 Plate preparation and seeding

Immediately after autoclaving, the closed media bottles were mixed on a magnetic plate to homogenize the agar. Afterwards the media were placed into a 55°C water bath to cool down. Immediately before plating the medium was stirred for 5-10minutes on a magnetic plate again. Under a laminar flow or downflow clean bench, 50mL of warm medium was filled into a square petri dish using a falcon to measure volume (Greiner Bio-One, GB688102). The plates were stacked and allowed to cool and solidify for ~1h. Imbibed seeds were then placed with a cut 200µl tip onto the plates. Depending on experiment, seeds were pipetted individually or in a narrow line. The plates were sealed with one layer of micropore tape (3M-ID 7100036504)

8.2.3.2 Tissue staining, imaging and analysis

For suberin staining, plants were grown for the indicated time and stained using Fluorol Yellow (Lux et al., 2005b). In brief, small customized 3D-printed baskets, designed with Fusion360 (Autodesk) and printed with “High_Temp_v2” resin using a Form3B (formlabs) 3D printer, were placed into 12-well plates (Greiner CELLSTAR M9187-100EA). The wells were filled with 3.5mL 0.02% (w/v) Fluorol Yellow 088 (Merck, CAS 81-37-8) dissolved in 85% (w/w) lactic acid (Merck, CAS 50-21-5). Seedlings were immersed into the solution using forceps and incubated at 70°C for 30min – 60min in darkness. Afterwards, new 12-well plates were filled with 3.5mL deionized water per well and seedlings were washed three times for 3 – 5min by transferring the whole basket with the plants inside between the wells. Another plate was prepared in the same way containing 0.5% (w/v) aniline blue (Sigma-Aldrich 415049-50G) for which the samples are transferred and incubated for at least another 30min but not exceeding 6h in darkness. Just before preparing the microscopy slides, the samples were washed twice as described before by transferring them in a 50% glycerol (ROTH Art.Nr.: 3783.1) solution. Depending on the experiment up to 6 slides with up to 30 seedlings per slide were imaged at a time. Fluorescence was detected using an epifluorescence stereomicroscope (Zeiss Axio Zoom.V16) with excitation at 488nm (Lumencor LED) and GFP signal detection using a MF475-35 filter. Depending on the seedling age, 3-12 seedlings were imaged within one tile using the software autofocus and an exposure time of 200-300ms. The suberization zones were measured via the segmented lines tool of Fiji (Schindelin et al., 2012). The unsuberized zone was defined from the root tip until the first suberized cell was visible. The patchy zone was defined thereafter until the whole endodermal cylinder was suberized for the first time. Thereafter, the suberized zone was defined until the root-hypocotyl junction. Passage cells

were counted as unsuberized cells within the suberized zone. For expression analysis plants were fixed, cleared and, if indicated, stained with Calcofluor White (Ursache et al., 2018). Images were obtained via a Zeiss LSM980 CLSM microscope. Calcofluor White (excitation = 405nm, detection = 425-475nm) and GFP (excitation = 488nm, detection = 510-560nm) signals were detected in separate channels. The images were then analysed using the Fiji software (Schindelin et al., 2012; Schneider et al., 2012).

8.2.3.3 Translating Ribosome Affinity purification (TRAP)

Seeds were prepared as described in 8.2.1 and sown onto pre-cut, autoclaved nylon mesh (SEFAR, NITEX 03-100/44, 11cm x 11cm). On each plate, seeds were pipetted in 3 rows containing approximately 200 seeds each. Aroud 20 to 40 plates were prepared per treatment and genotype (Appendix Figure and table). After eight days, plants were cut below the hypocotyl and ca. 3-5 mm above the meristems to enrich for the differentiated root partition. The meristem and the differentiated root fractions were collected separately by scraping the mesh with a feather-weight forceps and snap freezing the samples in liquid nitrogen. Samples were stored at -70°C until extraction. TRAP RNA was obtained as previously described (Thellmann et al., 2020). In brief, the protocol was adapted for the following steps: During tissue homogenization [(Thellmann et al., 2020) Step 6.2.4] 5mL Polysome Extraction Buffer (PEB) was transferred to the homogenizer and the ground sample added directly into the homogenizer. The lysate was cleared using an Avanti J-25 centrifuge from Beckman-Coulter. Microcentrifuge tubes were autoclaved before each run. GFP-binding (Step 6.6.2) was carried out by placing the 15mL Falcon tubes (Falcon™ 352096) containing the samples on a horizontal rotator at <30rpm at 4°C. For subsequent bead washes (Steps 6.6.3-6.6.4), the samples were placed from the rotator into an ice bucket and the beads were allowed to settle down for 10min. Afterwards the Falcon tubes were placed into a 3D-printed rack lined with neodymium magnets (Omnicube N35 Neodym Mini Magnete Extra Stark, 5x1mm) along the conical part of the Falcon tubes. The rack was designed using Fusion360 and printed with “White_v4” resin using a Form3B (formlabs) 3D printer. The beads were precipitated for 10min, before removing the supernatant. RNA extraction was carried out as previously described (16 Appendix II: TRAP protocol”). During the TRAP protocol all surfaces were periodically treated with RNAzap (Sigma-Aldrich R2020-250ML). After RNA extraction the samples were sent to Novogene Co., Ltd. for quality control and sequenced via Low Input RNAseq (https://www.novogene.com).

8.2.3.4 Plant growth and tissue preparation of NLS-NLP7 overexpressing plants

One row of ~200 seeds were sown on 1/2 MS plates as described for the TRAP experiment (8.2.3.3) and grown vertically for eight days. Three to five roots per genotype were stained with Fluorol Yellow as described before to confirm the phenotype of the NLS-NLP7 overexpressing line. Afterwards, the root was cut below the hypocotyl and harvested as described for the TRAP experiment.

8.2.3.5 KNO_3 transfer experiments

8.2.3.5.1 Assessing endodermal suberization upon nitrogen re-supply

Sterilized and imbibed seeds were pipetted individually on plates containing 1/2 MS-N medium. Two individual plates were prepared per genotype. The plates were transferred and grown vertically for 6 days under standard conditions. Afterwards, the plates were opened under a

laminar flow clean bench and 6 physiologically similar seedlings were transferred onto a new plate containing either 1/2 MS-N, 1/2 MS or 1/2 MS-N + 30mM KNO_3. The root tip was marked with a pen to assess the growth rate after transfer. All genotypes were placed onto the same plate. The experiment was carried out with 3 replicate treatment plates each. Afterwards, the plants were grown for additional two days before taking images for root growth measurements. Root length measurements were carried out using the segmented line tool of the Fiji software (Schindelin et al., 2012). After the pictures were taken, the plants were pooled across all 3 replicates, jointly stained with Fluorol Yellow and imaged as described above.

8.2.3.5.2 Plant growth and tissue preparation for RNAseq upon nitrogen resupply.

One row of ~200 seeds were sown on 1/2 MS-N as described for the TRAP experiment (8.2.3.3) and then incubated vertically for six days. Afterwards, the plates were opened under a laminar flow clean bench. The nylon mesh was carefully lifted off the plate using two surface sterilized coverslip forceps and transferred to a new plate with either 1/2 MS-N or 1/2 MS-N + 30mM KNO_3. Afterwards, the plates were re-sealed with micropore tape and incubated for another 2 days, before cutting the root below the hypocotyl and harvesting the root material like described for the TRAP. Three to five roots per genotype were stained with Fluorol Yellow as described before to confirm the phenotype of the NLS-NLP7 overexpressing line grown on the nylon mesh. The experiment was carried out with four replicates.

8.2.3.6 Coumarin extraction

Plants were sown, grown, dissected and harvested as described for the TRAP experiment (8.2.3.3). Coumarins were extracted from the differentiated root fractions. Frozen tissue was homogenized by adding a metal ball for 1min at 30Hz (Qiagen TissueLyser). Samples were kept on ice. Then, 1mL of pre-cooled extraction buffer (40% Acetonitrile, 40% Methanol, 20% H_2O) was added and samples were gently mixed by inverting. Samples were incubated for 30min at 40°C and 1500rpm and afterwards centrifuged for 10min at 4°C and 21000x g. The pellet was used for protein quantification as previously described (Bradford, 1976). The supernatant was transferred to a new tube and dried in a CentriVap evaporator (Labconco) at 10°C and 1000rpm for 6h. The dried pellet was subsequently used for targeted analysis via Gas chromatography-Mass spectrometry (GC-MS). For quantification of scopolin, scopoletin, fraxin and fraxetin, reference spikes were used to determine the m/z-score and retention time specific peaks. For the quantification of sideretin, the m/z score and retention time were approximated.

8.2.4 Greenhouse experiments

Table 9: Summary of experiments on soil, dates in brackets indicate the date of transfer from plates onto soil

ID	Name	Start	End	Genotypes	Soils	Treatments	Measured parameters
CAS I	Greenhouse setup	08.06.2022 (15.06.2022)	25.06.2022	*Col-0* *pGPAT5::Citrine-SYP122* *pELTP::NLS-NLP7 #4-20* *pELTP::NLS-NLP7 #5-15* *pELTP::NIGT1.1 #1-17* *pELTP::NIGT1 #6-2*	Potting soil CAS (natural)	Rainwater	Pictures (end)

ID	Name	Start	End	Genotypes	Soils	Treatments	Measured parameters
CAS II	Fertilization of agricultural soil	20.06.2022 (27.06.2022)	12.08.2023	*Col-0* *pGPAT5::Citrine-SYP122* *pELTP::NLS-NLP7 #4-20* *pELTP::NLS-NLP7 #5-15* *pELTP::NIGT1.1 #1-17* *pELTP::NIGT1 #6-2*	Potting soil CAS (natural)	Rainwater Calcinite WUXAL	Pictures (end) Shoot weight
CAS III	Nitrogen fertilizer usage of endodermis mutant lines	02.02.2023 (09.03.2023)	30.03.2023	*Col-0* *pGPAT5::Citrine-SYP122* *pELTP::NLS-NLP7 #4-20* *gelp*^{quintuple}	CAS (natural) CAS (sterile)	ddH_2O Calcinite	Pictures (weekly) Shoot weight Shoot transcriptome Shoot NO_3^-, SO_4^{2-},PO_4^{3-} Soil microbiome Rhizosphere Endosphere Soil pH, NO_3^-, Fe
CAS IV	Nitrogen fertilizer usage in mutants of ion uptake and secondary metabolism	29.03.2023 (05.04.2023)	26.04.2023	*Col-0* *f6'h1* *cyp79b2b3* *cyp79b2b3f6'h1* *irt1* *amt1.2* *nrt2.1* *nlp7*	CAS (natural) CAS (sterile)	ddH_2O Calcinite	Pictures (weekly) Shoot weight
CAS V	Nitrogen fertilizer usage in interdependence with Fraxetin and FeDTPA	05.05.2023 (12.05.2023)	02.06.2023	*Col-0* *f6'h1* *pGPAT5::Citrine-SYP122* *pELTP::NLS-NLP7 #4-20*	CAS (natural)	ddH_2O Calcinite ddH_2O + 50µM Fraxetin Calcinite + 50µM Fraxetin ddH_2O + 35µM FeDTPA Calcinite + 35µM FeDTPA	Pictures (weekly) Shoot weight
CAS VI	Microbe re-inoculation of sterilized soil before nitrogen fertilization	25.05.2023 (01.06.2023)	22.06.2023	*Col-0* *f6'h1* *pGPAT5::Citrine-SYP122* *pELTP::NLS-NLP7 #4-20*	CAS (sterile)	Mock Soil wash	Pictures (weekly) Shoot weight

8.2.4.1 Greenhouse setup

Besides the first experiments ('CAS I' and 'CAS II'), all experiments were carried out in two full factorial replicates, consisting of one tray of each combination of soil and treatment with three pots which contained four plants per genotype. This resulted in 24 individual measurements per experiment.

8.2.4.1.1 Pilot experiment

During a first iteration (experiment 'CAS I'), we tested the best suitable conditions for our experiments. The plants were grown at short day conditions in the semi-sterile greenhouse (8h of sunlight). Trays were prepared by placing flat plastic stands into greenhouse trays. An oversized capillary greenhouse mat (Vivaplus 3-Layer Capillary Matting, Thorntrees Amenity LTD) was placed onto the stand. The tray thus acted as a reservoir to supply the plants with irrigation medium throughout the experiment. Twenty four 9*9*9.5 (cm*cm*cm) square pots (e.g. growland Artikelnr. 15773, ca. 0.5L) in plastic grids were placed onto the capillary mats.

The plants were then transferred into the dry soil settled with water from the top. Afterwards the plants were watered with an initial 2L of rain water from the bottom.

8.2.4.1.2 Tray preparation

As described in (8.2.4.1.1), 12 – 24 pots per tray were filled with soil and directly placed into plastic trays containing the respective irrigation solution. The soil was then allowed to soak from the bottom for one to three hours. After 10-15 minutes, the CAS changed visibly in colour as it was saturating with liquid. We used this as visual confirmation of soil moisture saturation. Four seedlings per pot were then transferred to the indicated soil condition with either standard potting soil (only used for experiment 'CAS II') or CAS.

8.2.4.1.3 Sowing

Plants were germinated for 7 days on 1/2 MS agar plates as described above. The agar plates were opened in the greenhouse cabin. Next, a single seedling was picked up at the hypocotyl-root junction using a toothpick. The seedlings were carefully laid on top of the soaked soil and the roots gently pressed into the substrate with the toothpick.

8.2.4.1.4 Transfer and tray layout

Meanwhile, fresh capillary mat trays were prepared as indicated above and labelled for each condition. The individual pots were then transferred onto the capillary mat. Three pots with four plants per genotype were placed into each tray. Their position was randomly assigned and noted. If there was any remaining liquid from the soaking process it was added to the reservoir. After all pots were transferred, a picture was taken with a cell-phone camera (Samsung Galaxy S10 Lite) for documentation and the trays were covered with a transparent propagator lid for seven days.

8.2.4.1.5 Irrigation regiment

Upon seedling transfer the pots were initially soaked (7DAG/0DAT). In here, 1/6L was used per pot in each tray (e.g.: 24pots/tray = 4L irrigation liquid). After one additional week (14DAG), the propagator lid was removed and 1/12L per pot was added to the reservoir of each tray. After one additional week (21DAG), another 1/6L per pot was added to the reservoir of each tray. The plants were always irrigated with a fix volume and fertilizer concentration. No liquid was drained or added otherwise and mineral content can be considered to be cumulative throughout the experiments.

8.2.4.2 Fertilization of agricultural soil

For this experiment ('CAS II'), *Col-0* plants, two independent lines overexpressing NLS-NLP7 and NIGT1.1 in *pGPAT5::Citrine-SYP122* background as well as their parental line, *pGPAT5::Citrine-SYP122* were used. Plants were watered with rainwater, collected in a big reservoir outside the greenhouse (50°57'28.8"N 6°51'21.6"E). Since the rainwater showed visible algae growth, it was not used for following experiments. As fertilizer treatments 'Calcinite' and 'Wuxal' were mixed with rainwater as indicated above. The experiment was carried out in one tray per condition and four pots per genotype (n = 16). The pot location was not traced. Three weeks after transplantation, the trays were transported to the laboratory, the rosettes were cut and weighted with a fine scale.

8.2.4.3 Nitrogen fertilizer usage of endodermis mutant lines

For this experiment ('CAS III'), *Col-0, gelp*^{quintuple} and *pELTP::NLS-NLP7#4-20* in *pGPAT5::Citrine-SYP122* background as well as its parental line *pGPAT5::Citrine-SYP122* were used. Five pots per genotype were prepared as described above. Additionally, three empty pots containing four tooth picks were used as "unplanted" control. Each tray consisted of 24 pots The plants were sown onto natural and sterilized CAS and irrigated with de-ionized water, as well as Calcinite in de-ionized water. Three weeks after transplantation, soil, plant rosettes, and their root and rhizosphere, together with the soil matrix were harvested directly outside the greenhouse chamber. To do so, all individual rosettes were cut weighted and directly frozen in liquid nitrogen. The samples were stored at -70°C before being further processed for shoot transcriptomics and ionomics separately. Afterwards the pots were transported to the laboratory and the microbial samples were harvested.

For soil microbiome samples, ~1cm³ from "unplanted" pots was harvested with a metal spatula dispersed into a collection tube containing Lysing Matrix E (FastDNA Spin Kit for Soil, MP Biomedicals). For rhizosphere and endosphere samples, the moist soil and roots were taken out of the pot and split into two. The roots were then extracted by grasping the hypocotyl-root junction with a forceps and removing the majority of the soil, by ejecting ddH_2O onto the root system. Two root systems extracted that way were pooled and immersed into a 15mL Falcon tube containing 10mL deionized water. Thus, the majority of the remaining soil was washed off and collected in the tube. The root systems were removed for the endosphere samples and the tubes were stored at -20°C. For the rhizosphere samples the tubes were allowed to thaw at 4°C for 24h. Afterwards the supernatant was discarded. The sedimented soil was resuspended with a 1000µl pipette using a cut tip. Then, 300µl of the resuspension were added to a collection tube containing Lysing Matrix E snap frozen in liquid nitrogen and stored at -20°C until DNA extraction. For the endosphere samples, the two root systems were again immersed in a 15mL Falcon tube containing 10mL deionized water. The remaining soil particles were gently removed using metal forceps. The roots were then added to a collection tube containing Lysing Matrix E snap frozen in liquid nitrogen and stored at -20°C until DNA extraction.

This way, three soil microbiome samples, as well as six rhizosphere samples and six endosphere samples were collected per replicate and genotype. For natural soil, samples from all genotypes were extracted, while for sterile soil only samples from *Col-0* were extracted. Microbiome samples of the first replicate of all conditions and genotypes were retrieved on the day of harvest. The remaining pots were then stored at 4°C over night before harvesting the next day.

8.2.4.4 Nitrogen fertilizer usage in mutants of ion uptake and secondary metabolism

For this experiment ('CAS IV'), the following genotypes were used: *Col-0* wild-type plants in comparison to mutant plants impaired in *f6'h1* coumarin synthesis, *cyp79b2b3* indole glucosinolate biosynthesis, *f6'h1cyp78b2b3* secondary metabolite synthesis, *irt1* ferrous iron uptake¸ *amt1.2* high affinity ammonium uptake mutant, *nrt2.1* high affinity nitrate uptake mutant and *nlp7* nitrate signalling transcription factor. All genotypes were prepared and sown on natural and sterilized CAS and irrigated with water. After three weeks (28DAG) the plants were

moved to the laboratory and weighted using a fine scale. The individual rosettes were snap frozen in liquid nitrogen and stored at -20°C.

8.2.4.5 Nitrogen fertilizer usage in interdependence with Fraxetin and FeDTPA

For this experiment ('CAS V'), *Col-0, f6'h1* and *pELTP::NLS-NLP7#4-20* in *pGPAT5::Citrine-SYP122* background as well as its parental line *pGPAT5::Citrine-SYP122* were used. All genotypes were prepared and sown on natural and sterilized CAS. A tray consisted of 12 pots for this experiment. As control, the plants were irrigated with either 'Calcinite' or ddH_2O as indicated above. Additionally, the plants were supplicated with either 50µM Fraxetin (10.4085mg/L, Merck CAS 574-84-5) or 35µM Fe-DTPA (291.84µl/L IJzerchelaat DTPA 6%, Van Iperen International). Both chemicals were dissolved in either water or 'Calcinite'. The treatment was applied during each irrigation cycle. Two days before harvest (26DAG), each tray was supplied with an additional 2L of water only to keep the plants hydrated. After three weeks (28DAG) the plants were moved to the laboratory and weighted using a fine scale. The individual rosettes were snap frozen in liquid nitrogen and stored at -20°C.

8.2.4.6 Microbe re-inoculation of sterilized soil before nitrogen fertilization

A soil wash was generated from a new batch of CAS ('CAS-17') extracted from the same soil sampling-site in April 2023, removing the first 30cm of top soil (Durán et al., 2022; Harbort et al., 2020). The soil wash was obtained by modifying a previously established procedure (Durán et al., 2022) using 10kg of 'CAS-17' to generate 90mL of soil wash. First, the soil was transferred to a big open plastic container (620mm*360mm*320mm, polypropylen). Afterwards, 15L of extraction buffer consisting of 10mM tris(hydroxymethyl)aminomethane (TRIS, Sigma-Aldrich E201-064-4) pH 7.5, 0.1mM ethylenediaminetetraacetic acid disodium salt dihydrate (Na_2EDTA, Sigma-Aldrich E6635-100G) and 0.1% Triton X-100 (Sigma-Aldrich, CAS 9002-93-1) were added. To release the soil microbes, the soil and extraction buffer were continuously stirred for 45min using a metal shovel. Afterwards, the large soil particles were allowed to settle down for 15min. The supernatant was transferred into 400mL centrifugation tubes using a soup ladle and a plastic funnel which resulted to 9.6L of harvested extract. To eliminate the remaining soil particles, the extract was centrifuged for 5min at 300g (Beckman-Coulter, Avanti J-25, JA-10 Rotor). The supernatant, still turbid, was transferred to fresh 400mL centrifugation bottles. To obtain the microbial pellet, the samples were centrifuged for another 20min at 2000g. The supernatant was discarded. 80mL of 10mM $MgCl_2$ (sterile filtered, particle size <22µm) were added to one bottle and resuspended by shaking the bottle for ~1-3min. The resuspension was then transferred to the next bottle and the process repeated until all 24 pellets were resuspended in 10mM $MgCl_2$ into a total volume of 90mL. Lastly, the soil wash was split into two aliquots of 45mL. One aliquot was used as soil inoculum and the other one was passed again through a 0.22µm filter, using a vacuum pump, and served as a mock treatment. To confirm the presence of microorganism and the effective filtering of the mock treatment we then plated the solution onto TSB plates (see 8.1.4). Using inoculation loops, we streak-plated 5µl of the mock treatment as well as 5µl of a 1:1, $1:10^3$, $1:10^6$, $1:10^9$ dilutions.

For this experiment ('CAS VI'), the same genotypes; *Col-0, f6'h1* and *pELTP::NLS-NLP7#4-20* in *pGPAT5::Citrine-SYP122* background as well as its parental line *pGPAT5::Citrine-SYP122* were used. We modified the 9cm*9cm*9.5cm plastic pots by cutting them, effectively reducing their height by half. We then distributed the remaining 20kg of sterilized soil into eight

trays with 12 pots each, resulting in ~200g of soil per pot. We then placed them in a tray and added 1/6L per pot of 'Calcinite' or ddH_2O as described above. Additionally, we added 10mL of either soil wash or mock treatment to each tray. The trays were then covered with propagator lids and incubated overnight before continuing with the transplantation as described (8.2.4.1.4). The microbe inoculation was only performed once at the start of the experiment.

After three weeks (28DAG), the shoots were harvested and stored as described for previous experiments. Additionally, soil microbiome samples and rhizosphere and endosphere were collected from *Col-0* plants as described above (8.2.4.3).

8.2.5 Nucleic acid extractions

8.2.5.1 Plant DNA extraction

Plant DNA was extracted using hexadecyltrimethylammonium bromide (CTAB) (adapted from Porebski et al., 1997). In brief, sampling material was collected (leaf, root, flower etc.) in 1.1 micro dilution tubes with a metal ball-bearing inside. Samples were frozen in liquid N_2 and were ground with homogenizer (Qiagen TissueLyser II Bead Mill) for at 30Hz for 45s. Samples were thawed on ice for 15min then 200µl of CTAB buffer were added into each tube and incubated at 70°C for 1h. Samples were cooled down for 10min at room temperature before adding 200µl of Chloroform and vortexing. Debris was precipitated by centrifugation at 3900rpm for 10min (or 6000rpm for 5min, depending on the centrifuge used). After centrifugation 125µl of the upper aqueous phase was transferred into the new microfuge tube containing 125µl isopropanol and were pipette mixed. Samples were centrifuged at 3900rpm for 25min (or 6000rpm for 15min) to pellet out the DNA. The supernatant was discarded and 150µl of 70% EtOH was added to wash the pellet with another centrifugation at 3900rpm for 10min (or 6000rpm for 5min). Supernatant was removed and the pellets were air-dried for 30min under a fume hood. DNA was resuspended in 100µl Tris-EDTA buffer and dissolved by incubating for 30min at 37°C whilst shaking.

Table 10: CTAB extraction buffer

Chemical	Concentration	For 400 mL	Remark
Cetyl-trimetyl-ammonium bromide (CTAB)	2% (w/v)	8g	Toxic, use fume hood
NaCl	1.4 M	32.72g	
Tris-HCl (pH 8)	100 mM	4.85g / 40mL (40mL 1M)	Add some HCl to dissolve
EDTA-NaOH (pH 8)	20mM	2.978g / 16mL (16mL 0.5M)	

Table 11 TE buffer (pH 8.0)

Chemical	Concentration	For 100 ml	Remark
TRIS	10mM	1mL 1M TRIS-HCl (pH 8.0)	Add some HCl to dissolve
EDTA	1mM	0.2mL 0.5M EDTA-NaOH (pH 8.0)	

8.2.5.2 Microbial DNA extraction

Microbial DNA was isolated following the user manual for the FastDNA™ SPIN Kit for Soil (MP Biomedicals)

8.2.5.3 RNA extraction

For the TRAP experiments RNA was extracted using a TRIzol™ (Invitrogen Cat. No.15596-026) and chloroform-based extraction (122 Appendix II: TRAP protocol"). Total RNA was extracted adapted from the user manual for the ReliaPrep™ RNA Tissue Miniprep System (Promega, Z6112). Here the tissue lysis and RNA extraction was performed using a TRIzol™ (Invitrogen Cat. No.15596-026) and chloroform-based extraction (122 Appendix II: TRAP protocol"). After incubation the precipitation, wash and DNase I treatment were performed as per user manual (ReliaPrep™ RNA Tissue Miniprep System (Promega, Z6112).

8.2.6 DNA amplification

8.2.6.1 Plant genotyping

We used polymerase chain reaction (PCR) (Schochetman et al., 1988). Transgenic lines overexpressing either NLP7 or NIGT1.1 were previously generated. We confirmed the insertion by amplifying a sequence from the promoter region of *ELTP* into the coding sequence of either *NLP7* or *NIGT1.1* (Table 12). Amplification of a PCR product is only possible if the construct is present (Figure 15).

Table 12: Primers used for genotyping in this study

Nr.	Name	Sequence 5´-->3´	Size	Annealing temp	Description	By
TGA_363	NLS_For	CCAAAGAAGAAGAGGAAGGTT	21	54	Full At "nucleus localization signal" (NLS) sequence	Tonni Grube Andersen
TGA_364	NLS_Rev	AACCTTCCTCTTCTTCTTTGG	21	54	Full reverse At "nucleus localization signal" (NLS) sequence	Tonni Grube Andersen
TGA_567	GFP_QPCR_For	CCTGAAGTTCATCTGCACCA	20			Federica Locci
TGA_568	GFP_QPCR_Rev	GGTCTTGTAGTTGCCGTCGT	20			Federica Locci
TGA_780	Gt_pELTP_FOR	tcatgtctacgtggcgttgt	20	59	Genotyping_close to ATG	Noah Kürtös
TGA_781	Gt_gNLP7_REV	CGGAAAGAAGGAACACCGGA	20	57	Genotyping_ first exon	Noah Kürtös
TGA_782	Gt_gNIGT1_REV	AGGGAGCTCACGTTGAAAGA	20	56	Genotyping_ first exon	Noah Kürtös
TGA_868	Gt_pCASP1_For	TTTTTGTTTGGGCTGGCGCT	20	61	Genotyping	Noah Kürtös
TGA_869	Gt_CDEF_CDS_Rev	AAACACGAAGTAACACGGCG	20	59	Genotyping	Noah Kürtös
TGA_870	Gt_pELTP_For_v2	TCTTCCGGTGACGATGCTTTA	21	58	Genotyping early pELTP promotor region	Noah Kürtös

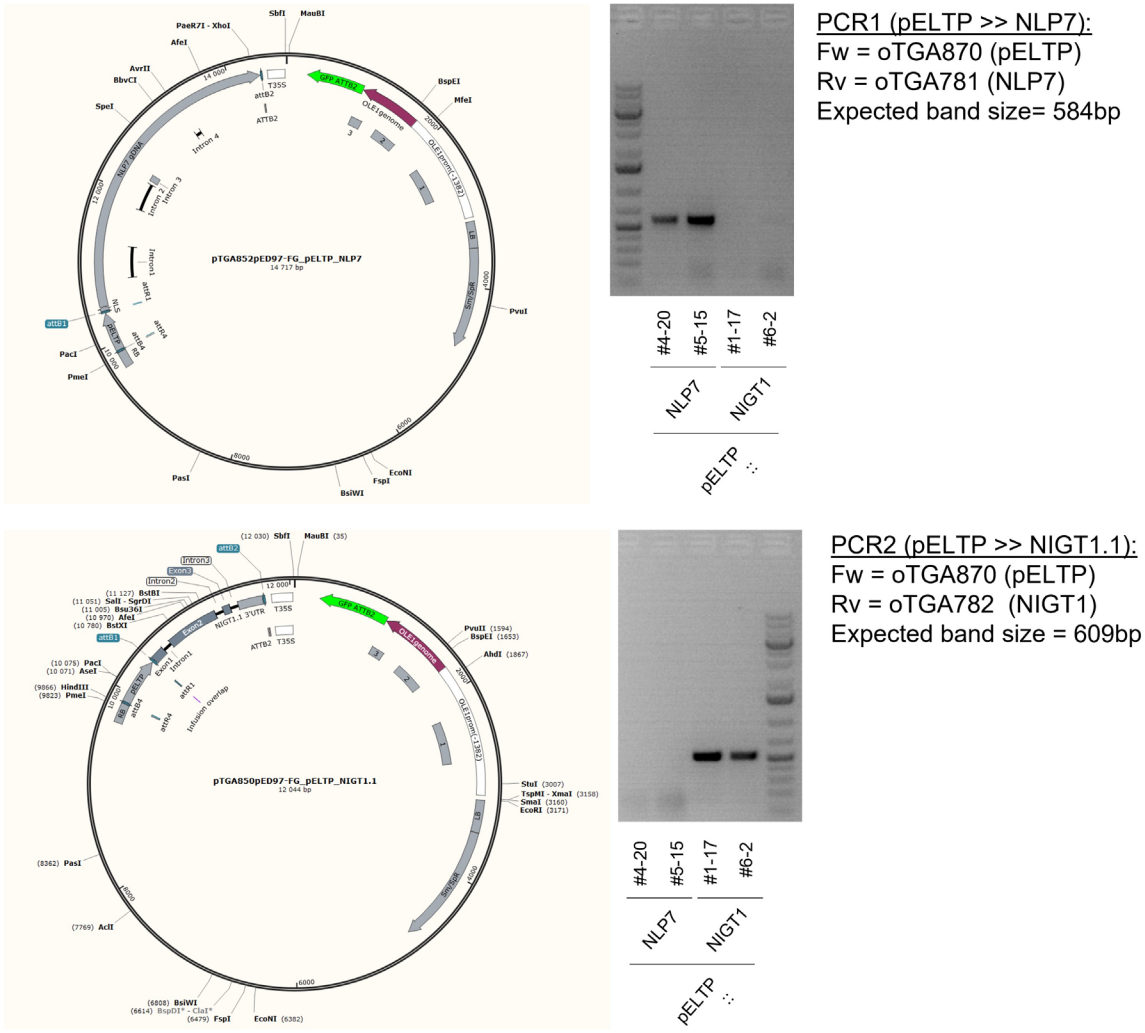

Figure 15: ***Vectormaps for endodermal overexpression constructs and PCR validation of the insertion in the T_3 lines used in this study:***

8.2.6.2 16S and ITS amplification

The amplification of bacterial 16S rRNA and internal transcribed spacer (ITS) was performed as previously described (Harbort et al., 2020; Shen et al., 2023; Wippel et al., 2021) using primers designed for the NovoSeq pipeline. In brief, after isolation (8.2.5.2), DNA was quantified using SYBR® Green I nucleic acid gel stain (Merck, 163795-75-3) and DNA was diluted to <1ng/µl. The 16S or ITS DNA from individual microbial samples was amplified in a first PCR (PCR1). Residual primers and enzymes were then digested using antarctic phosphatase (New England Biolabs, M0289L). DNA quantity was estimated via agarose gel electrophoresis and the input for the next PCR adjusted to 5-10µl. In the second PCR (PCR2) individual barcodes were added to each sample (multiplexing). Lastly the samples were pooled and the 16S amplicon was purified via a second agarose gel electrophoresis followed by gel purification (Gel and PCR Clean-up, MACHERY-NAGEL GmbH & Co. KG, 74060.50). PCR2 products were then concentrated using AMPure XP (Beckman Coulter, A63882) magnetic beads. Pooled DNA was stored at -20°C before sending for sequencing by Novogene UK Ltd.

8.2.7 Shoot and soil ion concentration measurements

After harvest, soil and shoot material used for ionomic analysis was freeze-dried using a lyophilizer for 2-4 days (CHRIST, Alpha 1-4 LSC, Ser.No.14492). Soil was then analysed for pH, nitrate (NO_3^-) content and iron ($Fe^{2+/3+}$) content by the Mediterranean Agronomic Institute of Chania, Greece (CIHEAM). Dried shoots were analysed for shoot nitrate (NO_3^-), sulphate (SO_4^{2-}) and phosphate (PO_4^{3-}) content via IC-MS by Dr. Sabine Metzger at the University of Cologne (UoC)

8.2.8 Bioinformatics

Sequencing data was processed in a Linux shell environment on a local processing unit (MPIPZ, dell-node-11). Sequencing results were trimmed using *trimmomatic* (Bolger et al., 2014) and aligned to the *Arabidopsis thaliana genome* [Araport11 genome release, (Cheng et al., 2017)] via *HISAT2* (Kim et al., 2019) and count tables were generated using *HTSeq* (Anders et al., 2015). Differentially expressed gene (DEG) analysis was carried out in an R environment using DESeq2 (Love et al., 2014) and *edgeR* (Y. Chen et al., 2014). As indicated, the reads were filtered for minimum counts per million (cpm) across all samples (threshold = 3*n) and a minimum cpm within all samples per condition (threshold = 10) to account for outliers and non-expressed genes (DeSEQ2_TMM.R, Table 13). To determine top DEGs, a score was calculated by combining the adjusted p-value and the log2(fold change). The detailed analysis of TRAPseq data is highlighted in (15 Appendix I: Translating ribosome affinity purification as tool to resolve tissue-specific post-transcriptional profiles). Further processing of the data is indicated in the respective figures generated and in the scripts used to generate them (Table 13).

Table 13: List of R scripts and functions created for this work and the packages used within

Name	Type	Packages used	Usage	Contributors
DeSEQ2_TMM.R **DeSEQ2_TMM_NT3.R** **DeSEQ2_TMM_CAS3.R**	script	edgeR, glue, stringr, dplyr, DESeq2, sva, tibble	TRAPseq RNAseq	Noah Kürtös Niklas Kiel
k-means_clustering_analysis_cluster_abundance.R **k-means_clustering_analysis_heatmap.R**	script	'readr', 'magrittr', 'tibble', 'tidyr', 'dplyr', 'glue', 'dynamicTreeCut', 'DESeq2', 'cluster', 'gplots, 'dendextend', 'ggplot2', 'ggtree', 'ggdendro', 'RColorBrewer', 'gridExtra' 'grid', 'scales', 'ggrepel'	TRAPseq	Noah Kürtös
DeSEQ2_gene_expression_v2.R **DEG_HeatmapsNT3.R**	script	'readr', 'magrittr', 'tibble', 'tidyr', 'dplyr' 'glue', 'dynamicTreeCut', 'DESeq2' 'cluster', 'gplots', 'ggh4x', 'ggplot2' 'ggdendro', 'RColorBrewer', 'gridExtra' 'grid', 'scales', 'ggrepel', patchwork	TRAPseq RNAseq	Noah Kürtös

Name	Type	Packages used	Usage	Contributors
geom_volcanoplot_v7.R	function	ggplot2, ggrepel, glue, DESeq2, dplyr	TRAPseq RNAseq	Noah Kürtös
plotPCA_modified.R	function	DESeq2	TRAPseq RNAseq	Michael Love Noah Kürtös
counts_roots_heatmap.R	function	glue, DESeq2, cowplot	TRAPseq	Noah Kürtös
dend_data_custom.R	function	None	TRAPseq	Noah Kürtös
geom_counts.R	function	DESeq2, tidyverse glue	TRAPseq	Noah Kürtös
tidy_suberin_df_v2.R	function	None	Suberization plots	Noah Kürtös
ggplot_suberin_df_v5.R	function	tidyverse	Suberization plots	Noah Kürtös
Tukey_Segami_v2.R **tukey_df_v1.R** **tukey_suberin_df_v2.R**	function	Glue, dplyr, multcomp	Suberization plots	Shoji Segami Noah Kürtös
geom_suberin_abs_v4.R **geom_suberin_rel_v3.R**	function	Tidyverse, scales	Suberization plots	Noah Kürtös
empty_map.R	function	ggplot2 tidyverse maps, dplyr	GWAS analysis Katz et al., 2022	Noah Kürtös
GWAS_raw_performance.R **GWAS_no3_preference.R**	function	tidyverse ggrepel	GWAS analysis Katz et al., 2022	Noah Kürtös

8.2.8.1 Statistics

The data was tested for normal distribution using a variance test for normality (Shapiro & Wilk, 1965). If not stated otherwise, statistical differences were calculated as indicated by the post-hoc Tukey's HSD (honestly significant difference) test (Tukey, 1949) using the *multcomp* package in R (Hothorn et al., 2008).

8.2.8.2 Data visualisation

All plots were generated using the packages of the *tidyverse* library (Wickham et al., 2019) or their extensions (Table 13). in R studio (rstudio.com) using R (https://cran.r-project.org/).

8.2.8.3 Data availability

All raw data and scripts and stl designs used in this study are available on request and will be published on GitHub at the same time of respective peer reviewed article(s) emerging from this study.

9 Author Contributions

The project was conceptualized and initiated by Dr. Tonni Grube Andersen (TGA) and Noah Kürtös (NoK). Funding was obtained by TGA (Alexander von Humboldt foundation) and NoK (IMPRS). The project was supervised by Prof. Dr. Paul Schulze-Lefert (PSL), TGA as well as, Dr. Ruben-Garrido Oter (RGO) and coordinated by Dr. Stephan Wagner (SW). Dr. Eliza Loo (EL) provided valuable input. Vector construction and cloning was carried out by TGA. Phylogenetic analysis of *NRT* and *NPF* genes was carried out by Oliver Johandrees (OJ). The protocol for total RNA extraction was adapted by Dr. Julia Holbein (JH). The RNAseq pipeline was established jointly with Niklas Kiel (NiK). Coumarin extraction was done together with Silvina Perin (SP). GC-MS and subsequent analysis was done by SP. During 'CAS III' Bart Boesten (BB) and TGA assisted with plant rosette harvesting and Dr. Sebastian Samwald (BS), Swati Mahiwal (SwM) and BB assisted with the acquisition of the microbial samples. Dr. Sabine Metzger (SaM) measured the shoot ion content of the 'CAS III' experiment. Lioba Rüger (LR) helped during the setup, irrigation and harvest of the experiments 'CASIV', 'CAS V' and 'CAS VI'. Dr. Stéphane Hacquard (SH) and Dr. Paloma Duran (PD), provided information on the soil wash protocol ('CAS VI'). Ralf Equit (RE) cut the pots for 'CAS VI'. DNA extraction, amplicon and library preparation, as well as microbiome analysis was carried out collaboratively with LR. ASV table generation from 16S amplicons was performed by LR using a pipeline from Dr. Pengfan Zhang (PZ). Information on greenhouse environmental conditions and CAS soil parameters were obtained by Aristeidis Stamatakis (AS).

10 Corrigendum

Between the submission of this work (25.09.2023) and its publication on the Kölner UniversitätsPublikationsServer (KUPS, https://kups.ub.uni-koeln.de/, 29.01.2024), some grammatical erros and typos were corrected in the monograph. The scientifically non-relevant sections 11 "Acknowledgments" and 12 "PhD Metadata" were extended. Moreover, there was an error in the design file used to plot the data in Figure 13 leading to missannotation of some data points and wrong colour assignment in panel C. The figure was corrected but the original, faulty figure was attached as Supplemental figure 18.

11 Acknowledgments

First and foremost, I would like to thank **Tonni Grube Andersen.** We experienced science during the Covid19 pandemic together, we recovered from failed experiments and samples lost in custom. But we also had great discussions, pondering about the wonders of life. You were very supportive of my scientific career and in the end I consider this project a result of our collective effort.

Paul Schulze-Lefert, I would like to thank for supporting me during my TAC meetings throughout the last three years but also for taking me in with the Rooters. I was quite oblivious towards plant-microbe interactions before I started this PhD and I learned so, so much. Similarly I would like to thank **Ruben Garido-Oter** and **Eliza Loo** for being part of my TAC meetings and giving me critical advice but also support in the beginning of the journey. Here I would also like to thank the IMPRS and **Stephan Wagner**, who was a pillar of professionalism and always took the time to discuss also individual matters. It was also a pleasure to work together with you during my time as a PhD representative

Anne Krapp, Stanislav Kopriva and **Bart Thomma** I would like to thank for taking the time of reading through my thesis and being part of my defense committee. I am greatly looking forward to our discussion.

I would also like to thank all of my colleages at the MPIPZ for supporting my endeavours during this time: from the **Greenhouse Team** I would like to thank especially Aristeidis Stamatakis, Andreas Lautscham, Monika Bürgel, Sybille Richter and John Sattelberger. From **IT**, I would like to thank especially Marc Thoben, Marco Rupp, Erik Nießen, José Reza and Gunter Thiel. From the **Technical Service** I would like to thank especially Ralf Equit and Renate Michalowski-Schröder.

I would also like to thank all **my friends inside and outside the institute** who contributed to this work by discussing with me encouraging me or just enduring my “scientific fun facts” and lastly **my family and close friends** who gave me love and support especially in the final stretches. I will make sure to let them know of their contributions in the following. Words can not express how much your big and small gestures helped me through the PhD but I tried anyway:

Aaron Lawson	for being the definition of dedication. You are a beast and great motivation!
Alessandro Popoli	for reminding my why science can be awesome: looking beyond the edge of human knowledge
Ananda Buchmüller	die beste Schwester der Welt zu sein. Immer für mich da zu sein. Mir zu sagen, dass ich okay bin so wie ich bin!
Annabelle Mattern	für gemeinsame Back-, Koch und Gesangsstunden
Anthony Piro	for kind words of support especially during the writing phase, and for coumarin discussions (written and spoken)

Birgitta Kürtös	dafür, dass du eine liebevolle Mutter bist und auch wenn unsere Lebensansätze unterschiedlich sind versuchst mich in allem zu unterschützen was ich tue
Carlos Duran Ballesteros	garcias por las sonrisas, todos los abrazos, las chismes y por pedir contra mi en ping pong
Charles Copeland	for being polite and indismissive about my weird sceintific ideas ideas but also for being a great party host
Christoph Köhler	for sharing my passion for metal and crustaceans and the many shared journeys
Clara Stock	proving that avocados can survive if taken care of well enough(so i should care enough!) and for teaching me an important lesson about evolution and languages and arrogance
Claudia Buzdumovic	dafür dass du bedingslos liebevoll bist. Ob es gebackene Plätzchen, Fotoalben oder Pflänzchen sind
Daniel Scholten	for his trust in my abilities and treating me level-headed from the start
Danijel Majic	dafür zu zeigen, dass Familie und Science auch vereinbar sein können und für 3D-Project-Unterstüzung
Defeng Shen	for his advice and proof reading the results
Dirk Keller	for his incredible trust and discovering his love for plants, like me, a bit later in life
Enric Bertran Garcia de Olalla	por veniste conmigo por todo la camina desde heidelberg hasta colonia
Everardo Rodriguez	por ser mi amigo. Que ha empezó con una camina en Heidelberg culminó en viajes juntos. Te estoy admirando por tambien trabajando en industria quedes tu curiosidad sceintifico.
Fantin Mesny	for helping me out of ditch autoclaving dirt together
Federica Locci	for advice but also the occasional cigarette and for creating podcast-worthy voice messages
Felix Getzke	together with Jana you were the senior PhDs to look up to, thanks for providing advice
Florian Kümmel	for being my favorite island boy
Frederick Finckh	for his love, respect and astonishing intellect. All the way from introducing me to honey mead, the physics of black holes to introducing me to Noah junior
Frederickson Dayag Entila	Salamat Panginon! For all the time we spent together in the gym, all the banter, all the PhD-support-group talks we had and lastly for also reading through my materials and methods in the end

Gauthier Weissbart	for sharing some of my quirky philosophical views and pre-/post-gym beers
Giuliana Hessler	für die GuMos aus dem Off und für konditionslose Schokoladenriegelfinanzierungshilfen
Hannah Walter	dafür der beste Support der Welt zu sein. Danke für die unterstützenden Worte, Korrekturlesen und Kaffeepausen. Für Brettspielabende und Roadtrips. Für alles!
Hennriette Läßle	Wir sind Macher*innen!
Jana Ordon	together with Felix you were the senior PhDs to look up to, thanks for providing advice
Jazmin Reyes Hernandez	por mostrarme el mundo y compartir mi amor por las cosas verde (Somos hobbits orgullosos!).
Jesús Praena-Tamayo	por compartir mi fascinación por la ciencia (+fiction), por compartir la cultura de nerdismo y mostrarme su hogar
Joel Fernandes	for sharing coffee, ping pong and chess enthusiasm
Johannes Lehmann	for his love and inadequate admiration. For taking us and himself not too seriously. For shared glasses of wine, shared tears and smoked cigars
Joram Dongus	for integrating me into the institute society rather swiftly.
José Flores-Uribe	por tu experiencia bioinformatica y en cocinar mole
Jozefien Van de Velde	Dankjewel for your respect and trust in me as a friend
Junli Wang	for german-mandarin practice and for using my volcano-plot script
Ka-Wai Ma	for encouraging words on the occasional bus-stroll.
Kathrin Wippel	for great discussions and for being a great scientist to look up to!
Keeichi Hasegawa	ごはんそしてビールはありがとうございました
Lara Van Dijck	Dankjewel for all the bike rides together, encouraging smiles and being the bold direct person you are. Please don't change!
Lars Hellweg	du alter Bufferino! Ich bewundere deine kompromisslos saubere Wissenschaft und deine geerdete Art
Laura Armbrust	for listening to my troubles, consulting me for plant shenanigans, joint cooking and hosting me for not always (completely) sober occasions
Laura Ruppert	for journeying togehter with me to islands and through the PhD. I hope we will enjoy our harbours
Lea Rehm	for sharing her fascination on pokémon and bacterial motility with me

Leonie Kraska	for all the shared lunches, pizza, fights, beers, bike rides and scientific discussions. Especially during the pandemic you kept my sanity together. You were, are and will be a great scientist!
Lioba Rüger	for her physical help with managing the final soil experiments, her bioinformatic help untangling the microbiome data and lastly for mental support and chocolate croissants
Lisa Brombach (Clark)	for supporting me from afar (a.k.a another building) and for being a great co-rep
Lisa Over	for walks around the pond in the rain and reminding me gently of how little i know outside the four walls of my mind
Lukas Engling	for being a great friend over long years. Always having an open ear and expanding my horizons
Lukas Stier	for my being my great little bro. You took a different path but damn you are dedicated. Thanks for being there when needed, no questions asked
Marc Somssich	for proof-reading the intro. Thanks for your hard words.
Marco Castellani	Il diacono! Thank you for being a great and gentle support, joint climbing sessions and always being upbeat.
Marian Gropp	for being one of my best friends. For all the times we drank, danced, discussed, terraformed mars and conquered middl earth. I am proud of you becoming a dad and I am looking forward to us getting old together
Marion Jespersen (MJ)	for many shared adventures and for going through the same but very different struggle at the same time. I admire your scientific grit! A lot.
Martha Thellmann	for the TRAP protocoll and TRAP lines and for a supportive call when things weren't working.
Megan Sierz	for sharing a passion for Spanish, Japanese and swimming
Milena Malisic	for the great discussions we have about science but also evenings spend together hugs and words of support when needed
Mohamed Redha El Amine Herma	for being PhD rep with me and our joint effort to improve things at the institute
Nawid Albinger	for the incredible friendship we share for more than a decade! For many discussions about science (I look up to you so much), magic, life and life science xRaptorGenesisP. To many more shared decades and our contributions.
Niklas Bub	for as despite our physical distance we grow closer every year. I admire you for your fusion of science and spirituality. Thank you

	for being my crutch when i needed you and allowing me to be yours when you needed one.
Niklas Kiel	for all the coding sessions together sucessfully in bash or less sucessfully in javascript. For the SWARM!
Nora Papadima-Karanikou	for productive Sunday café sessions and many shared beers over the years
Oliver Johanndrees	for your help with the iTOL but also sharing the office with me. Your ability to stay calm in distress ("resilient") is admirable.
Paloma Duran	por su ayuda con llavar la tierra pero tambien por nuestros discussiones durante nuestro tiempo juntos aqui
Pascal Krohn	I am quite glad I could convince you to be the coffee lord with me. Thank you for the drinks shared, early morning coffee rides and blundered chess games
Paul Kajdewicz	für seine besonne Art und den kleinen Lötkurs zwischendurch
Pegah Jabbari Lak	for making me fall in love with this city and making me feel at home whenever we are together
Peter Pavlasek	dafür dass du deinen Teil dazu beigetragen hast, dass ich hier bin
Philip Stier	mein geliebter Bruder. Danke, dass du mich teilweise durch die schwierigeren Phasen gecarried hast. Unsere gemeinsamen LoL und HerrDerRinge Abende bedeuten mir die Welt
Philipp Scherer	for being a phenomenon of a person. You are a wizard: Always appearing when least expected but mostly appropriate. Thanks for helping me to take me less seriously
Qiaochu Shen	for the occasional snack keeping me sane during the writing period
Rainer Waadt	like three years back: thank you for your teachings of order and death metal and for your respect
Ram-Sevak Raja-Kumar	நன்றி for your support your warm laughter and hugs when needed!
Réjane Carron	of course for the last three years but especially for going through the writing phase together with me. I am curious where life will take us but building that vegan cheese factory with Leonie didn't sound too bad
Rigel Salinas-Gamboa	gracias tía por las noches de bailar, de deporte y compartir nuestras vidas con nosotras. Te apprecio.
Sabine Görtz	for always sharing a smile of encouragement
Sebastian Samwald	for being part of the Andersen family and for reading through my materials and methods

Shawn Kramer	for having the heart of a lion! Thank you for your hugs, your respect and your hosted parties.
Simone Remmel	für die Zeit die gemeinsame Zeit im Andersen Labor.
Siva Subramanian Ayeraselvan	நன்றி for the unconditional kindness of letting me crash at the guesthouse to safe time while writing
Sonja Krabatnik	for the bond we share. I think you are a powerfull scientist and I admire your brains but also the ability to keep your balance. Thank you for hosting me in Copenhagen
Sonja Vögeler	dafür dass du mir hilfst meine Leidenschaft in meiner Haut zu verewigen
Sophie-Asako Xerri	朝食のサポートはありがとう
Stefan Strütt	für Schach und ggplot Lektionen
Stéphane Hacquard	pour son conseil mais aussi pour les mots honnêtes sur la vie en science
Swati Mahiwal	for occasional snacks and words of encouragement. Ich weiß das sehr zu schätzen
Tak Lee	가함삼니다 for untangling some of the theory of clustering
Thomas Ryohei Nakano	一番コーヒー飲む人
Thomas Stier	for being my father, for being the driver of my curiousity. For teaching me that logic and the scientific method can solve most problems. For supporting phyiscally, finacially and emotionally in times of need. I am what I am because of you
Tobias Kleefisch	for being a great roommate, a great personal trainer, for making me feel at home in cologne and last but not least for being a great pasta to charcoal converter
Viktor Mamontov	Спасибо for your calm but friendly way and your willingness to help
Yang An	for being my brother from another mother. Even if we don't talk much or in less intervals I always carry you. But nonetheless, I will be better! I am proud of what we became
Yasir Tamal	for his enouragement and support and outdoor chess sessions, despite his unwillingness to wear a jacket in winter
Yoonkeum Oh	가함삼니다 for her dedication, for tasty 비빔밥 and to our work and kindness thereafter.
Zsófia Winter	türelméért és megnyugtató szavaiért

12 PhD Metadata

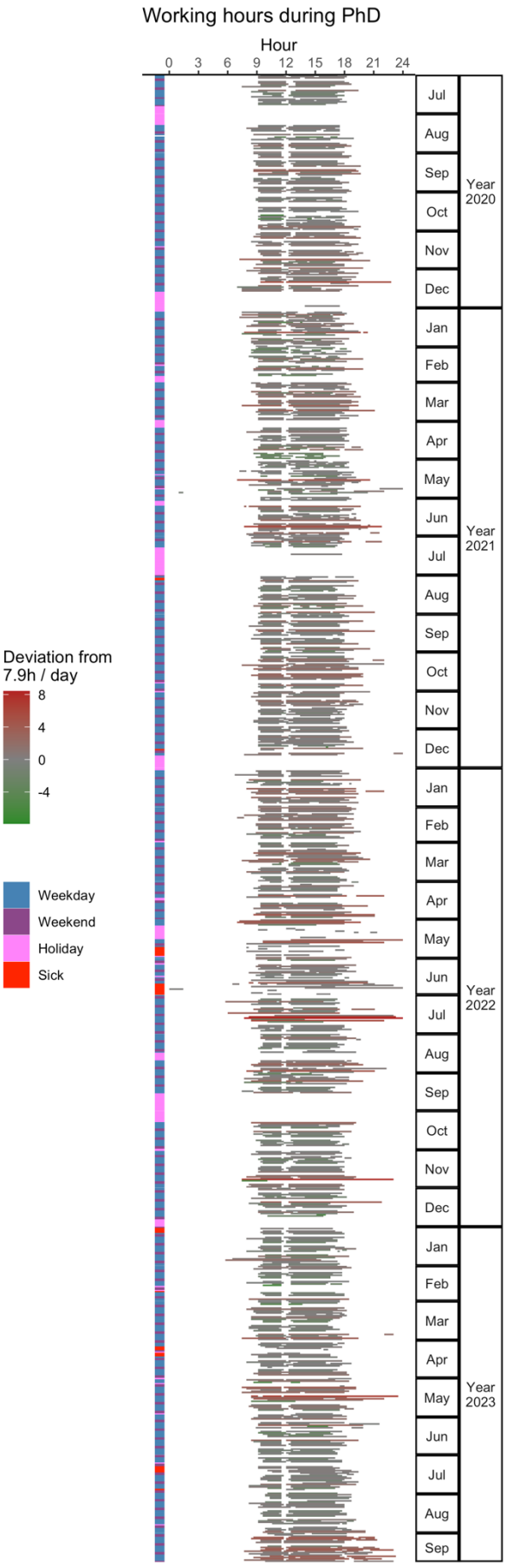

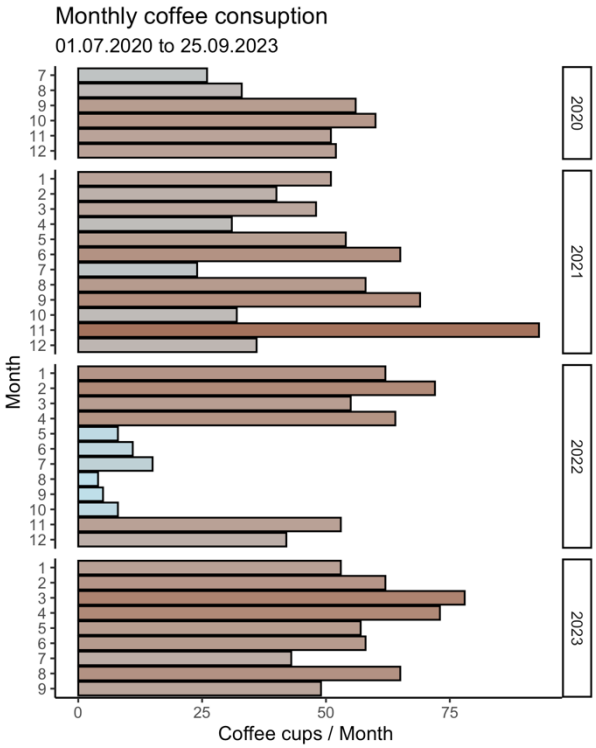

Total cups of coffee consumed:	1816
Liters of coffee consumer:	218L
Grams Caffeine consumed:	87g
Money spent on coffee:	454€

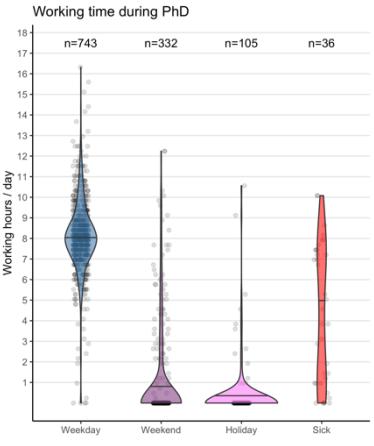

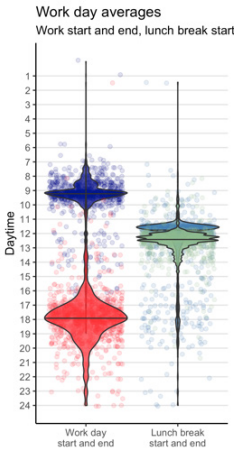

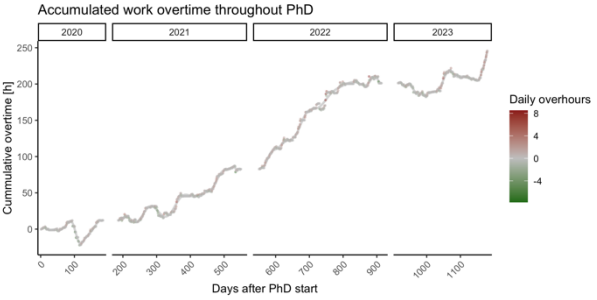

13 List of abbreviations

Abbrevi-ation	Description
4CL	4-COUMARATE-COA LIGASE
AA	amino acid
AAP	AMINO ACID PERMEASE
ABA	abscisic acid
ABCG	ATP-BINDING-CASSETTE transporter G-family PROTEIN
ABI2	ABA-INSENSITIVE 2
AGI	*Arabidopsis thaliana* gene identifier
AGT	ALANINE:GLYOXYLATE AMINOTRANSFERASE
AHC	ALKYL HYDROXY CINNAMATE
AIC	Akaike information criterion
Ala	Alanine, amino acid
AMT1	AMMONIUM TRANSPORTER 1
AMT2	AMMONIUM TRANSPORTER 2
ANS	ANTHOCYANIDIN SYNTHASE
AON	autoregulation of nodulation
Arg	Arginine, amino acid
ASFT	ALIPHATIC SUBERIN FERULOYL TRANSFERASE
BIC	Bayesian information criterion
bp	base pairs
BR	Brassinosteroid
BSK1	BR-SIGNALLING KINASE 1, BRASSINOSTEROID SIGNALLING KINASE 1
BT1	BTB DOMAINE CONTAINING PROTEIN 1
BT2	BTB DOMAINE CONTAINING PROTEIN 2
C3H	COUMARATE 3-HYDROXYLASE
C4H	CINNAMIC ACID 4-HYDROXYLASE
CAD	CINNAMYL ALCOHOL DEHYDROGENASE
CAP1	[Ca2+]cyt-ASSOCIATED PROTEIN KINASE 1
CBL	CALCINEURIN-B LIKE PROTEIN
CCoAOMT	CAFFEOYL CoA3-O-METHYLTRANSFERASE
CCR	CINNAMOYL-COA REDUCTASE
CDEF1	CUTICLE DESTRUCTION FACTOR !
CEP	C-TERMINALLY ENCODED PEPTIDE
CEPR	CEP-RECEPTOR 1, C-TERMINALLY ENCODED PEPTIDE RECEPTOR
ChIP-seq	Chromatin ImmunoPrecipitation DNA-Sequencing
CHS	CHALCONE SYNTHASE
CIPK	CBL-INTERACTING PROTEIN KINASE
CIPK2	CALCINEURIN B-LIKE PROTEIN-INTERACTING PROTEIN KINASE 2
CK	Cytokinin
Cl^-	chloride
CLE	CLAVATA/ESR-RELATED
CLSM	confocal laser scanning microscope
CLV1	CLAVATA1 (CLV1)

Abbrevi-ation	Description
CoA	CoenzymeA
COMT	CAFFEATE/5-HYDROXYFERULATE3-O-METHYLTRANSFERASE
CPK	CALCIUM DEPENDENT KINASE
CPL3	RNA POLYMERASE II C-TERMINAL DOMAIN PHOSPHATASE-LIKE 3
CS	Casparian Strip
CST	CAST AWAy
CTAB	hexadecyltrimethylammonium bromide
CW	Calcufluor white
CYP86A1	CYTOCHROME P450 ENZYME 86A1, HORST
CYP86B1	CYTOCHROME P450 ENZYME 86B1, RALPH
DAG	Days after germination
DAT	Days after transfer
DEG	Differentially expressed gene
DFR	FIHYDROFLAVONOL 4-REDUCTASE
DNA	Desoxyribonucleic acid
DUR	DEGRADATION OF UREA
EDTA	ethylenediaminetetraacetic acid disodium salt dihydrate
ELTP	ENDODERMIS LIPID TRANSFER PROTEIN, LTPG16
ER	endoplasmatic reticulum
F3'H	FLAVANONE 3'-HYDROXYLASE
F5H	FERULATE 5'-HYDROXYLASE
F6'H1	FERULOYL-COA 6-HYDROXYLASE1
FACT	FATTY ALCOHOL:CAFFEOYL-CoA CAFFEOYL TRANSFERASE
FAD	Flavin adenine dinucleotide
FAR	FATTY ACYL REDUCTASE
FRO2	FERRIC REDUCTION OXIDASE 2
FY	Fluorol Yellow 088
GA	gibberellin
GELP	GDSL-TYPE ESTERASE/LIPASE
GFP	GREEN FLUORESCENT PROTEIN
Gln	Glutamine, amino acid
GLR	GLUTAMATE LIKE RECEPTORS
Glu	Glutamate, amino acid
Gly	Glycine, amino acid
GO	gene ontology
GOGAT	GLUTAMINE OXOGLUTARATE AMINOTRANSFERASE, GLUTAMATE SYNTHASE
GPAT	GLYCEROL-3-PHOSPHATE ACYLTRANSFERASE 5
GSL	glucosinolates
H	His, histidine, amino acid
H_2	elemental hydrogen
ha^{-1}	per hectare
HATS	High Affinity Transport System
HCT	HYDROXYCINNAMOYL-COA SHIKIMATE/QUINATE HYDROXYCINNAMOYL TRANSFERASE

Abbrevi-ation	Description
HHO	HOMOLOGUE OF HRS1
HNO_3	nitric acid
HRS	HYPERSENSITIVE TO LOW PI-ELICITED PRIMARY ROOT SHORTENING
HY5	ELONGATED HYPOCOTYL5
IAA	indole-3-acetic acid
IC-MS	ion chromatography couple mass spectrometry
ICP-MS	inductively coupled plasma mass spectrometry
IOS1	IMPAIRED OOMYCETE SUSCEPTIBILITY 1
IRT1	IRON-REGULATED TRANSPORTER1
ITS	internal transcribed spacer
JA	jasmonate
K	potassium
KCS2	BETA-KETOACYL-COA SYNTHASE2, DAISY
KCS20	BETA-KETOACYL-COA SYNTHASE20
KIN7	KINASE 7
LACS	LONG-CHAIN ACYL-COA SYNTHETASE
LATS	Low Affinity Transport System
LBD	LATERAL BOUNDARY DOMAIN 37
LHT	LYS/HIS TRANSPORTER
LR	lateral root
MAP	PUTATIVE MITOGEN-ACTIVATED PROTEIN KINASE
Mg	Magnesium
miR	micro RNA
mM	millimole, 10^{-3} M
Mo-MPT	molybdenum-molybdopterin
mRNA	messenger RNA
MS	Murashige and Skoop 1962 plant media
MYB	MYB DOMAIN PROTEIN
N	nitrogen
N_2	elemental dinitrogen
NAR1.1	NUCLEAR ARCHITECTURE RELATED homologue
NAR2.1	NITRATE ASSIMILATION RELATED 2.1
NEK6	NEVER IN MITOSIS GENE A-RELATED KINASE 6
NFC	nitrogen fixing clade
NH_3	ammonia
NH_4^+	ammonium
NIA1	NITRATE REDUCTASE 1, NR1
NIA2	NITRATE REDUCTASE 2, NR2
NIGT1.1	NITRATE-INDUCIBLE, GARP-TYPE TRANSCRIPTIONAL REPRESSOR 1.1, HRS1 HOMOLOGUE 1, HHO3
NIGT1.2	NITRATE-INDUCIBLE, GARP-TYPE TRANSCRIPTIONAL REPRESSOR 1.2, HRS1 HOMOLOGUE 1, HHO2
NIGT1.3	NITRATE-INDUCIBLE, GARP-TYPE TRANSCRIPTIONAL REPRESSOR 1.3, HRS1 HOMOLOGUE 1, HHO1

Abbrevi-ation	Description
NIGT1.4	NITRATE-INDUCIBLE, GARP-TYPE TRANSCRIPTIONAL REPRESSOR 1.4, HRS
NiR	NITRITE REDUCTASE, NiR1
NLP	NIN-LIKE PROTEIN 1, NODULE-INCEPTION-LIKE PROTEIN
NO	nitric oxide
NO_2	nitrogen dioxide
NO_2^-	nitrite
NO_3^-	nitrate
NPF	NRT1/PTR FAMILY, NITRATE TRANSPORTER 1 / PEPTIDE TRANSPORTER FAMILY
NPF1.1	NRT1/PTR FAMILY, NITRATE TRANSPORTER 1 / PEPTIDE TRANSPORTER FAMILY 1.1, NRT1.12
NPF1.2	NRT1/PTR FAMILY, NITRATE TRANSPORTER 1 / PEPTIDE TRANSPORTER FAMILY 1.2, NRT1.11
NPF2.12	NRT1/PTR FAMILY, NITRATE TRANSPORTER 1 / PEPTIDE TRANSPORTER FAMILY 2.12, NRT1.6
NPF2.13	NRT1/PTR FAMILY, NITRATE TRANSPORTER 1 / PEPTIDE TRANSPORTER FAMILY2.13, NRT1.7
NPF2.3	NRT1/PTR FAMILY, NITRATE TRANSPORTER 1 / PEPTIDE TRANSPORTER FAMILY 2.3
NPF2.7	NRT1/PTR FAMILY, NITRATE TRANSPORTER 1 / PEPTIDE TRANSPORTER FAMILY 2.7, NITRATE EFFLUX 1
NPF2.9	NRT1/PTR FAMILY, NITRATE TRANSPORTER 1 / PEPTIDE TRANSPORTER FAMILY 2.9, NRT1.9
NPF4.6	NRT1/PTR FAMILY, NITRATE TRANSPORTER 1 / PEPTIDE TRANSPORTER FAMILY 4.6, NRT1.2
NPF5.5	NRT1/PTR FAMILY, NITRATE TRANSPORTER 1 / PEPTIDE TRANSPORTER FAMILY 5.5
NPF6.2	NRT1/PTR FAMILY, NITRATE TRANSPORTER 1 / PEPTIDE TRANSPORTER FAMILY 6.2, NRT1.4
NPF6.3	NRT1/PTR FAMILY, NITRATE TRANSPORTER 1 / PEPTIDE TRANSPORTER FAMILY 6.3, NRT1.1
NPF7.2	NRT1/PTR FAMILY, NITRATE TRANSPORTER 1 / PEPTIDE TRANSPORTER FAMILY 7.2, NRT1.8
NR	NITRATE REDUCTASE
NRE	nitrate responsive *cis*-element
NRT1	NITRATE TRANSPORTER
NRT2	NITRATE TRANSPORTER 2
NRT3	NITRATE TRANSPORTER3, *Chlamydomonas rheinhardtii* NAR2.1 homologue
NUE	nitrogen use efficiency
PAL	PHENYLALANINE AMMONIALYASE
PC	Passage Cells
PC	Principal component
PCA	Principal component analysis
PCD	programmed cell deat
PCoA	Principil Coordinate Analysis
PCR	polymerase chain reaction
PDLP	PLASMODESMATA-LOCATED PROTEIN
PEP	ENDOPEPTIDASE

Abbrevi-ation	Description
pH	power of hydrogen, potential of hydrogen, pondus hydrogenI
PHO1	PHOSPHATE1
P_i	inorganic phosphorus
PM	plasma membrane
PNR	PRIMARY NITRATE RESPONSE
PPP	phenylpropanoid pathway
ProT	PROLINE TRANSPORTER
RIN	RNA integrity score
RNA	Ribonucleic acid
ROS	reactive oxygen species
RPL18	RIBOSOMAL PROTEIN L18
RSA	root system architecture
S8H	SCOPOLETIN 8-HYDROXYLASE
SCR	SCARECROW
scRNAseq	single cell RNA sequencing
SNRK2.4	SUCROSE NONFERMENTING 1-RELATED KINASE 2.4
SSS	SODIUM-SOLUTE SYMPORTERS
SynCom	synthetic microbial community
TGA1	TGACG SEQUENCE-SPECIFIC BINDING PROTEIN 1
TGA4	TGACG SEQUENCE-SPECIFIC BINDING PROTEIN 4
TM	transmembrande domain
TMM	trimmed mean of M values
TOR	TARGET OF RAPAMYCIN
T-PMT	transmitted detection module with a photon counting module
TRAP	Translating Ribosome Affinity Purification
TRAPseq	Translating Ribosome Affinity Purification sequencing
TRIS	tris(hydroxymethyl)aminomethane
UMAMIT	USUALLY MULTIPLE ACIDS MOVE IN AND OUT TRANSPORTER
WRKY53	WRKY DNA-BINDING PROTEIN 53
WSS	within sum of squares

14 List of figures

14.1 Main text figures

14.2 Supplemental figures

14.3 Appendix figures

15 List of tables

16 Supplementary figures

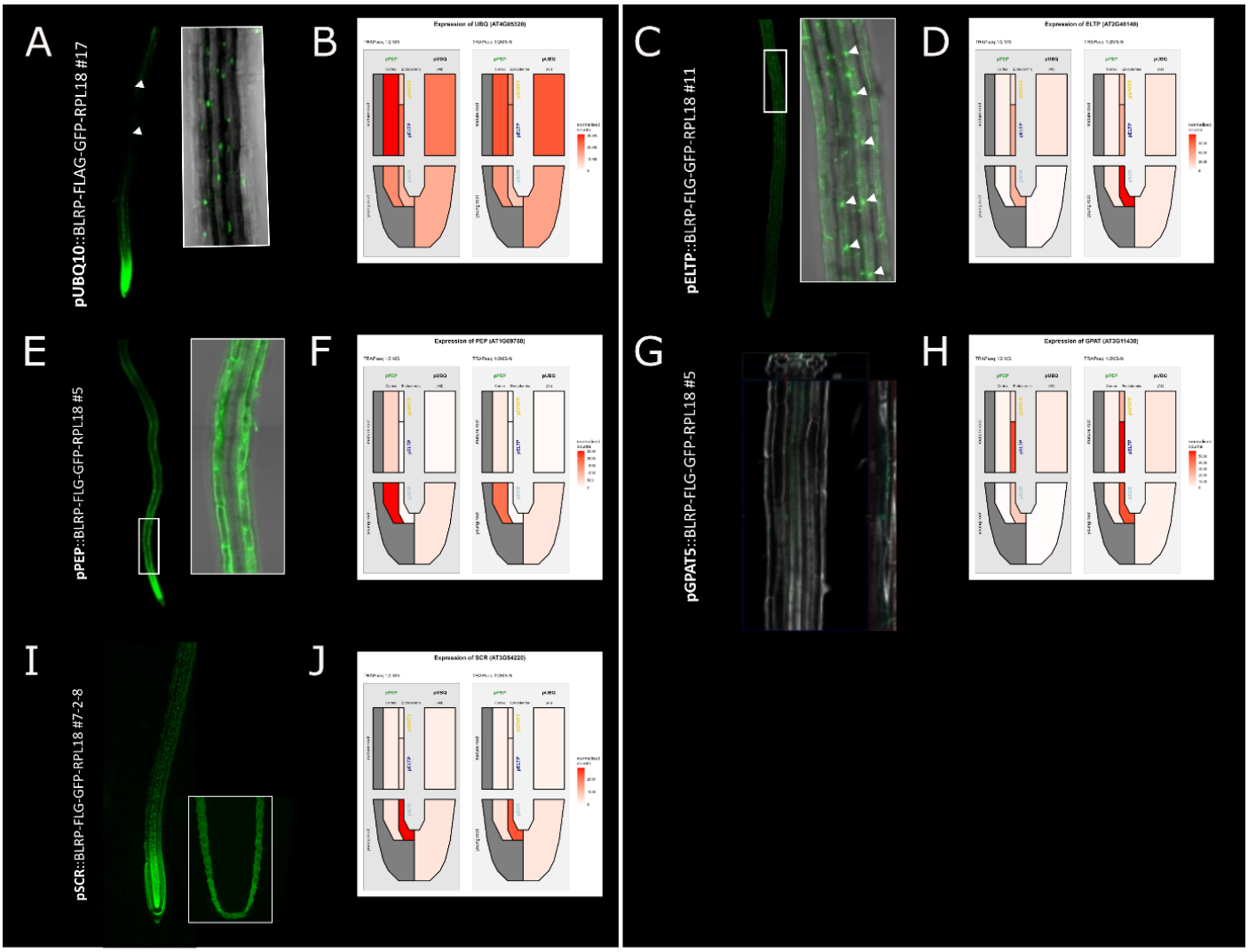

Supplemental figure 1: **Expression of the TRAP construct under tissue-specific promoters:** Ubiquitous (pUBQ), cortex-specific (pPEP), young endodermis (pSCR), mature endodermis (pELTP) and suberizing cells (pGPAT). Plants were grown for 8 days on 1/2 MS. A, C, E, Whole root was imaged as tiled scan using CLSM. Magnifications show an overlay of the T-PMT and GFP channel. A, C Arrowheads indicate nucleoli. C, E White rectangles indicate magnified area if applicable. G Seedlings stained with calcofluor white (CW) before imaging. Image depicts an overlay of CW and GFP. I Image of whole root was taken with an epifluorescence stereo microscope. Magnification shows airy scan of a root from a different experiment. B, D, F, H, J Minecraft-plots for the indicated gene itself after bioinformatic processing. Left plot indicates 1/2 MS condition and right plot indicates 1/2 MS-N condition.

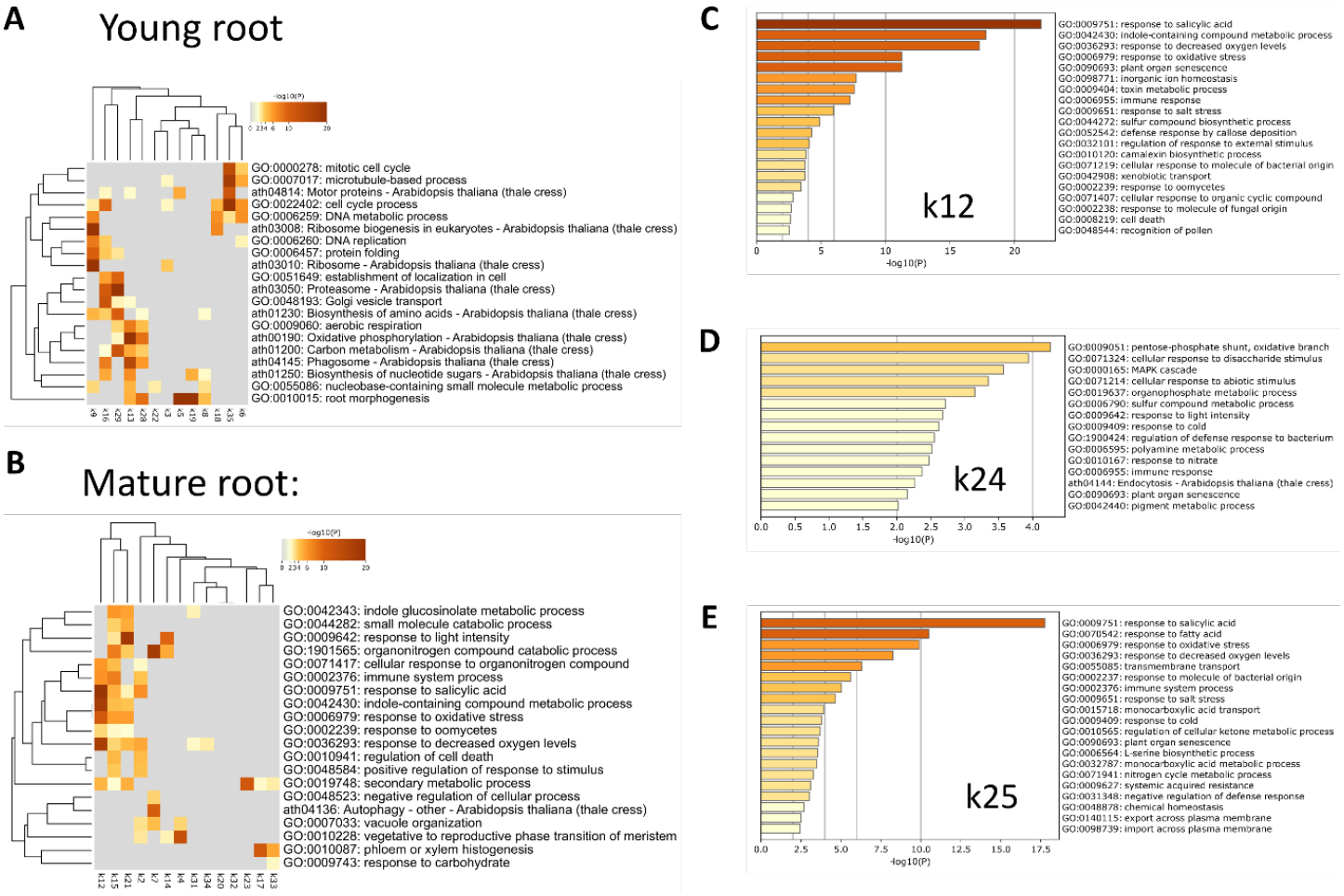

Supplemental figure 2 ***Gene ontology term analysis performed with Metascape****:* (Zhou et al., 2019)*: **A-B** GO terms determined for all genes across clusters specific to the root zones. Color indicates significance of enrichment. Grey colour indicates that the GO-term was not significantly enriched in that cluster. **A** GO analysis of young root. **B** Go analysis of mature root. **C** GO enrichment for all genes in cluster k12. **D** GO enrichment for all genes in cluster k24. **E** GO enrichment for all genes in cluster k125.*

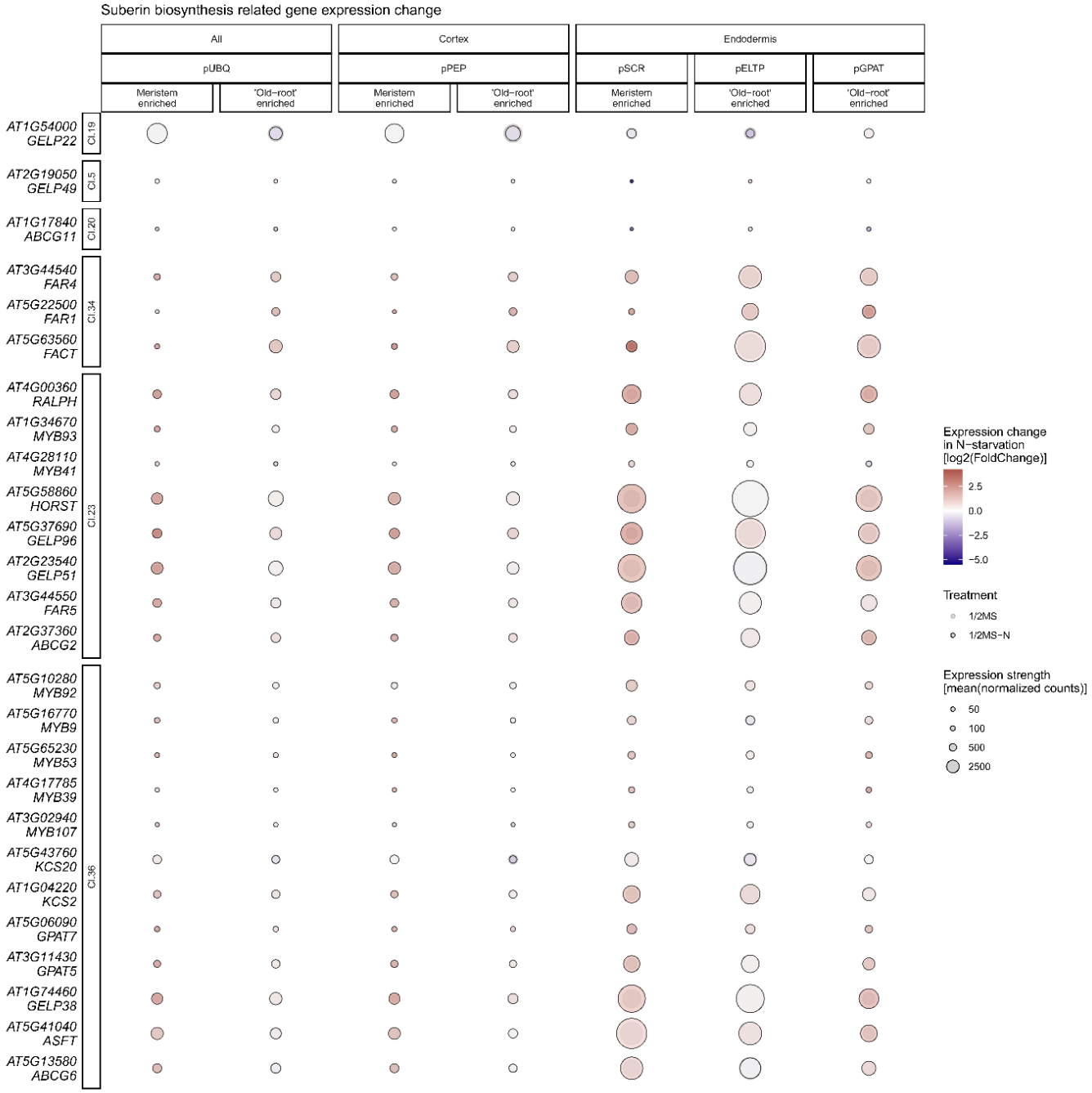

Supplemental figure 3 ***Expression halo-plot of suberin synthesis genes:*** *Grey circles indicate the mean, normalized counts of TRAPseq profiles from 1/2 MS grown plants. Colored circles indicated the mean, normalized counts of TRAPseq profiles form 1/2 MS-N grown plants. Color indicates the log2(FoldChange). Accordingly, larger red circles indicate induction upon nitrogen starvation and smaller blue circles indicate repression upon nitrogen starvation. The x-axis is facetted for the tissue, then promoters, then young and mature root. The y-axis is facetted for the individual k-clusters. Genes are indicated by name and AGI.*

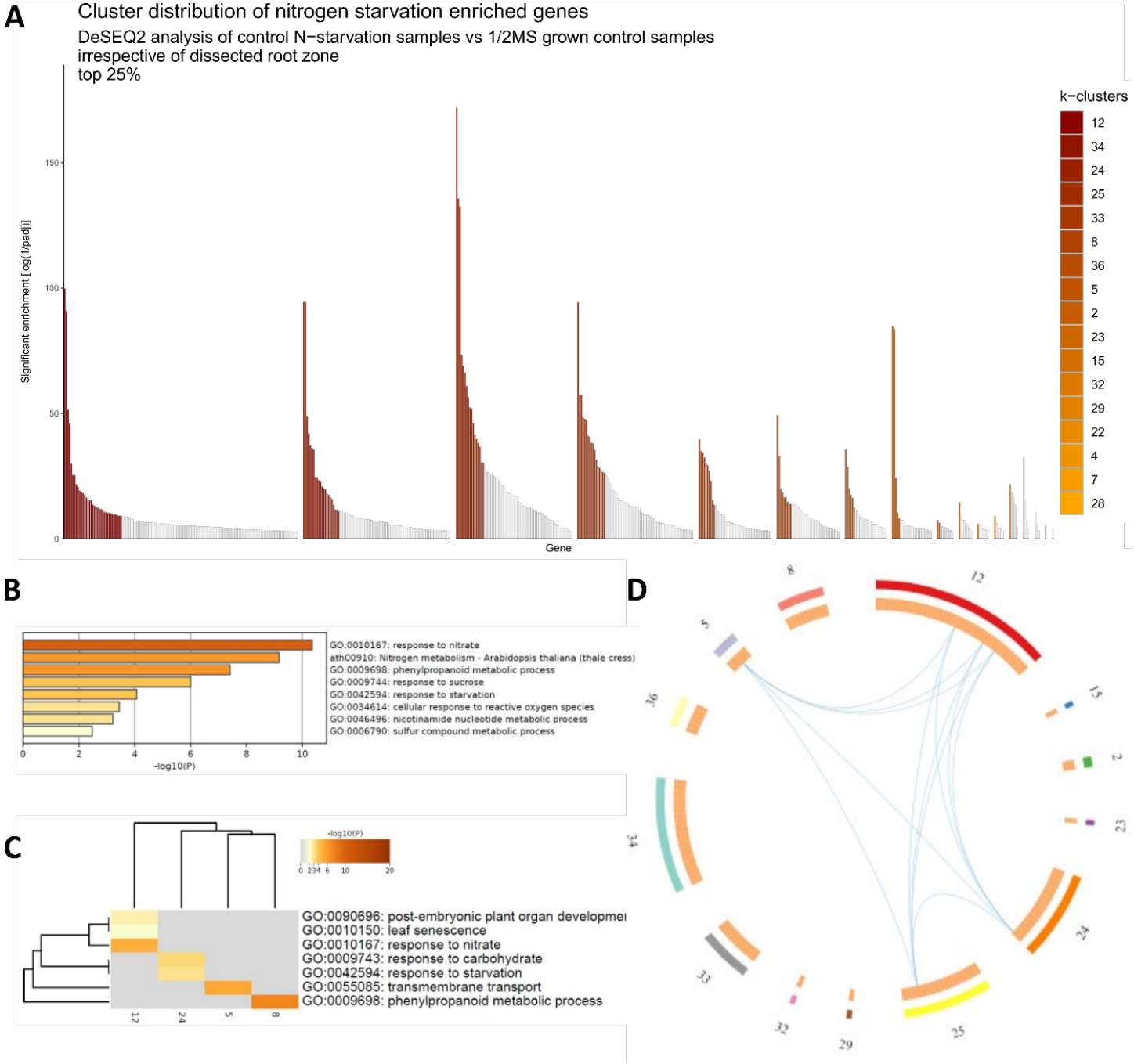

Supplemental figure 4 ***Tissue unspecific nitrogen starvation cluster gene ontology term analysis performed with Metascape*** (Zhou et al., 2019)*: **A** DEG analysis of "UBQ" post-transcriptome grown on 1/2 MS-N vs "UBQ" post-transcriptome grown on 1/2 MS. Genes are facetted per cluster and the top 25% of each cluster are highlighted. The colors indicated the cluster. These genes (n=127) were then used for GO-enrichment analysis. **B** Bulk GO terms across clusters. **C** GO-enrichment across clusters. **D** Overlap of gene ontologies across clusters.*

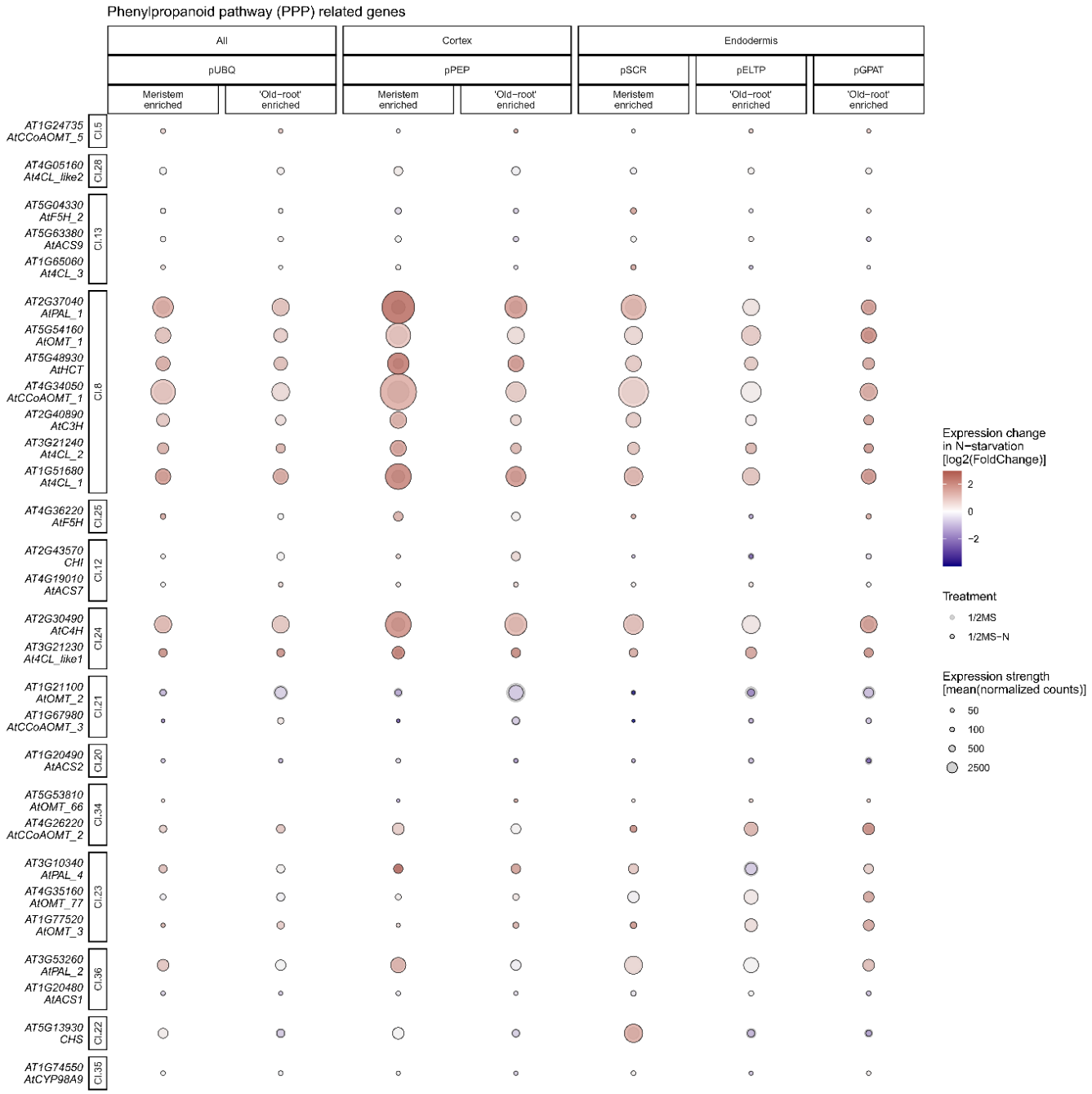

Supplemental figure 5 ***Expression halo-plot of phenylpropanoid pathway (PPP) genes:*** *Grey circles indicate the mean, normalized counts of TRAPseq profiles from 1/2 MS grown plants. Colored circles indicated the mean, normalized counts of TRAPseq profiles form 1/2 MS-N grown plants. Color indicates the log2(FoldChange). Accordingly, larger red circles indicate induction upon nitrogen starvation and smaller blue circles indicate repression upon nitrogen starvation. The x-axis is facetted for the tissue, then promoters, then young and mature root. The y-axis is facetted for the individual k-clusters. Genes are indicated by name and AGI.*

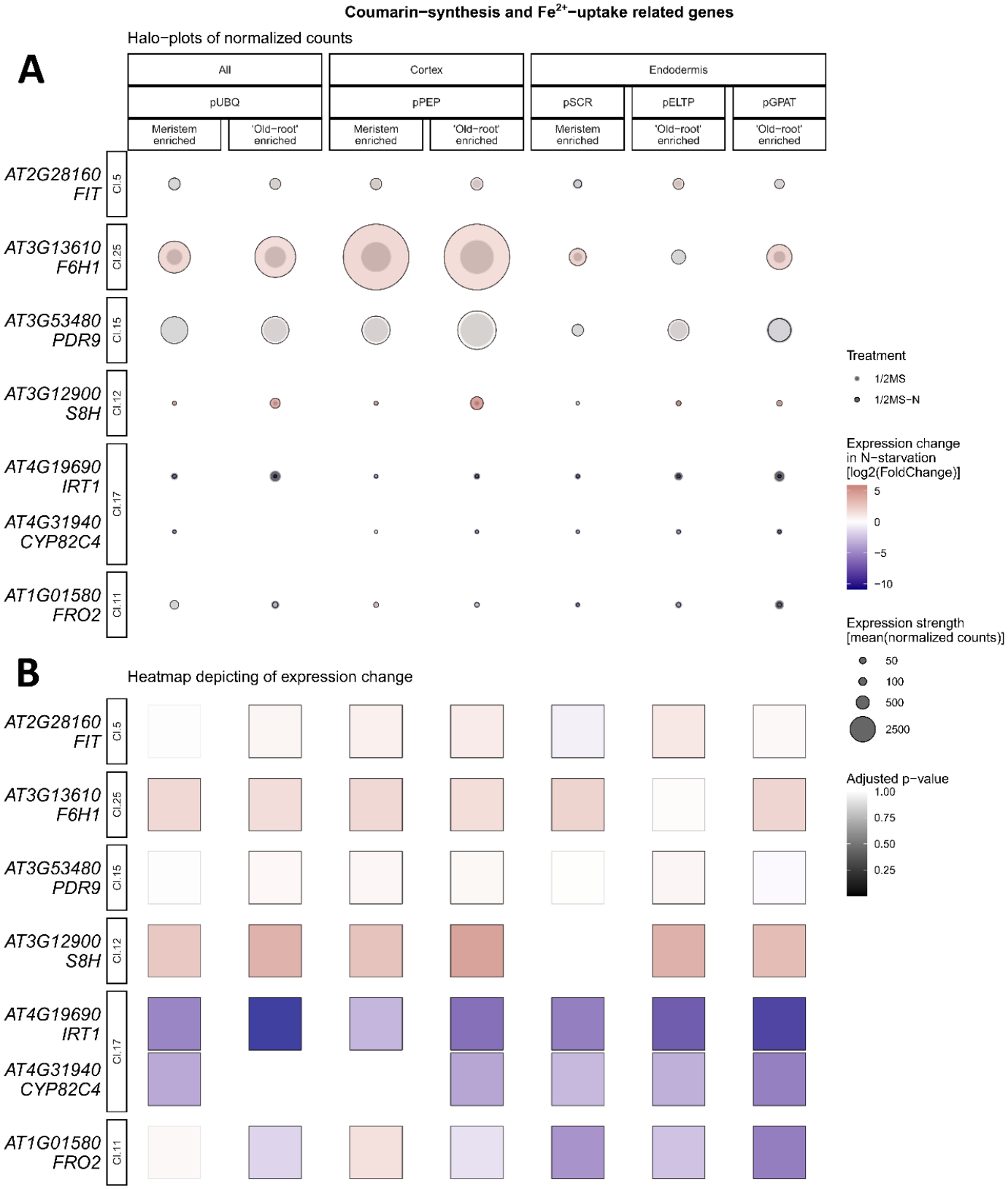

Supplemental figure 6 ***Expression Coumarin biosynthesis and related Fe²⁺-uptake genes: A*** *Halo-plot. Grey circles indicate the mean, normalized counts of TRAPseq profiles from 1/2 MS grown plants. Colored circles indicated the mean, normalized counts of TRAPseq profiles form 1/2 MS-N grown plants. Color indicates the log2(FoldChange). Accordingly, larger red circles indicate induction upon nitrogen starvation and smaller blue circles indicate repression upon nitrogen starvation. The x-axis is facetted for the tissue, then promoters, then young and mature root. The y-axis is facetted for the individual k-clusters. Genes are indicated by name and AGI.* ***B*** *Heatmap. Color indicates log2(FoldChange) as above and borders indicated adjusted p-values*

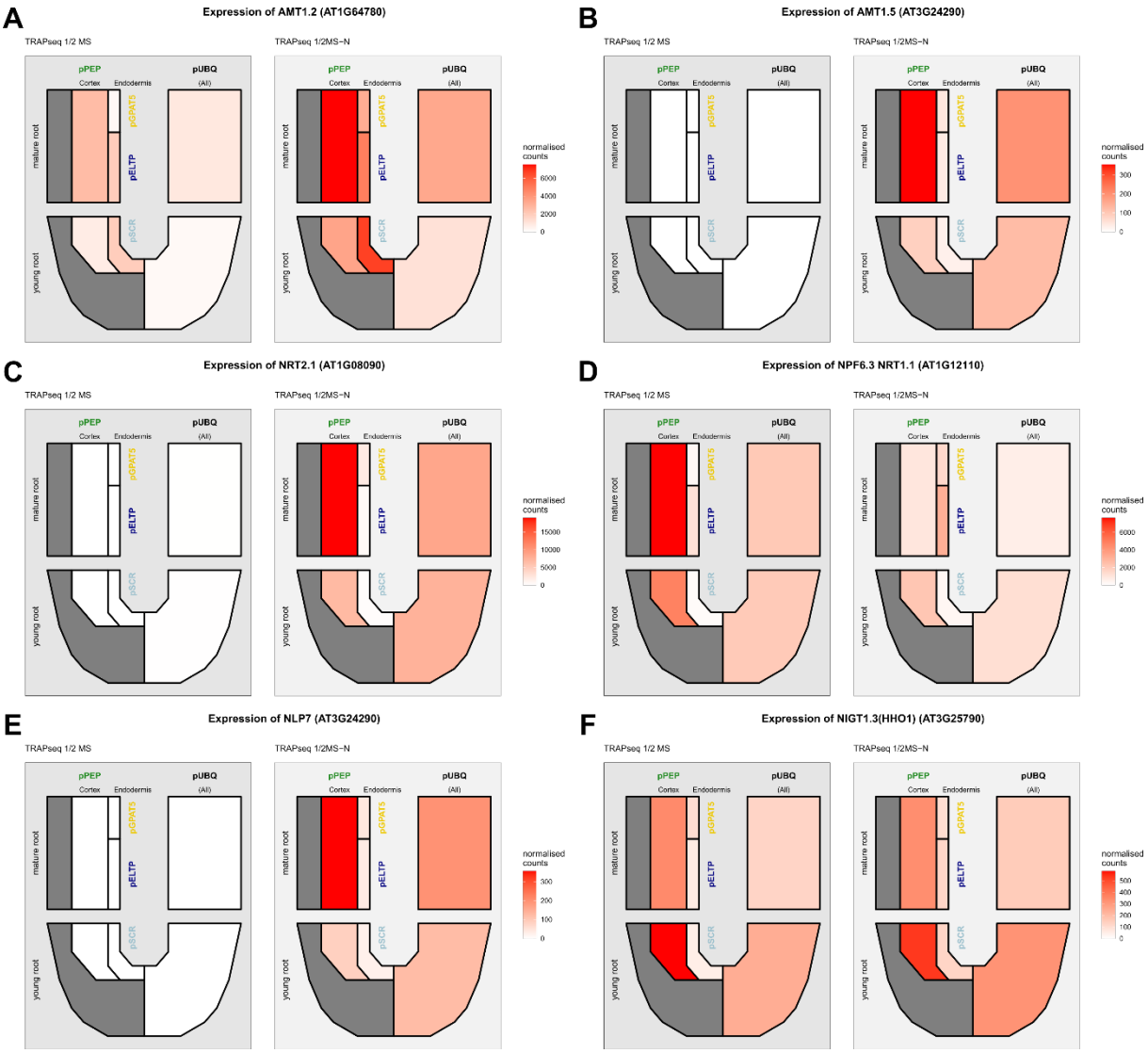

Supplemental figure 7 ***Minecraft-plots for genes related to nitrogen transport or transcriptional regulation:*** *Minecraft plots were done after bioinformatic processing. Left plot indicates 1/2 MS condition and right plot indicates 1/2 MS-N condition.* ***A*** *AMT1.2 expression.* ***B*** *AMT1.5 expression.* ***C*** *NRT2.1 expression.* ***D*** *NPF6.3 expression.* ***E*** *NLP7 expression.* ***F*** *NIGT1.3 expression.*

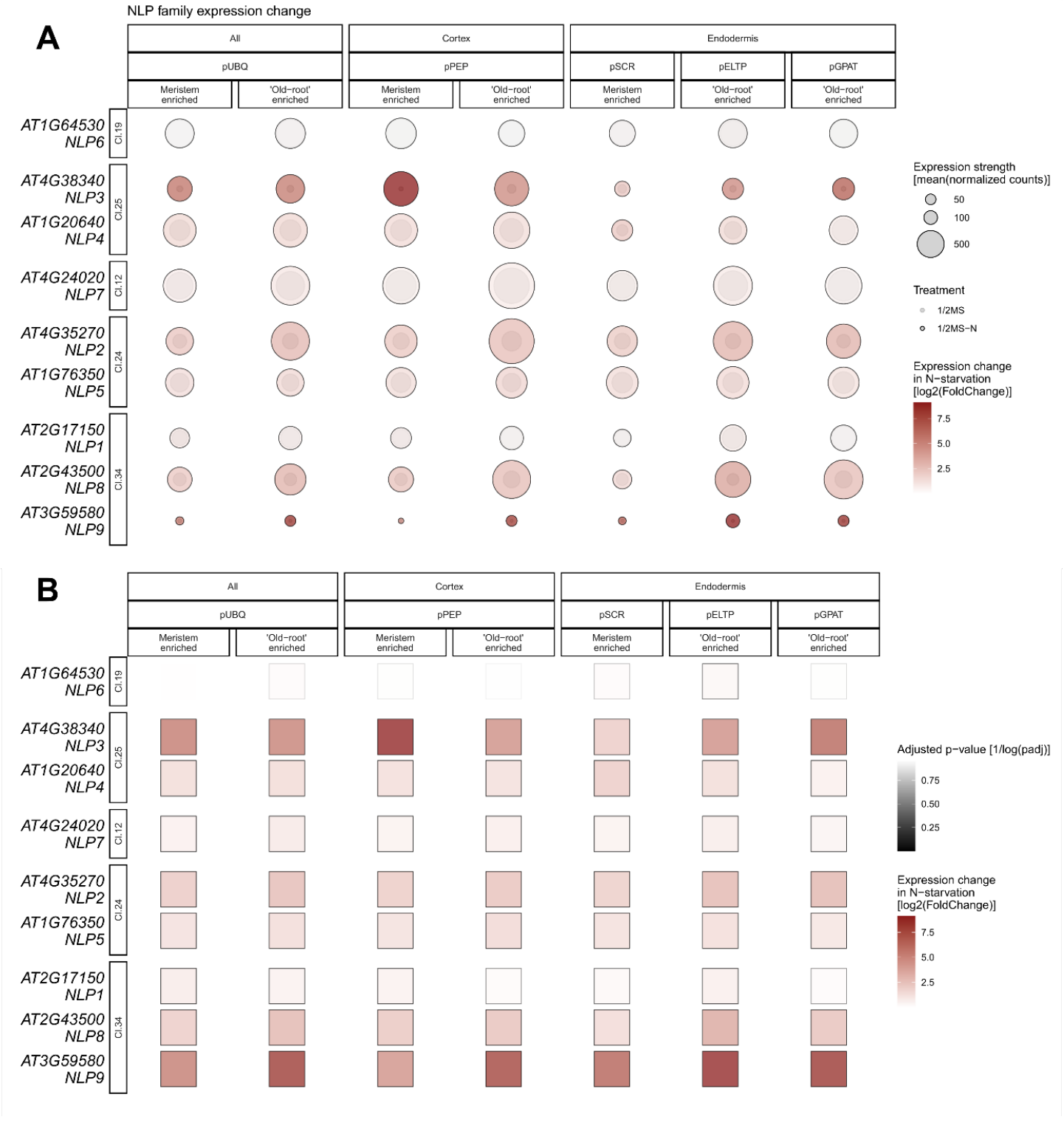

Supplemental figure 8 ***Expression NLP genes: A*** *Halo-plot. Grey circles indicate the mean, normalized counts of TRAPseq profiles from 1/2 MS grown plants. Colored circles indicated the mean, normalized counts of TRAPseq profiles form 1/2 MS-N grown plants. Color indicates the log2(FoldChange). Accordingly, larger red circles indicate induction upon nitrogen starvation and smaller blue circles indicate repression upon nitrogen starvation. The x-axis is facetted for the tissue, then promoters, then young and mature root. The y-axis is facetted for the individual k-clusters. Genes are indicated by name and AGI.* ***B*** *Heatmap. Color indicates log2(FoldChange) as above and borders indicated adjusted p-values.*

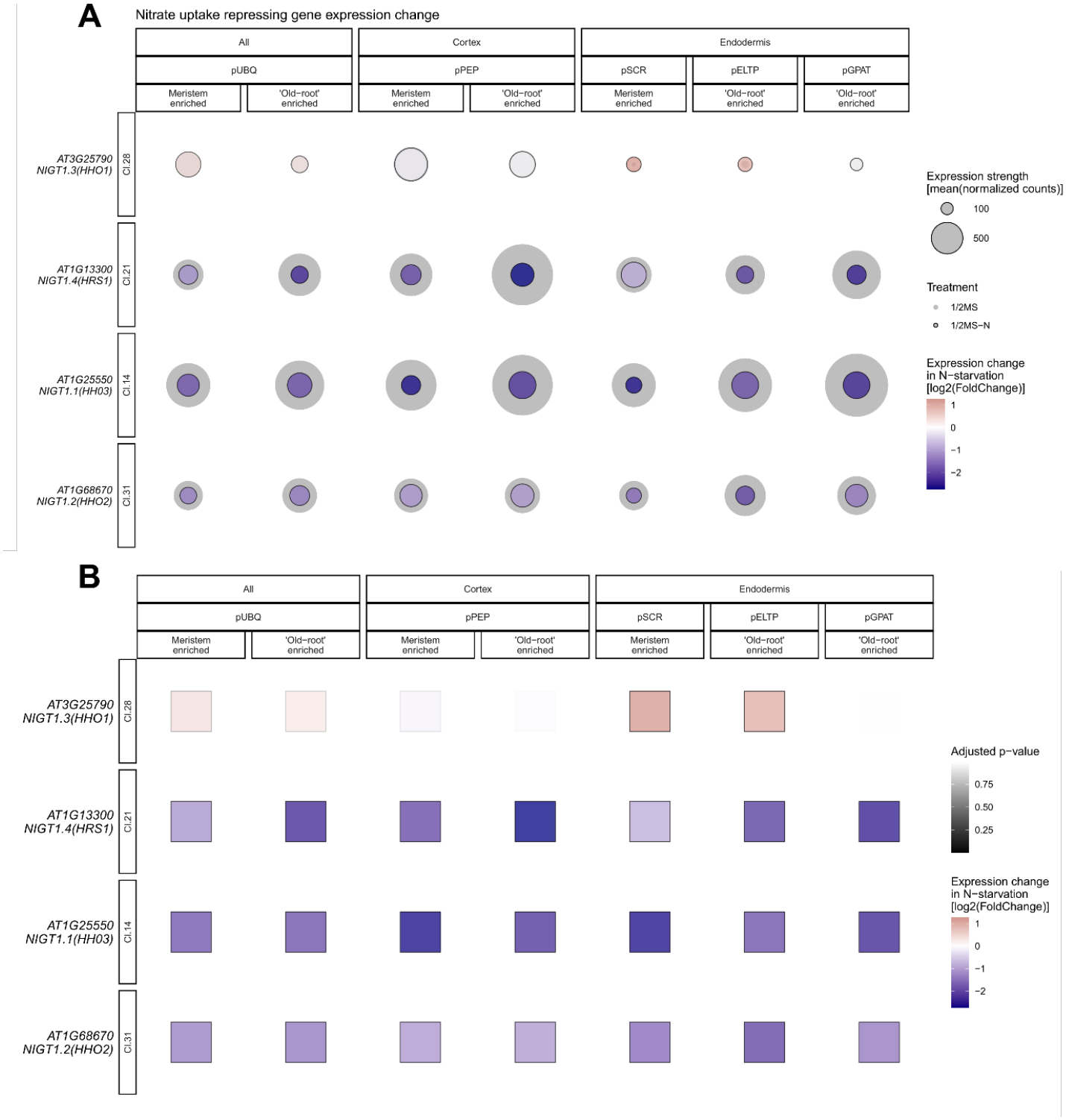

Supplemental figure 9 ***TRAPseq Expression NIGT genes: A*** *Halo-plot. Grey circles indicate the mean, normalized counts of TRAPseq profiles from 1/2 MS grown plants. Colored circles indicated the mean, normalized counts of TRAPseq profiles form 1/2 MS-N grown plants. Color indicates the log2(FoldChange). Accordingly, larger red circles indicate induction upon nitrogen starvation and smaller blue circles indicate repression upon nitrogen starvation. The x-axis is facetted for the tissue, then promoters, then young and mature root. The y-axis is facetted for the individual k-clusters. Genes are indicated by name and AGI.* ***B*** *Heatmap. Color indicates log2(FoldChange) as above and borders indicated adjusted p-values.*

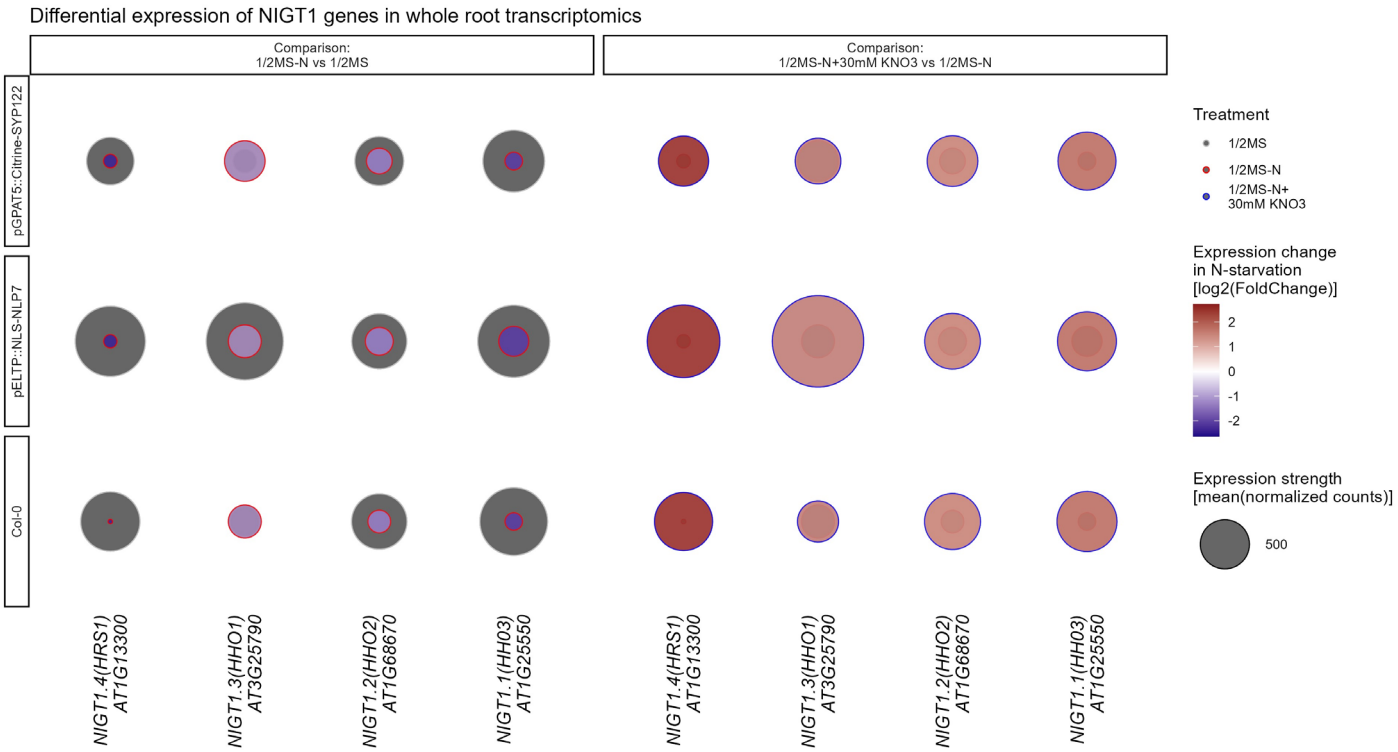

Supplemental figure 10 ***RNAseq Expression NIGT genes:*** *Halo-plot. Grey circles indicate the base mean, normalized counts of RNAseq profiles from 1/2 MS grown plants 8 DAG. Colored circles indicated the mean, normalized counts of RNAseq profiles from 1/2 MS-N grown plants 6 DAG + 2 DAT. Fill color indicates the log2(FoldChange). Circle edge color indicates the treatment. Fill color indicates the log2(FoldChange). Circle edge color indicates the treatment. Larger red filled circles indicate induction and smaller blue circles indicate repression. The x-axis is facetted for the respective DEG analysis. The y-axis is facetted for genotypes. Genes are indicated by name and AGI on the x-axis.*

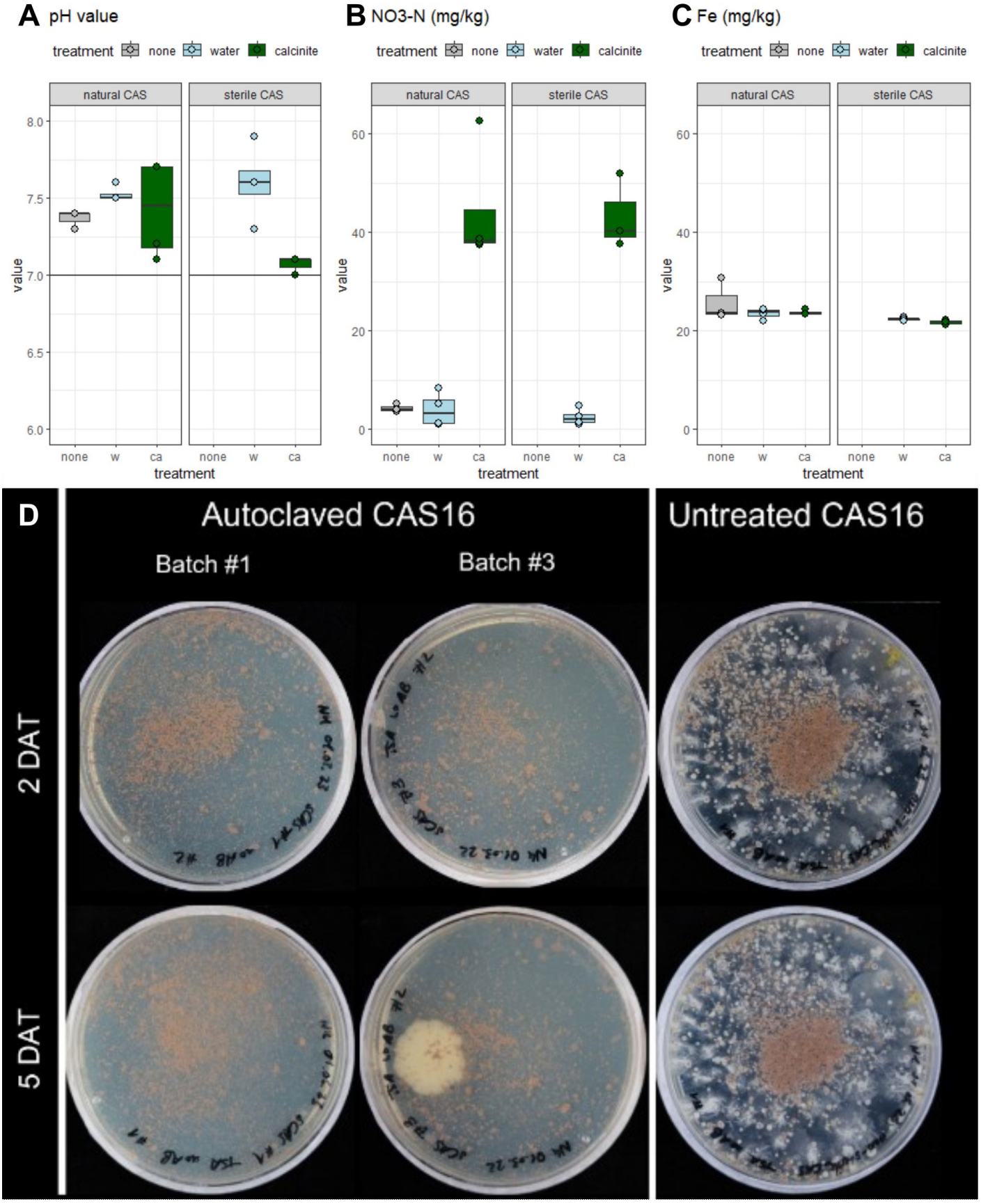

Supplemental figure 11 ***Soil properties measurements:*** *Parameters either after 3weeks of plant cultivation under the respective treatment or without treatment* ***A*** *pH.* ***B*** *Nitrate.* ***C*** *Dissolvable iron.* ***D*** *plates after soil sterilization (before plant transfer)*

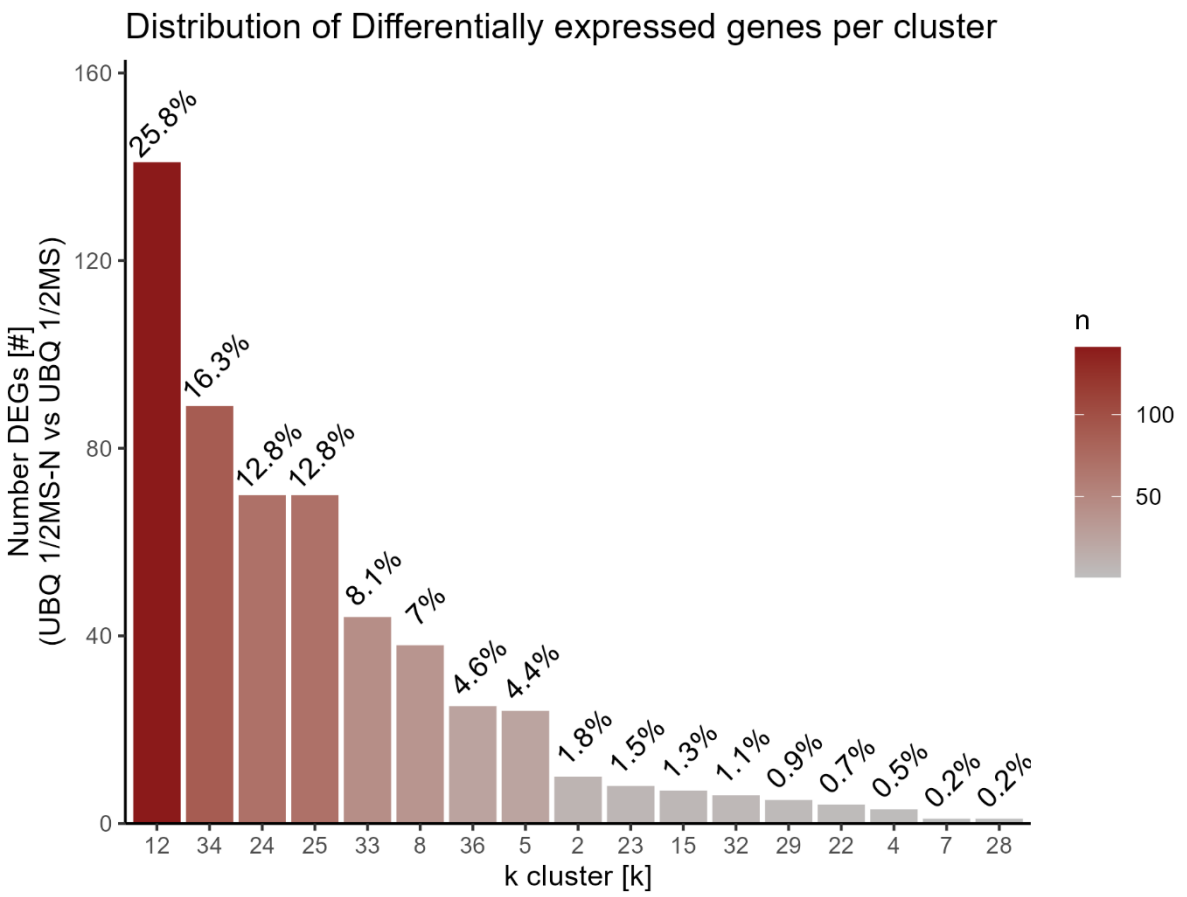

Supplemental figure 12 ***Cluster distribution of DEGs upon nitrogen starvation:*** *DEG analysis was performed on UBQ TRAPseq profiles of 1/2 MS-N grown seedlings versus 1/2 MS grown seedlings. Young and mature root samples were merged per treatment, sum(n_{DEG} = 546).*

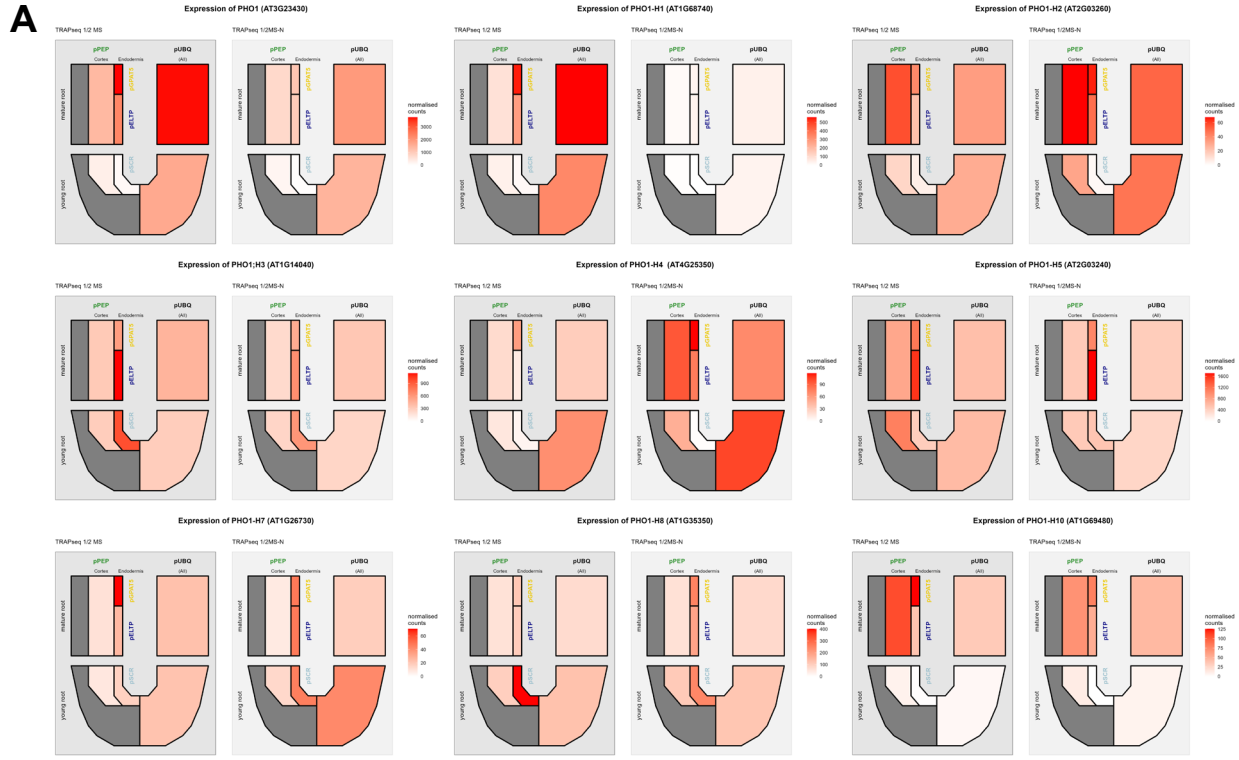
A
Expression of PHO1 (AT3G23430)
Expression of PHO1-H1 (AT1G68740)
Expression of PHO1-H2 (AT2G03260)
Expression of PHO1;H3 (AT1G14040)
Expression of PHO1-H4 (AT4G25350)
Expression of PHO1-H5 (AT2G03240)
Expression of PHO1-H7 (AT1G26730)
Expression of PHO1-H8 (AT1G35350)
Expression of PHO1-H10 (AT1G69480)
TRAPseq 1/2 MS
TRAPseq 1/2MS-N
pPEP
pUBQ
mature root
young root
normalised counts

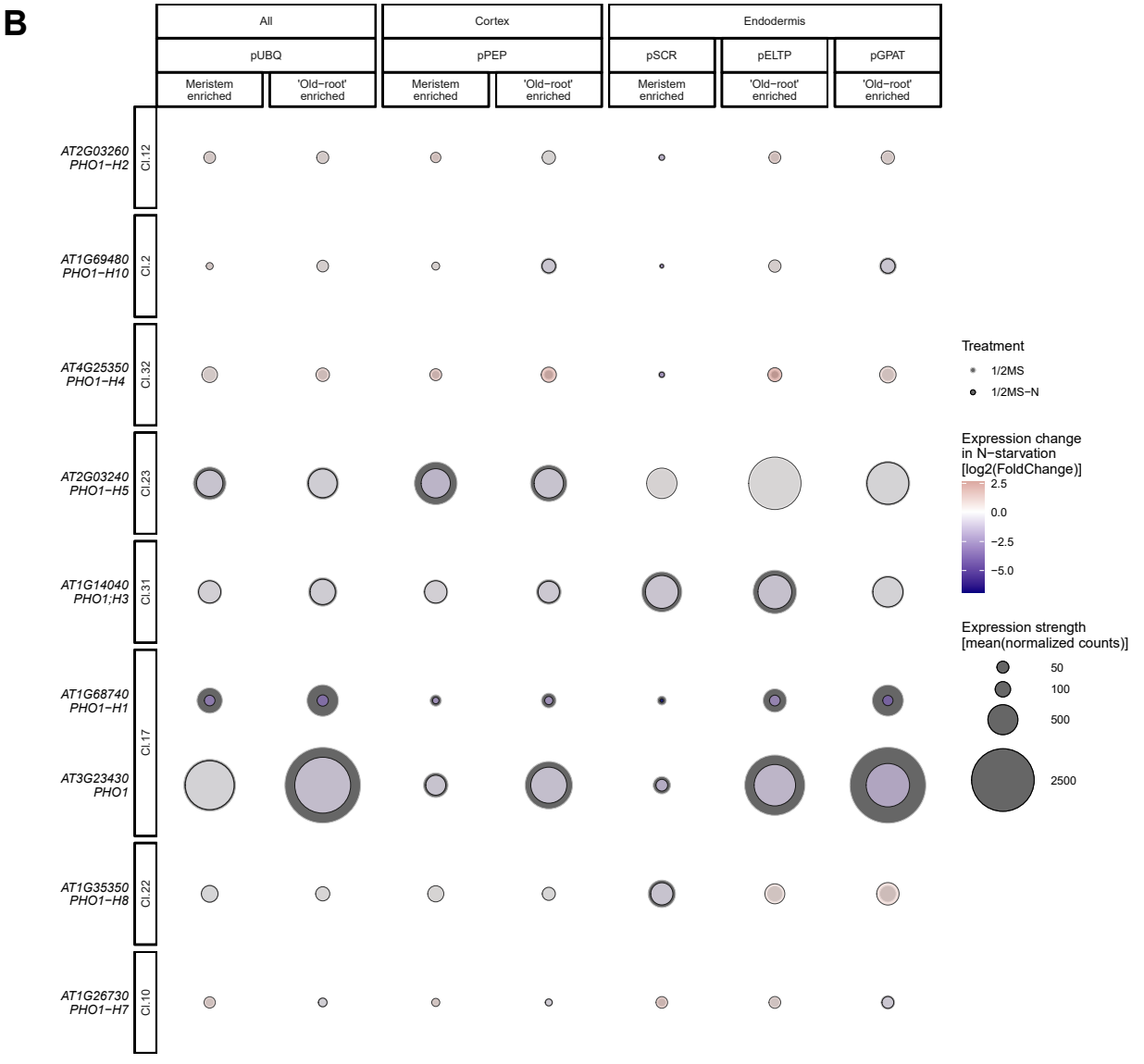
B
All
Cortex
Endodermis
pUBQ
pPEP
pSCR
pELTP
pGPAT
Meristem enriched
'Old−root' enriched
AT2G03260 PHO1−H2
AT1G69480 PHO1−H10
AT4G25350 PHO1−H4
AT2G03240 PHO1−H5
AT1G14040 PHO1;H3
AT1G68740 PHO1−H1
AT3G23430 PHO1
AT1G35350 PHO1−H8
AT1G26730 PHO1−H7
Cl.12
Cl.2
Cl.32
Cl.23
Cl.31
Cl.17
Cl.22
Cl.10
Treatment
1/2MS
1/2MS−N
Expression change in N−starvation [log2(FoldChange)]
2.5
0.0
−2.5
−5.0
Expression strength [mean(normalized counts)]
50
100
500
2500

Supplemental figure 13 ***TRAPseq PHO1 genes expression A*** *Minecraft plots were done after bioinformatic processing. Left plot indicates 1/2 MS condition and right plot indicates 1/2 MS-N condition.* ***B*** *Halo-plot. Grey circles indicate the mean, normalized counts of TRAPseq profiles from 1/2 MS grown plants. Colored circles indicated the mean, normalized counts of TRAPseq profiles form 1/2 MS-N grown plants. Color indicates the log2(FoldChange). Accordingly, larger red circles indicate induction upon nitrogen starvation and smaller blue circles indicate repression upon nitrogen starvation. The x-axis is facetted for the tissue, then promoters, then young and mature root. The y-axis is facetted for the individual k-clusters. Genes are indicated by name and AGI*

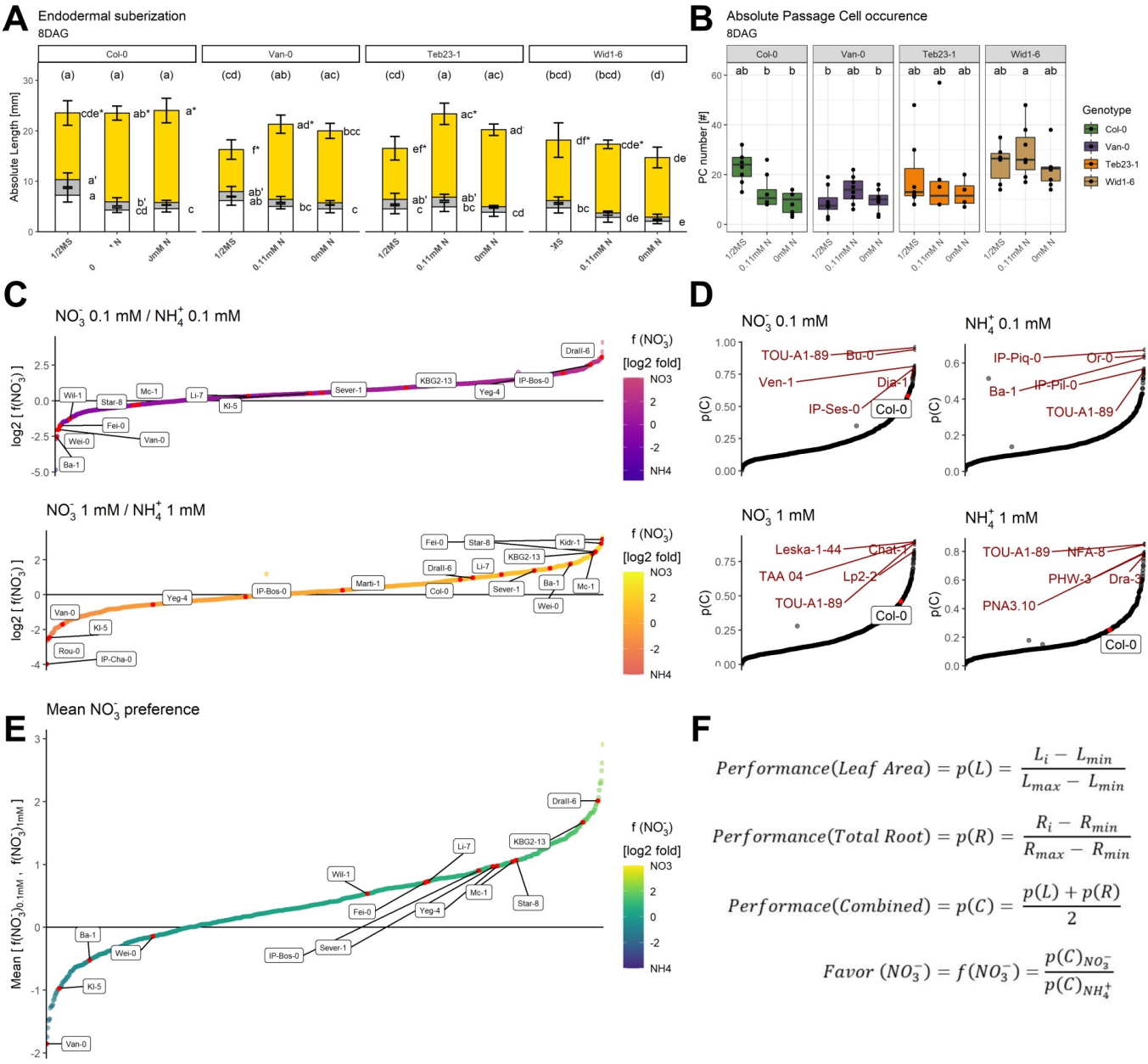

Supplemental figure 14 ***Natural variation in passage cell occurrence and nitrogen preference: A*** *Endodermal suberization in limiting nitrogen conditions and absolute root length. Quantification of endodermal suberization of seedlings grown for 8 DAG (n = 8). Error bars indicate bi-directional standard deviation per zone as mean plus standard deviation. Statistics are performed as Tukey post-hoc HSD within each experiment and per zone as well as on the total root length. Statistics are indicated as: (a) = total root length, a = unsuberized zone, a' = patchy zone and a* = suberized zone.* ***B*** *Quantification of passage cells after 8 DAG (n = 8). Passage cells are defined as unsuberized cells in the fully suberized zone. Statistics are performed as Tukey post-hoc HSD* ***C*** *Preference of individual lines towards nitrate when exposed to low nitrate or ammonium conditions* (Katz et al., 2022) ***D*** *Relative performance of accessions in individual conditions of low and intermediate nitrate and ammonium supply* ***B*** *Preference of accession to nitrate in combined low and high concentrations* ***D*** *Formulas used to evaluate nitrogen preference of individual accessions.*

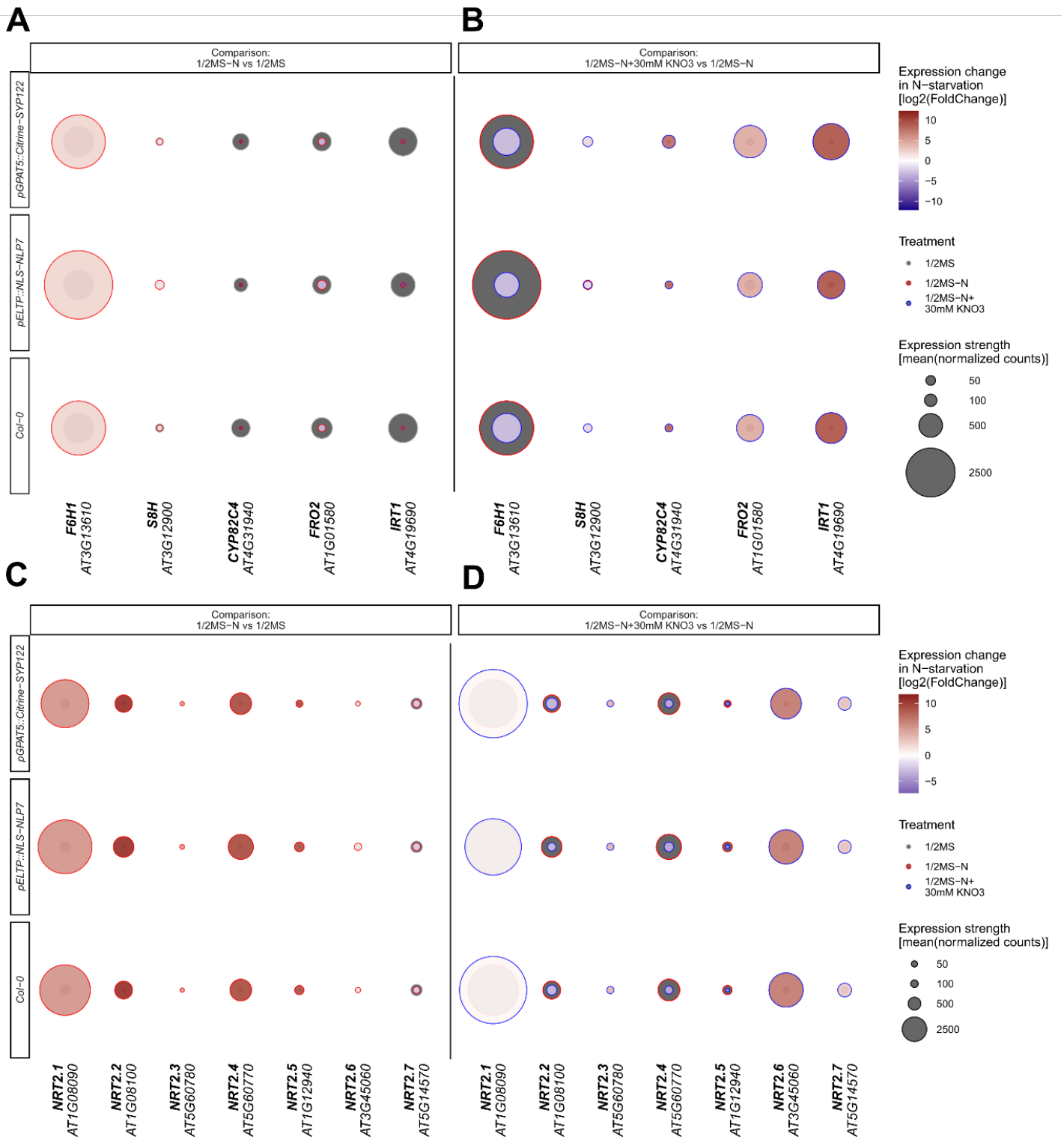

Supplemental figure 15 ***Halo plots of whole root transcriptomic analysis: A,B*** *coumarin biosynthesis and iron uptake genes* ***C,D*** *NRT2 high affinity nitrate transporters* ***A,C:*** *Nitrogen starvation. Grey circles indicate the base mean, normalized counts of RNAseq profiles from 1/2 MS grown plants 8DAG. Colored circles indicated the mean, normalized counts of RNAseq profiles from 1/2 MS-N grown plants 6DAG + 2DAT. Fill color indicates the log2(FoldChange). Circle edge color indicates the treatment.* ***B,D*** *Halo-plot. Grey circles indicate the base mean, normalized counts of RNAseq profiles from 1/2 MS-N grown plants 6DAG+2DAT. Colored circles indicated the mean, normalized counts of RNAseq profiles from 1/2 MS-N+30mMKNO_3 grown plants 6DAG + 2DAT. Fill color indicates the log2(FoldChange). Circle edge color indicates the treatment. Larger red filled circles indicate induction upon nitrogen starvation and smaller blue circles indicate repression upon nitrogen starvation. The x-axis is facetted for the respective DEG analysis. The y-axis is facetted for genotypes. Genes are indicated by name and AGI on the x-axis*

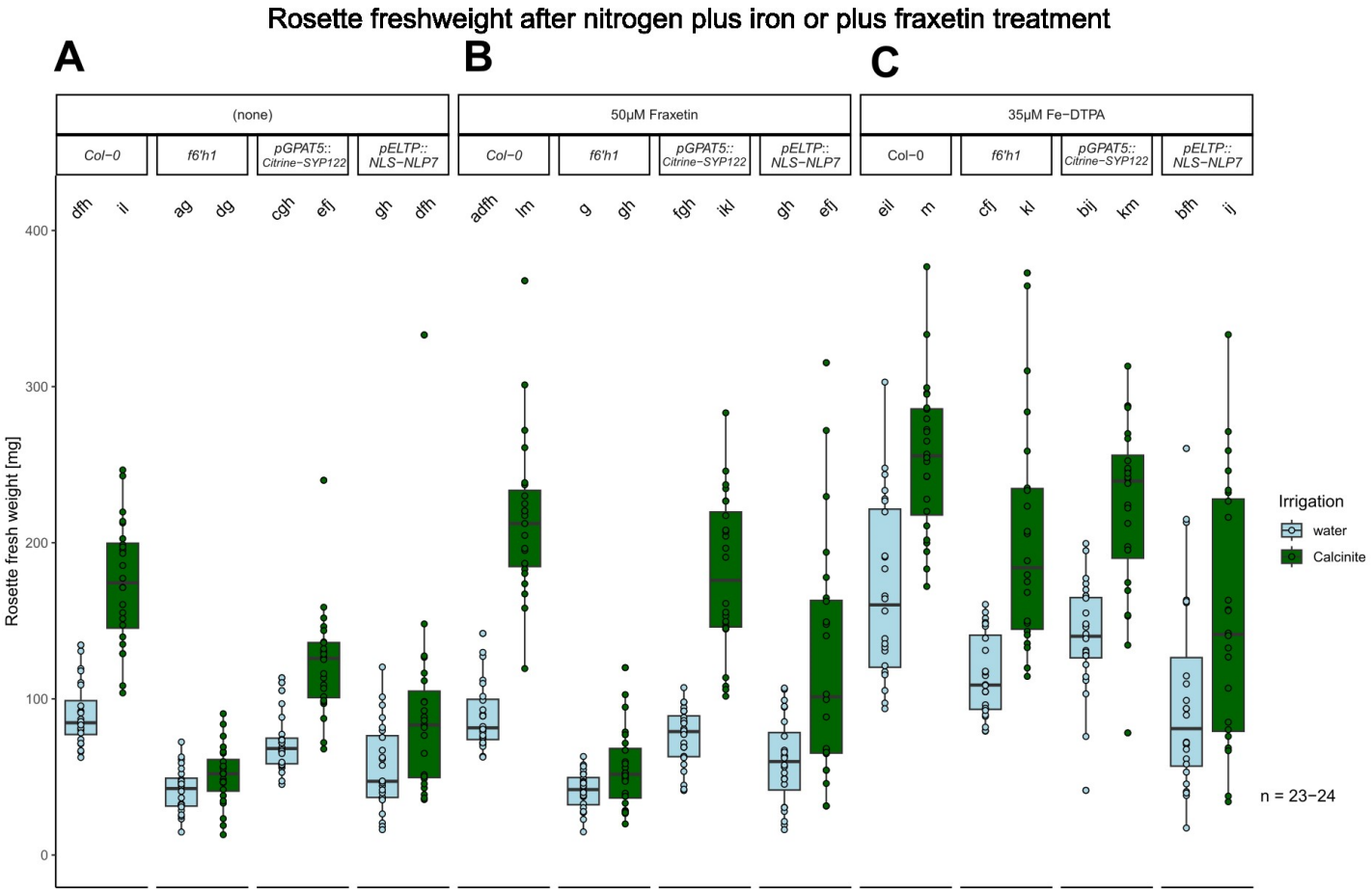

Supplemental figure 16: ***Iron and fraxetin resupply to natural soil: A*** *Control plants grown without additional treatment and were irrigated weekly with either water or Calcinite* ***B*** *Plants were irrigated with 50µM fraxetin weekly dissolved in water or Calcinite irrigation medium* ***C*** *Plants were irrigated with 35µM Fe-DTPA weekly dissolved in water or Calcinite irrigation medium. Statistics were performed as Tukey HSD across all conditions.*

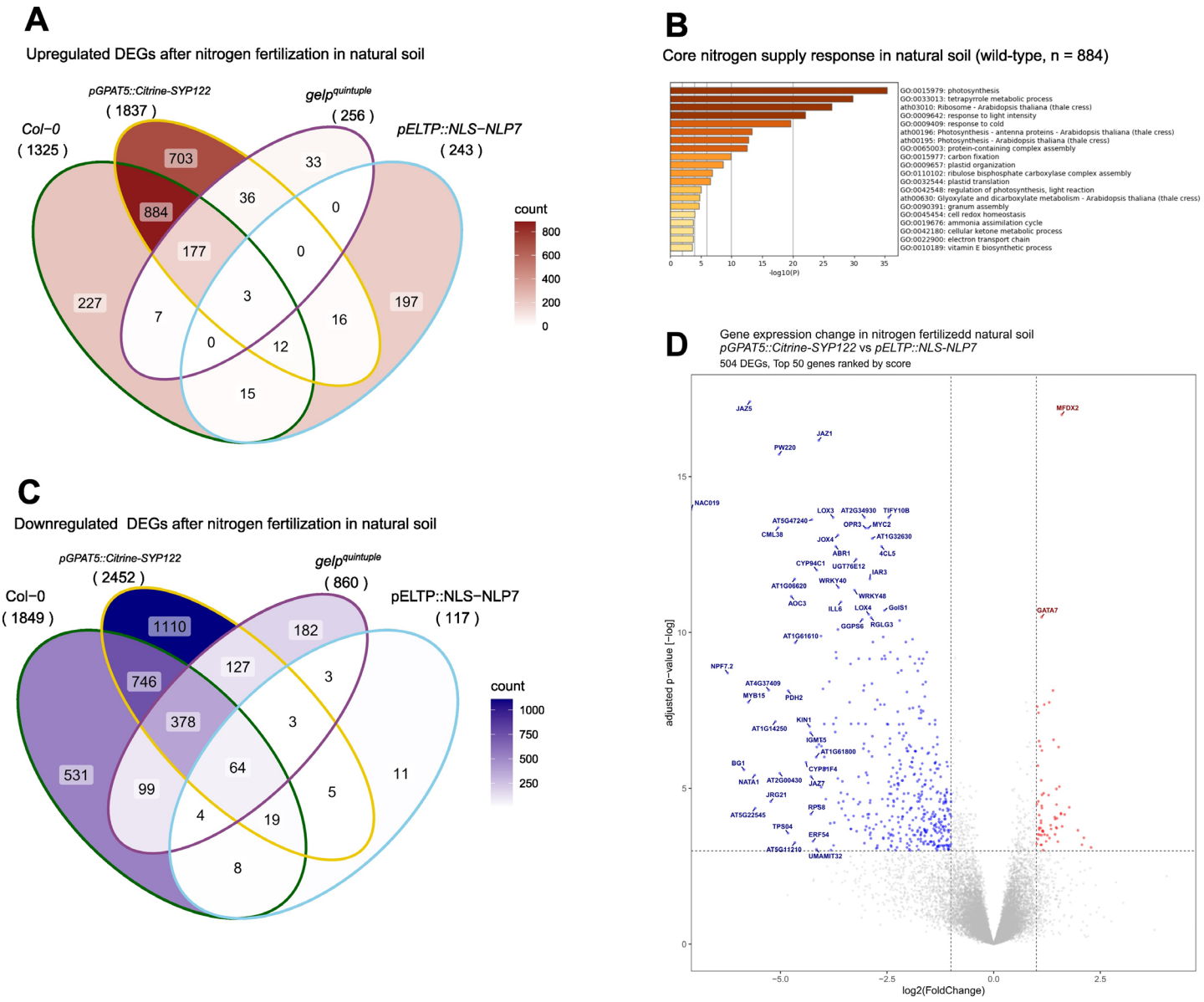

Supplemental figure 17 ***Preliminary analysis of shoot transcriptomics of nitrogen fertilized plants: A*** *Venn diagram showing the overlap of upregulated DEGs in natural soil after nitrogen fertilization versus unfertilized soil* ***B*** *GO-terms of core wild-type nitrogen fertilizer response* (Zhou et al., 2019)***C*** *Venn diagram showing the overlap of downregulated DEGs in natural soil after nitrogen fertilization versus unfertilized soil* ***D*** *Volcano plot of wild-type pGPAT5::Citrine-SYP122 versus pELTP::NLS-NLP7 DEG* analysis

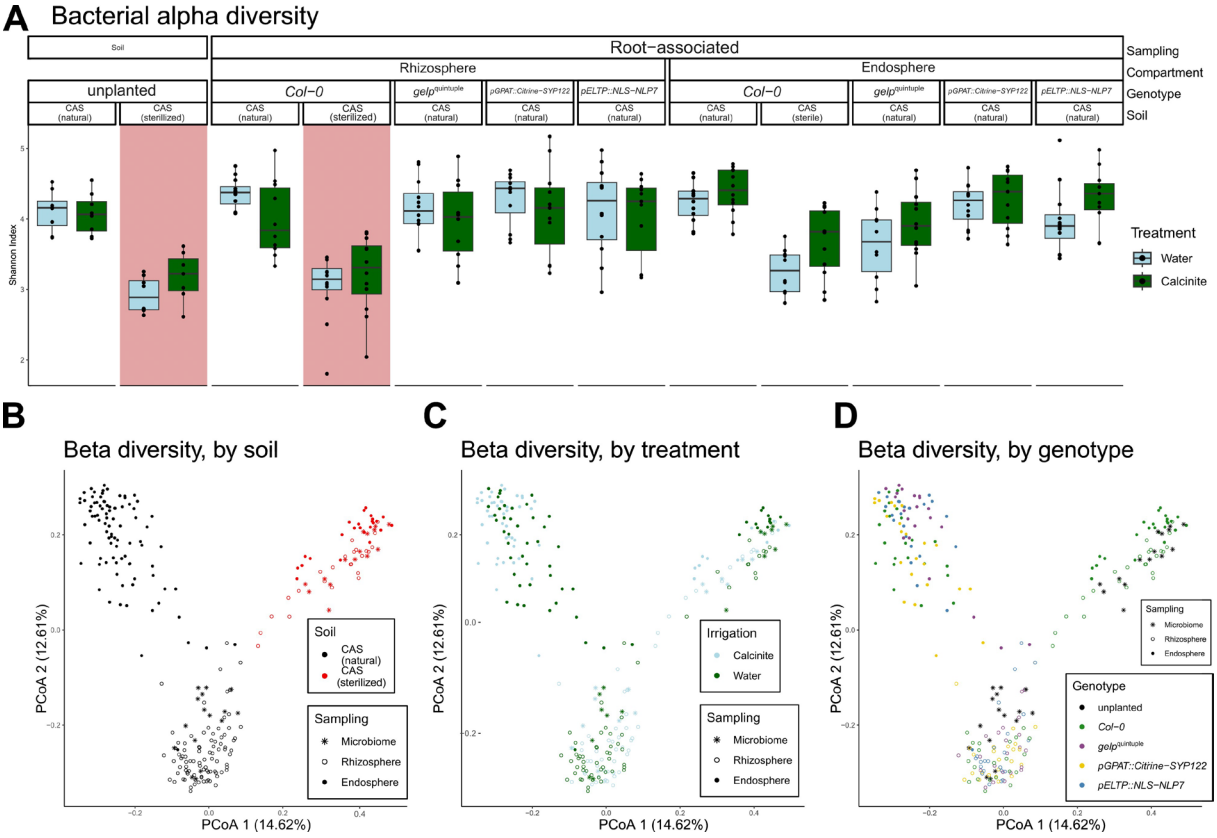

Supplemental figure 18: ***CORRIGENDUM*** *this figure was originally figure 13 and replaced upon error correction* ***Diversity of the bacterial community.*** *Bacterial taxa were identified based on their 16S amplicon sequence as (Shen et al., 2023; Wippel et al., 2021)* ***A*** *Alpha diversity calculated as Shannon index* (Shannon, 1948)*, red rectangle indicate samples obtained from sterilized soil. Numbers below the boxplots indicate sample size* ***B,C,D*** *Beta diversity as Bray-Curtis dissimilarity.* ***B*** *Beta diversity soil.* ***C*** *Beta diversity treatment.* ***D*** *beta diversity genotype.*

17 Appendix I: Translating ribosome affinity purification as tool to resolve tissue-specific post-transcriptional profiles

Currently, there are two methods to assess tissue specific transcriptional profiles of plants cells: Single cell transcriptomics (scRNAseq) and translating ribosome affinity purification (TRAPseq). Recently, scRNAseq has traction to investigate regulatory networks in the young root meristem (Denyer et al., 2018, 2019; Jean-Baptiste et al., 2019; Ryu et al., 2019; Shulse et al., 2019; Zhang et al., 2019). Less well established are TRAPseq approaches (Fröschel et al., 2021; Leal et al., 2022; Mustroph et al., 2009; Thellmann et al., 2020; Vragović et al., 2015), as they require the knowledge of tissue specific promoters and the establishment of transgenic material. Here, I want to highlight the methodology of the TRAPseq approach used for this study, the performed bioinformatic analysisas well as compare it to a whole root RNAseq dataset acquired during this study.

17.1 Spatial separation of nitrogen responses requires tissue-specific sequencing approaches in order to expose/investigate specific regulatory mechanisms

TRAPseq uses tissue specific promoters to express the 60S ribosomal subunit protein RPL18 connected to an antigen, in our case GFP (11 List of abbreviations) which allows to purify the polysome-bound mRNA through magnetic beads, and thus retrieve transcriptomes exclusively from the tissue of interest (Mustroph et al., 2009; Thellmann et al., 2020; Zanetti et al., 2005). In contrast to the alternative method to assess tissue-specific transcriptional profiles, single-cell RNAseq (scRNAseq), TRAPseq is not dependent on protoplasting and sorting the root material. This has two advantages; on the one hand, individual tissues protoplastelyse/degrate at different rates dependent on their cell-wall digestibility by the protoplasting enzyme cocktail (Birnbaum et al., 2005). The endodermis, as the primary root barrier tissues, thus is notoriously difficult to protoplast and requires long/prolonged enzyme treatments. In fact, previous scRNAseq datasets do not capture genes involved in suberization (Ryu et al. 2019). On the other hand, long protoplasting treatment is altering the transcriptional profile of the isolated cells, potentially masking treatment and/or cell-type specific transcriptional profiles. For TRAPseq the root material is immediately frozen after harvesting and individual profiles are thus preserved.

For this study, we selected promoters allow us to understand the observed phenotype of the ground tissue in response to the applied nitrogen starvation stress. We chose the promoters of SCR and ELTP which were shown to be expressed in the young and late endodermis respectively (Barberon et al., 2016; Di Laurenzio et al., 1996; Koizumi & Gallagher, 2013). Late endodermal cells undergo suberization selectively (Andersen et al. 2018), which appears to be influenced by the nitrogen status of the plant (Figure 1). Thus, we included the promoter for the acyltransferase GPAT5 which is required for Suberin synthesis (Beisson et al. 2005). Lastly, we used the promoter of the endopeptidase PEP, which was shown to be cortex specific and was used for TRAPseq before (Fröschel et al., 2021). To account for biases, introduced to our dataset due to our experimental conditions or RNA purification, we also extracted RNA from GFP-tagged polysomes expressed under a ubiquitously active promoter (UBQ10). Thus, we generated a dataset comprising 14 different conditions with 3-6 replicates. Each condition

represents a combination of the dissected root zone, the promoter under which the TRAP-construct is expressed, and the treatment under which the plants were grown (Table 14)

Table 14: ***Design table for samples used for TRAPseq in this study.*** *Quality assessment of RNA integrity values (RIN), library preparation and sequencing were performed by Novogene UK Ltd.*

Library	Project	Sample ID	Sequenced	Tissue	Promotor	Line	Treatment	Rep	Experiment	Extraction	Date	Plates [n]	Fresh weight	Total RNA [ng]	RIN
D16	5376	UBQ_0	1	mature root	UBQ10	12	1_2MS	0	1	1	02.12.2021	20	1183	1372.6	9.8
E16	5376	UBQ_N_0	1	mature root	UBQ10	12	1_2MS-N	0	1	1	02.12.2021	20	1564	990.31	9.9
G16	5376	PEP_0	1	mature root	PEP	5	1_2MS	0	1	1	02.12.2021	20	1365	715.25	9.8
D16	5407	UBQ_1	1	mature root	UBQ10	12	1_2MS	1	2	2	17.01.2022	20	923.8	448	8.6
E16	5407	UBQ_N_1	1	mature root	UBQ10	12	1_2MS-N	1	2	2	17.01.2022	20	829.2	340	9.3
F16	5407	PEP_1	1	mature root	PEP	5	1_2MS	1	2	2	17.01.2022	20	1504.4	136	8.1
G16	5407	PEP_N_1	1	mature root	PEP	5	1_2MS-N	1	2	2	17.01.2022	20	665.2	112	9.1
H16	5407	ELTP_1	0	mature root	ELTP	9	1_2MS	1	2	2	17.01.2022	20	1012.8	17	5.5
A17	5407	ELTP_N_1	0	mature root	ELTP	9	1_2MS-N	1	2	2	17.01.2022	20	1165.8	75	1.6
B17	5407	GPAT_1	0	mature root	GPAT5	4	1_2MS	1	2	2	17.01.2022	20	1562.2	34	1.5
C17	5407	GPAT_N_1	1	mature root	GPAT5	4	1_2MS-N	1	2	2	17.01.2022	20	874.7	476	9.6
A01	5452	UBQ_2	1	mature root	UBQ10	12	1_2MS	2	3	3	06.02.2022	15	675.4	255	8.9
B01	5452	UBQ_N_2	1	mature root	UBQ10	12	1_2MS-N	2	3	3	06.02.2022	15	852.4	72	6.8
C01	5452	PEP_2	1	mature root	PEP	5	1_2MS	2	3	3	06.02.2022	19	1290.8	68	7.6
D01	5452	PEP_N_2	1	mature root	PEP	5	1_2MS-N	2	3	3	06.02.2022	20	678.3	51	7.5
E01	5452	ELTP_2	1	mature root	ELTP	9	1_2MS	2	3	3	06.02.2022	20	793.1	34	6.8
F01	5452	ELTP_N_2	0	mature root	ELTP	9	1_2MS	2	3	3	06.02.2022	20	1039.4	68	1.6
G01	5452	GPAT_2	0	mature root	GPAT5	4	1_2MS	2	3	3	06.02.2022	25	1441.6	17	1
H01	5452	GPAT_N_2	0	mature root	GPAT5	4	1_2MS-N	2	3	3	06.02.2022	25	811.9	17	1
A02	5452	UBQ_3	1	mature root	UBQ10	12	1_2MS	3	4	4	17.02.2022	14	626.5	391	8.7
B02	5452	UBQ_N_3	1	mature root	UBQ10	12	1_2MS-N	3	4	4	17.02.2022	20	675.7	323	8.8
C02	5452	PEP_3	1	mature root	PEP	5	1_2MS	3	4	4	17.02.2022	19	1455.2	160	8.4
D02	5452	PEP_N_3	1	mature root	PEP	5	1_2MS-N	3	4	4	17.02.2022	20	599.6	208	8.8
E02	5452	ELTP_3	1	mature root	ELTP	9	1_2MS	3	4	4	17.02.2022	20	774.4	128	9
F02	5452	ELTP_N_3	0	mature root	ELTP	9	1_2MS-N	3	4	4	17.02.2022	20	1111	17	1.6
G02	5452	GPAT_3	0	mature root	GPAT5	4	1_2MS	3	4	4	17.02.2022	25	1849.9	48	1
H02	5452	GPAT_N_3	0	mature root	GPAT5	4	1_2MS-N	3	4	4	17.02.2022	24	732.3	80	1
A01	5528	ELTP_4	1	mature root	ELTP	9	1_2MS	4	5	5	03.05.2022	40	1643.1	51	7.9
B01	5528	GPAT_4	0	mature root	GPAT5	4	1_2MS	4	5	5	03.05.2022	40	1963.6	51	1
C01	5528	GPAT_5	0	mature root	GPAT5	4	1_2MS	5	5	5	03.05.2022	40	2236.4	17	1.2
D01	5528	GPAT_6	0	mature root	GPAT5	4	1_2MS	6	5	5	03.05.2022	40	2067.4	32	1.1
E01	5528	ELTP_N_4	1	mature root	ELTP	9	1_2MS-N	4	5	5	03.05.2022	40	2178.6	17	1
F01	5528	ELTP_N_5	1	mature root	ELTP	9	1_2MS-N	5	5	5	03.05.2022	40	2194.4	17	1.7
G01	5528	ELTP_N_6	1	mature root	ELTP	9	1_2MS-N	6	5	5	03.05.2022	40	2034.9	16	2.5
H01	5528	GPAT_N_4	1	mature root	GPAT5	4	1_2MS-N	4	5	5	03.05.2022	40	2336.4	68	1.4
A02	5528	ELTP_N_7	1	mature root	ELTP	9	1_2MS-N	7	6	6	07.07.2022	22	1503.2	36	1
B02	5528	ELTP_N_8	1	mature root	ELTP	9	1_2MS-N	8	6	6	07.07.2022	22	1618.3	54	1
C02	5528	ELTP_N_9	1	mature root	ELTP	9	1_2MS-N	9	6	6	07.07.2022	22	1795.4	18	1
D02	5528	GPAT_7	1	mature root	GPAT5	4	1_2MS	7	6	6	07.07.2022	27	1728.8	9	1
E02	5528	GPAT_8	1	mature root	GPAT5	7	1_2MS	8	6	6	07.07.2022	27	1717.7	36	1
F02	5528	GPAT_9	1	mature root	GPAT5	7	1_2MS	9	6	6	07.07.2022	27	1687	36	6
G02	5528	GPAT_N_5	1	mature root	GPAT5	4	1_2MS-N	5	6	6	07.07.2022	27	2023.7	72	1
H02	5528	GPAT_N_6	0	mature root	GPAT5	7	1_2MS-N	6	6	6	07.07.2022	27	1588.3	54	1
A01	5828	Meri_MS_PEP_0	1	Meristem	PEP	5	1_2MS	0	1	7	26.01.2023	20	221	34	9.2
B01	5828	Meri_MS_PEP_1	1	Meristem	PEP	5	1_2MS	1	2	7	26.01.2023	19	245.9	11	8.9
C01	5828	Meri_MS_PEP_2	1	Meristem	PEP	5	1_2MS	2	3	7	26.01.2023	19	470	99	9.9
D01	5828	Meri_MS_PEP_3	1	Meristem	PEP	5	1_2MS	3	4	7	26.01.2023	19	231.2	5	8.4
E01	5828	Meri_N_PEP_0	1	Meristem	PEP	5	1_2MS-N	0	1	7	26.01.2023	20	267	11	7.7
F01	5828	Meri_N_PEP_1	1	Meristem	PEP	5	1_2MS-N	1	2	7	26.01.2023	20	289	4	6.5
G01	5828	Meri_N_PEP_2	1	Meristem	PEP	5	1_2MS-N	2	3	7	26.01.2023	20	408.3	24	9
H01	5828	Meri_N_PEP_3	1	Meristem	PEP	5	1_2MS-N	3	4	7	26.01.2023	20	251.5	13	8.9
A02	5828	Meri_MS_UBQ_0	1	Meristem	UBQ10	12	1_2MS	0	1	8	27.01.2023	20	85	14	9.3
B02	5828	Meri_MS_UBQ_1	1	Meristem	UBQ10	12	1_2MS	1	2	8	27.01.2023	15	331.9	26	9.3
C02	5828	Meri_MS_UBQ_2	1	Meristem	UBQ10	12	1_2MS	2	3	8	27.01.2023	15	332.8	28	9.1
D02	5828	Meri_MS_UBQ_3	1	Meristem	UBQ10	12	1_2MS	3	4	8	27.01.2023	14	278.8	28	9.2
E02	5828	Meri_N_UBQ_0	1	Meristem	UBQ10	12	1_2MS-N	0	1	8	27.01.2023	20	168	54	9.7
F02	5828	Meri_N_UBQ_1	1	Meristem	UBQ10	12	1_2MS-N	1	2	8	27.01.2023	15	306.4	23	9.3
G02	5828	Meri_N_UBQ_2	1	Meristem	UBQ10	12	1_2MS-N	2	3	8	27.01.2023	15	234.7	14	9.2
H02	5828	Meri_N_UBQ_3	1	Meristem	UBQ10	12	1_2MS-N	3	4	8	27.01.2023	20	302.6	16	8
A03	5828	Meri_MS_SCR_a	1	Meristem	SCR	2_7_8	1_2MS	0	7	9	28.01.2023	10	190	79	9.1

Library	Project	Sample ID	Sequenced	Tissue	Promotor	Line	Treatment	Rep	Experiment	Extraction	Date	Plates [n]	Fresh weight	Total RNA [ng]	RIN
B03	5828	Meri_MS_SCR_b	1	Meristem	SCR	2_7_8	1_2MS	1	7	9	28.01.2023	10	192.2	60	9.5
C03	5828	Meri_MS_SCR_c	1	Meristem	SCR	2_7_8	1_2MS	2	7	9	28.01.2023	9	184.7	16	9.3
D03	5828	Meri_MS_SCR_d	1	Meristem	SCR	2_7_8	1_2MS	3	7	9	28.01.2023	8	140.9	46	9.3
E03	5828	Meri_N_SCR_a	1	Meristem	SCR	2_7_8	1_2MS-N	0	7	9	28.01.2023	11	231	52	9
F03	5828	Meri_N_SCR_b	1	Meristem	SCR	2_7_8	1_2MS-N	1	7	9	28.01.2023	12	223.6	77	8.9
G03	5828	Meri_N_SCR_c	1	Meristem	SCR	2_7_8	1_2MS-N	2	7	9	28.01.2023	8	156.2	72	8.4

17.2 Unequal cell- and consequently, ribosomal density, across the longitudinal axis of the root, implies biases in whole root transcriptomic analysis

The 60S ribosome, of which we used the subunit RPL18 tagged to GFP for TRAPseq, is assembled in the nucleolus of the cell. It migrates into the cytoplasm in an inactive state and becomes activated through a second step of cytosplasmic maturation (Panse & Johnson, 2010). Due to this maturation delay, only ribosomal pull-downs from cells with cytoplasmic RLP18-GFP signal will contribute mRNA to the TRAPseq. Moreover, in the putative ubiquitously and cortex-specifically expressing lines (Supplemental figure 1), we also observed a much stronger signal closer to the root tip, associated to the higher cell density there. To address this experimental bias, we decided to cut the root during harvesting approx. 0.5cm above the meristem line (Appendix Figure 1). Next, we extracted the polysome-bound RNA from the meristem-enriched and mature-root-enriched fractions, separately. Interestingly, this observation was not reflected in the amount of yielded RNA per unit of root material. In the root tip, irrespective of treatment, approx100 pg of RNA could be extracted per mg of root material, while in the mature root 400 pg could be extracted per mg of root material (Table 14). This could be either due to a delay between BLRP-FLG-RPL18-GFP expression and 60S ribosome assembly and/or retention at the nucleosome (Fromont-Racine et al., 2003). This observation highlights the differences between cellular transcriptional and translational activity depending on the cellular maturation. Thus, we factored in the root zone into our subsequent analyses.

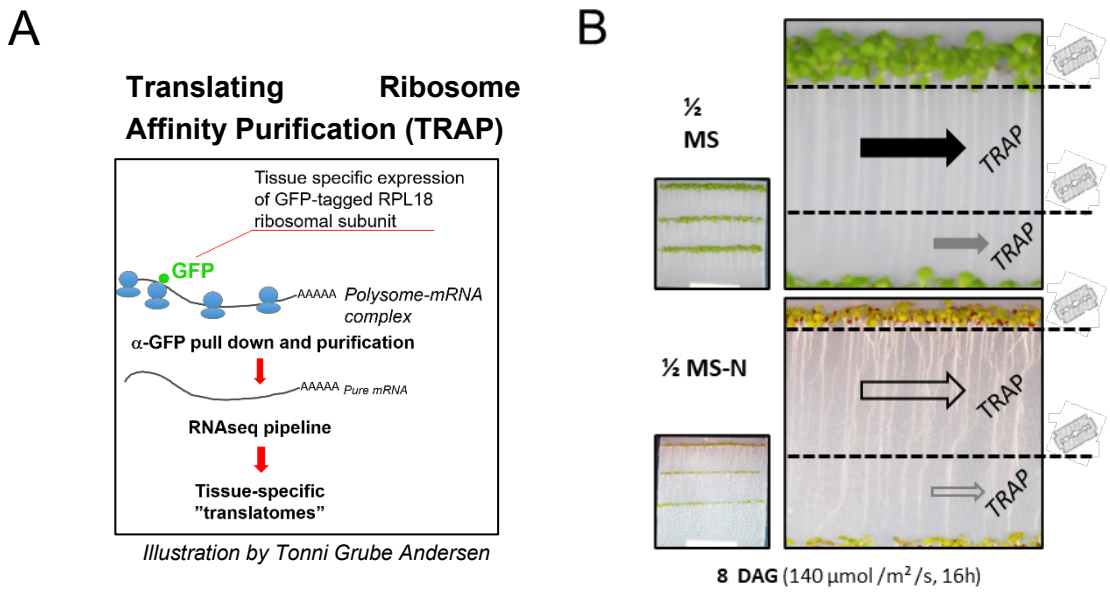

*Appendix Figure 1: **Visual explanation of TRAP seq approach: A** Cartoon explaining the process of obtaining tissue-specific posttranscriptional profiles ("translatomes") **B** Exemplary picture of plate grown seedlings of Arabidopsis thaliana 8 DAG. The top picture show 1/2 MS grown plants the bottom picture shows plants grown on 1/2 MS-N. Dotted lines indicate the height of dissection for obtaining "mature" and "young" root samples respectively.*

17.3 Data processing and cluster analysis

17.3.1 PCA and choice of genes included for variance assessment.

Frist, we removed genes with low counts. Here, we excluded genes that had below 10 counts in all samples of all conditions, i.e., if one condition featured more than 10 counts across all its replicates, the gene was kept. To improve the detection of DEGs (Sha et al., 2015), we additionally filtered genes that had below 159 (53*3) absolute counts, independent of count distribution within conditions. All following analyses were performed on the filtered counts. To analyse the principal components of the dataset, we chose the top 500 most varying genes (ntop = 500) (Appendix Figure 1A). Here, the first principal component explained 42% of the variance (Figure 6A,B,C,D). While increasing the number of included genes reduced the amount of explained variance by the first component (Appendix Figure 2B), it did not strongly affect the ordination of our samples along the first two principal components (Appendix Figure 2, Figure 6A), indicating that the top 500 most variable genes explained the sample behaviour to a similar extent as the full 21179 genes. PCA revealed clear distinctive profiles for the 14 conditions probed (n = 3-6).

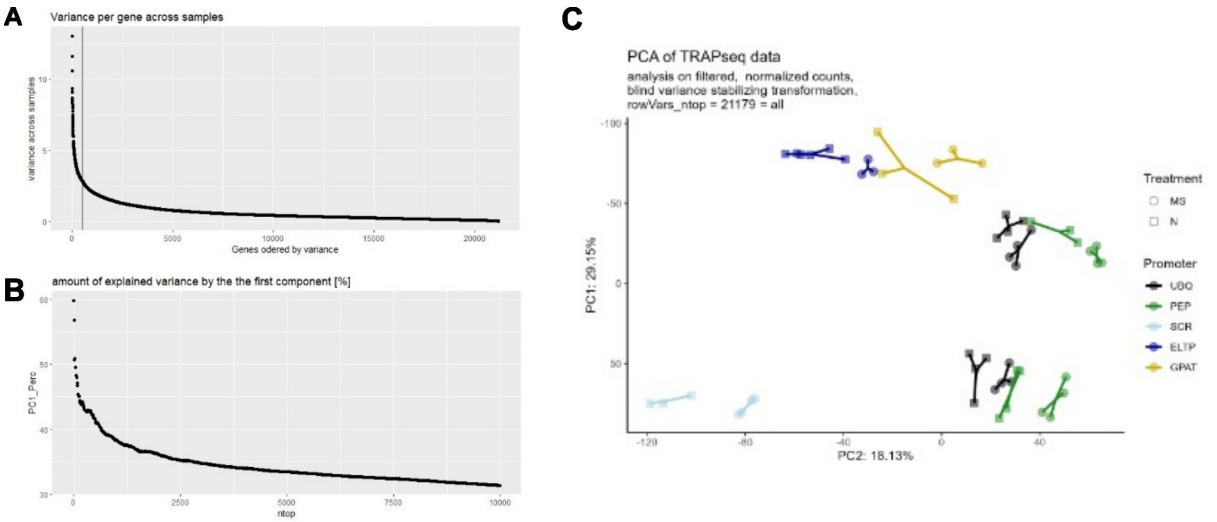

*Appendix Figure 2 **Choice of genes for variance analysis: A** Variance of individual genes post filtering **B** Contribution of the first principal component to the explained variance depending on the choice of included genes. **C** PCA plot of the first and second principal component including all genes regardless of variance*

17.3.2 Hierarchical clustering of individual samples and sample merging

In agreement with our conclusion from the PCA, the cluster hierarchy could be divided into different levels according to the physical dissection of the root, i.e., the tissue they were extracted from, the promoter used, and the treatment (Figure 6F). Interestingly, in young roots, the cortex (PEP) samples cluster separate from the endodermis-specific (SCR) and unspecific (UBQ) samples. In the mature root seems to be a subdivision between endodermis-specific samples (ELTP and GPAT5) apart from the cortex and the unspecific samples (PEP and UBQ).

On the first level samples clustered according to root zone. On the second level according to the tissue. On the third level, the samples cluster according to the different promoters under which the TRAP-construct was expressed. On the fourth level, the samples separated according to the nitrogen-starvation treatment. Lastly, on the fifth level, the samples separated into the individual replicates, indicating distinctive RNA abundance profiles for the different experimental conditions. We did not observe any clear clustering according to individual replicates, indicating that the biological variation with the conditions imposed in our experiment, is larger than the technical variation. Notably, one sample of the mature root under nitrogen starvation, expressing the TRAP-construct under the cortex-specific promoter, “PEP_N_1” did cluster closer to the unspecific samples (UBQ) under nitrogen starvation. Moreover, samples that were expressing the TRAP-construct under the “GPAT5” promoter and were grown under nitrogen starvation, GPAT_N, did not cluster together. Instead, GPAT_N_1 grouped together with samples of the late endodermis (ELTP) under nitrogen starvation. GPAT_N_4 grouped together with non-starved samples of the same promoter and GPAT_N_5 was grouped together with the unspecific mature root samples, irrespective of nitrogen status. This clustering poses a limitation to the interpretability of these specific samples. However, as the individual groupings are consistent with the premise of suberization, and thus GPAT5 expression, being primarily active in the late endodermis and suberization being increased upon nitrogen starvation. Altogether, the hierarchical clustering is consistent with the conclusions drawn from PCA, but highlights the higher variability of the data associated to suberizing cells under nitrogen starvation (“GPAT_N”) (Appendix Figure 3).

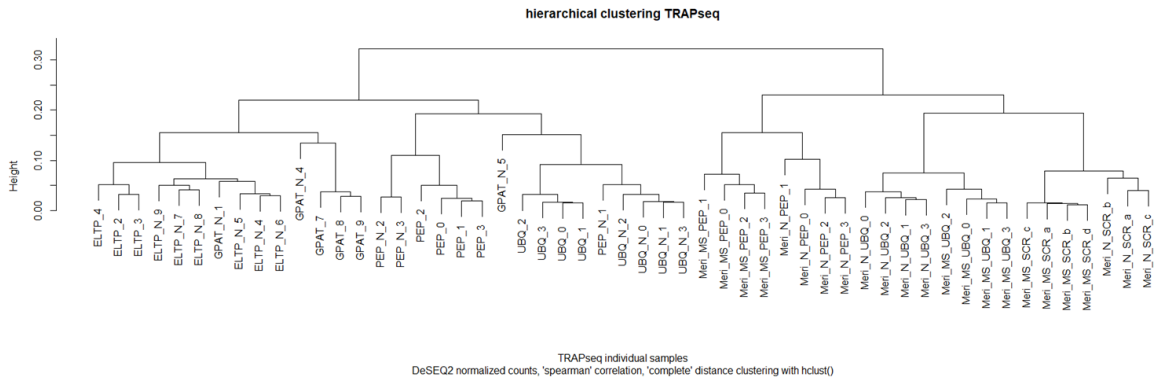

*Appendix Figure 3: **Hierarchical clustering of samples after filtering** The normalized counts were clustered using hclust() and the distances between the samples, according to spearman correlation, were plotted.*

17.3.3 K-means cluster determination based on Within Sum of Squares (WSS), Akaike Information Criterion (AIC) and Bayesian Information Criterion (BIC)

Next, we aimed to determine which genes behave similar in our dataset. Therefore, we chose to perform k-means clustering on our dataset. As indicated above, hierarchical clustering is an iterative but deterministic process in which the minimal distance between each node, across all dimensions, will be determined. In the first iteration each instance, i.e., a gene or a sample, represents a node. Then, the closest nodes are merged into a new node containing all dimensional information of its lower-level nodes and the process is repeated until all nodes are merged. In contrast, k-means clustering assigns a predetermined number of random vectors, so-called “centers” (MacQueen, 1967). Then, each data point is assigned to each nearest center and the center is redefined as centroid of all data points assigned to it. Again, all data

points are then assigned to the updated centers and the process is repeated/iterated until updating the centers does not change the data point assignment anymore. Accordingly, k-means cluster assignment is only semi-deterministic as it depends on the number and position of the initial centers. Because of the latter, it can happen that the algorithm converges early, in a local minimum, or doesn't converge at all, i.e., constant reassignment of data points. To combat convergence limitations, multiple random set of starting points are tested, in our case two. To determine the optimal number of k-centers, we assess the Within cluster Sum of Squares (WSS), which measures the distance between a center and all its assigned datapoints (Equation 2). The Akaike Information Criterion (AIC, Equation 3) and Bayesian Information Criterion (BIC, Equation 4) are derivatives of WSS and factor in the number of compared groups (AIC) or the number of compared groups as well as the number of observations (BIC) (Vrieze, 2012). The optimal number of k-centers is defined as the number where the addition of more centers does not further decrease the WSS, or the AIC and BIC reach a global minimum. Next, we tested our dataset for those criteria and for k-values between 2 and 150. We did not observe a minimum for AIC within these margins but found a minimum of k ≈ 100 (Appendix Figure 4A). However, selecting this many clusters would complicate the downstream analysis as well as the biological interpretation. Another controversial k-center selection method is the so-called "elbow-method", where the graphical representation of the WSS per k is used to determine the inflection point or in other words where the 2nd derivative equals 0 (Appendix Figure 4C). Additionally, we checked at which k the changes in WSS, AIC or BIC, so their first derivatives, were reduced by 99% (Appendix Figure 4C). Depending on the random start of the centers these values lay between k≈35-45. Subsequently, we chose to cluster gene similarity with k-means (k=36) for the analyses. For easier visualization and to get an impression of the relationship between the individual clusters, we determined the average z-score of all genes per cluster and condition and used these scores for hierarchical clustering. The distances between all individual samples were then calculated using the pairwise Pearson's correlation coefficient (Ma et al., 2021) (Figure 6G)

Equation 2 ***Within cluster Sum of Squares***

$$WSS = \left(\sum_{1}^{n}(k_i - x_i)^2\right)$$

Equation 3: ***Akaike Information Criterion***

$$AIC_i = Within\ cluster\ Sum\ of\ squares + 2 \cdot number\ of\ parameters$$
$$AIC_i = (\sum_{1}^{n}(k_i - x_i)^2) + 2 \cdot \left(k\ \cdot (j\ +\ 1)\right)$$

Equation 4 ***Bayesian Information Criterion***

$$BIC_i = Within\ cluster\ Sum\ of\ Squares + ln(number\ of\ observations\ ) \cdot number\ of\ parameters$$
$$BIC_i = (\sum_{1}^{n}(k_i - x_i)^2) + ln(n) \cdot \left(k\ \cdot (j\ +\ 1)\right)$$

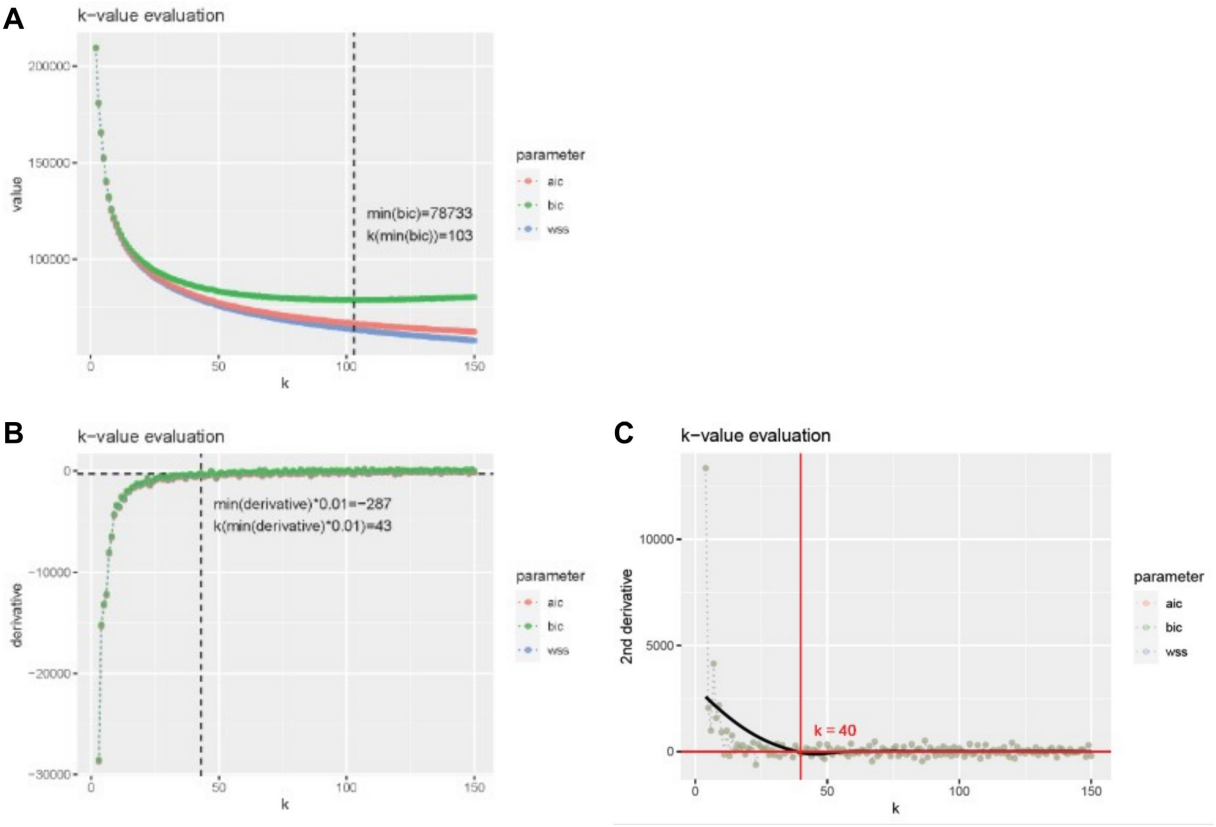

Appendix Figure 4: ***k-value evaluation*** *A computation of wss, aic and bic for the indicated k-values* ***B*** *first derivative of the wss, aic and bic values* ***C*** *second derivative of the wss, aic and bic values*

17.3.4 Comparison between clusters determined with hierarchical clustering and k-means clustering and cluster significance determination.

Hierarchical clustering and k-means clustering can be considered two distinct approaches to determine sample similarity across a large number of dimensions (n_genes = 21179). Thus, we also performed hierarchical clustering on the z-scores of all individual genes. The distances were calculated using Pearson correlation (Ma et al., 2021). Hence, the resulting tree had a maximum height of 2, as the maximum distance between perfect positive correlation (1) or perfect negative correlation (-1) (Appendix Figure 5). Next, we compared the genes that share similar behavior across conditions (hierarchical clustering) or shared a common center across conditions (kmeans). To obtain a comparable number of 36 clusters we cut the resulting tree at a height of 1.62 (Appendix Figure 5). Plotting the association of each gene between its respective clusters determined by kmeans or hierarchical clustering allowed us to assess the cluster stability. Clusters with a strong correspondence between h1.62 and k can be considered stable, i.e. k-cluster 4, 21 and 33, while clusters with a weaker correspondence can be considered less stable, i.e. k-cluster 7, 31 and 29. This should be considered when assessing the contents of these clusters respectively (Appendix Figure 6).

Lastly, we investigated the uniqueness of each cluster for our input parameters, being as stated above the condition (Appendix Figure 7A) promoter (Appendix Figure 7B), treatment or dissected root zone (Appendix Figure 7C). To see whether a cluster was significantly enriched for a specific condition, we performed a one-sided student's t-test on the z-scores of all genes within a cluster. For the purposes of the t-test, the z-scores of all parameters, that were not our

parameter of interested, were merged. Merging the samples this way produced vastly different sample sizes depending on cluster size. For this reason, p-values can be only compared within each cluster and parameter comparison respectively (Equation 5). However, comparing p-values generated this way indicates whether genes of a certain cluster are enriched for a certain condition of interest. This analysis allowed us to assign different gene clusters to the young and mature root and individual tissues, respectively. Indeed, when compared to previously published data, we saw a strong overlap of genes associated to the endodermis (pSCR and pELTP, k22, k36, k23, k34) (Figure 7D), albeit with varying stringency (Mustroph et al., 2009; Vragović et al., 2015).The overlap of cortex-associated genes (pPEP, k28, k13, k8, k25, k 15, k12), was less pronounced (Mustroph et al. 2009.).

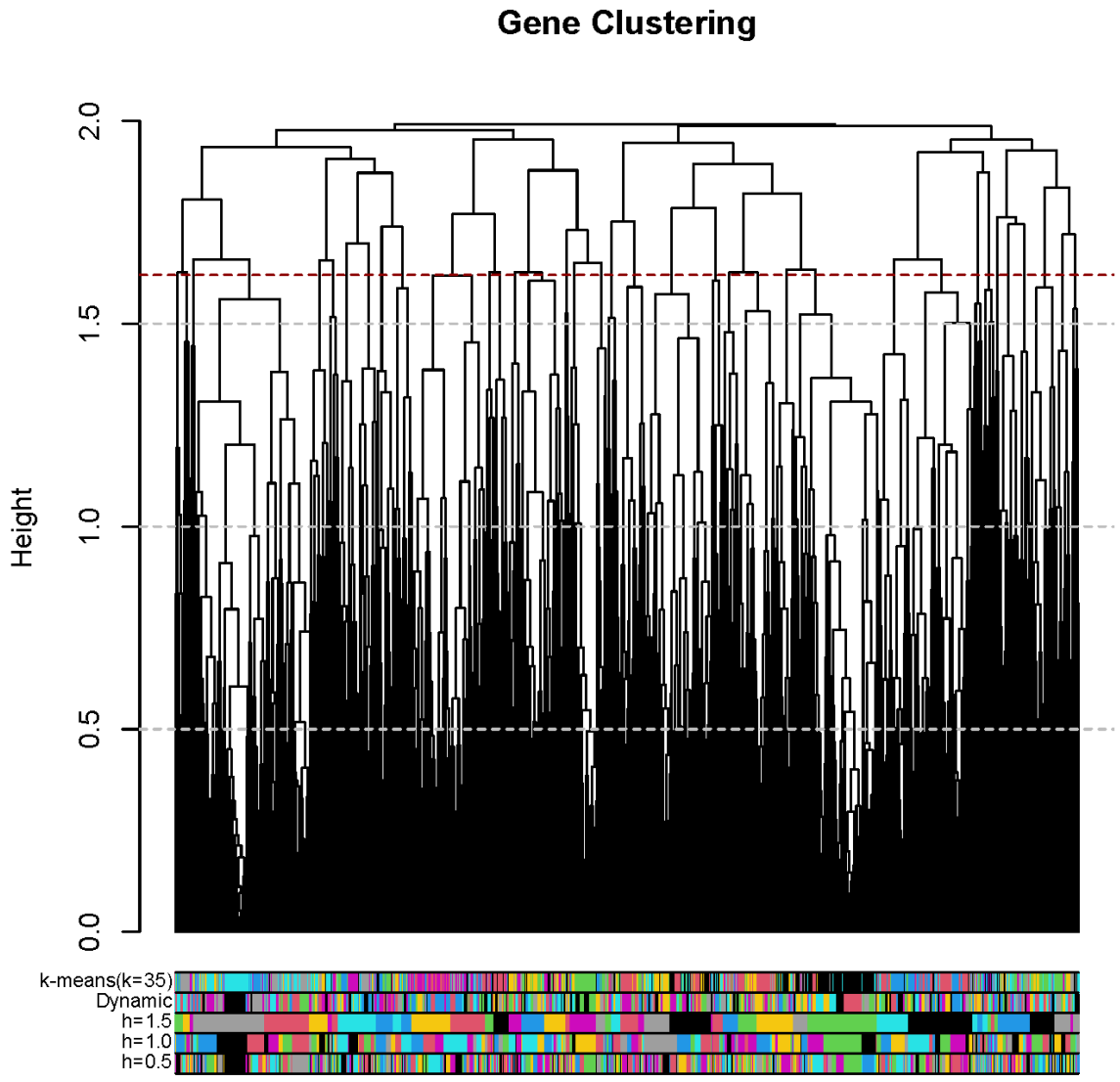

Appendix Figure 5: ***Hierarchical clustering of all genes post filtering:*** *The distances between all individual samples were then calculated according to the pairwise pearson correlation coefficients (Ma et al., 2021).*

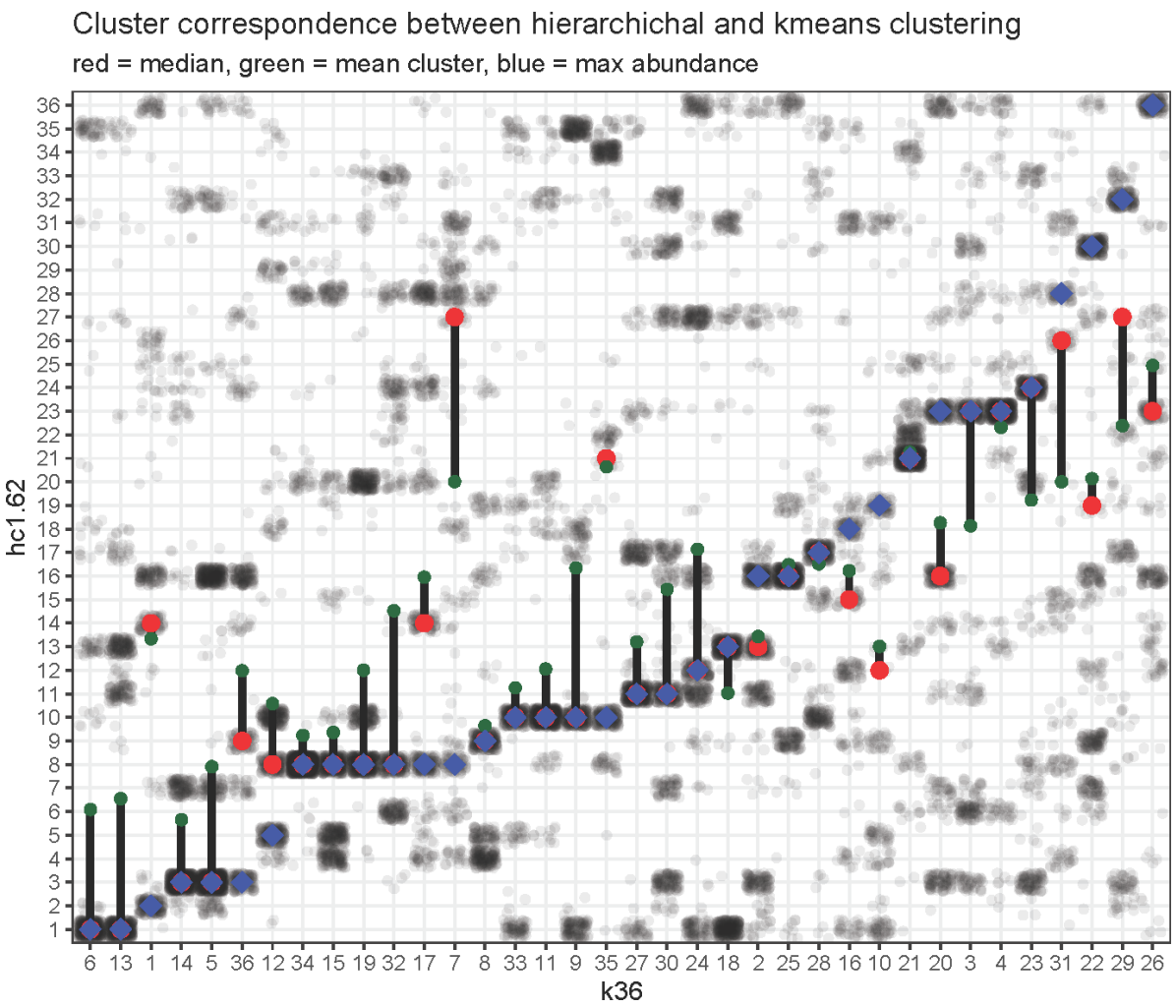

Appendix Figure 6: ***Cluster comparison of clusters determined by hierarchical clustering or kmeans clustering*** *The kmeans clusters (x-axis) were associated to the respective hierarchical clusters (y-axis) by determining the highest percentage of k-cluster genes associated to the respective hierarchical cluster (blue dot). Similarly mean (green) and median (red) abundance were determined. Grey dots represent individual genes.*

A

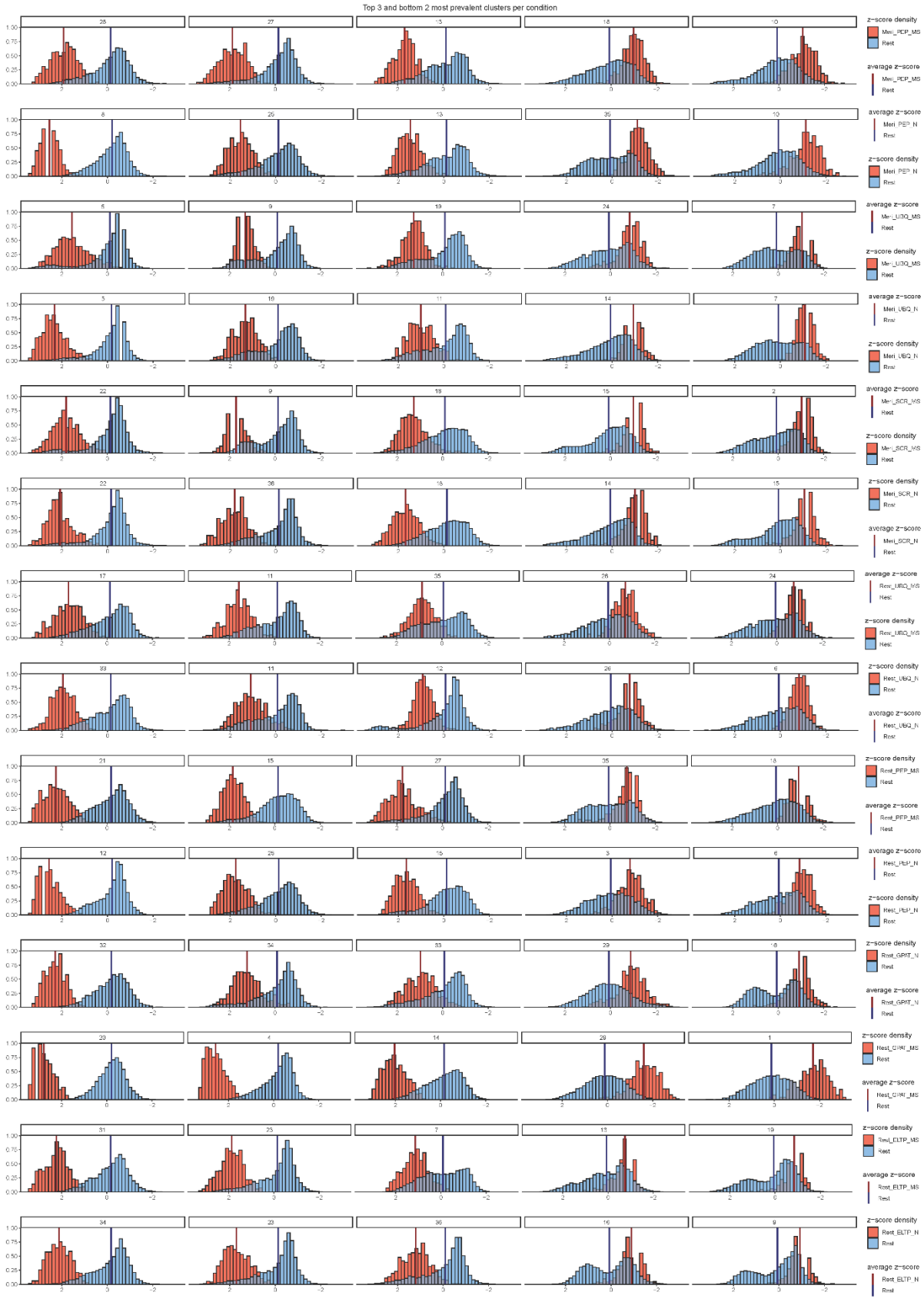
Top 3 and bottom 2 most prevalent clusters per condition
z-score density
average z-score

B

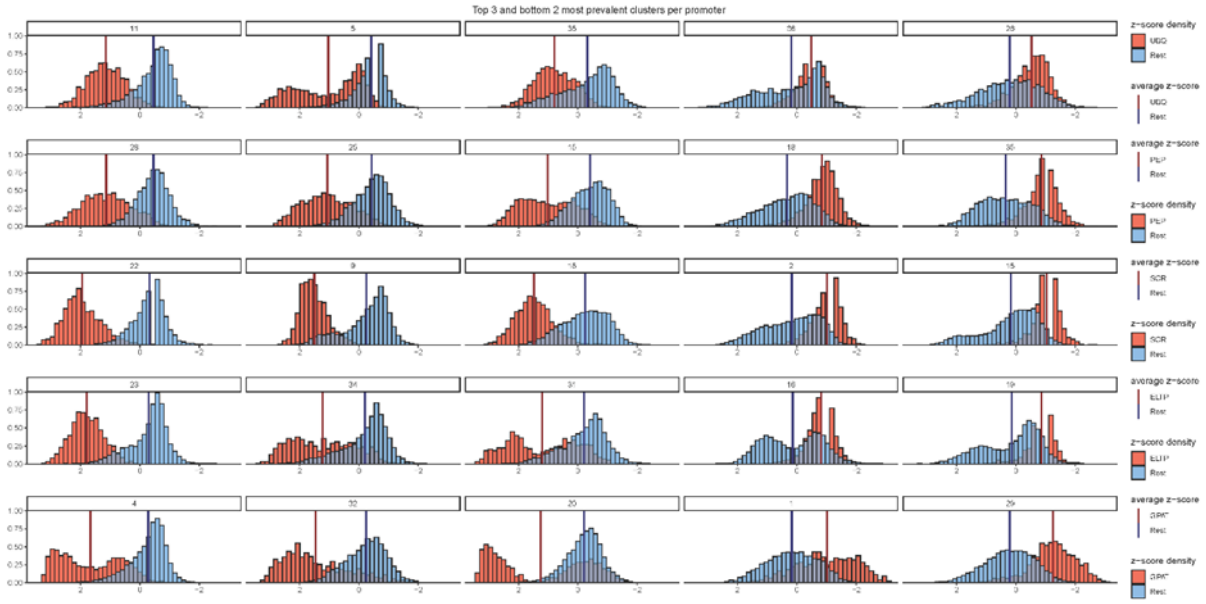

C

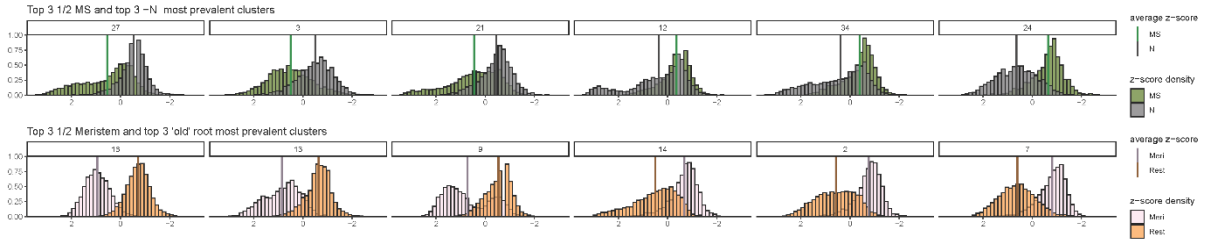

Appendix Figure 7: ***Evaluation of cluster uniqueness via one sided t-test.*** ***A,B*** *Subset of individual parameters (in red) versus the remaining samples unequal to the parameter of interest (blue). Exemplary the three most unique clusters as well as the two least unique clusters are shown per parameter* ***A*** *Cluster uniqueness for each of the 14 conditions* ***B*** *Cluster uniqueness for each of the five promoters* ***C*** *Cluster uniqueness for the two treatments, and for the the two zones respectively. Here only the two parameters were mutually exclusive.*

*Equation 5:****Determination of cluster significance between individual parameters of interest:***

$$Sample\ size_i = cluster\ size \cdot parameter\ conditions$$
$$Sample\ size\_i = cluster\ size \cdot non\_parameter\ conditions$$
$$n_{pUBQ\_N(Cluster24)} = 268 * 1 = 268$$
$$n_{Rest(Cluster24)} = 268 * 13 = 3484$$

17.4 Comparison of TRAPseq and whole root RNAseq highlights core nitrogen starvation genes but also differences between transcribed and translated mRNA.

In this study, we obtained a second transcriptional dataset the same growth conditions as used for the TRAPseq (8 Materials and Methods). Here RNAseq was performed on whole root total RNA. Besides the transfer of plants to a fresh 1/2MS-N plate 6DAG, the conditions for the RNAseq experiment were directly comparable to the setup used for TRAPseq. First, we investigated the robustness of our data. We individually processed both datasets and compared the counts present in both datasets. Despite the individual filtering, the differentially expressed genes in the final count tables were largely overlapping. Thus, we performed PCA on the remaining 20712 genes, representing 98% of the RNAseq (n=211332) dataset and the TRAPseq dataset (n=21179) respectively. The first principal component resolved the nitrogen

starvation treatment, while the second differentiated the differently dissected tissues the RNA was harvested from (Appendix Figure 8, Left). Despite the fact, that nitrate-resupply did not revert the suberization in wild-type plants 2 days after transfer (Figure 10D), the transcriptome of all genotypes after nitrate re-supply was clustering closer to transcriptomes of samples continuously grown under 1/2 MS (sufficient nitrogen) conditions. When performing DEG (list of abbreviations) analysis on the TRAPseq and the RNAseq data individually we found that 362 genes were upregulated in both TRAPseq and RNAseq, representing 66% (n=546) and 34% (n=1070) of the upregulated DEGs respectively (Appendix Figure 8**,** Right). We concluded that this the core nitrogen starvation response. GO-enrichment revealed that this primarily included the response to nitrogen compounds including amino acid-, nitrogen- and secondary metabolism such as nitrogen starvation (data not shown). However, we also found distinct DEGs for the TRAPseq and RNAseq, respectively. E.g., the previously observed phenylpropanoid metabolism was increased in nitrogen starvation regulation of programmed cell-death only in the TRAPseq data. While the response to hypoxia, the response to oxidative stress but also ureide metabolic processes are only visible in the RNAseq. Only *S8H* (AT3G12900) is upregulated in the TRAPseq but downregulated in the RNAseq. However, performing Gas Chromatography coupled to Mass Spectrometry (GC-MS) on extracts of whole roots grown under the same conditions as the TRAPseq, we found that indeed Scopoletin and Fraxetin levels were elevated, while Sideretin levels were not (Figure 8E). These preliminary results are in line with the elevated transcript levels of *F6'H1*, synthesizing Scopoletin, elevated levels of *S8H,* synthesizing Fraxetin and decreased levels of *CYP82C4,* synthesizing Sideretin (Figure 8A). This indicates that coumarins are indeed regulated as indicated by the TRAPseq. The differential regulation of *S8H* in the transfer RNAseq could be due to the different experimental procedure, i.e. the transfer to a fresh plate, or alternatively due to the difference between assessing the plant transcriptome or post-transcriptome ("translatome").

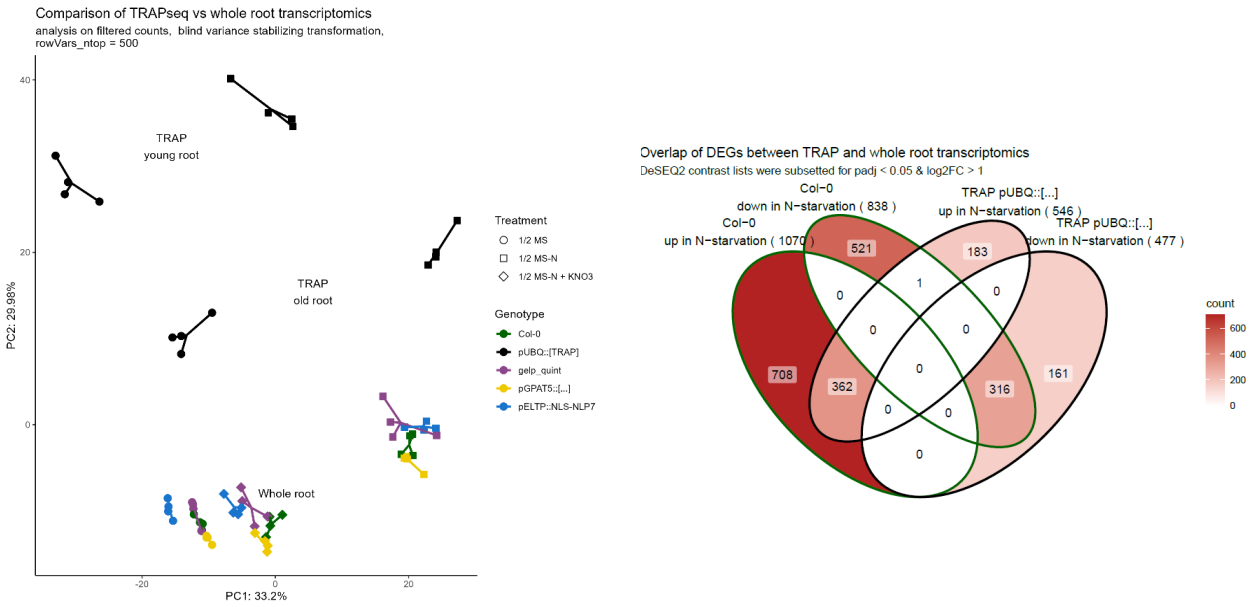

Appendix Figure 8: ***Comparison of whole root transcriptomics with TRAPseq data: Left*** *PCA analysis of TRAPseq data using the UBQ promoter.* ***Right*** *Venn diagram showing the overlap of DEGs when comparing the 1/2MS-N vs the 1/2MS condition within the individual experiments.*

18 Appendix II: TRAP protocol

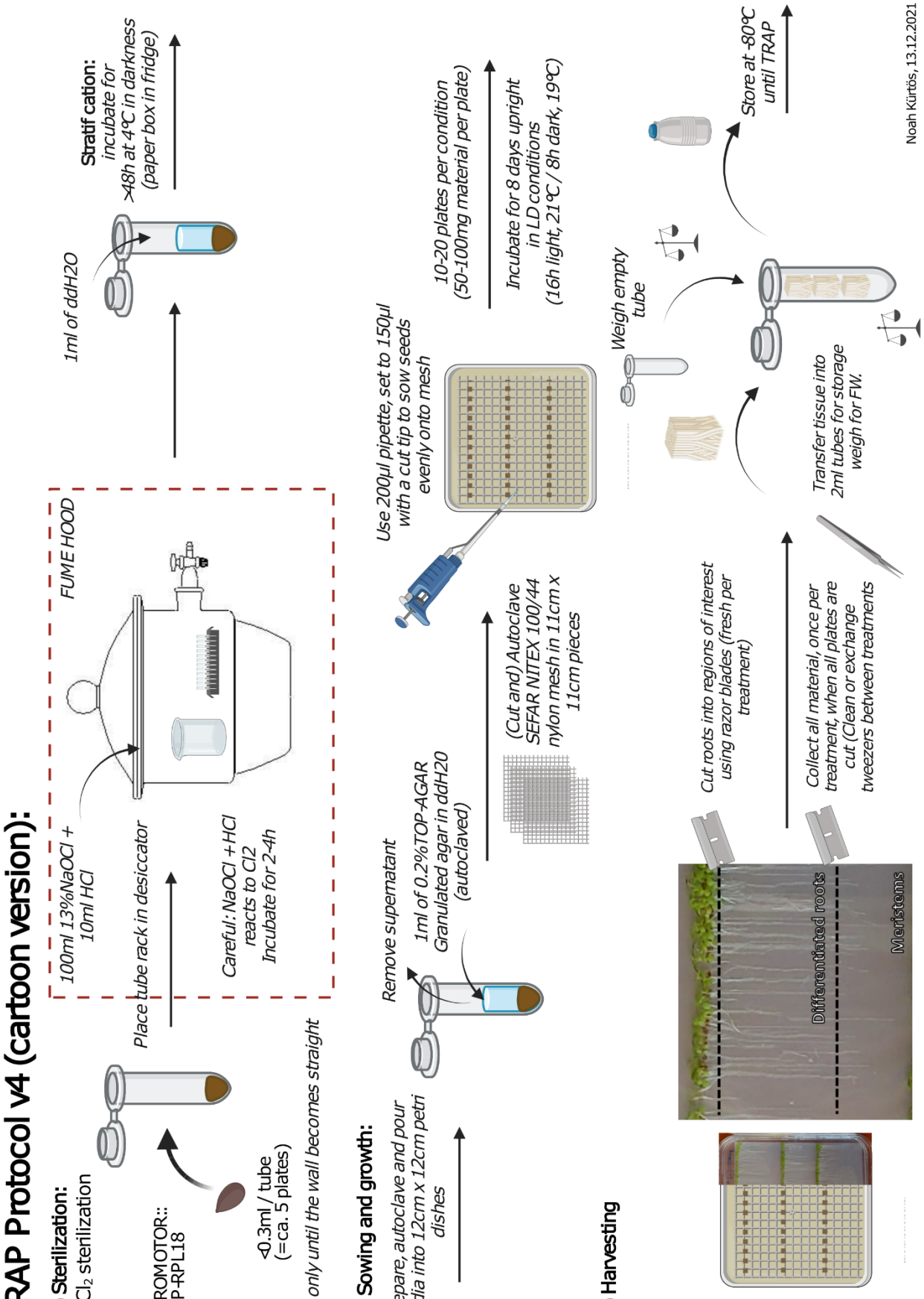

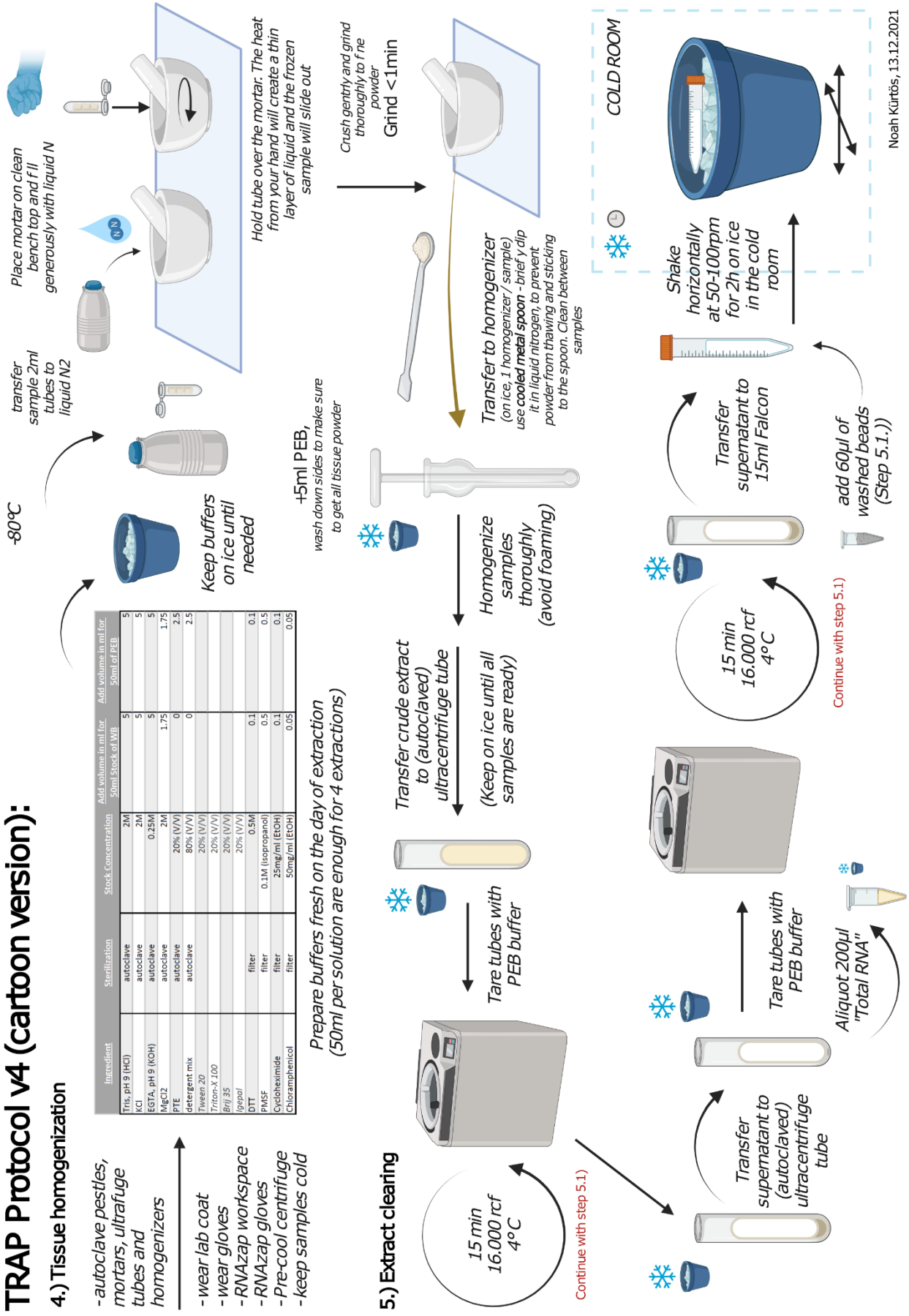

Ingredient	Sterilization	Stock Concentration	Add volume in ml for 50ml Stock of WB	Add volume in ml for 50ml of PEB
Tris, pH 9 (HCl)	autoclave	2M	5	5
KCl	autoclave	2M	5	5
EGTA, pH 9 (KOH)	autoclave	0.25M	5	5
MgCl2	autoclave	2M	1.75	1.75
PTE	autoclave	20% (V/V)	0	2.5
detergent mix	autoclave	80% (V/V)	0	2.5
Tween 20		20% (V/V)		
Triton-X 100		20% (V/V)		
Brij 35		20% (V/V)		
Igepal		20% (V/V)		
DTT	filter	0.5M	0.1	0.1
PMSF	filter	0.1M (isopropanol)	0.5	0.5
Cycloheximide	filter	25mg/ml [EtOH]	0.1	0.1
Chloramphenicol	filter	50mg/ml [EtOH]	0.05	0.05

TRAP Protocol v4 (cartoon version):

5.1.) Bead cleaning (while extract clearing centrifugations)

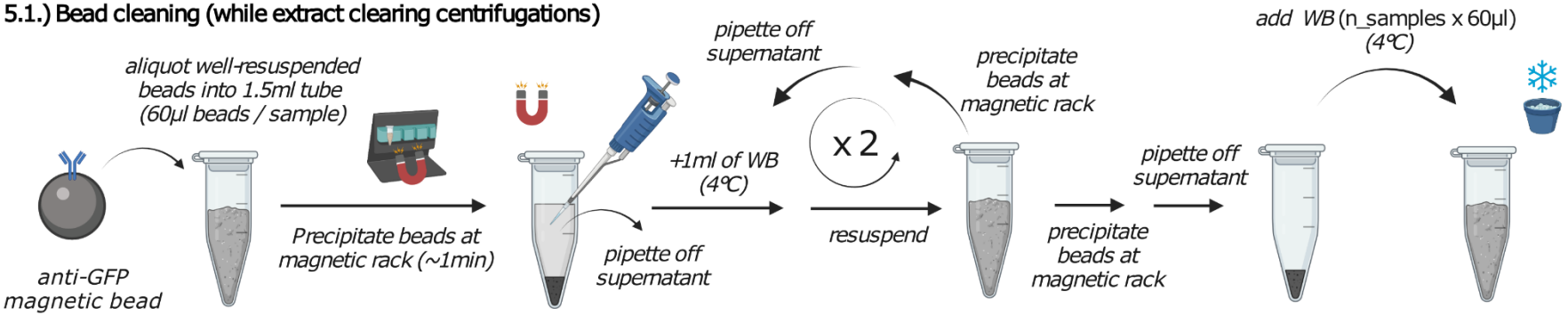

6.) Immunoprecipitation

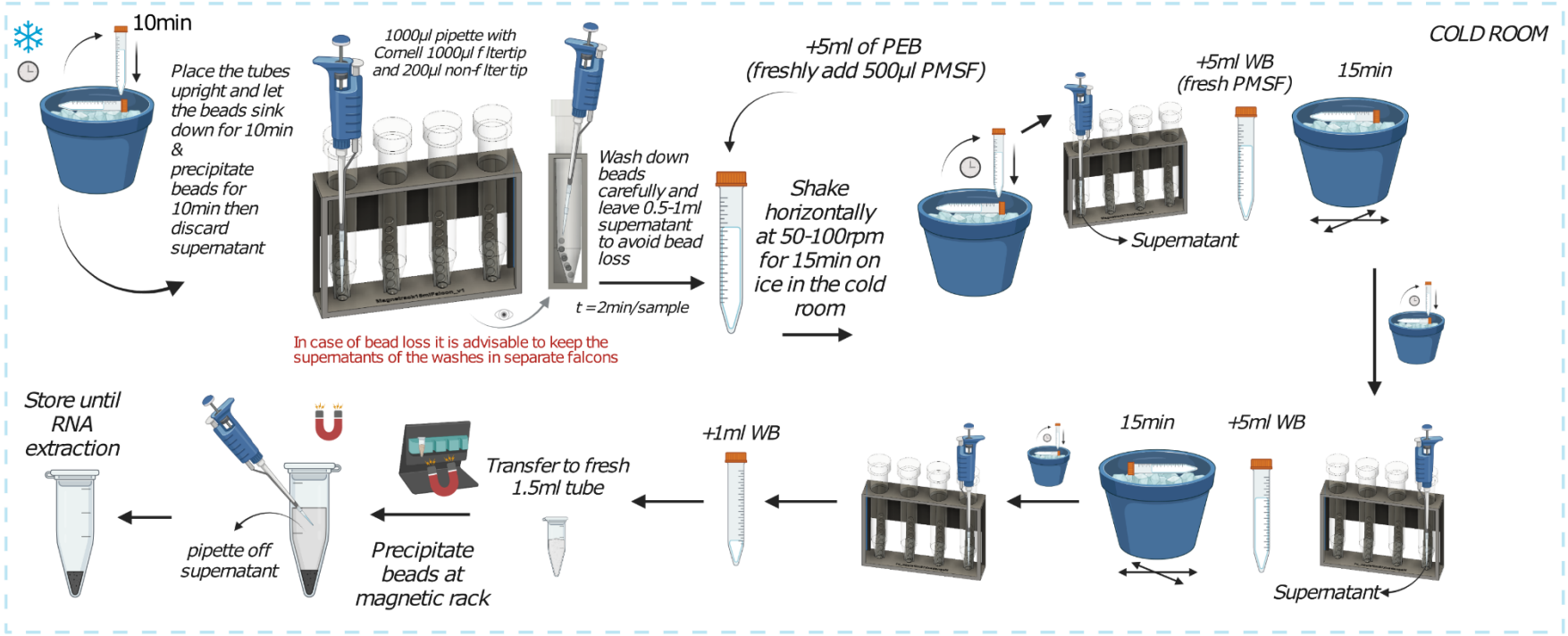

Noah Kürtös, 13.12.2021

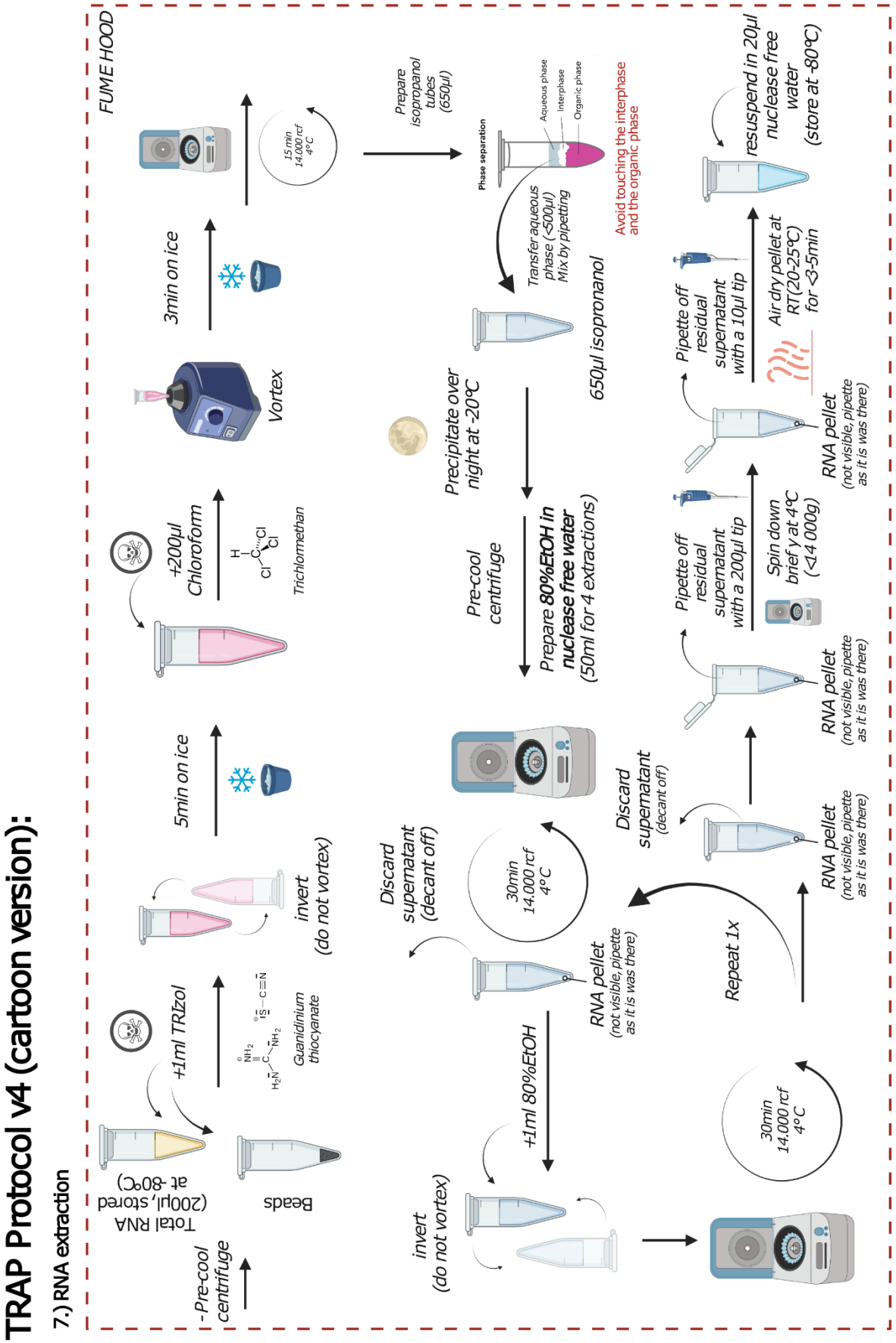

Noah Kürtös, 13.12.2021

19 References

Ågren, G. I., & Franklin, O. (2003). Root:shoot ratios, optimization and nitrogen productivity. *Annals of Botany*, *92*(6), 795–800. https://doi.org/10.1093/aob/mcg203

Almeida, T., Menéndez, E., Capote, T., Ribeiro, T., Santos, C., & Gonçalves, S. (2013). Molecular characterization of Quercus suber MYB1, a transcription factor up-regulated in cork tissues. *Journal of Plant Physiology*, *170*(2), 172–178. https://doi.org/10.1016/J.JPLPH.2012.08.023

Anders, S., Pyl, P. T., & Huber, W. (2015). HTSeq-A Python framework to work with high-throughput sequencing data. *Bioinformatics*, *31*(2), 166–169. https://doi.org/10.1093/bioinformatics/btu638

Andersen, T. G., Barberon, M., & Geldner, N. (2015). Suberization-the second life of an endodermal cell. *Current Opinion in Plant Biology*, *28*, 9–15. https://doi.org/10.1016/j.pbi.2015.08.004

Andersen, T. G., Molina, D., Kilian, J., Franke, R. B., Ragni, L., & Geldner, N. (2021). Tissue-Autonomous Phenylpropanoid Production Is Essential for Establishment of Root Barriers. *Current Biology*, *31*(5), 965-977.e5. https://doi.org/10.1016/j.cub.2020.11.070

Andersen, T. G., Naseer, S., Ursache, R., Wybouw, B., Smet, W., De Rybel, B., Vermeer, J. E. M., & Geldner, N. (2018). Diffusible repression of cytokinin signalling produces endodermal symmetry and passage cells. *Nature*, *555*(7697), 529–533. https://doi.org/10.1038/nature25976

Araya, T., Miyamoto, M., Wibowo, J., Suzuki, A., Kojima, S., Tsuchiya, Y. N., Sawa, S., Fukuda, H., Von Wirén, N., & Takahashi, H. (2014). CLE-CLAVATA1 peptide-receptor signaling module regulates the expansion of plant root systems in a nitrogen-dependent manner. *Proceedings of the National Academy of Sciences of the United States of America*, *111*(5), 2029–2034. https://doi.org/10.1073/PNAS.1319953111/-/DCSUPPLEMENTAL/PNAS.201319953SI.PDF

Arevalo, C. B. M., Drew, A. P., & Volk, T. A. (2005). The effect of common Dutch white clover (Trifolium repens L.), as a green manure, on biomass production, allometric growth and foliar nitrogen of two willow clones. *Biomass and Bioenergy*, *29*(1), 22–31. https://doi.org/10.1016/J.BIOMBIOE.2005.02.003

Armand, T., Cullen, M., Boiziot, F., Li, L., & Fricke, W. (2019). Cortex cell hydraulic conductivity, endodermal apoplastic barriers and root hydraulics change in barley (Hordeum vulgare L.) in response to a low supply of N and P. *Annals of Botany*, *124*(6), 1091–1107. https://doi.org/10.1093/aob/mcz113

Armijo, G., & Gutiérrez, R. A. (2017). Emerging Players in the Nitrate Signaling Pathway. *Molecular Plant*, *10*, 1019–1022. https://doi.org/10.1016/j.molp.2017.07.006

Bai, L., Ma, X., Zhang, G., Song, S., Zhou, Y., Gao, L., Miao, Y., & Song, C. P. (2014). A Receptor-Like Kinase Mediates Ammonium Homeostasis and Is Important for the Polar Growth of Root Hairs in Arabidopsis. *The Plant Cell*, *26*(4), 1497–1511. https://doi.org/10.1105/TPC.114.124586

Bai, L., Zhou, Y., Ma, X., Gao, L., & Song, C.-P. (2014). *Plant Signaling & Behavior Arabidopsis CAP1-mediated ammonium sensing required reactive oxygen species in plant cell growth*. https://doi.org/10.4161/psb.29582

Barbarino, E., & Lourenço, S. O. (2009). Comparison of CHN analysis and Hach acid digestion to quantify total nitrogen in marine organisms. *Limnology and Oceanography: Methods*, *7*(NOV), 751–760. https://doi.org/10.4319/lom.2009.7.751

Barberon, M. (2017). The endodermis as a checkpoint for nutrients. In *New Phytologist* (Vol. 213, Issue 4, pp. 1604–1610). Blackwell Publishing Ltd. https://doi.org/10.1111/nph.14140

Barberon, M., Vermeer, J. E. M., De Bellis, D., Wang, P., Naseer, S., Andersen, T. G., Humbel, B. M., Nawrath, C., Takano, J., Salt, D. E., & Geldner, N. (2016). Adaptation of Root Function by Nutrient-Induced Plasticity of Endodermal Differentiation. *Cell*, *164*(3), 447–459. https://doi.org/10.1016/j.cell.2015.12.021

Bar-On, Y. M., Phillips, R., & Milo, R. (2018). The biomass distribution on Earth. *Proceedings of the National Academy of Sciences of the United States of America*, *115*(25), 6506–6511. https://doi.org/10.1073/PNAS.1711842115/SUPPL_FILE/1711842115.SAPP.PDF

Barth, P., Stüeken, E. E., Helling, C., Rossmanith, L., Peng, Y., Walters, W., & Claire, M. (2023). Isotopic constraints on lightning as a source of fixed nitrogen in Earth's early biosphere. *Nature Geoscience 2023 16:6*, *16*(6), 478–484. https://doi.org/10.1038/s41561-023-01187-2

Baxter, I., Hosmani, P. S., Rus, A., Lahner, B., Borevitz, J. O., Muthukumar, B., Mickelbart, M. V., Schreiber, L., Franke, R. B., & Salt, D. E. (2009). Root suberin forms an extracellular barrier that affects water relations and mineral nutrition in Arabidopsis. *PLoS Genetics*, *5*(5). https://doi.org/10.1371/journal.pgen.1000492

Benvenuto, M. A., & Plaumann, H. (2021). Chapter 25 Nitric acid. *Industrial Catalysis*, 95–98. https://doi.org/10.1515/9783110542868-025/HTML

Berardini, T. Z., Reiser, L., Li, D., Mezheritsky, Y., Muller, R., Strait, E., & Huala, E. (2015). The arabidopsis information resource: Making and mining the "gold standard" annotated reference plant genome. *Genesis*, *53*(8), 474–485. https://doi.org/10.1002/DVG.22877

Berhe, A. A., Arnold, C., Stacy, E., Lever, R., McCorkle, E., & Araya, S. N. (2014). *Soil erosion controls on biogeochemical cycling of carbon and nitrogen.* Citation: Berhe, A. A., Arnold, C., Stacy, E., Lever, R., McCorkle, E. & Araya, S. N. (2014) Soil Erosion Controls on Biogeochemical Cycling of Carbon and Nitrogen. Nature Education Knowledge 5(8):2. https://www.nature.com/scitable/knowledge/library/soil-erosion-controls-on-biogeochemical-cycling-of-122160904/

Bezrutczyk, M., Yang, J., Eom, J. S., Prior, M., Sosso, D., Hartwig, T., Szurek, B., Oliva, R., Vera-Cruz, C., White, F. F., Yang, B., & Frommer, W. B. (2018). Sugar flux and signaling in plant–microbe interactions. *The Plant Journal*, *93*(4), 675–685. https://doi.org/10.1111/TPJ.13775

Birnbaum, K., Jung, J. W., Wang, J. Y., Lambert, G. M., Hirst, J. A., Galbraith, D. W., & Benfey, P. N. (2005). Cell type-specific expression profiling in plants via cell sorting of protoplasts from fluorescent reporter lines. In *NATURE METHODS* | (Vol. 2, Issue 8). http://www.arabidopsis.org/

Bolger, A. M., Lohse, M., & Usadel, B. (2014). Trimmomatic: A flexible trimmer for Illumina sequence data. *Bioinformatics*, *30*(15), 2114–2120. https://doi.org/10.1093/bioinformatics/btu170

Bouguyon, E., Brun, F., Meynard, D., Kubeš, M., Pervent, M., Leran, S., Lacombe, B., Krouk, G., Guiderdoni, E., Zazímalová, E., Hoyerová, K., Nacry, P., & Gojon, A. (2015). Multiple mechanisms of nitrate sensing by Arabidopsis nitrate transceptor NRT1.1. *Nature Plants*, *1*. https://doi.org/10.1038/nplants.2015.15

Bradford, M. M. (1976). A rapid and sensitive method for the quantitation of microgram quantities of protein utilizing the principle of protein-dye binding. *Analytical Biochemistry*, *72*(1–2), 248–254. https://doi.org/10.1016/0003-2697(76)90527-3

Bray, J. R., & Curtis, J. T. (1957). An Ordination of the Upland Forest Communities of Southern Wisconsin. *Ecological Society of Ameria*, *27*(4), 325–349.

Breazeale, J. F. (1906). The relation of sodium to potassium in soil and solution cultures. *Journal of the American Chemical Society*, *28*(8), 1013–1025. https://doi.org/10.1021/JA01974A008

Buathong, R., Chamchumroon, V., Schinnerl, J., Bacher, M., Santimaleeworagun, W., Kraichak, E., & Vajrodaya, S. (2019). Chemovariation and antibacterial activity of extracts and isolated compounds from species of Ixora and Greenea (Ixoroideae, Rubiaceae). *PeerJ*, *2019*(5), e6893. https://doi.org/10.7717/PEERJ.6893/SUPP-3

Bulgarelli, D., Mimmo, T., Mathesius, U., Canarini, A., Kaiser, C., Merchant, A., Richter, A., & Wanek, W. (2019). *Root Exudation of Primary Metabolites: Mechanisms and Their Roles in Plant Responses to Environmental Stimuli*. *10*. https://doi.org/10.3389/fpls.2019.00157

Bulgarelli, D., Schlaeppi, K., Spaepen, S., Van Themaat, E. V. L., & Schulze-Lefert, P. (2013). Structure and functions of the bacterial microbiota of plants. In *Annual Review of Plant Biology* (Vol. 64, pp. 807–838). https://doi.org/10.1146/annurev-arplant-050312-120106

Campbell, W. H. (2001). Structure and function of eukaryotic NAD(P)H:nitrate reductase. *CMLS, Cell. Mol. Life Sci*, *58*, 194–204.

Caspary, R. (1866). Bemerkungen ueber die Schutzscheide und die Bildung des Stammes und der Wurzel. *Jahrbuecher Fuer Wissenschaftliche Botanik*, *4*, 101–123.

Chamizo-Ampudia, A., Sanz-Luque, E., Llamas, A., Galvan, A., & Fernandez, E. (2017). Nitrate Reductase Regulates Plant Nitric Oxide Homeostasis. *Trends in Plant Science*, *22*, 163–174. https://doi.org/10.1016/j.tplants.2016.12.001

Chen, X., Yao, Q., Gao, X., Jiang, C., Harberd, N. P., & Fu, X. (2016). Shoot-to-Root Mobile Transcription Factor HY5 Coordinates Plant Carbon and Nitrogen Acquisition. *Current Biology*, *26*(5), 640–646. https://doi.org/10.1016/J.CUB.2015.12.066

Chen, Y., Lun, A. T. L., & Smyth, G. K. (2014). Differential Expression Analysis of Complex RNA-seq Experiments Using edgeR. *Statistical Analysis of Next Generation Sequencing Data*, 51–74. https://doi.org/10.1007/978-3-319-07212-8_3

Cheng, C. Y., Krishnakumar, V., Chan, A. P., Thibaud-Nissen, F., Schobel, S., & Town, C. D. (2017). Araport11: a complete reannotation of the Arabidopsis thaliana reference genome. *Plant Journal*, *89*(4), 789–804. https://doi.org/10.1111/tpj.13415

Chislock, M. F., Doster, E., Zitomer, R., & Wilson, A. E. (2013). *Eutrophication: Causes, Consequences, and Controls in Aquatic Ecosystems*. Chislock, M. F., Doster, E., Zitomer, R. A. & Wilson, A. E. (2013) Eutrophication: Causes, Consequences, and Controls in Aquatic Ecosystems. Nature Education Knowledge 4(4):10.

Chopin, F., Orsel, M., Dorbe, M. F., Chardon, F., Truong, H. N., Miller, A. J., Krapp, A., & Daniel-Vedele, F. (2007). The Arabidopsis ATNRT2.7 Nitrate Transporter Controls Nitrate Content in Seeds. *The Plant Cell*, *19*(5), 1590. https://doi.org/10.1105/TPC.107.050542

Christensen, N. L. (1973). Fire and the Nitrogen Cycle in California Chaparral. *Science*, *181*(4094), 66–68. https://doi.org/10.1126/SCIENCE.181.4094.66

Corratgé-Faillie, C., & Lacombe, B. (2017). Substrate (un)specificity of Arabidopsis NRT1/PTR FAMILY (NPF) proteins. *Journal of Experimental Botany*, *68*(12), 3107–3113. https://doi.org/10.1093/JXB/ERW499

Cosme, M., Fernández, I., Declerck, S., van der Heijden, M. G. A., & Pieterse, C. M. J. (2021). A coumarin exudation pathway mitigates arbuscular mycorrhizal incompatibility in Arabidopsis thaliana. *Plant Molecular Biology*, *106*(4–5), 319–334. https://doi.org/10.1007/S11103-021-01143-X

Courty, P. E., Smith, P., Koegel, S., Redecker, D., & Wipf, D. (2015). Inorganic Nitrogen Uptake and Transport in Beneficial Plant Root-Microbe Interactions. *Critical Reviews in Plant Sciences*, *34*, 4–16. https://doi.org/10.1080/07352689.2014.897897

Croswell, K. (1996). *The alchemy of the heavens.*

Cuin, T. A., Pedas, P., Hegelund, J. N., Shabala, S., Schjoerring, J. K., & Jahn, T. P. (2010). Competition between uptake of ammonium and potassium in barley and Arabidopsis roots: molecular mechanisms and physiological consequences. *Journal of Experimental Botany*, *61*(9), 2303–2315. https://doi.org/10.1093/jxb/erq057

Czaban, W., Jämtgård, S., Näsholm, T., Rasmussen, J., Nicolaisen, M., & Fomsgaard, I. S. (2016). Direct acquisition of organic N by white clover even in the presence of inorganic N. *Plant and Soil*, *407*(1–2), 91–107. https://doi.org/10.1007/S11104-016-2896-Z/FIGURES/4

de Vries, J., & Archibald, J. M. (2018). Plant evolution: landmarks on the path to terrestrial life. *New Phytologist*, *217*(4), 1428–1434. https://doi.org/10.1111/NPH.14975

Denyer, T., Ma, X., Klesen, S., Scacchi, E., Nieselt, K., & Timmermans, M. (2018). Spatiotemporal Developmental Trajectories in the Arabidopsis Root Revealed Using High-Throughput Single Cell RNA Sequencing. *SSRN Electronic Journal*. https://doi.org/10.2139/ssrn.3300042

Denyer, T., Ma, X., Klesen, S., Scacchi, E., Nieselt, K., & Timmermans, M. C. P. (2019). Spatiotemporal Developmental Trajectories in the Arabidopsis Root Revealed Using High-Throughput Single-Cell RNA Sequencing. *Developmental Cell*, *48*(6), 840-852.e5. https://doi.org/10.1016/j.devcel.2019.02.022

Di Laurenzio, L., Wysocka-Diller, J., Malamy, J. E., Pysh, L., Helariutta, Y., Freshour, G., Hahn, M. G., Feldmann, K. A., & Benfey, P. N. (1996). The SCARECROW gene regulates an asymmetric cell division that is essential for generating the radial organization of the Arabidopsis root. *Cell*, *86*(3), 423–433. https://doi.org/10.1016/S0092-8674(00)80115-4

Diaz, R. J., & Rosenberg, R. (2008). Spreading dead zones and consequences for marine ecosystems. *Science*, *321*(5891), 926–929. https://doi.org/10.1126/SCIENCE.1156401/SUPPL_FILE/1156401-DIAZ-SOM.PDF

Doblas, V. G., Geldner, N., & Barberon, M. (2017). The endodermis, a tightly controlled barrier for nutrients. In *Current Opinion in Plant Biology* (Vol. 39, pp. 136–143). Elsevier Ltd. https://doi.org/10.1016/j.pbi.2017.06.010

Doblas, V. G., Smakowska-Luzan, E., Fujita, S., Alassimone, J., Barberon, M., Madalinski, M., Belkhadir, Y., & Geldner, N. (2017). Root diffusion barrier control by a vasculature-derived peptide binding to the SGN3 receptor. *Science (New York, N.Y.)*, *355*(6322), 280–284. https://doi.org/10.1126/SCIENCE.AAJ1562

Dolan, L., Janmaat, K., Willemsen, V., Linstead, P., Poethig, S., Roberts, K., & Scheres, B. (1993). Cellular organisation of the Arabidopsis thaliana root. *Development*, *119*(1), 71–84.

Dong, N. Q., & Lin, H. X. (2021). Contribution of phenylpropanoid metabolism to plant development and plant–environment interactions. *Journal of Integrative Plant Biology*, *63*(1), 180–209. https://doi.org/10.1111/JIPB.13054

Durán, P., Ellis, T. J., Thiergart, T., Ågren, J., & Hacquard, S. (2022). Climate drives rhizosphere microbiome variation and divergent selection between geographically distant Arabidopsis populations. *New Phytologist*, *236*(2), 608–621. https://doi.org/10.1111/nph.18357

Durand, M., Brehaut, V., Clement, G., Kelemen, Z., Macé, J., Feil, R., Duville, G., Launay-Avon, A., Roux, C. P. Le, Lunn, J. E., Roudier, F., & Krapp, A. (2023). The Arabidopsis transcription factor NLP2 regulates early nitrate responses and integrates nitrate assimilation with energy and carbon skeleton supply. *The Plant Cell*, *35*(5), 1429–1454. https://doi.org/10.1093/PLCELL/KOAD025

El-Showk, S., & Mähönen, A. P. (2018). A cellular passage to the root interior. *Nature*, *555*(7697), 454–455. https://doi.org/10.1038/d41586-018-02861-x

Erb, K. H., Kastner, T., Plutzar, C., Bais, A. L. S., Carvalhais, N., Fetzel, T., Gingrich, S., Haberl, H., Lauk, C., Niedertscheider, M., Pongratz, J., Thurner, M., & Luyssaert, S. (2017). Unexpectedly large impact of forest management and grazing on global vegetation biomass. *Nature 2018 553:7686*, *553*(7686), 73–76. https://doi.org/10.1038/nature25138

Erisman, J. W., Sutton, M. A., Galloway, J., Klimont, Z., & Winiwarter, W. (2008). How a century of ammonia synthesis changed the world. *Nature Geoscience 2008 1:10*, *1*(10), 636–639. https://doi.org/10.1038/ngeo325

Fan, J., Xiao, J., Liu, D., Ye, G., Luo, J., Houlbrooke, D., Laurenson, S., Yan, J., Chen, L., Tian, J., & Ding, W. (2017). *Effect of application of dairy manure, effluent and inorganic fertilizer on nitrogen leaching in clayey fluvo-aquic soil: A lysimeter study*. https://doi.org/10.1016/j.scitotenv.2017.03.060

Fan, S. C., Lin, C. S., Hsu, P. K., Lin, S. H., & Tsay, Y. F. (2009). The Arabidopsis Nitrate Transporter NRT1.7, Expressed in Phloem, Is Responsible for Source-to-Sink Remobilization of Nitrate. *The Plant Cell*, *21*(9), 2750. https://doi.org/10.1105/TPC.109.067603

Fan, X., Naz, M., Fan, X., Xuan, W., Miller, A. J., & Xu, G. (2017). Plant nitrate transporters: from gene function to application. *Journal of Experimental Botany*, *68*(10), 2463–2475. https://doi.org/10.1093/JXB/ERX011

Fang, X. Z., Fang, S. Q., Ye, Z. Q., Liu, D., Zhao, K. L., & Jin, C. W. (2021). NRT1.1 Dual-Affinity Nitrate Transport/Signalling and its Roles in Plant Abiotic Stress Resistance. *Frontiers in Plant Science*, *12*, 715694. https://doi.org/10.3389/FPLS.2021.715694

Fernández, I., Cosme, M., Stringlis, I. A., Yu, K., de Jonge, R., van Wees, S. C. M., Pozo, M. J., Pieterse, C. M. J., & van der Heijden, M. G. A. (2019). Molecular dialogue between arbuscular mycorrhizal fungi and the nonhost plant Arabidopsis thaliana switches from initial detection to antagonism. *New Phytologist*, *223*(2), 867–881. https://doi.org/10.1111/NPH.15798

Finch, H. J. S., Samuel, A. M., & Lane, G. P. F. (2014). Fertilisers and manures. *Lockhart & Wiseman's Crop Husbandry Including Grassland*, 63–91. https://doi.org/10.1533/9781782423928.1.63

Fred, E. B. (1932). *Root nodule bacteria and leguminous plants - Chapter 1: The history of the leguminosae in agriculture* (5th ed., Vol. 52). University of Wisconsin.

Fromont-Racine, M., Senger, B., Saveanu, C., & Fasiolo, F. (2003). Ribosome assembly in eukaryotes. In *Gene* (Vol. 313, Issues 1–2, pp. 17–42). Elsevier. https://doi.org/10.1016/S0378-1119(03)00629-2

Fröschel, C., Komorek, J., Attard, A., Marsell, A., Lopez-Arboleda, W. A., Le Berre, J., Wolf, E., Geldner, N., Waller, F., Korte, A., & Dröge-Laser, W. (2021). Plant roots employ cell-layer-specific programs to respond to pathogenic and beneficial microbes. *Cell Host and Microbe*, *29*(2), 299-310.e7. https://doi.org/10.1016/j.chom.2020.11.014

Garrido-Oter, R., Nakano, R. T., Dombrowski, N., Ma, K. W., McHardy, A. C., & Schulze-Lefert, P. (2018). Modular Traits of the Rhizobiales Root Microbiota and Their Evolutionary Relationship with Symbiotic Rhizobia. *Cell Host & Microbe*, *24*(1), 155-167.e5. https://doi.org/10.1016/J.CHOM.2018.06.006

Geldner, N. (2013). The endodermis. In *Annual Review of Plant Biology* (Vol. 64, pp. 531–558). https://doi.org/10.1146/annurev-arplant-050312-120050

Gent, L., & Forde, B. G. (2017). How do plants sense their nitrogen status? *Journal of Experimental Botany*, *68*(10), 2531–2539. https://doi.org/10.1093/JXB/ERX013

Giehl, R. F. H., Laginha, A. M., Duan, F., Rentsch, D., Yuan, L., & von Wirén, N. (2017). A Critical Role of AMT2;1 in Root-To-Shoot Translocation of Ammonium in Arabidopsis. *Molecular Plant*, *10*(11), 1449–1460. https://doi.org/10.1016/j.molp.2017.10.001

Giehl, R. F. H., & von Wirén, N. (2014). Root nutrient foraging. *Plant Physiology*, *166*(2), 509–517. https://doi.org/10.1104/pp.114.245225

Gioseffi, E., De Neergaard, A., & Schjoerring, J. K. (2012). Interactions between uptake of amino acids and inorganic nitrogen in wheat plants. *Biogeosciences*, *9*(4), 1509–1518. https://doi.org/10.5194/bg-9-1509-2012

Glass, A. D. M. (2010). Nitrogen Use Efficiency of Crop Plants: Physiological Constraints upon Nitrogen Absorption. *Https://Doi.Org/10.1080/07352680390243512*, *22*(5), 453–470. https://doi.org/10.1080/07352680390243512

Govindarajulu, M., Pfeffer, P. E., Jin, H., Abubaker, J., Douds, D. D., Allen, J. W., Bücking, H., Lammers, P. J., & Shachar-Hill, Y. (2005). Nitrogen transfer in the arbuscular mycorrhizal symbiosis. *Nature 2005 435:7043*, *435*(7043), 819–823. https://doi.org/10.1038/nature03610

Gower, J. C. (1966). Some distance properties of latent root and vector methods used in multivariate analysis. In *Biometrika* (Vol. 53). https://academic.oup.com/biomet/article/53/3-4/325/246598

Gruber, B. D., Giehl, R. F. H., Friedel, S., & von Wirén, N. (2013). Plasticity of the Arabidopsis root system under nutrient deficiencies. *Plant Physiology*, *163*(1), 161–179. https://doi.org/10.1104/pp.113.218453

Guiry, E. J., Buckley, M., Orchard, T. J., Hawkins, A. L., Needs-Howarth, S., Holm, E., & Szpak, P. (2020). Deforestation caused abrupt shift in Great Lakes nitrogen cycle. *Limnology and Oceanography*, *65*(8), 1921–1935. https://doi.org/10.1002/LNO.11428

Hachiya, T., Inaba, J., Wakazaki, M., Sato, M., Toyooka, K., Miyagi, A., Kawai-Yamada, M., Sugiura, D., Nakagawa, T., Kiba, T., Gojon, A., & Sakakibara, H. (2021). Excessive ammonium assimilation by plastidic glutamine synthetase causes ammonium toxicity in Arabidopsis thaliana. *Nature Communications 2021 12:1*, *12*(1), 1–10. https://doi.org/10.1038/s41467-021-25238-7

Hamburger, D., Rezzonico, E., Somerville, C., & Poirier, Y. (2002). Identification and Characterization of the Arabidopsis PHO1 Gene Involved in Phosphate Loading to the Xylem. *The Plant Cell*, *14*(April), 889–902. https://doi.org/10.1105/tpc.000745.the

Harbort, C. J., Hashimoto, M., Inoue, H., Niu, Y., Guan, R., Rombolà, A. D., Kopriva, S., Voges, M. J. E. E. E., Sattely, E. S., Garrido-Oter, R., & Schulze-Lefert, P. (2020). Root-Secreted Coumarins and the Microbiota Interact to Improve Iron Nutrition in Arabidopsis. *Cell Host and Microbe*, *28*(6), 825-837.e6. https://doi.org/10.1016/j.chom.2020.09.006

Harrison, M. T., Edwards, E. J., Farquhar, G. D., Nicotra, A. B., & Evans, J. R. (2009). Nitrogen in cell walls of sclerophyllous leaves accounts for little of the variation in photosynthetic nitrogen-use efficiency. *Plant, Cell and Environment*, *32*(3), 259–270. https://doi.org/10.1111/j.1365-3040.2008.01918.x

Hawkesford, M. J., Cakmak, I., Coskun, D., De Kok, L. J., Lambers, H., Schjoerring, J. K., & White, P. J. (2023). Functions of macronutrients. *Marschner's Mineral Nutrition of Plants*, 201–281. https://doi.org/10.1016/B978-0-12-819773-8.00019-8

Hestrin, R., Hammer, E. C., Mueller, C. W., & Lehmann, J. (2019). Synergies between mycorrhizal fungi and soil microbial communities increase plant nitrogen acquisition. *Communications Biology 2019 2:1*, *2*(1), 1–9. https://doi.org/10.1038/s42003-019-0481-8

Hill, R. D., Rinker, R. G., & Dale Wilson, H. (1980). Atmospheric Nitrogen Fixation by Lightning. *N: Journal of the Atmospheric Sciences*, *37*(1), 179–192. https://journals.ametsoc.org/view/journals/atsc/37/1/1520-0469_1980_037_0179_anfbl_2_0_co_2.xml

Hiruma, K., Gerlach, N., Sacristán, S., Nakano, R. T., Hacquard, S., Kracher, B., Neumann, U., Ramírez, D., Bucher, M., O'Connell, R. J., & Schulze-Lefert, P. (2016). Root Endophyte Colletotrichum tofieldiae Confers Plant Fitness Benefits that Are Phosphate Status Dependent. *Cell*, *165*(2), 464–474. https://doi.org/10.1016/j.cell.2016.02.028

Ho, C. H., & Tsay, Y. F. (2010). Nitrate, ammonium, and potassium sensing and signaling. *Current Opinion in Plant Biology*, *13*(5), 604–610. https://doi.org/10.1016/J.PBI.2010.08.005

Hoopen, F. Ten, Cuin, T. A., Pedas, P., Hegelund, J. N., Shabala, S., Schjoerring, J. K., & Jahn, T. P. (2010). Competition between uptake of ammonium and potassium in barley and Arabidopsis roots: molecular mechanisms and physiological consequences. *Journal of Experimental Botany*, *61*(9), 2303. https://doi.org/10.1093/JXB/ERQ057

Hose, E., Clarkson, D. T., Steudle, E., Schreiber, L., & Hartung, W. (2001). The exodermis: a variable apoplastic barrier. *Journal of Experimental Botany*, *52*(365), 2245–2264. https://doi.org/10.1093/JEXBOT/52.365.2245

Hosmani, P. S., Kamiya, T., Danku, J., Naseer, S., Geldner, N., Guerinot, M. Lou, & Salt, D. E. (2013). Dirigent domain-containing protein is part of the machinery required for formation of the lignin-based Casparian strip in the root. *Proceedings of the National Academy of Sciences of the United States of America*, *110*(35), 14498–14503. https://doi.org/10.1073/PNAS.1308412110

Hothorn, T., Bretz, F., & Westfall, P. (2008). Simultaneous inference in general parametric models. *Biometrical Journal*, *50*(3), 346–363. https://doi.org/10.1002/bimj.200810425

Howitt, S. M., & Udvardi, M. K. (2000). Structure, function and regulation of ammonium transporters in plants. *Biochimica et Biophysica Acta (BBA) - Biomembranes*, *1465*(1–2), 152–170. https://doi.org/10.1016/S0005-2736(00)00136-X

Hu, Q. Q., Shu, J. Q., Li, W. M., & Wang, G. Z. (2021). Role of Auxin and Nitrate Signaling in the Development of Root System Architecture. *Frontiers in Plant Science*, *12*, 690363. https://doi.org/10.3389/FPLS.2021.690363/BIBTEX

Ijato, T., Porras-Murillo, R., Ganz, P., Ludewig, U., & Neuhäuser, B. (2021). Concentration-dependent physiological and transcriptional adaptations of wheat seedlings to ammonium. *Physiologia Plantarum*, *171*(3), 328–342. https://doi.org/10.1111/PPL.13113

Jacquot, A., Chaput, V., Mauries, A., Li, Z., Tillard, P., Fizames, C., Bonillo, P., Bellegarde, F., Laugier, E., Santoni, V., Hem, S., Martin, A., Gojon, A., Schulze, W., & Lejay, L. (2020). NRT2.1 C-terminus phosphorylation prevents root high affinity nitrate uptake activity in Arabidopsis thaliana. *New Phytologist*, *228*(3), 1038–1054. https://doi.org/10.1111/NPH.16710

Jamet, E., Heredia, A., Ralph, J., Herburger KlausHerburger, K., address, P., Xin, A., & Herburger, K. (2021). *Mini Review: Transport of Hydrophobic Polymers Into the Plant Apoplast*. https://doi.org/10.3389/fpls.2020.590990

Jean-Baptiste, K., McFaline-Figueroa, J. L., Alexandre, C. M., Dorrity, M. W., Saunders, L., Bubb, K. L., Trapnell, C., Fields, S., Queitsch, C., & Cuperusa, J. T. (2019). Dynamics of gene expression in single root cells of arabidopsis thaliana. *Plant Cell*, *31*(5), 993–1011. https://doi.org/10.1105/tpc.18.00785

Jollife, I. T., & Cadima, J. (2016). Principal component analysis: A review and recent developments. In *Philosophical Transactions of the Royal Society A: Mathematical, Physical and Engineering Sciences* (Vol. 374, Issue 2065). Royal Society of London. https://doi.org/10.1098/rsta.2015.0202

Jones, D. L., Shannon, D., Junvee-Fortune, T., & Farrar, J. F. (2005). Plant capture of free amino acids is maximized under high soil amino acid concentrations. *Soil Biology and Biochemistry*, *37*(1), 179–181. https://doi.org/10.1016/j.soilbio.2004.07.021

Kamiya, T., Borghi, M., Wang, P., Danku, J. M. C., Kalmbach, L., Hosmani, P. S., Naseer, S., Fujiwara, T., Geldner, N., & Salt, D. E. (2015). The MYB36 transcription factor orchestrates Casparian strip formation. *Proceedings of the National Academy of Sciences of the United States of America*, *112*(33), 10533–10538. https://doi.org/10.1073/PNAS.1507691112/-/DCSUPPLEMENTAL

Kang, J., & Turano, F. J. (2003). The putative glutamate receptor 1.1 (AtGLR1.1) functions as a regulator of carbon and nitrogen metabolism in Arabidopsis thaliana. *Proceedings of the National Academy of Sciences*, *100*(11), 6872–6877. https://doi.org/10.1073/PNAS.1030961100

Kant, S. (2018). Understanding nitrate uptake, signaling and remobilisation for improving plant nitrogen use efficiency. *Seminars in Cell & Developmental Biology*, *74*, 89–96. https://doi.org/10.1016/J.SEMCDB.2017.08.034

Katz, E., Knapp, A., Lensink, M., Stefani, J., Li, J.-J., Shane, E., Tuermer-Lee, K., Bloom, A. J., & Kliebenstein, D. J. (2022). Differential genetic variation underlying Ammonium and Nitrate responses in Arabidopsis thaliana. *BioRxiv*, 2022.04.27.489730.

Kiba, T., Feria-Bourrellier, A. B., Lafouge, F., Lezhneva, L., Boutet-Mercey, S., Orsel, M., Bréhaut, V., Miller, A., Daniel-Vedele, F., Sakakibara, H., & Krapp, A. (2012). The Arabidopsis nitrate transporter NRT2.4 plays a double role in roots and shoots of nitrogen-starved plants. *Plant Cell*, *24*(1), 245–258. https://doi.org/10.1105/tpc.111.092221

Kiba, T., Inaba, J., Kudo, T., Ueda, N., Konishi, M., Mitsuda, N., Takiguchi, Y., Kondou, Y., Yoshizumi, T., Ohme-Takagi, M., Matsui, M., Yano, K., Yanagisawa, S., & Sakakibara, H. (2018). Repression of nitrogen starvation responses by members of the arabidopsis GARP-type transcription factor NIGT1/HRS1 subfamily. *Plant Cell*, *30*(4), 925–945. https://doi.org/10.1105/tpc.17.00810

Kiba, T., & Krapp, A. (2016). Plant Nitrogen Acquisition Under Low Availability: Regulation of Uptake and Root Architecture. *Plant and Cell Physiology*, *57*(4), 707–714. https://doi.org/10.1093/PCP/PCW052

Kim, D., Paggi, J. M., Park, C., Bennett, C., & Salzberg, S. L. (2019). Graph-based genome alignment and genotyping with HISAT2 and HISAT-genotype. *Nature Biotechnology*, *37*(8), 907–915. https://doi.org/10.1038/s41587-019-0201-4

Koizumi, K., & Gallagher, K. L. (2013). Identification of SHRUBBY, a SHORT-ROOT and SCARECROW interacting protein that controls root growth and radial patterning. *Development*, *140*(6), 1292–1300. https://doi.org/10.1242/dev.090761

Konishi, M., & Yanagisawa, S. (2011). Roles of the transcriptional regulation mediated by the nitrate-responsive cis-element in higher plants. *Biochemical and Biophysical Research Communications*, *411*(4), 708–713. https://doi.org/10.1016/J.BBRC.2011.07.008

Konishi, M., & Yanagisawa, S. (2013). Arabidopsis NIN-like transcription factors have a central role in nitrate signalling. *Nature Communications 2013 4:1*, *4*(1), 1–9. https://doi.org/10.1038/ncomms2621

Kosma, D. K., Murmu, J., Razeq, F. M., Santos, P., Bourgault, R., Molina, I., & Rowland, O. (2014). AtMYB41 activates ectopic suberin synthesis and assembly in multiple plant species and cell types. *The Plant Journal*, *80*(2), 216–229. https://doi.org/10.1111/TPJ.12624

Kotur, Z., Mackenzie, N., Ramesh, S., Tyerman, S. D., Kaiser, B. N., & Glass, A. D. M. (2012). Nitrate transport capacity of the Arabidopsis thaliana NRT2 family members and their interactions with AtNAR2.1. *New Phytologist*, *194*(3), 724–731. https://doi.org/10.1111/J.1469-8137.2012.04094.X

Krapp, A., David, L. C., Chardin, C., Girin, T., Marmagne, A., Leprince, A.-S., Chaillou, S., Ferrario-Méry, S., Meyer, C., & Daniel-Vedele, F. (2014). Nitrate transport and signalling in Arabidopsis. *Journal of Experimental Botany*, *65*(3), 789–798. https://doi.org/10.1093/jxb/eru001

Kreszies, T., Shellakkutti, N., Osthoff, A., Yu, P., Baldauf, J. A., Zeisler-Diehl, V. V., Ranathunge, K., Hochholdinger, F., & Schreiber, L. (2019). Osmotic stress enhances suberization of apoplastic barriers in barley seminal roots: analysis of chemical, transcriptomic and physiological responses. *New Phytologist*, *221*(1), 180–194. https://doi.org/10.1111/NPH.15351

Kroemer, H. (1903). *Hypodermis und Endodermis der Angiospermenwurzel*. Schweizerbart Science Publishers. http://www.schweizerbart.de//publications/detail/artno/144005900/Bibliotheca_Botanica_Heft_59

Krömer, K. (1903). *Wurzelhaut, Hypodermis und Endodermis der Angiospermenwurzel*. Bibl. Bot. 59. Stuttgart: Verlag von Erwin Nägele.

Krouk, G., Tillard, P., & Gojon, A. (2006). Regulation of the High-Affinity NO3− Uptake System by NRT1.1-Mediated NO3− Demand Signaling in Arabidopsis. *Plant Physiology*, *142*(3), 1075. https://doi.org/10.1104/PP.106.087510

Lanquar, V., & Frommer, W. B. (2010). Adjusting ammonium uptake via phosphorylation. *Plant Signaling and Behavior*, *5*(6), 736–738. https://doi.org/10.4161/psb.5.6.11696

Lanquar, V., Loqué, D., Hörmann, F., Yuan, L., Bohner, A., Engelsberger, W. R., Lalonde, S., Schulze, W. X., von Wirén, N., & Frommer, W. B. (2009). Feedback Inhibition of Ammonium Uptake by a Phospho-Dependent Allosteric Mechanism in Arabidopsis. *The Plant Cell*, *21*(11), 3610–3622. https://doi.org/10.1105/TPC.109.068593

Leal, A. R., Barros, P. M., Parizot, B., Sapeta, H., Vangheluwe, N., Andersen, T. G., Beeckman, T., & Oliveira, M. M. (2022). Translational profile of developing phellem cells in Arabidopsis thaliana roots. *Plant Journal*, *110*(3), 899–915. https://doi.org/10.1111/tpj.15691

Lehmann, J., Pereira da Silva Jr, J., Steiner, C., Nehls, T., Zech, W., & Glaser, B. (2003). Nutrient availability and leaching in an archaeological Anthrosol and a Ferralsol of the Central Amazon basin: fertilizer, manure and charcoal amendments. *Plant and Soil*, *249*, 343–357.

Lehmann, J., & Schroth, G. (2009). Nutrient leaching. *Trees, Crops and Soil Fertility: Concepts and Research Methods*, 151–166. https://doi.org/10.1079/9780851995939.0151

Lezhneva, L., Kiba, T., Feria-Bourrellier, A. B., Lafouge, F., Boutet-Mercey, S., Zoufan, P., Sakakibara, H., Daniel-Vedele, F., & Krapp, A. (2014). The Arabidopsis nitrate transporter NRT2.5 plays a role in nitrate acquisition and remobilization in nitrogen-starved plants. *Plant Journal*, *80*(2), 230–241. https://doi.org/10.1111/tpj.12626

Li, J. Y., Fu, Y. L., Pike, S. M., Bao, J., Tian, W., Zhang, Y., Chen, C. Z., Zhang, Y., Li, H. M., Huang, J., Li, L. G., Schroeder, J. I., Gassmann, W., & Gong, J. M. (2010). The Arabidopsis Nitrate Transporter NRT1.8 Functions in Nitrate Removal from the Xylem Sap and Mediates Cadmium Tolerance. *The Plant Cell*, *22*(5), 1633–1646. https://doi.org/10.1105/TPC.110.075242

Li, W., Wang, Y., Okamoto, M., Crawford, N. M., Siddiqi, M. Y., & Glass, A. D. M. (2007). Dissection of the AtNRT2.1:AtNRT2.2 Inducible High-Affinity Nitrate Transporter Gene Cluster. *Plant Physiology*, *143*(1), 425–433. https://doi.org/10.1104/PP.106.091223

Liang, J., & He, J. (2018). Protective role of anthocyanins in plants under low nitrogen stress. *Biochemical and Biophysical Research Communications*, *498*(4), 946–953. https://doi.org/10.1016/j.bbrc.2018.03.087

Lindsey, B. E., Rivero, L., Calhoun, C. S., Grotewold, E., & Brkljacic, J. (2017). Standardized Method for High-throughput Sterilization of Arabidopsis Seeds. *Journal of Visualized Experiments : JoVE*, *2017*(128). https://doi.org/10.3791/56587

Liu, K. H., Diener, A., Lin, Z., Liu, C., & Sheen, J. (2020). Primary nitrate responses mediated by calcium signalling and diverse protein phosphorylation. *Journal of Experimental Botany*, *71*(15), 4428–4441. https://doi.org/10.1093/JXB/ERAA047

Liu, K. H., Liu, M., Lin, Z., Wang, Z. F., Chen, B., Liu, C., Guo, A., Konishi, M., Yanagisawa, S., Wagner, G., & Sheen, J. (2022). NIN-like protein 7 transcription factor is a plant nitrate sensor. *Science*, *377*(6613), 1419–1425. https://doi.org/10.1126/science.add1104

Liu, T., Ren, T., White, P. J., Cong, R., & Lu, J. (2018). Storage nitrogen co-ordinates leaf expansion and photosynthetic capacity in winter oilseed rape. *Journal of Experimental Botany*, *69*(12), 2995–3007. https://doi.org/10.1093/jxb/ery134

Liu, Y., & Von Wirén, N. (2017). Ammonium as a signal for physiological and morphological responses in plants. *Journal of Experimental Botany*, *68*(10), 2581–2592. https://doi.org/10.1093/JXB/ERX086

Loqué, D., Tillard, P., Gojon, A., & Lepetit, M. (2003). Gene expression of the NO3- transporter NRT1.1 and the nitrate reductase NIA1 is repressed in Arabidopsis roots by NO2-, the product of NO3- reduction. *Plant Physiology*, *132*(2), 958–967. https://doi.org/10.1104/PP.102.018523

Love, M. I., Huber, W., & Anders, S. (2014). Moderated estimation of fold change and dispersion for RNA-seq data with DESeq2. *Genome Biology*, *15*(12). https://doi.org/10.1186/s13059-014-0550-8

Lupini, A., Mercati, F., Araniti, F., Miller, A. J., Sunseri, F., & Abenavoli, M. R. (2016). NAR2.1/NRT2.1 functional interaction with NO3- and H+ fluxes in high-affinity nitrate transport in maize root regions. *Plant Physiology and Biochemistry*, *102*, 107–114. https://doi.org/10.1016/J.PLAPHY.2016.02.022

Lux, A., Morita, S., Abe, J., & Ito, K. (2005a/b). An improved method for clearing and staining free-hand sections and whole-mount samples. *Annals of Botany*, *96*(6), 989–996. https://doi.org/10.1093/aob/mci266

Ma, K. W., Niu, Y., Jia, Y., Ordon, J., Copeland, C., Emonet, A., Geldner, N., Guan, R., Stolze, S. C., Nakagami, H., Garrido-Oter, R., & Schulze-Lefert, P. (2021). Coordination of microbe–host homeostasis by crosstalk with plant innate immunity. *Nature Plants*, *7*(6), 814–825. https://doi.org/10.1038/s41477-021-00920-2

MacQueen, J. (1967). *Some methods for classification and analysis of multivariate observations*.

Maeda, Y., Konishi, M., Kiba, T., Sakuraba, Y., Sawaki, N., Kurai, T., Ueda, Y., Sakakibara, H., & Yanagisawa, S. (2018). A NIGT1-centred transcriptional cascade regulates nitrate signalling and incorporates phosphorus starvation signals in Arabidopsis. *Nature Communications*, *9*(1). https://doi.org/10.1038/s41467-018-03832-6

Mamatova, A. S., Korona-Glowniak, I., Skalicka-Woźniak, K., Józefczyk, A., Wojtanowski, K. K., Baj, T., Sakipova, Z. B., & Malm, A. (2019). Phytochemical composition of wormwood (Artemisia gmelinii) extracts in respect of their antimicrobial activity. *BMC Complementary and Alternative Medicine*, *19*(1), 1–8. https://doi.org/10.1186/S12906-019-2719-X/TABLES/3

Marchive, C., Roudier, F., Castaings, L., Bréhaut, V., Blondet, E., Colot, V., Meyer, C., & Krapp, A. (2013). Nuclear retention of the transcription factor NLP7 orchestrates the early response to nitrate in plants. *Nature Communications*, *4*. https://doi.org/10.1038/ncomms2650

Mark Winter. (2023). *WebElements: THE periodic table on the WWW [www.webelements.com] Copyright 1993-2023 Mark Winter [The University of Sheffield and WebElements Ltd, UK]. All rights reserved.* www.webelements.com

Marschner, H. (1995). *Mineral Nutrition of Higher Plants 2nd Edition*. https://doi.org/10.1016/S0167-5648(08)71011-6

Mathieu, E., Rodés-Guirao, L., & Roser, M. (2023). What are the sources for Our World in Data's population estimates? *Our World in Data*. https://ourworldindata.org/population-sources

Medici, A., Marshall-Colon, A., Ronzier, E., Szponarski, W., Wang, R., Gojon, A., Crawford, N. M., Ruffel, S., Coruzzi, G. M., & Krouk, G. (2015). AtNIGT1/HRS1 integrates nitrate and phosphate signals at the Arabidopsis root tip. *Nature Communications*, *6*. https://doi.org/10.1038/ncomms7274

Meier, M., Liu, Y., Lay-Pruitt, K. S., Takahashi, H., & von Wirén, N. (2020). Auxin-mediated root branching is determined by the form of available nitrogen. *Nature Plants*, *6*(9), 1136–1145. https://doi.org/10.1038/s41477-020-00756-2

Melino, V. J., Plett, D. C., Bendre, P., Thomsen, H. C., Zeisler-Diehl, V. V., Schreiber, L., & Kronzucker, H. J. (2021). Nitrogen depletion enhances endodermal suberization without restricting transporter-mediated root NO3- influx. *Journal of Plant Physiology*, *257*. https://doi.org/10.1016/j.jplph.2020.153334

Millard, P. (1988). The accumulation and storage of nitrogen by herbaceous plants. *Plant, Cell & Environment*, *11*(1), 1–8. https://doi.org/10.1111/j.1365-3040.1988.tb01769.x

Miller, R. E., & Woodrow, I. E. (2008). Resource availability and the abundance of an n-based defense in Australian tropical rain forests. *Ecology*, *89*(6), 1503–1509. https://doi.org/10.1890/07-0335.1

Miller, S. L. (1953). A production of amino acids under possible primitive earth conditions. *Science*, *117*(3046), 528–529. https://doi.org/10.1126/science.117.3046.528

Mu, X., & Luo, J. (2019). Evolutionary analyses of NIN-like proteins in plants and their roles in nitrate signaling. *Cellular and Molecular Life Sciences 2019 76:19*, *76*(19), 3753–3764. https://doi.org/10.1007/S00018-019-03164-8

Murashige, T., & Skoog, F. (1962). A Revised Medium for Rapid Growth and Bio Assays with Tobacco Tissue Cultures. *Physiologia Plantarum*, *15*(3), 473–497. https://doi.org/10.1111/J.1399-3054.1962.TB08052.X

Muratore, C., Espen, L., & Prinsi, B. (2021). Nitrogen Uptake in Plants: The Plasma Membrane Root Transport Systems from a Physiological and Proteomic Perspective. *Plants*, *10*(4). https://doi.org/10.3390/PLANTS10040681

Mustroph, A., Zanetti, M. E., Jang, C. J. H., Holtan, H. E., Repetti, P. P., Galbraith, D. W., Girke, T., & Bailey-Serres, J. (2009). Profiling translatomes of discrete cell populations resolves altered cellular priorities during hypoxia in Arabidopsis. *Proceedings of the National Academy of Sciences of the United States of America*, *106*(44), 18843–18848. https://doi.org/10.1073/pnas.0906131106

Nacry, P., Bouguyon, E., & Gojon, A. (2013). Nitrogen acquisition by roots: physiological and developmental mechanisms ensuring plant adaptation to a fluctuating resource. *Plant and Soil 2013 370:1*, *370*(1), 1–29. https://doi.org/10.1007/S11104-013-1645-9

Naegle, E. R., Burton, J. W., Carter, T. E., & Rufty, T. W. (2005). Influence of seed nitrogen content on seedling growth and recovery from nitrogen stress. *Plant and Soil*, *271*(1–2), 329–340. https://doi.org/10.1007/S11104-004-3242-4/METRICS

Napiroon, T., Bacher, M., Balslev, H., Tawaitakham, K., Santimaleeworagun, W., & Vajrodaya, S. (2018). Scopoletin from Lasianthus lucidus Blume (Rubiaceae): A potential antimicrobial against multidrug-resistant Pseudomonas aeruginosa. *Journal of Applied Pharmaceutical Science*, *8,*(9), 001–006. https://doi.org/10.7324/JAPS.2018.8901

Naseer, S., Lee, Y., Lapierre, C., Franke, R., Nawrath, C., & Geldner, N. (2012). Casparian strip diffusion barrier in Arabidopsis is made of a lignin polymer without suberin. *Proceedings of the National Academy of Sciences of the United States of America*, *109*(25), 10101–10106. https://doi.org/10.1073/pnas.1205726109

Noguero, M., & Lacombe, B. (2016). Transporters involved in root nitrate uptake and sensing by Arabidopsis. *Frontiers in Plant Science*, *7*(September), 213266. https://doi.org/10.3389/FPLS.2016.01391/BIBTEX

Novoa, R., & Loomis, R. S. (1981). 1981 Novoa and Loomis, nitrogen and plant production. *Plant and Soil*, *58*, 177–204.

Obata, T. (2019). Metabolons in plant primary and secondary metabolism. *Phytochemistry Reviews 2019 18:6*, *18*(6), 1483–1507. https://doi.org/10.1007/S11101-019-09619-X

O'brien, J. A., Vega, A., Onore Bouguyon, E., Krouk, G., Gojon, A., Coruzzi, G., & Gutié Rrez, R. A. (2016). Nitrate Transport, Sensing, and Responses in Plants. *Molecular Plant*, *9*, 837–856. https://doi.org/10.1016/j.molp.2016.05.004

Ohkubo, Y., Tanaka, M., Tabata, R., Ogawa-Ohnishi, M., & Matsubayashi, Y. (2017). Shoot-to-root mobile polypeptides involved in systemic regulation of nitrogen acquisition. *Nature Plants 2017 3:4*, *3*(4), 1–6. https://doi.org/10.1038/nplants.2017.29

Ohyama, Takuji., & Sueyoshi, Kuni. (2010). *Nitrogen assimilation in plants*. Research Signpost.

Oji, Y., & Izawa, G. (1971). Rapid synthesis of glutamine during the initial period of ammonia assimilation in roots of barley plants. *Plant and Cell Physiology*, *12*(5), 817–821. https://doi.org/10.1093/OXFORDJOURNALS.PCP.A074684

Okamoto, M., Kumar, A., Li, W., Wang, Y., Siddiqi, M. Y., Crawford, N. M., & Glass, A. D. M. (2006). High-affinity nitrate transport in roots of Arabidopsis depends on expression of the NAR2-like gene AtNRT3.1. *Plant Physiology*, *140*(3), 1036–1046. https://doi.org/10.1104/PP.105.074385

Okumoto, S., & Pilot, G. (2011). Amino Acid Export in Plants: A Missing Link in Nitrogen Cycling. *Molecular Plant •*, *4*, 453–463. https://doi.org/10.1093/mp/ssr003

O'Neill, A. (2022, June 21). *Global population 10,000BCE-2100 | Statista*. Population of the World 10,000BCE-2100. https://www.statista.com/statistics/1006502/global-population-ten-thousand-bc-to-2050/

Ordon, J., Kiel, N., Becker, D., Kretschmer, C., Schulze-Lefert, P., & Stuttmann, J. (2023). Targeted gene deletion with SpCas9 and multiple guide RNAs in Arabidopsis thaliana: four are better than two. *Plant Methods*, *19*(1), 1–11. https://doi.org/10.1186/S13007-023-01010-4/FIGURES/3

Ordon, J., Thouin, J., Nakano, R. T., Ma, K.-W., Zhang, P., Huettel, B., Garrido-Oter, R., & Schulze-Lefert, P. (2023). Simultaneous tracking of near-isogenic bacterial strains in synthetic Arabidopsis microbiota by chromosomally-integrated barcodes. *BioRxiv*, 2023.04.20.537712. https://doi.org/10.1101/2023.04.20.537712

Orsel, M., Krapp, A., & Daniel-Vedele, F. (2002). Analysis of the NRT2 Nitrate Transporter Family in Arabidopsis. Structure and Gene Expression. *Plant Physiology*, *129*(2), 886. https://doi.org/10.1104/PP.005280

Panse, V. G., & Johnson, A. W. (2010). Maturation of eukaryotic ribosomes: acquisition of functionality. In *Trends in Biochemical Sciences* (Vol. 35, Issue 5, pp. 260–266). https://doi.org/10.1016/j.tibs.2010.01.001

Parker, J. L., & Newstead, S. (2014). Molecular basis of nitrate uptake by the plant nitrate transporter NRT1.1. *Nature 2014 507:7490*, *507*(7490), 68–72. https://doi.org/10.1038/nature13116

Parvin, S., Uddin, S., Tausz-Posch, S., Armstrong, R., & Tausz, M. (2020). Carbon sink strength of nodules but not other organs modulates photosynthesis of faba bean (Vicia faba) grown under elevated [CO2] and different water supply. *New Phytologist*, *227*(1), 132–145. https://doi.org/10.1111/NPH.16520

Peng, M., Hudson, D., Schofield, A., Tsao, R., Yang, R., Gu, H., Bi, Y. M., & Rothstein, S. J. (2008). Adaptation of Arabidopsis to nitrogen limitation involves induction of anthocyanin synthesis which is controlled by the NLA gene. *Journal of Experimental Botany*, *59*(11), 2933–2944. https://doi.org/10.1093/JXB/ERN148

Perchlik, M., Foster, J., & Tegeder, M. (2014). Different and overlapping functions of Arabidopsis LHT6 and AAP1 transporters in root amino acid uptake. *Journal of Experimental Botany*, *65*(18), 5193–5204. https://doi.org/10.1093/JXB/ERU278

Peterson, C. A., & Enstone, D. E. (1996). Functions of passage cells in the endodermis and exodermis of roots. *Physiologia Plantarum*, *97*(3), 592–598. https://doi.org/10.1034/j.1399-3054.1996.970323.x

Pfister, A., Barberon, M., Alassimone, J., Kalmbach, L., Lee, Y., Vermeer, J. E. M., Yamazaki, M., Li, G., Maurel, C., Takano, J., Kamiya, T., Salt, D. E., Roppolo, D., & Geldner, N. (2014). A receptor-like kinase mutant with absent endodermal diffusion barrier displays selective nutrient homeostasis defects. *ELife*, *3*, e03115. https://doi.org/10.7554/eLife.03115

Porebski, S., Bailey, L. G., & Baum, B. R. (1997). Modification of a CTAB DNA extraction protocol for plants containing high polysaccharide and polyphenol components. *Plant Molecular Biology Reporter*, *15*(1), 8–15. https://doi.org/10.1007/BF02772108/METRICS

Prosser, J. I. (1990). Autotrophic Nitrification in Bacteria. *Advances in Microbial Physiology*, *30*(C), 125–181. https://doi.org/10.1016/S0065-2911(08)60112-5

Pudelski, B., Kraus, S., Soll, J., & Philippar, K. (2010). The plant PRAT proteins - preprotein and amino acid transport in mitochondria and chloroplasts. *Plant Biology*, *12*(SUPPL. 1), 42–55. https://doi.org/10.1111/J.1438-8677.2010.00357.X

Putz, M., Schleusner, P., Rütting, T., & Hallin, S. (2018). *Relative abundance of denitrifying and DNRA bacteria and their activity determine nitrogen retention or loss in agricultural soil*. https://doi.org/10.1016/j.soilbio.2018.05.006

Qin, D. Bin, Liu, M. Y., Yuan, L., Zhu, Y., Li, X. D., Chen, L. M., Wang, Y., Chen, Y. F., Wu, W. H., & Wang, Y. (2020). CALCIUM-DEPENDENT PROTEIN KINASE 32-mediated phosphorylation is essential for the ammonium transport activity of AMT1;1 in Arabidopsis roots. *Journal of Experimental Botany*, *71*(16), 5087–5097. https://doi.org/10.1093/JXB/ERAA249

Raab, T. K., Lipson, D. A., & Monson, R. K. (1999). Soil amino acid utilization among species of the Cyperaceae: Plant and soil processes. *Ecology*, *80*(7), 2408–2419. https://doi.org/10.1890/0012-9658(1999)080[2408:SAAUAS]2.0.CO;2

Ramakrishna, P., & Barberon, M. (2019). Polarized transport across root epithelia. *Current Opinion in Plant Biology*, *52*, 23–29. https://doi.org/10.1016/J.PBI.2019.05.010

Rashid, M., Bera, S., Banerjee, M., Medvinsky, A. B., Sun, G. Q., Li, B. L., Sljoka, A., & Chakraborty, A. (2020). Feedforward Control of Plant Nitrate Transporter NRT1.1 Biphasic Adaptive Activity. *Biophysical Journal*, *118*(4), 898. https://doi.org/10.1016/J.BPJ.2019.10.018

Rashid, M., Bera, S., Medvinsky, A. B., Sun, G.-Q., Li, B.-L., & Chakraborty, A. (2018). Adaptive Regulation of Nitrate Transceptor NRT1.1 in Fluctuating Soil Nitrate Conditions. *ISCIENCE*, *2*, 41–50. https://doi.org/10.1016/j.isci.2018.03.007

Raven, J. A. (1994). Physiological analyses of aspects of the functioning of vascular tissue in early plants. *Botanical Journal of Scotland*, *47*(1), 49–64. https://doi.org/10.1080/03746609408684817

Rawat, S. R., Silim, S. N., Kronzucker, H. J., Siddiqi, M. Y., & Glass, A. D. M. (1999). AtAMT1 gene expression and NH4+ uptake in roots of Arabidopsis thaliana: evidence for regulation by root glutamine levels. *The Plant Journal*, *19*(2), 143–152. https://doi.org/10.1046/J.1365-313X.1999.00505.X

Ritchie, H., & Roser, M. (2019). *Land Use - Our World in Data*. Hannah Ritchie and Max Roser (2013) - 'Land Use'. Published Online at OurWorldInData.Org. Retrieved from: "https://Ourworldindata.Org/Land-Use" [Online Resource]. https://ourworldindata.org/land-use#citation

Robbins, N. E., Trontin, C., Duan, L., & Dinneny, J. R. (2014). Beyond the barrier: Communication in the root through the endodermis. *Plant Physiology*, *166*(2), 551–559. https://doi.org/10.1104/pp.114.244871

Robinson, M. D., & Oshlack, A. (2010). *A scaling normalization method for differential expression analysis of RNA-seq data*. http://genomebiology.com/2010/11/3/R25

Rubin, G., Tohge, T., Matsuda, F., Saito, K., & Scheible, W. R. (2009). Members of the LBD Family of Transcription Factors Repress Anthocyanin Synthesis and Affect Additional Nitrogen Responses in Arabidopsis. *The Plant Cell*, *21*(11), 3567–3584. https://doi.org/10.1105/TPC.109.067041

Ruffel, S. (2018). Nutrient-Related Long-Distance Signals: Common Players and Possible Cross-Talk. *Plant and Cell Physiology*, *59*(9), 1723–1732. https://doi.org/10.1093/PCP/PCY152

Ruffel, S., & Gojon, A. (2017). *Systemic nutrient signalling: On the road for nitrate*. https://doi.org/10.1038/nplants.2017.40

Russell, J. B. (2009). Rumen. *Encyclopedia of Microbiology, Third Edition*, 163–174. https://doi.org/10.1016/B978-012373944-5.00061-4

Ryu, K. H., Huang, L., Kang, H. M., & Schiefelbein, J. (2019). Single-cell RNA sequencing resolves molecular relationships among individual plant cells. *Plant Physiology*, *179*(4), 1444–1456. https://doi.org/10.1104/pp.18.01482

Safi, A., Medici, A., Szponarski, W., Martin, F., Clément-Vidal, A., Marshall-Colon, A., Ruffel, S., Gaymard, F., Rouached, H., Leclercq, J., Coruzzi, G., Lacombe, B., & Krouk, G. (2021). GARP transcription factors repress Arabidopsis nitrogen starvation response via ROS-dependent and -independent pathways. *Journal of Experimental Botany*, *72*(10), 3881–3901. https://doi.org/10.1093/JXB/ERAB114

Salas-González, I., Reyt, G., Flis, P., & Custódio, V. (2020). *Coordination between microbiota and root endodermis supports plant mineral nutrient homeostasis*. *2507*(1), 1–9.

Salas-González, I., Reyt, G., Flis, P., Custódio, V., Gopaulchan, D., Bakhoum, N., Dew, T. P., Suresh, K., Franke, R. B., Dangl, J. L., Salt, D. E., & Castrillo, G. (2021). Coordination between microbiota and root endodermis supports plant mineral nutrient homeostasis. *Science*, *371*(6525). https://doi.org/10.1126/science.abd0695

Sanz-Luque, E., Chamizo-Ampudia, A., Llamas, A., Galvan, A., & Fernandez, E. (2015). Understanding nitrate assimilation and its regulation in microalgae. *Frontiers in Plant Science*, *6*(OCTOBER). https://doi.org/10.3389/FPLS.2015.00899/ABSTRACT

Sato, T., Maekawa, S., Konishi, M., Yoshioka, N., Sasaki, Y., Maeda, H., Ishida, T., Kato, Y., Yamaguchi, J., & Yanagisawa, S. (2016). *Direct transcriptional activation of BT genes by NLP transcription factors is a key component of the nitrate response in Arabidopsis*. https://doi.org/10.1016/j.bbrc.2016.12.135

Schindelin, J., Arganda-Carreras, I., Frise, E., Kaynig, V., Longair, M., Pietzsch, T., Preibisch, S., Rueden, C., Saalfeld, S., Schmid, B., Tinevez, J. Y., White, D. J., Hartenstein, V., Eliceiri, K., Tomancak, P., & Cardona, A. (2012). Fiji: An open-source platform for biological-image analysis. In *Nature Methods* (Vol. 9, Issue 7, pp. 676–682). https://doi.org/10.1038/nmeth.2019

Schneider, C. A., Rasband, W. S., & Eliceiri, K. W. (2012). NIH Image to ImageJ: 25 years of image analysis. *Nature Methods 2012 9:7*, *9*(7), 671–675. https://doi.org/10.1038/nmeth.2089

Schochetman, G., Ou, C.-Y., & Jones, W. K. (1988). Polymerase Chain Reaction. *Source: The Journal of Infectious Diseases*, *158*(6), 1154–1157. https://www.jstor.org/stable/30137034

Serra, O., Mähönen, A. P., Hetherington, A. J., & Ragni, L. (2022). *The Making of Plant Armor: The Periderm*. https://doi.org/10.1146/annurev-arplant-102720

Sha, Y., Phan, J. H., & Wang, M. D. (2015). Effect of low-expression gene filtering on detection of differentially expressed genes in RNA-seq data. *Conference Proceedings : ... Annual International Conference of the IEEE Engineering in Medicine and Biology Society. IEEE Engineering in Medicine and Biology Society. Annual Conference*, *2015*, 6461. https://doi.org/10.1109/EMBC.2015.7319872

Shannon, C. E. (1948). A Mathematical Theory of Communication. *The Bell System Technical Journal*, *27*(3).

Shapiro, A. S. S., & Wilk, M. B. (1965). Biometrika Trust An Analysis of Variance Test for Normality (Complete Samples) Published by : Oxford University Press on behalf of Biometrika Trust Stable. *Biometrika*, *52*(3), 591–611.

Shen, D., Wippel, K., Remmel, S., Zhang, P., Kuertoes, N., Neumann, U., Kopriva, S., & Andersen, T. G. (2023). Timing of root barriers controls soil-to-shoot integration of rhizosphere status. *BioRxiv*, 2023.04.19.537470. https://doi.org/10.1101/2023.04.19.537470

Shimada, T. L., Shimada, T., & Hara-Nishimura, I. (2010). A rapid and non-destructive screenable marker, FAST, for identifying transformed seeds of Arabidopsis thaliana: TECHNICAL ADVANCE. *Plant Journal*, *61*(3), 519–528. https://doi.org/10.1111/j.1365-313X.2009.04060.x

Shimizu, B. I. (2014). 2-Oxoglutarate-dependent dioxygenases in the biosynthesis of simple coumarins. In *Frontiers in Plant Science* (Vol. 5, Issue November). Frontiers Media S.A. https://doi.org/10.3389/fpls.2014.00549

Shin, D. H., Choi, M., Kim, K., Bang, G., Cho, M., Choi, S. B., Choi, G., & Park, Y. Il. (2013). HY5 regulates anthocyanin biosynthesis by inducing the transcriptional activation of the MYB75/PAP1 transcription factor in Arabidopsis. *FEBS Letters*, *587*(10), 1543–1547. https://doi.org/10.1016/J.FEBSLET.2013.03.037

Shukla, V., Han, J. P., Cléard, F., Lefebvre-Legendre, L., Gully, K., Flis, P., Berhin, A., Andersen, T. G., Salt, D. E., Nawrath, C., & Barberon, M. (2021). Suberin plasticity to developmental and exogenous cues is regulated by a set of MYB transcription factors. *Proceedings of the National Academy of Sciences of the United States of America*, *118*(39), e2101730118. https://doi.org/10.1073/PNAS.2101730118/SUPPL_FILE/PNAS.2101730118.SAPP.PDF

Shulse, C. N., Cole, B. J., Ciobanu, D., Lin, J., Yoshinaga, Y., Gouran, M., Turco, G. M., Zhu, Y., O'Malley, R. C., Brady, S. M., & Dickel, D. E. (2019). High-Throughput Single-Cell Transcriptome Profiling of Plant Cell Types. *Cell Reports*, *27*(7), 2241-2247.e4. https://doi.org/10.1016/j.celrep.2019.04.054

Silva, S. P., Sabino, M. A., Fernandas, E. M., Correlo, V. M., Boesel, L. F., & Reis, R. L. (2013). Cork: properties, capabilities and applications. *Https://Doi.Org/10.1179/174328005X41168*, *50*(6), 345–365. https://doi.org/10.1179/174328005X41168

Smith, C., Hill, A. K., & Torrente-Murciano, L. (2020). Current and future role of Haber–Bosch ammonia in a carbon-free energy landscape. *Energy & Environmental Science*, *13*(2), 331–344. https://doi.org/10.1039/C9EE02873K

Soliday, C. L., Kolattukudy, P. E., & Davis, R. W. (1979). Chemical and ultrastructural evidence that waxes associated with the suberin polymer constitute the major diffusion barrier to water vapor in potato tuber (Solanum tuberosum L.). *Planta*, *146*(5), 607–614. https://doi.org/10.1007/BF00388840/METRICS

Sonoda, Y., Ikeda, A., Saiki, S., Yamaya, T., & Yamaguchi, J. (2003). Feedback Regulation of the Ammonium Transporter Gene Family AMT1 by Glutamine in Rice. *Plant and Cell Physiology*, *44*(12), 1396–1402. https://doi.org/10.1093/PCP/PCG169

Straub, T., Ludewig, U., & Neuhäuser, B. (2017). The Kinase CIPK23 Inhibits Ammonium Transport in Arabidopsis thaliana. *The Plant Cell*, *29*(2), 409–422. https://doi.org/10.1105/TPC.16.00806

Streeter, J. G. (1985). Nitrate Inhibition of Legume Nodule Growth and Activity : I. Long Term Studies with a Continuous Supply of Nitrate. *Plant Physiology*, *77*(2), 321. https://doi.org/10.1104/PP.77.2.321

Stringlis, I. A., Yu, K., Feussner, K., De Jonge, R., Van Bentum, S., Van Verk, M. C., Berendsen, R. L., Bakker, P. A. H. M., Feussner, I., & Pieterse, C. M. J. (2018). MYB72-dependent coumarin exudation shapes root microbiome assembly to promote plant health. *Proceedings of the National Academy of Sciences of the United States of America*, *115*(22), E5213–E5222. https://doi.org/10.1073/PNAS.1722335115/-/DCSUPPLEMENTAL

Strodtman, K. N., & Emerich, D. W. (2015). Nodule Metabolism. *Nitrogen Fixation in Crop Production*, *52*, 95–124. https://doi.org/10.2134/AGRONMONOGR52.C5

Sugiura, M., Georgescu, M. N., & Takahashi, M. (2007). A Nitrite Transporter Associated with Nitrite Uptake by Higher Plant Chloroplasts. *Plant and Cell Physiology*, *48*(7), 1022–1035. https://doi.org/10.1093/PCP/PCM073

Sun, J., & Zheng, N. (2015). Molecular mechanism underlying the plant NRT1.1 dual-affinity nitrate transporter. In *Frontiers in Physiology* (Vol. 6, Issue DEC). Frontiers Media S.A. https://doi.org/10.3389/fphys.2015.00386

Tabata, R., Sumida, K., Yoshii, T., Ohyama, K., Shinohara, H., & Matsubayashi, Y. (2014). Perception of root-derived peptides by shoot LRR-RKs mediates systemic N-demand signaling. *Science*, *346*(6207), 343–346. https://doi.org/10.1126/SCIENCE.1257800/SUPPL_FILE/TABATASM.PDF

Taleski, M., Chapman, K., Novák, O., Schmülling, T., Frank, M., & Djordjevic, M. A. (2023). CEP peptide and cytokinin pathways converge on CEPD glutaredoxins to inhibit root growth. *Nature Communications 2023 14:1*, *14*(1), 1–11. https://doi.org/10.1038/s41467-023-37282-6

Tegeder, M., & Masclaux-Daubresse, C. (2018). Source and sink mechanisms of nitrogen transport and use. In *New Phytologist* (Vol. 217, Issue 1, pp. 35–53). Blackwell Publishing Ltd. https://doi.org/10.1111/nph.14876

The Arabidopsis Genome Initiative. (2000). Analysis of the genome sequence of the flowering plant Arabidopsis thaliana. *Nature*, *408*. www.nature.com

Thellmann, M., Andersen, T. G., & Vermeer, J. E. M. (2020). Translating ribosome affinity purification (Trap) to investigate arabidopsis thaliana root development at a cell type-specific scale. *Journal of Visualized Experiments*, *2020*(159). https://doi.org/10.3791/60919

Tinker, P. B. (Philip B., & Nye, P. H. (2000). *Solute movement in the rhizosphere*. 444.

Topham, S. A. (1985). *The History of the Catalytic Synthesis of Ammonia*.

Tsay, Y. F., Schroeder, J. I., Feldmann, K. A., & Crawford, N. M. (1993). The herbicide sensitivity gene CHL1 of Arabidopsis encodes a nitrate-inducible nitrate transporter. *Cell*, *72*(5), 705–713. https://doi.org/10.1016/0092-8674(93)90399-B

Tukey, J. W. (1949). Comparing Individual Means in the Analysis of Variance Author (s): John W . Tukey Published by : International Society Stable URL : http://www.jstor.org/stable/3001913 REFERENCES Linked references are available on JSTOR for this article : You may need t. *Biometric*, *5*(2), 99–114.

Tyree, M. T. (2003). Plant hydraulics: The ascent of water. *Nature 2003 423:6943*, *423*(6943), 923–923. https://doi.org/10.1038/423923a

Ursache, R., Andersen, T. G., Marhavý, P., & Geldner, N. (2018). A protocol for combining fluorescent proteins with histological stains for diverse cell wall components. *Plant Journal*, *93*(2), 399–412. https://doi.org/10.1111/tpj.13784

Ursache, R., De Jesus Vieira Teixeira, C., Dénervaud Tendon, V., Gully, K., De Bellis, D., Schmid-Siegert, E., Grube Andersen, T., Shekhar, V., Calderon, S., Pradervand, S., Nawrath, C., Geldner, N., & Vermeer, J. E. M. (2021). GDSL-domain proteins have key roles in suberin polymerization and degradation. *Nature Plants 2021 7:3*, *7*(3), 353–364. https://doi.org/10.1038/s41477-021-00862-9

Ursache, R., Vieira-Teixeira, C. D. J., Tendon, V. D., Gully, K., Bellis, D. De, Schmid-Siegert, E., Andersen, T. G., Shekhar, V., Calderon, S., Pradervand, S., Nawrath, C., Geldner, N., & Vermeer, J. E. M. (2020). GDSL-domain containing proteins mediate suberin biosynthesis and degradation, enabling developmental plasticity of the endodermis during lateral root emergence. *BioRxiv*, *1*, 2020.06.25.171389. https://doi.org/10.1101/2020.06.25.171389

Vallon, O., & Spalding, M. H. (2009). Amino Acid Metabolism. *The Chlamydomonas Sourcebook 3-Vol Set*, *2*, 115–158. https://doi.org/10.1016/B978-0-12-370873-1.00012-5

Van Bel, A. J. E. (1984). Quantification of the xylem-to-phloem transfer of amino acids by use of inulin [14C]carboxylic acid as xylem transport marker. *Plant Science Letters*, *35*(1), 81–85. https://doi.org/10.1016/0304-4211(84)90162-7

Van Bel, A. J. E. (1990). Xylem-Phloem Exchange Via the Rays: The Undervalued Route of Transport. *Journal of Experimental Botany*, *41*(6), 631–644. https://doi.org/10.1093/JXB/41.6.631

Van Deynze, A., Zamora, P., Delaux, P. M., Heitmann, C., Jayaraman, D., Rajasekar, S., Graham, D., Maeda, J., Gibson, D., Schwartz, K. D., Berry, A. M., Bhatnagar, S., Jospin, G., Darling, A., Jeannotte, R., Lopez, J., Weimer, B. C., Eisen, J. A., Shapiro, H. Y., … Bennett, A. B. (2018). Nitrogen fixation in a landrace of maize is supported by a mucilage-associated diazotrophic microbiota. *PLOS Biology*, *16*(8), e2006352. https://doi.org/10.1371/JOURNAL.PBIO.2006352

van Puijenbroek, P. J. T. M., Beusen, A. H. W., & Bouwman, A. F. (2019). Global nitrogen and phosphorus in urban waste water based on the Shared Socio-economic pathways. *Journal of Environmental Management*, *231*, 446–456. https://doi.org/10.1016/J.JENVMAN.2018.10.048

Verbon, E. H., Liberman, L. M., Zhou, J., Yin, J., Pieterse, C. M., Benfey, P. N., Stringlis, I. A., de Jonge, R., Cmj, P., & Jonge, de R. (2023). *Cell-type-specific transcriptomics reveals that root hairs and endodermal barriers play important roles in beneficial plant-rhizobacterium interactions*. https://doi.org/10.1016/j.molp.2023.06.001

Vidal, E. A., Alvarez, J. M., Araus, V., Riveras, E., Brooks, M. D., Krouk, G., Ruffel, S., Lejay, L., Crawford, N. M., Coruzzi, G. M., & Gutiérrez, R. A. (2020). Nitrate in 2020: Thirty Years from Transport to Signaling Networks. *The Plant Cell*, *32*(7), 2094–2119. https://doi.org/10.1105/TPC.19.00748

Vishwanath, S. J., Delude, C., Domergue, F., & Rowland, O. (2015). Suberin: biosynthesis, regulation, and polymer assembly of a protective extracellular barrier. *Plant Cell Reports*, *34*(4), 573–586. https://doi.org/10.1007/S00299-014-1727-Z/FIGURES/2

Vitousek, P. M., Hättenschwiler, S., Olander, L., & Allison, S. (2002). Nitrogen and nature. *Ambio*, *31*(2), 97–101. https://doi.org/10.1579/0044-7447-31.2.97

Voges, M. J. E. E. E., Bai, Y., Schulze-Lefert, P., & Sattely, E. S. (2019). Plant-derived coumarins shape the composition of an Arabidopsis synthetic root microbiome. *Proceedings of the National Academy of Sciences of the United States of America*, *116*(25), 12558–12565. https://doi.org/10.1073/PNAS.1820691116/SUPPL_FILE/PNAS.1820691116.SD01.XLSX

von Wangenheim, D., Hauschild, R., Fendrych, M., Barone, V., Benková, E., & Friml, J. (2017). Live tracking of moving samples in confocal microscopy for vertically grown roots. *ELife*, *6*. https://doi.org/10.7554/ELIFE.26792

Vragović, K., Selaa, A., Friedlander-Shani, L., Fridman, Y., Hacham, Y., Holland, N., Bartom, E., Mockler, T. C., & Savaldi-Goldstein, S. (2015). Translatome analyses capture of opposing tissuespecific brassinosteroid signals orchestrating root meristem differentiation. *Proceedings of the National Academy of Sciences of the United States of America*, *112*(3), 923–928. https://doi.org/10.1073/PNAS.1417947112

Vrieze, S. I. (2012). Model selection and psychological theory: A discussion of the differences between the Akaike information criterion (AIC) and the Bayesian information criterion (BIC). *Psychological Methods*, *17*(2), 228–243. https://doi.org/10.1037/a0027127

Wagner, S. C. (2011). *Biological Nitrogen Fixation*. Wagner, S. C.. (2011) Biological Nitrogen Fixation. Nature Education Knowledge 3(10):15.

Wang, W., Hu, B., Li, A., & Chu, C. (2020). NRT1.1s in plants: functions beyond nitrate transport. *Journal of Experimental Botany*, *71*(15), 4373–4379. https://doi.org/10.1093/JXB/ERZ554

Wang, X., Luo, Z., Hu, Q., Tang, W., Lu, H., Ma, C., Wang, Z., Baltaevich, A. M., & Kong, X. (2023). Light induced shoot-sourced transcription factor HY5 regulates the nitrate uptake of cotton by shoot-to-root signal transport. *Plant Physiology and Biochemistry : PPB*, *200*. https://doi.org/10.1016/J.PLAPHY.2023.107738

Webb, M., Jouannic, S., Foreman, J., Linstead, P., & Dolan, L. (2002). Cell specification in the Arabidopsis root epidermis requires the activity of ectopic root hair 3 - A katanin-p60 protein. *Development*, *129*(1), 123–131.

Weiland, M., Mancuso, S., Baluska, F., Weiland, M., Mancuso, S., & Baluska, F. (2015). Signalling via glutamate and GLRs in Arabidopsis thaliana. *Functional Plant Biology*, *43*(1), 1–25. https://doi.org/10.1071/FP15109

Welsh, A., Chee-Sanford, J. C., Connor, L. M., Löffler, F. E., & Sanford, R. A. (2014). *Refined NrfA Phylogeny Improves PCR-Based nrfA Gene Detection*. https://doi.org/10.1128/AEM.03443-13

Wickham, H., Averick, M., Bryan, J., Chang, W., McGowan, L., François, R., Grolemund, G., Hayes, A., Henry, L., Hester, J., Kuhn, M., Pedersen, T., Miller, E., Bache, S., Müller, K., Ooms, J., Robinson, D., Seidel, D., Spinu, V., … Yutani, H. (2019). Welcome to the Tidyverse. *Journal of Open Source Software*, *4*(43), 1686. https://doi.org/10.21105/joss.01686

Wippel, K., Tao, K., Niu, Y., Zgadzaj, R., Kiel, N., Guan, R., Dahms, E., Zhang, P., Jensen, D. B., Logemann, E., Radutoiu, S., Schulze-Lefert, P., & Garrido-Oter, R. (2021). Host preference and invasiveness of commensal bacteria in the Lotus and Arabidopsis root microbiota. *Nature Microbiology 2021 6:9*, *6*(9), 1150–1162. https://doi.org/10.1038/s41564-021-00941-9

Wirth, J., Chopin, F., Santoni, V., Viennois, G., Tillard, P., Krapp, A., Lejay, L., Daniel-Vedele, F., & Gojon, A. (2007). Regulation of root nitrate uptake at the NRT2.1 protein level in Arabidopsis thaliana. *Journal of Biological Chemistry*, *282*(32), 23541–23552. https://doi.org/10.1074/jbc.M700901200

Wolinska, K. W., Vannier, N., Thiergart, T., Pickel, B., Gremmen, S., Piasecka, A., Piślewska-Bednarek, M., Nakano, R. T., Belkhadir, Y., Bednarek, P., & Hacquard, S. (2021). Tryptophan metabolism and bacterial commensals prevent fungal dysbiosis in Arabidopsis roots. *Proceedings of the National Academy of Sciences of the United States of America*, *118*(49). https://doi.org/10.1073/PNAS.2111521118/-/DCSUPPLEMENTAL

Wong, P. P. (1988). Inhibition of legume nodule formation and n2 fixation by nitrate. *Critical Reviews in Plant Sciences*, *7*(1), 1–23. https://doi.org/10.1080/07352688809382257/ASSET//CMS/ASSET/010E676B-5F0E-4F4E-A184-31879FF6C411/07352688809382257.FP.PNG

Woolfson, K. N., Esfandiari, M., & Bernards, M. A. (2022). Suberin Biosynthesis, Assembly, and Regulation. *Plants*, *11*(4). https://doi.org/10.3390/PLANTS11040555

Wu, X., Liu, T., Zhang, Y., Duan, F., Neuhaüser, B., Ludewig, U., Schulze, W. X., & Yuan, L. (2019). Ammonium and nitrate regulate NH4+ uptake activity of Arabidopsis ammonium transporter AtAMT1;3 via phosphorylation at multiple C-terminal sites. *Journal of Experimental Botany*, *70*(18), 4919–4930. https://doi.org/10.1093/JXB/ERZ230

Wunderling, A., Ripper, D., Barra-Jimenez, A., Mahn, S., Sajak, K., Targem, M. Ben, & Ragni, L. (2018). A molecular framework to study periderm formation in Arabidopsis. *New Phytologist*, *219*(1), 216–229. https://doi.org/10.1111/NPH.15128

Xiao, C., Sun, D., Liu, B., Fang, X., Li, P., Jiang, Y., He, M., Li, J., Luan, S., & He, K. (2022). Nitrate transporter NRT1.1 and anion channel SLAH3 form a functional unit to regulate nitrate-dependent alleviation of ammonium toxicity. *Journal of Integrative Plant Biology*, *64*(4), 942–957. https://doi.org/10.1111/jipb.13239

Xu, G., Fan, X., & Miller, A. J. (2012). Plant Nitrogen Assimilation and Use Efficiency. *Https://Doi.Org/10.1146/Annurev-Arplant-042811-105532*, *63*, 153–182. https://doi.org/10.1146/ANNUREV-ARPLANT-042811-105532

Xu, N., Wang, R., Zhao, L., Zhang, C., Li, Z., Lei, Z., Liu, F., Guan, P., Chu, Z., & Crawford, N. M. (2016). The Arabidopsis NRG2 Protein Mediates Nitrate Signaling and Interacts with and Regulates Key Nitrate Regulators. *The Plant Cell*, *28*(2), 485–504. https://doi.org/10.1105/TPC.15.00567

Yamazaki, K., Ohmori, Y., & Fujiwara, T. (2020). A Positive Tropism of Rice Roots toward a Nutrient Source. *Plant and Cell Physiology*, *61*(3), 546–553. https://doi.org/10.1093/PCP/PCZ218

Yang, X., Poelmans, W., Grones, C., De Rybel, B., Motte, H., Beeckman, T., Lakehal, A., Pevernagie, J., Van Bel, M., Njo, M., Xu, L., & Nelissen, H. (2023). Spatial transcriptomics of a lycophyte root sheds light on root evolution. *Current Biology*, *33*. https://doi.org/10.1016/j.cub.2023.08.030

Ye, J. Y., Tian, W. H., & Jin, C. W. (2019). A reevaluation of the contribution of NRT1.1 to nitrate uptake in Arabidopsis under low-nitrate supply. *FEBS Letters*, *593*(15), 2051–2059. https://doi.org/10.1002/1873-3468.13473

Yu, L. H., Wu, J., Tang, H., Yuan, Y., Wang, S. M., Wang, Y. P., Zhu, Q. S., Li, S. G., & Xiang, C. Bin. (2016). Overexpression of Arabidopsis NLP7 improves plant growth under both nitrogen-limiting and -sufficient conditions by enhancing nitrogen and carbon assimilation. *Scientific Reports 2016 6:1*, *6*(1), 1–13. https://doi.org/10.1038/srep27795

Yu, P., He, X., Baer, M., Beirinckx, S., Tian, T., Moya, Y. A. T., Zhang, X., Deichmann, M., Frey, F. P., Bresgen, V., Li, C., Razavi, B. S., Schaaf, G., von Wirén, N., Su, Z., Bucher, M., Tsuda, K., Goormachtig, S., Chen, X., & Hochholdinger, F. (2021). Plant flavones enrich rhizosphere Oxalobacteraceae to improve maize performance under nitrogen deprivation. *Nature Plants*, *7*(4), 481–499. https://doi.org/10.1038/s41477-021-00897-y

Yuan, L., Loqué, D., Kojima, S., Rauch, S., Ishiyama, K., Inoue, E., Takahashi, H., & Von Wiréna, N. (2007). The Organization of High-Affinity Ammonium Uptake in Arabidopsis Roots Depends on the Spatial Arrangement and Biochemical Properties of AMT1-Type Transporters. *The Plant Cell*, *19*(8), 2636–2652. https://doi.org/10.1105/TPC.107.052134

Zanetti, M. E., Chang, I. F., Gong, F., Galbraith, D. W., & Bailey-Serres, J. (2005). Immunopurification of polyribosomal complexes of Arabidopsis for global analysis of gene expression. In *Plant Physiology* (Vol. 138, Issue 2, pp. 624–635). American Society of Plant Biologists. https://doi.org/10.1104/pp.105.059477

Zhang, T. Q., Xu, Z. G., Shang, G. D., & Wang, J. W. (2019). A Single-Cell RNA Sequencing Profiles the Developmental Landscape of Arabidopsis Root. *Molecular Plant*, *12*(5), 648–660. https://doi.org/10.1016/j.molp.2019.04.004

Zhao, C., Pratelli, R., Yu, S., Shelley, B., Collakova, E., & Pilot, G. (2021). Detailed characterization of the UMAMIT proteins provides insight into their evolution, amino acid transport properties, and role in the plant. *Journal of Experimental Botany*, *72*(18), 6400–6417. https://doi.org/10.1093/JXB/ERAB288

Zhao, L., Liu, F., Crawford, N. M., & Wang, Y. (2018). Molecular Regulation of Nitrate Responses in Plants. *International Journal of Molecular Sciences*, *19*(7). https://doi.org/10.3390/IJMS19072039

Zhao, M., Ding, H., Zhu, J. K., Zhang, F., & Li, W. X. (2011). Involvement of miR169 in the nitrogen-starvation responses in Arabidopsis. *New Phytologist*, *190*(4), 906–915. https://doi.org/10.1111/J.1469-8137.2011.03647.X

Zhou, Y., Zhou, B., Pache, L., Chang, M., Khodabakhshi, A. H., Tanaseichuk, O., Benner, C., & Chanda, S. K. (2019). Metascape provides a biologist-oriented resource for the analysis of systems-level datasets. *Nature Communications*, *10*(1). https://doi.org/10.1038/s41467-019-09234-6

Zhu, X., Wang, D., Xie, L., Zhou, T., Zhao, J., Zhang, Q., Yang, M., Wu, W., & Lian, X. (2022). Rice transcription factors OsLBD37/38/39 regulate nitrate uptake by repressing OsNRT2.1/2.2/2.3 under high-nitrogen conditions. *The Crop Journal*, *10*(6), 1623–1632. https://doi.org/10.1016/J.CJ.2022.03.011

20 Declaration on the application for admission to the doctoral examinations

Erklärung zur Dissertation
gemäß der Promotionsordnung vom 12. März 2020

Diese Erklärung muss in der Dissertation enthalten sein.
(*This version must be included in the doctoral thesis*)

„Hiermit versichere ich an Eides statt, dass ich die vorliegende Dissertation selbstständig und ohne die Benutzung anderer als der angegebenen Hilfsmittel und Literatur angefertigt habe. Alle Stellen, die wörtlich oder sinngemäß aus veröffentlichten und nicht veröffentlichten Werken dem Wortlaut oder dem Sinn nach entnommen wurden, sind als solche kenntlich gemacht. Ich versichere an Eides statt, dass diese Dissertation noch keiner anderen Fakultät oder Universität zur Prüfung vorgelegen hat; dass sie - abgesehen von unten angegebenen Teilpublikationen und eingebundenen Artikeln und Manuskripten - noch nicht veröffentlicht worden ist sowie, dass ich eine Veröffentlichung der Dissertation vor Abschluss der Promotion nicht ohne Genehmigung des Promotionsausschusses vornehmen werde. Die Bestimmungen dieser Ordnung sind mir bekannt. Darüber hinaus erkläre ich hiermit, dass ich die Ordnung zur Sicherung guter wissenschaftlicher Praxis und zum Umgang mit wissenschaftlichem Fehlverhalten der Universität zu Köln gelesen und sie bei der Durchführung der Dissertation zugrundeliegenden Arbeiten und der schriftlich verfassten Dissertation beachtet habe und verpflichte mich hiermit, die dort genannten Vorgaben bei allen wissenschaftlichen Tätigkeiten zu beachten und umzusetzen. Ich versichere, dass die eingereichte elektronische Fassung der eingereichten Druckfassung vollständig entspricht."

Teilpublikationen:

Keine

Datum, Name und Unterschrift

21.09.2023, Noah Kürtös

Declaration for the doctoral thesis (dissertation)

according to the doctoral regulations published 12th March 2020

Non-official English translation of the "Erklärung zur Dissertation"
(*The German version must be included in the doctoral thesis*)

"I hereby declare that I have completed the present dissertation independently and without the use of any aids or literature other than those referred to. All passages that have been taken, either literally or in sense, from published and unpublished works, are marked as such. I declare that this dissertation has not been submitted to any other faculty or university; that - apart from the partial publications and included articles and manuscripts listed below - it has not yet been published, and that I will not publish the dissertation before completing my doctorate without the permission of the PhD Committee. I am aware of the terms of the doctoral regulations. In addition, I hereby declare that I am aware of the "Regulations for Safeguarding Good Scientific Practice and Dealing with Scientific Misconduct" of the University of Cologne, and that I have observed them during the work on the thesis project and the written doctoral thesis. I hereby commit myself to observe and implement the guidelines mentioned there in all scientific activities. I assure that the submitted electronic version is identical to the submitted printed version".

Partial publications of the thesis:

None

Date, name, and signature

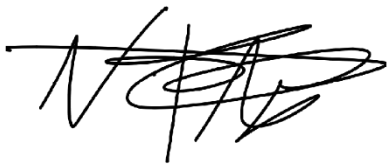

21.09.2023, Noah Kürtös

Erklärung zum Gesuch um Zulassung zur Promotion

gemäß der Promotionsordnung vom 12. März 2020

1. Zugänglichkeit von Daten und Materialien

Die Dissertation beinhaltet die Gewinnung von Primärdaten oder die Analyse solcher Daten oder die Reproduzierbarkeit der in der Dissertation dargestellten Ergebnisse setzt die Verfügbarkeit von Datenanalysen, Versuchsprotokollen oder Probenmaterial voraus.

Trifft nicht zu

✓ Trifft zu.
In der Dissertation ist dargelegt wie diese Daten und Materialien gesichert und zugänglich sind (entsprechend den Vorgaben des Fachgebiets beziehungsweise der Betreuerin oder des Betreuers).

2. Frühere Promotionsverfahren

Ich habe bereits einen Doktortitel erworben oder ehrenhalber verliehen bekommen.
Oder: Für mich ist an einer anderen Fakultät oder Universität ein Promotionsverfahren eröffnet worden, aber noch nicht abgeschlossen.
Oder: Ich bin in einem Promotionsverfahren gescheitert.

✓ Trifft nicht zu
Zutreffend
Erläuterung:

3. Straftat

Ich bin nicht zu einer vorsätzlichen Straftat verurteilt worden, bei deren Vorbereitung oder Begehung der Status einer Doktorandin oder eines Doktoranden missbraucht wurde.

Ich versichere, alle Angaben wahrheitsgemäß gemacht zu haben.

Datum	Name	Unterschrift
21.09.2023	Noah Kürtös	

01-2021

Declaration on the application for admission to the doctoral examinations

according to the doctoral regulations published 12th March 2020

1. Accessibility of data and materials

The dissertation involves the acquisition of primary data or the analysis of such data or the reproducibility of the results presented in the dissertation requires the availability of data analyses, experimental protocols or sample material.

not applicable

✓ applicable

I have described in the dissertation how these data and materials are secured and accessible (according to the specifications of the subject area or supervisor).

2. Previous doctoral examinations

I have already obtained a doctorate or been awarded an honorary doctoral degree.

Or: A doctoral examination has been opened at another faculty or university, but not yet completed.

Or: I have failed in a doctoral examination.

✓ not applicable

applicable

explanatory note:

3. Criminal offense

I have not been convicted of a deliberate criminal offence in the preparation or commission of which the status as a doctoral candidate was abused.

I declare that all information provided is truthful.

Date	Name	Signature
21.09.2023	Noah Kürtös